

This project was supported by the Centre for Global Eco-Innovation and is part financed by the European Regional Development Fund.

**Recycling and reuse of metal powders for various applications in additively manufactured products**

By

**DANIEL POWELL**

In collaboration with

**CROFT ADDITIVE MANUFACTURING LTD**



Engineering

Lancaster  
University



**Recycling and reuse of metal powders for various applications  
in additively manufactured products**

Author Daniel Powell  
Supervisor Dr Allan EW Rennie

MSc Engineering (by Research)  
Lancaster University Engineering Department

Initial submission: 24/01/2020

Amended submission: 07/04/2020

Lancaster University  
Faculty of Science and Technology  
Engineering Department

**Signed Declaration on the submission of a dissertation**

I declare that this dissertation is my own work and has not been submitted in substantially the same form towards the award of a degree or other qualification at this, or any other, institutions of higher education.

Acknowledgement is made in the text of assistance received and all major sources of information are properly referenced. I confirm that I have read and understood the publication *Guidance on Writing Technical Reports* published by the Engineering Department.

Signed .....

Date .....

## Contents

Contents.....	iv
List of Figures.....	vi
List of Tables.....	x
List of Abbreviations and Acronyms.....	xii
Nomenclature.....	xii
Contributions to Knowledge.....	xiii
Research Outputs.....	xiv
Acknowledgements.....	xiv
Abstract.....	xv
1. Introduction.....	1
1.1 Background of additive manufacturing.....	1
1.2 Croft Additive Manufacturing Ltd.....	2
1.3 Metal powder-based additive manufacturing.....	2
1.4 Waste metal powder.....	3
1.5 Objectives of research.....	5
1.6 Proposed solutions.....	6
2. Literature Review.....	8
2.1 Methodology for selecting literature.....	9
2.2 Methods of powder production.....	9
2.3 Particle and powder properties.....	11
2.3.1 Particle size distribution.....	11
2.3.2 Packing density.....	13
2.3.3 Particle morphology.....	15
2.3.4 Chemical composition.....	18
2.3.5 Flowability.....	21
2.4 Component properties.....	22
2.4.1 Chemical composition.....	22
2.4.2 Density and porosity.....	23
2.4.3 Tensile properties and hardness.....	24
2.4.4 Surface roughness.....	26
2.5 Combining virgin and recycled powder.....	27
2.6 End of life powder.....	28
3. Feasibility Analysis of Proposed Solutions.....	30
3.1 Proposed solutions by Croft AM.....	30
3.2 Further proposed solutions.....	35

3.3	Matrix analysis .....	43
3.4	Concepts carried forwards.....	49
4.	Powder Analysis .....	51
4.1	Introduction.....	51
4.2	Methodology.....	54
4.3	Results .....	56
4.3.1	SEM Imaging .....	56
4.3.2	EDS Analysis.....	66
4.3.3	Particle Size Distribution .....	77
4.4	Discussion.....	82
4.5	Conclusions.....	87
5.	Breakdown of Support Structures into Metal Powder .....	89
5.1	Establishing further understanding of support structures.....	89
5.2	Proposed breakdown techniques .....	91
5.3	Experimental Procedure.....	92
5.4	Results .....	93
5.5	Discussion.....	94
5.6	Conclusion .....	95
6.	Continuation of support structure breakdown through ball milling.....	96
6.1	Environmental justification.....	96
6.2	Initial experimentation .....	97
6.2.1	Methodology.....	97
6.2.2	Results .....	99
6.2.3	Discussion.....	113
6.2.4	Conclusions.....	115
6.3	Further experimentation.....	116
6.3.1	Methodology.....	116
6.3.2	Results .....	117
6.3.3	Discussion.....	137
6.3.4	Conclusion .....	139
7.	Conclusions.....	141
8.	Further Work .....	143
	References.....	145
	Appendix A – Poster presented at the Eco-I Conference 2019.....	xix
	Appendix B – Carbon Reductions Calculations.....	xvi
	Appendix C – Programme of work for plasma spheroidisation .....	xxiv

## List of Figures

Figure 1-1 – The Selective Laser Melting process (figure provided by Croft AM) .....	3
Figure 2-1 – Representation of the increasing number of particles present, from an individual particle through to the manufactured component .....	8
Figure 2-2 – A simplified diagram of the atomisation process .....	10
Figure 2-3 – Random packing of uniformly sized particles .....	13
Figure 2-4 – Random packing of various sized particles.....	14
Figure 2-5 – Distribution of spherical particles (Left: model. Right: SEM image).....	14
Figure 2-6 – Distribution of agglomerate particles (Left: model. Right: SEM image) The rectangular outline on the model shows the region where, assuming the powder has been fed by gravity from the top of the diagram, the packing density is negatively influenced due to the agglomerates .....	14
Figure 2-7 – Interparticle forces between two smooth particles.....	16
Figure 2-8 – Interparticle forces between two rough particles .....	16
Figure 2-9 – A particle with satellites on it (Left: model. Right: SEM image) .....	17
Figure 2-10 – An agglomerate particle made of two individual particles (Left: model. Right: SEM image) .....	17
Figure 2-11 – An example of low surface roughness between layers.....	26
Figure 2-12 – An example of high surface roughness between layers.....	26
Figure 3-1 – Particle sizes used by the different metal powder based AM techniques. Thick lines indicate the desirable particle sizes for each process, whilst dashed lines indicate usable but less acceptable particle sizes. ....	31
Figure 3-2 – Representation of the air jigging principle with a mixed powder. Air flows from the bottom of the chamber upwards. Denser particles are presented by darker grey, whilst less dense particles are lighter grey. ....	35
Figure 3-3 – An example of ball milling .....	36
Figure 3-4 – An overview of plasma spheroidisation.....	41
Figure 4-1 – Visual comparison of 316L stainless steel metal powders. Left: virgin powder. Right: double overflow powder.....	53
Figure 4-2 – Quantified particles to allow visual analysis of roundness (x) and sphericity (y) and (Krumbein and Sloss 1963).....	54
Figure 4-3a (top left), Figure 4-3b (top right), Figure 4-3c (bottom left) & Figure 4-3d (bottom right) – x60, x140, x400 and x1,000 magnifications of Powder 1 (respectively).....	56
Figure 4-4a (top left), Figure 4-4b (top right), Figure 4-4c (bottom left) & Figure 4-4d (bottom right) – x60, x140, x400 and x1,000 magnifications of Powder 2 (respectively).....	57

Figure 4-5a (top left), Figure 4-5b (top right), Figure 4-5c (bottom left) & Figure 4-5d (bottom right) – x60, x140, x400 and x1,000 magnifications of Powder 3 (respectively).....	58
Figure 4-6a (top left), Figure 4-6b (top right), Figure 4-6c (bottom left) & Figure 4-6d (bottom right) – x60, x140, x400 and x1,000 magnifications of Powder 4 (respectively).....	59
Figure 4-7a (top left), Figure 4-7b (top right), Figure 4-7c (bottom left) & Figure 4-7d (bottom right) – x60, x140, x400 and x1,000 magnifications of Powder 7 (respectively).....	60
Figure 4-8a (top left), Figure 4-8b (top right), Figure 4-8c (bottom left) & Figure 4-8d (bottom right) – x60, x140, x400 and x1,000 magnifications of Powder 8 (respectively).....	61
Figure 4-9a (top left), Figure 4-9b (top right), Figure 4-9c (bottom left) & Figure 4-9d (bottom right) – x60, x140, x400 and x1,000 magnifications of Powder 9 (respectively).....	62
Figure 4-10a (top left), Figure 4-10b (top right), Figure 4-10c (bottom left) & Figure 4-10d (bottom right) – x60, x140, x400 and x1,000 magnifications of Powder 10 (respectively) .....	63
Figure 4-11a (top left), Figure 4-11b (top right), Figure 4-11c (bottom left) & Figure 4-11d (bottom right) – x60, x140, x400 and x1,000 magnifications of Powder 11 (respectively) .....	64
Figure 4-12a (top left), Figure 4-12b (top right), Figure 4-12c (bottom left) & Figure 4-12d (bottom right) – x60, x140, x400 and x1,000 magnifications of Powder 12 (respectively) .....	65
Figure 4-13 – EDS site locations for Powder 1.....	67
Figure 4-14 – EDS site locations for Powder 2.....	68
Figure 4-15 – EDS site locations for Powder 3.....	69
Figure 4-16 – EDS site locations for Powder 4.....	70
Figure 4-17 – EDS site locations for Powder 5.....	71
Figure 4-18 – EDS site locations for Powder 6.....	72
Figure 4-19 – EDS site locations for Powder 7.....	73
Figure 4-20 – EDS site locations for Powder 8.....	74
Figure 4-21 – EDS site locations for Powder 9.....	75
Figure 4-22 – EDS site locations for Powder 10.....	76
Figure 4-23 – PSDs of powders used by Croft AM at various stages of reuse .....	77
Figure 4-24 – PSDs of powders from different companies compared to virgin powder and acceptable powder used by Croft AM .....	79
Figure 4-25 – PSDs of overflow powders compared with virgin and acceptable powder.....	80
Figure 4-26 – PSD of black powder compared with virgin and acceptable powder .....	81
Figure 4-27a (top left) – Initial particle size analysis image Figure 4-27b (top right) – Adjusted particle size image analysis to include larger particles Figure 4-27c (bottom left) – Overlaid image of Figure	

4-27a and Figure 4-27b Figure 4-27d (bottom right) – SEM image of Powder 3 at x140 magnification, from which Figure 4-27a and Figure 4-27b were derived .....	83
Figure 5-1 – Supports used for breakdown analysis, overlaid on a 5x5mm grid. From left to right: light hatch, dense hatch, light border support, dense border support.....	92
Figure 5-2 – Broken down support structures, overlaid on a 5x5mm grid. From left to right: light hatch, dense hatch, light border support, dense border support, variety of chips from all support types ....	93
Figure 6-1 – Examples of the chips included in each sample, overlaid on a 5x5mm grid. Left: standard chips. Right: oversized chips .....	97
Figure 6-2 – Side-by-side comparison of the 15ml samples of standard (left) and oversized (right) chips, occupying the same volume .....	98
Figure 6-3 – Powder formed from standard chips in the ball milling process .....	99
Figure 6-4 – Powder formed from oversized chips in the ball milling process .....	99
Figure 6-5 – Powder adhered to both the mixing bowl and balls .....	101
Figure 6-6a (top left), Figure 6-6b (top right), Figure 6-6c (middle left), Figure 6-6d (middle right), Figure 6-6e (bottom left), Figure 6-6f (bottom right) & Figure 6-6g (bottom centre) – x200 magnification SEM images of the powder produced from standard chips.....	102
Figure 6-7a (top left), Figure 6-7b (top right), Figure 6-7c (middle left), Figure 6-7d (middle right), Figure 6-7e (bottom left) & Figure 6-7f (bottom right) – x200 magnification SEM images of the powder produced from oversized chips .....	103
Figure 6-8 – PSDs of the powders created from ball milling and the theoretical blended powders they could create.....	104
Figure 6-9 – PSDs of the theoretical blended powders compared with virgin and used powders ....	106
Figure 6-10 – EDS site locations for powder produced from standard chips .....	108
Figure 6-11 – EDS site locations for powder produced from oversized chips .....	109
Figure 6-12 – Comparison of the average chemical composition of powders formed from standard and oversized chips with virgin powder (see Table 4-3) and used but acceptable powder (see Table 4-4) .....	110
Figure 6-13 – EDS peaks produced for analysis, detecting only the main constituent elements of 316L stainless steel. Yellow regions = a typical particle from virgin powder. Grey regions = a typical particle from oversized powder (minus carbon).....	111
Figure 6-14 – EDS peaks produced for analysis, allowing the software to pair peaks to the most likely element detected. Yellow regions = a typical particle from virgin powder. Grey regions = a typical particle from oversized powder (minus carbon).....	111

Figure 6-15 – EDS peaks produced before analysis, allowing the software to pair peaks to the most likely element detected. Yellow regions = a typical particle from virgin powder. Grey regions = a typical particle from standard powder (minus carbon).....	112
Figure 6-16 – Examples of the chips included in each sample, overlaid on a 5x5mm grid. Left: assorted chips. Right: overfilled assorted chips. Circled regions show example of thick chips .....	116
Figure 6-17 – Side-by-side comparison of the samples of assorted (left) and overfilled assorted (right) chips.....	117
Figure 6-18 – The powders formed from assorted chips (top left) and the overfilled chip sample (top right) compared with virgin powder (bottom) .....	118
Figure 6-19a (top left), Figure 6-19b (top right), Figure 6-19c (middle left), Figure 6-19d (middle right) and Figure 6-19e (centre bottom) – x50 magnification SEM images of the powder produced from the assorted sample after 30, 60, 90, 120 and 150 minutes respectively.....	120
Figure 6-20a (top left), Figure 6-20b (top right), Figure 6-20c (middle left), Figure 6-20d (middle right) and Figure 6-20e (centre bottom) – x50 magnification SEM images of the powder produced from the overfilled sample after 30, 60, 90, 120 and 150 minutes respectively .....	122
Figure 6-21 – PSD of the powder produced from assorted chips after various durations of ball milling .....	124
Figure 6-22 – PSD of the powder produced from the overfilled chip sample after various durations of ball milling .....	125
Figure 6-23 – PSD curves of the powders produced from ball milling compared with powders used by Croft AM .....	126
Figure 6-24a (left), Figure 6-24b (centre) and Figure 6-24c (right) – Comparison of d10, d50, d90 and mean values for the powder produced at various stages by both the assorted and overfilled chips	127
Figure 6-25 – EDS site locations for powder produced from assorted chips after 60 minutes of ball milling.....	129
Figure 6-26 – EDS site locations for powder produced from assorted chips after 120 minutes of ball milling.....	130
Figure 6-27 – EDS site locations for powder produced from assorted chips after 180 minutes of ball milling.....	131
Figure 6-28 – EDS site locations for powder produced from assorted chips after 270 minutes of ball milling.....	132
Figure 6-29 – EDS site locations for powder produced from the overfilled sample after 60 minutes of ball milling .....	133

Figure 6-30 – EDS site locations for powder produced from the overfilled sample after 120 minutes of ball milling .....	134
Figure 6-31 – EDS site locations for powder produced from the overfilled sample after 180 minutes of ball milling .....	135
Figure 6-32 – EDS site locations for powder produced from the overfilled sample after 270 minutes of ball milling .....	136

## List of Tables

Table 3-1 – Scoring system breakdown used in the concept-scoring matrix .....	43
Table 3-2 – Concept-scoring matrix filled in by Respondent 1 .....	45
Table 3-3 – Concept-scoring matrix filled in by Respondent 2 .....	46
Table 3-4 – Concept-scoring matrix filled in by Respondent 3 .....	47
Table 3-5 – Average scores and rankings based on the completed concept-scoring matrices.....	48
Table 4-1 – Powder details .....	52
Table 4-2 – Powder descriptors.....	52
Table 4-3 – Chemical composition of each site in Figure 4-13 .....	67
Table 4-4 – Chemical composition of each site in Figure 4-14 .....	68
Table 4-5 – Chemical composition of each site in Figure 4-15 .....	69
Table 4-6 – Chemical composition of each site in Figure 4-16 .....	70
Table 4-7 – Chemical composition of each site in Figure 4-17 .....	71
Table 4-8 – Chemical composition of each site in Figure 4-18 .....	72
Table 4-9 – Chemical composition of each site in Figure 4-19 .....	73
Table 4-10 – Chemical composition of each site in Figure 4-20.....	74
Table 4-11 – Chemical composition of each site in Figure 4-21.....	75
Table 4-12 – Chemical composition of each site in Figure 4-22.....	76
Table 4-13 – d10, d50, d90 and mean particle sizes for powders used by Croft AM at various stages of reuse .....	77
Table 4-14 – d10, d50, d90 and mean particle sizes for powders from different companies with numerous reuses compared to virgin powder and acceptable powder .....	79
Table 4-15 – d10, d50, d90 and mean particle sizes for overflow powder and derivatives compared to virgin powder and acceptable powder .....	80
Table 4-16 – d10, d50, d90 and mean particle sizes for black powder compared to virgin powder and acceptable powder .....	81

Table 5-1 – A summary of the four support structures used for breakdown analysis .....	93
Table 6-1 – The composition of standard and oversized samples.....	98
Table 6-2 – Mass comparison of input support structure and output powder .....	100
Table 6-3 – d10, d50, d90 and mean particle sizes for powders created from ball milling and the theoretical blended powders they could create.....	105
Table 6-4 – Percentage of particles smaller than 15µm and 45µm for powders created from ball milling and the theoretical blended powders they could create .....	105
Table 6-5 – d10, d50, d90 and mean particle sizes for the theoretical blended powders created from ball milling compared with virgin and used powders .....	106
Table 6-6 – Chemical composition of each site in Figure 6-10 .....	108
Table 6-7 – Chemical composition of each site in Figure 6-11 .....	109
Table 6-8 – Energy consumption calculations based on the data collected.....	114
Table 6-9 – The volume of chips, mass and theoretical volume of powder for each sample.....	117
Table 6-10 – The mass of powder produced after 270 minutes of ball milling .....	118
Table 6-11 – d10, d50, d90 and mean values of the powder produced from assorted and overfilled chip samples after various durations of ball milling.....	125
Table 6-12 – Percentage of particles within various size ranges for powders created from 270 minutes of ball milling .....	126
Table 6-13 – Chemical composition of each site in Figure 6-25.....	129
Table 6-14 – Chemical composition of each site in Figure 6-26.....	130
Table 6-15 – Chemical composition of each site in Figure 6-27.....	131
Table 6-16 – Chemical composition of each site in Figure 6-28.....	132
Table 6-17 – Chemical composition of each site in Figure 6-29.....	133
Table 6-18 – Chemical composition of each site in Figure 6-30.....	134
Table 6-19 – Chemical composition of each site in Figure 6-31.....	135
Table 6-20 – Chemical composition of each site in Figure 6-32.....	136
Table 6-21 – Average Wt% of tungsten present at all sites in each powder sample .....	137
Table 6-22 – Energy consumption calculations based on the data collected (see Chapter 6.2) .....	138

## List of Abbreviations and Acronyms

AM	– Additive Manufacturing
ASTM	– American Society for Testing and Materials
BJ	– Binder Jetting
BSE	– Backscattered-Electron
CGE	– Centre for Global Eco-Innovation
Croft AM	– Croft Additive Manufacturing Ltd
DED	– Directed Energy Deposition
DMLS	– Direct Metal Laser Sintering
EBM	– Electron Beam Melting
EDS	– Energy-Dispersive x-ray Spectroscopy
EoL	– End-of-Life
EOS	– Electro Optical Systems
GE	– General Electric Company
ICP-OES	– Inductively Coupled Plasma – Optical Emission Spectroscopy
ISO	– International Standards Organisation
PBF	– Powder Bed Fusion
PSD	– Particle Size Distribution
SEM	– Scanning Electron Microscopy
SLM	– Selective Laser Melting
SLS	– Selective Laser Sintering
SME	– Small and Medium-sized Enterprises
UK	– United Kingdom
UTS	– Ultimate Tensile Strength
YS	– Yield Strength

## Nomenclature

$\mu\text{m}$	– Micrometre/micron
bn	– Billion
d10	– 10% of particles are below this size in the sample
d50	– 50% of particles are below this size in the sample
d90	– 90% of particles are below this size in the sample
g	– Grams
kg	– Kilograms
MJ	– Megajoules
ml	– Millilitres
Wt%	– Percentage of chemical composition by weight

## Contributions to Knowledge

A comprehensive literature review has been carried out, providing any reader with a strong understanding of the methods through which powder degrades and the subsequent effect this has on components produced by AM. This compilation of the most recent research can be used as a starting point for future researchers.

Without extensive powder testing facilities, AM users may find it difficult to understand the quality of their powders and thus be unable to determine their suitability for use in AM. Where limited resources are available, it has been shown that the PSD of powders can be determined with an acceptable level of accuracy by taking SEM images of powder samples and utilising ImageJ, an image processing software. This can eliminate the necessity for particle size analysers, although should not be considered as a replacement for this superior technology.

The production of powders suitable for use in AM through ball milling has been shown to consume less energy than the alternative recycling methods used to produce AM powders from scrap metals. This also identifies another use for support structures, which had previously been considered as waste for scrap.

The collection of research investigating plasma spheroidisation has identified this process as a means of upcycling EoL powder. The suggestion that AM users consider this technology to prevent waste rather than produce very high-quality powders has not previously been made. Experimentation has been set up to determine the effectiveness of this solution, likely to be the basis of an academic paper (following completion of this thesis) to be published in the public domain, aiming to further encourage the adoption of this technology.

Identification of powder suppliers as the likely driving force and adopters of powder recycling solutions has not been highlighted previously. Without their resources and influence over the AM market, it is unlikely that any solutions adopted by AM users will be able to compete with the scale of powder production by AM suppliers.

## Research Outputs

- Powell, D., Rennie, A. E. W., Molyneux, A., Burns, N. & Geekie, L. (2019) “Repurposing of metal support structures to form powder for use in additive manufacturing” *Proceedings of the 16<sup>th</sup> Rapid Design, Prototyping and Manufacturing Conference (RDPM 2019)*, Uxbridge, UK, 4<sup>th</sup>-5<sup>th</sup> April 2019, ISBN: 978-1-5272-5164-9. See Chapter 5 for the basis of this manuscript. [Research Paper Lead Author; Presenter]
- Powell, D. & Rennie, A. (2019) “Reducing waste in additive manufacturing: the powder problem” *Eco-Innovation Conference*, Lancaster, UK, 19<sup>th</sup>-20<sup>th</sup> September 2019. [Poster Lead Author; Presenter; Appendix A]
- Powell, D., Rennie, A., Geekie, L. & Burns, N. (n.d.) “Understanding powder degradation in metal additive manufacturing and investigating powder upcycling solutions” *Journal of Cleaner Production*, Under Review. See Chapter 2 for the basis of this manuscript. [Lead Author]

## Acknowledgements

I wish to extend my gratitude to Dr Louise Geekie and Neil Burns of Croft Additive Manufacturing Ltd, alongside Dr Allan EW Rennie of Lancaster University. Without their guidance and expertise, the presented work would not have been possible. The moral support of Emily Shuck has also been invaluable throughout the project.

I further acknowledge the support of The University of Manchester’s Dalton Cumbrian Facility, a partner in the National Nuclear User Facility, the EPSRC UK National Ion Beam Centre and the Henry Royce Institute. I am grateful to Gyorgyi Glodan for her assistance during the milling process and SEM imaging/EDS analysis of the results, and to Sara Baldock for assisting with internal SEM imaging and EDS analysis.

## Abstract

Additive manufacturing has the potential to create almost no waste; only material that is required for the component (and any support structures) is used in the build process. Despite this, large quantities of metal powders are sent to landfill every year due to powder degradation, caused by continual reuse of the powder. An understanding of powder formation and degradation has been presented in an extensive literature review, enabling the viability of potential waste-reducing solutions to be assessed. Plasma spheroidisation is identified as a promising method of upcycling end-of-life powders, likely to reduce powder waste by 80%. An experimental procedure was established to allow future investigation into this technology. Sustainable powder manufacturing methods were identified as under-researched. A method of breaking down support structures in powders through shear shredding and ball milling was shown to consume less energy than current virgin powder production methods. The powder produced was of a lower quality than virgin powders used in selective laser melting; further refining of the milling procedure is likely to improve this powder quality. The work done showed improvements in both resource and energy efficiency, although developing these processes beyond proof of concept remains a challenge.

# 1. Introduction

## 1.1 Background of additive manufacturing

Additive Manufacturing (AM) has seen a significant development in the last decade in both the public eye and within an industrial setting. There has been a recent shift away from predominantly utilising AM as a rapid prototyping technology, instead adopting it as a method of manufacture for end-use products and bespoke components (Li *et al.*, 2016). Through layer-by-layer construction of components, with each layer typically tens of microns thick, components once perceived impossible to produce by conventional manufacturing methods can now be fabricated. The potential of this technology has not gone unnoticed by industries; it was expected that the output of additively manufactured products, as opposed to prototypes and artistic builds, would increase from 20% in 2012 to 50% by 2020 (The Economist, 2011).

Innovate UK (a funding body for research and development within the UK) have also highlighted the potential of AM technologies, having set up a dedicated “Additive Manufacturing UK” body. In their “National Strategy 2018-25” (Additive Manufacturing UK, 2017), they speculated that the global market for AM in 2017 was £6bn, with expectations of this market to rise to anywhere between £17bn and £52bn by 2025. Much of this growth is expected to come from high-value manufactured components and AM service provision, with a minimum estimated compound annual growth rate of 30%.

One of the reasons AM has become widely adopted is the efficiency of the process. From an economic stance, achieving the maximum product output from raw materials yields maximised potential profits. This is where AM excels, using only the material required for the manufacture of the product, alongside any necessary support structures and occasionally heat sinks. Through AM, material usage can be reduced by up to 40% versus conventional subtractive machining methods (Reeves, 2008; cited in The Economist, 2011).

The polymer materials initially used to create prototypes within the AM industry were ideal for rapid accurate production and easy utility. However, as AM has been increasingly considered for the manufacture of high-quality end-use products, such as within the aerospace industry, polymers rarely meet the design needs. This encouraged the development of several metal AM processes, designed to produce components that are ready-for-market. The revenue from metals has seen a continual growth of over 40% since 2014, indicating the increasing adoption of AM for production applications (Wohlers *et al.*, 2019).

## 1.2 Croft Additive Manufacturing Ltd

Croft Additive Manufacturing Ltd (Croft AM) are renowned for being one of the early Small and Medium-sized Enterprise (SME) adopters and pioneers of metallic AM. Founded in 2012, Croft AM manufacture bespoke 316L stainless steel products, notably fluid filters and complex housings, for clients across a diverse range of industrial sectors. Using a Realizer, designing and producing components through Selective Laser Melting is routine work, although the company plan to adopt further AM technologies in the future. Their expertise in the field has led to them becoming a recognised name in the industry.

Being a small company, Croft AM does not have the resources to undertake large research and development programmes themselves. In order to advance the global knowledge in the metallic AM industry, Croft AM partner with universities to assist student researchers with relevant projects, offering their expertise whilst applying the research to their work.

## 1.3 Metal powder-based additive manufacturing

Of the seven recognised AM processes defined by the American Society for Testing and Materials (ASTM) (ASTM Standard 52900, 2015), there are three main categories that utilise metal powders: Powder-Bed Fusion, Directed Energy Deposition and Binder Jetting.

Powder Bed Fusion (PBF) targets either a laser or electron beam on a flattened “bed” of metal powder, fusing particles together by melting them. Once a layer has been formed, the powder bed drops down by a predetermined layer thickness. More powder is added to the build chamber and distributed as an even layer using a spreading mechanism. The laser or electron beam then melts this new layer, fusing with the previously melted layer beneath. This is repeated until the build is complete. Through this process, detailed parts can be manufactured to a high standard. Metallic PBF processes include Selective Laser Melting (SLM), Electron Beam Melting (EBM) and Direct Metal Laser Sintering (DMLS). PBF machines make up 54% of the technologies available on the metal AM market (Cherdo, 2019). An example can be seen in Figure 1-1.

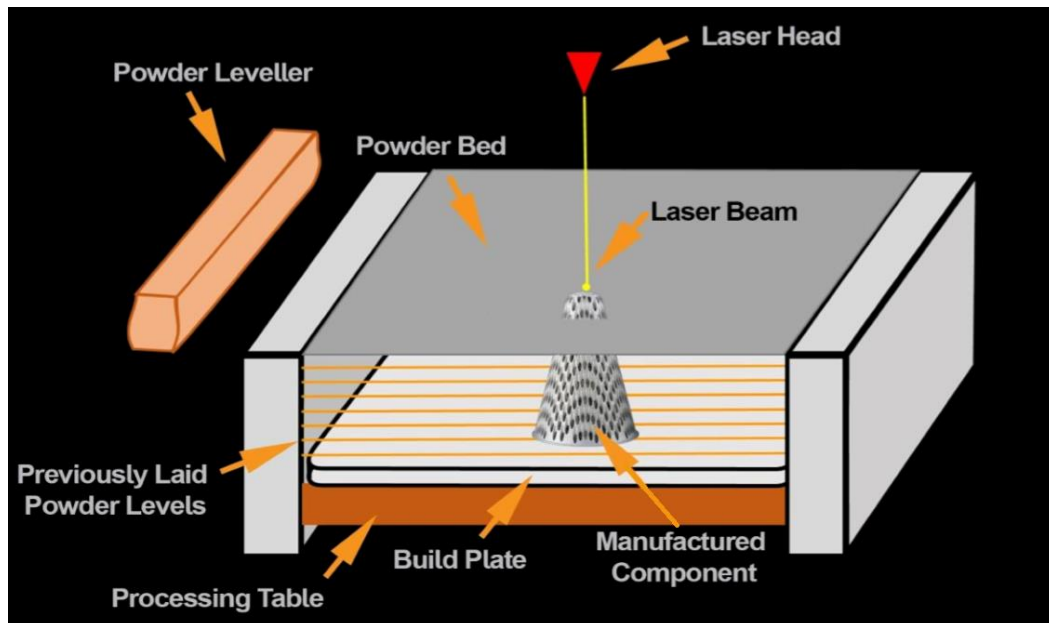


Figure 1-1 – The Selective Laser Melting process (figure provided by Croft AM)

Directed Energy Deposition (DED) directs a constant stream of powder metal feedstock from a nozzle (although wire can be used) onto the surface of an already constructed object. This feedstock is melted by a laser or electron beam, depositing metal onto the surface where the laser is focused. The object remains stationary, whilst the nozzle can move freely, allowing material to be added anywhere on the object. Typically, DED is used for the repair or maintenance of large components, owing to a poorer finish quality, although it can be used to build new components. As there is less demand for this application, DED machines account for 16% of all machines available in the metal AM market (Cherdo, 2019).

Binder Jetting (BJ) utilises a liquid binder to adhere layers of metal powder together. Alternating layers of powder and binder are deposited, releasing binder only where adhesion is necessary. As in PBF, once one layer of powder and binder has been deposited, the build platform is lowered by a set layer thickness and the process repeats until the component is fully built. BJ components lack the part accuracy and mechanical properties of their PBF counterparts so are less common in the metal AM industry, accounting for 16% of machines on the AM market (Cherdo, 2019).

#### 1.4 Waste metal powder

Whilst the above processes are additive and considered to be “clean”, producing little-to-no waste (Bourhis *et al.*, 2014; Campbell *et al.*, 2011), there are problems associated with powder-based AM systems that reduce the material efficiency of the process. In PBF and BJ, it is not possible to produce a 1cm<sup>3</sup> component from 1cm<sup>3</sup> of metal powder, as the powder bed requires a minimum volume of powder dependent on the build chamber size, regardless of the desired component’s size. This often

results in a very small material usage percentage. In DED, as little as 50.2% of the powder feedstock is utilised and added to the component (Takemura *et al.*, 2019), with the remaining powder being dispersed into the build chamber. This raises an important question: what can be done with the remaining unused powder?

With increased societal and governmental pressure on companies to be environmentally friendly, disposal of this unused powder would be unacceptable. A widely adopted practice is to recycle any unused powder and use it in future builds. Reeves (2008; cited in The Economist, 2011) believed that the recycle rates of powder are between 90-95%, whilst Petrovic *et al.* (2010) suggest that between 95-98% of powder not used in the build can be reused.

Steps need to be taken to ensure any reused powder remains of an acceptable quality for use in AM. This typically means ensuring the powder properties are as similar as possible to the virgin powder produced by the supplier. To ensure this happens, well-established powder handling procedures are employed. The powder is kept in an inert environment during building and whilst in storage to prevent oxidation and wetting, with minimal exposure to the air. Any powder that was not incorporated into the component is collected from the build chamber and sieved using one of a number of techniques, removing any oversized particles or other debris resulting from the fabrication process. Strict cleaning regulations of equipment are maintained to prevent potential contamination of the powder. This process is not currently regulated by any standards and is based on user experience, causing a great deal of variation throughout the industry (Leicht, 2018).

There are a number of benefits to reusing metal powders. A range of metals are used to build with in AM, including Ti6Al4V, Inconel 718, AlSi10Mg, 316L stainless steel and 304L stainless steel, varying in cost from £30 to £300 or more per kilogram of virgin powder (Ian Brooks 2019, personal communication). As material cost can make up 31% of the cost of the entire build (Piller *et al.*, 2018), recycling this metal powder has significant economic benefits to AM users. This was shown in a case study by LPW Technology Ltd, seeing a 92% reduction in material costs if a powder was reused 15 times (Rushton, 2019).

Reducing the quantity of unused “virgin” powder manufactured is also beneficial for the environment. The production of the metal powder uses a process called atomisation. Faludi *et al.* (2016) found that the energy consumption during gas atomisation of an aluminium alloy used to produce one part could be up to 24.5% of the energy consumption used in the PBF manufacturing process from start to finish, gram for gram. With repeated reuse of the powder, the impact of the production of metal powders reduces.

The rapidly developing AM industry has carried out research into the consequence of continually reusing metal powder in AM, finding changes in powder properties with reuse. This in turn affects the properties and quality of the manufactured components, raising concerns with the reuse of metal powders. Despite the growing quantity of research, the production, usage and recycling of metal powders are still identified as issues in AM and 'require more attention' (Javidrad et al., 2018). Croft AM are amongst the companies that have investigated powder degradation, aiming to progress the AM industry through further research into this field.

### 1.5 Objectives of research

As a part of their 2018-25 strategy, *Additive Manufacturing UK* actively encourage research and development, believing it to be necessary to enable further adoption of the technology (Additive Manufacturing UK, 2017). They note that research and development into AM materials and processes will assist with "increasing productivity, process stability and other areas". It is highlighted that there are many issues, such as intellectual property, standards and material consistency that currently prevent adoption and further development of AM, indicating that research aiming to overcome such issues will benefit the UK's AM industry.

High value parts produced in industries such as the aerospace and medical sectors will reuse a powder as few as one to five times, as they are concerned that the quality of the produced components is not maintained as the powder is recycled (Croft Additive Manufacturing Ltd, 2018, personal communication). Rather than disposing of this, an effective method of regrading this powder would allow less demanding industries to reuse this powder with confidence in the quality of the end-product. The regrading process could then be repeated, until finally the powder is considered unsuitable for further use in the AM industry.

A concern with accepting used powder stock from another company is that there is no guarantee that the powder is free of contaminant particles. This acts as a barrier to the concept of regrading and redistributing powder within the AM industry. If a method could be devised to quickly and cheaply determine the powder quality, companies could guarantee the quality of any powder they redistribute or purchase. Without this grading capability, companies will be reluctant to purchase recycled powder, having little faith in the powder quality.

A similar issue arises if a company accidentally contaminates a batch of powder. Currently, they would likely need to dispose of the powder, costing money and creating waste. The aforementioned method to quantify the level of contamination would therefore allow them to determine if the powder is still usable. Should the level of contamination become unacceptable, a method of separating out different

materials within the powder mix may prevent the powder from being rendered useless, creating new, pure powders. This would both reduce waste and save money.

Currently there is no cost-effective use for End-of-Life (EoL) powder. It can even be difficult for companies to dispose of metal powders due to their health, safety and environmental risks (HSE, 2017). Other industries or applications could be identified that can utilise this EoL powder, either through other AM processes or completely different manufacturing techniques. This would allow the AM industry to see more economical returns on their virgin powder investment whilst also achieving close to 100% material usage. Representatives from Renishaw plc and BAE Systems plc, both large AM adopters, have confirmed that they have large EoL powder batches in storage, unsure currently what to do with them (Stephen Crownshaw 2018, personal communication; Jenny Manning 2018, personal communication), demonstrating the necessity for an EoL powder solution. Unused metal powder no longer considered suitable for use in AM is sent to landfill, as there is currently no alternative destination.

Due to environmental considerations, efficient technologies are sought after globally. AM offers the chance to be the most efficient manufacturing technique for complex components. Fullenwider *et al.* (2019) state that 'environmentally sustainable feedstock alternatives need to be explored to attain the sustainability of additive manufacturing', highlighting a need for alternative metal powder production or recycling methods. Identification of a method that produces viable powder for use in AM without using more energy than the atomisation process would further increase the energy-saving potential of AM technologies.

In summary, Croft AM are seeking to employ methods to achieve maximum economical returns from utilising metal powder, whether it is virgin or used. The main priority is to establish what can be done with EoL powder, due to the accumulating powder stores globally that have no current use. Being able to reliably utilise used powder in AM is another highly desirable objective. Methods to minimise outgoing waste or reduce the need to purchase virgin powder should be highlighted. Identified solutions should be shown to have a beneficial impact on the environment with the potential to have an impact on the wider AM community.

## 1.6 Proposed solutions

With the increasing popularity of the metallic AM industry, there is a rising demand for the raw materials and feedstock. The issue of powder waste may not seem severe currently, but widespread adoption of AM in the future can only increase the impact of powder waste. Action needs to be taken now to ensure the growth of the AM industry is sustainable.

With their extensive industrial experience, Croft AM considered some potential solutions to the problems faced with metal powders. Each proposed solution requires further understanding of the AM process and impact of recycling metal powders and can therefore only be investigated once a literature review has been conducted. The viability of these solutions is discussed in Chapter 3.1.

- 1) Larger-diameter particles can be sieved into size fractions. New smaller-diameter powder fractions can be purchased and the powders remixed into relevant proportions. This could then be resold or reused as suitable for AM.
- 2) Re-sized fractions with larger particles may be suitable for use in other AM technologies. Alternatively, the powders could be used in other powder-based industries.
- 3) The powder may be remelted into another format for use in other additive procedures, such as wire, usable in wire deposition metal AM. Alternatively, the powder could be formed into solid metal materials for use in other industries.
- 4) Some metallic powders become mixed. These powders could be separated into representative material fractions for recombination as single material, allowing reuse in another industry.

Alternative potential solutions were identified as the project developed. These concepts are further explored in Chapter 3.2.

- 5) Large conglomerates, sieved out rejects and support structures could be reground through ball milling to produce a metal powder suitable for use in AM.
- 6) End of life metal powder could be sold on and embedded within a polymer matrix to enhance the material properties, in either AM or other industries.
- 7) Powders could be simply graded through measuring their flowability to predict the component properties, based upon the correlation between these properties.
- 8) The laser settings and coating arm speed could be adjusted when utilising recycled powders to reduce the negative effects associated with powder reuse.
- 9) Powder could be returned to the supplier for regrading after it has been used, then redistributed by the supplier.
- 10) Plasma spheroidisation can be utilised to upcycle poor quality powders into powders suitable for use in AM.

## 2. Literature Review<sup>1</sup>

There are a number of factors to consider when determining solutions that could be effective. An overview of the research to date provides information that can help to identify the key issues. Further investigation assists in validating the proposed solutions whilst highlighting new avenues for research.

The background research has been separated into sections, building from a micro to macro level, as properties at the individual particle level can influence the overall powder behaviour, in turn influencing the final built component. This is represented in Figure 2-1; many individual particles make up a powder, with even more particles fusing to form a component. As a preliminary discussion, consideration is given in Chapter 2.1 to the methodology for choosing the literature to be reviewed. Chapter 2.2 gives a brief overview of the methods of powder production used within the AM industry. Chapter 2.3 investigates the individual powder particle properties that are determined from the powder production phase, considering how these interact with one another to influence powder properties. The impact of the changes due to recycling powder on built components is reviewed in Chapter 2.4. Chapter 2.5 looks at literature that has used a mixture of virgin and recycled powder. Consideration is then given to end-of-life (EoL) powder and the current common practices for the disposal or reuse of this powder in Chapter 2.6.

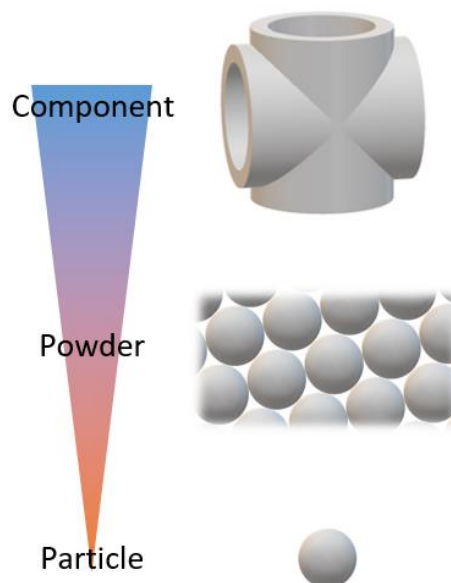


*Figure 2-1 – Representation of the increasing number of particles present, from an individual particle through to the manufactured component*

---

<sup>1</sup> The following chapter includes the majority of a paper currently under second review for publication in the Journal of Cleaner Production. This paper has therefore not been included as an appendix to reduce paper consumption, in line with the environmental focus of this thesis.

## 2.1 Methodology for selecting literature

It is difficult to narrow down a literature review to exclusively 316L stainless steel, as used by Croft AM, as there would not be a wide enough range of data available. Furthermore, it would limit the application of this review to one material, throttling the impact of this work on the wider AM community. The literature reviewed therefore includes a wide variety of metallic powders. Comments are made when necessary if any findings are notably different as a result of the material.

Exclusively searching for sources on SLM, also used by Croft AM, would further bottleneck the impact of this research. The problems identified with powder recycling by Croft AM are suffered by all powder-based AM users. By considering the research of the three previously identified metal AM processes (see Chapter 1.3), a broader understanding of the problem is given. Further to this, these sources may offer potential solutions that may not have been identified in a restricted literature review. However, an emphasis is placed upon PBF, as this is the most common metallic AM process (Cherdo, 2019).

Work of a similar nature had been undertaken by Vock *et al.* (2019), reviewing powder properties and touching upon the impact of recycling on these properties. As such, their work offered a starting point for the collection of literature. However, their review does not provide a detailed analysis of each study, nor does it offer understanding as to why observed changes had taken place. Their review instead aimed to identify processes to qualify powder, whilst the work within aims to promote understanding of the methods through which powder degrades, ultimately intending to identify methods to upcycle degraded powders.

## 2.2 Methods of powder production

Before the AM process can begin, powder feedstock needs to be created. This is done through a process called “atomisation”, identified as the best way to form metal powders for use in AM (Dawes *et al.*, 2015). As is the case in all manufacturing procedures, the quality of the material feedstock will affect the quality of a produced component. Investigation into the atomisation process enables understanding of the quality of virgin powder available for use in AM. Although several types of atomisation exist, there are three preferred methods within the AM industry that are to be focused on: water atomisation, gas atomisation and plasma atomisation.

All three procedures operate on similar principles. The metal feedstock is melted prior to being fed into an atomisation chamber, where it is blasted by jets of either water, gas or plasma, resulting in the rapid dispersion and solidification of the metal into small particles. This is illustrated in Figure 2-2, with each process discussed below. Chapter 2.3 provides further context to why some methods are considered preferable.

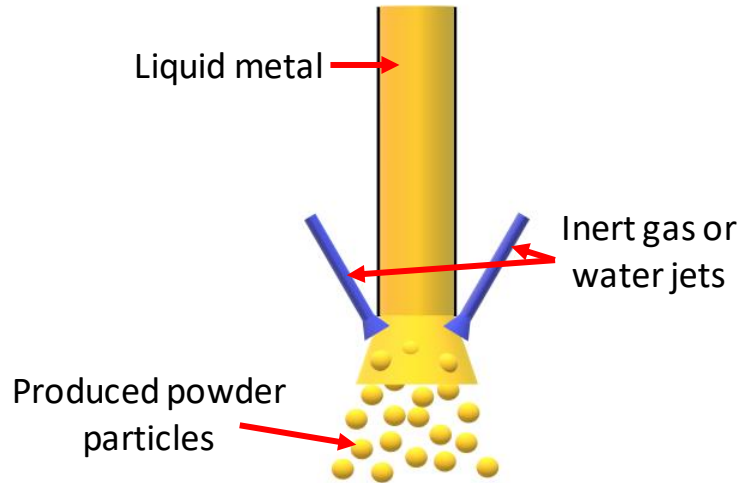


Figure 2-2 – A simplified diagram of the atomisation process

Powder produced through water atomisation is typically highly irregular in morphology, making it less preferable for use in the AM industry (Irrinki *et al.*, 2016; Dawes *et al.*, 2015). A further disadvantage of water atomisation was identified by Li *et al.* (2010) and Herzog *et al.* (2016), finding an increased oxygen content in water atomised powders versus gas atomised powders. Water atomised powder also requires post-processing to dry the powder. Despite this, due to the relative simplicity of the procedure, water atomised powder is the cheapest AM suitable powder, making it appealing to some AM users (Dawes *et al.*, 2015).

Gas atomised powder utilises inert gases to reduce the risk of oxidation and contamination of the powder. Due to the lower heat capacity of gases, the particles have longer to cool, allowing spherical particles to form (Dawes *et al.*, 2015). This has been widely accepted to be preferable to water atomisation (Kelkar, 2018; Herzog *et al.*, 2016; Li *et al.*, 2010).

Plasma atomisation uses either wire or powder feedstock that is melted and immediately atomised to minimise any chance of contamination. The particles created by plasma atomisation are highly spherical (Dawes *et al.*, 2015). As powder can be used as a feedstock, this process has been adapted to improve lower quality powders, such as those produced by the cheap water atomisation process. This has been successfully demonstrated by Kelkar (2018). However, the plasma atomisation process is more expensive than water or gas atomisation and is therefore typically only used to produce very high-quality powders (Dawes *et al.*, 2015).

Morrow *et al.* (2007) showed that the direct atomisation of tool steel consumed 17.62MJ per kilogram of powder produced from raw materials. If a steel plate were to be created and then remelted for use in the atomisation process, 32.81MJ of energy would be consumed per kilogram of powder produced, using 86.2% more energy than direct atomisation. This provides a benchmark for energy usage against

which future solutions can be compared. If a method of reclaiming powder consumes less energy than the atomisation process, the environmental benefit is twofold; less powder is sent to landfill, whilst less energy is used to produce new virgin powder for use in AM.

If alternative powder feedstocks can be identified for use in the atomisation process, the energy consumption in the AM cycle may be further reduced. Morrow *et al.* (2007) showed that 6.25MJ is required to remelt one kilogram of steel, whilst only 1MJ is required to atomise this melted steel into one kilogram of powder. Therefore, producing powder from already-produced steel only requires 41.1% of the energy used in creating powder from direct atomisation, indicating that scrap metals could provide a far more sustainable feedstock material than raw materials in the atomisation process.

### 2.3 Particle and powder properties

Through the gas atomisation process, powder particles tens of microns in diameter are produced. There are up to 1 billion particles in one kilogram of powder (Harrison, 2019). Each of these particles will vary in size, shape and often slightly in chemical composition. It is accepted that the properties of these particles have a large influence on the quality of the powder and the properties of the manufactured component (Vock *et al.*, 2019; Sames *et al.*, 2016). These are further discussed in Chapter 2.4.

Only literature that reuses powder repeatedly (without mixing in any virgin powder) is reviewed here, allowing the impact of powder recycling on each of these properties to be analysed in a “worst case scenario”. The practice of mixing virgin and recycled powder is discussed in Chapter 2.5.

#### 2.3.1 Particle size distribution

The Particle Size Distribution (PSD) is a measure of the frequency of various sized particles within a powder, commonly represented by a cumulative frequency diagram or a histogram. Wider PSD ranges allow for more closely packed particles (explained in Chapter 2.3.2). As such, PSD graphs can be indicative of powder properties and behaviour, as the particle interactions can influence bulk powder properties.

In order to measure the PSD, particles are assumed to be perfectly spherical. This allows the diameter of each particle to represent their overall 3-dimensional size. The graphs produced are often complimented by the mean, d10, d50 and d90 values. The d10 value marks the point where 10% of particles in the powder are below this size. The d50 and d90 values are similar, with 50% and 90% of particles being smaller than this value respectively. This allows for a quick understanding of the makeup of the powder, enabling users to determine the suitability of a powder for an application.

Powder reuse within PBF has been shown to have various effects on the PSD of powder. Slotwinski *et al.* (2014) compared eight 316L stainless steel powders after repeated reuse in SLM using an 80 $\mu$ m sieve, seeing a gradual increase in the d10, d50 and d90 values with powder recycling. Sartin *et al.* (2017) found a statistical difference after reusing 316L stainless steel powder seven times in SLM with an 80 $\mu$ m sieve, with an increase in the presence of particles over 45 $\mu$ m. A shift towards larger particles in SLM was also observed by Ardila *et al.* (2014) using Inconel 718 and a 63 $\mu$ m sieve, although there seemed to be very little change in the first seven builds from virgin powder. The notable change was instead observed between the seventh and fourteenth reuse of the powder. A comparison on EBM and SLM PSDs in the same study showed that recycling powder in the SLM process caused the PSD to increase, whilst in EBM the reverse occurred. This is most likely due to the recycled EBM powder having been treated by blasting to break the bonds between particles, a common practice with EBM powders, whilst the SLM powder was only sieved. Ti-6Al-4V was observed by Seyda *et al.* (2012) to shift in PSD, with fewer small particles present after six powder use cycles passing through a n 80 $\mu$ m sieve. This trend continued after 12 cycles, showing a slow but steady increase in the percentage of large particles present in the powder. A white paper produced in 2016 by Renishaw plc, one of the leading manufacturers of AM systems, showed a very slight increase in the d10, d50 and d90 values of a Ti6Al4V powder recycled 38 times with sieving. The absence of smaller particles was also observed in images obtained from a Scanning Electron Microscope (SEM). The increase in particle size was, however, smaller than other literature found.

Similar results have also been observed in DED processes. Renderos *et al.* (2016) observed an immediate change in PSD after just one use of Inconel 718 virgin powder passed through a 150 $\mu$ m sieve, with considerably less small particles present. The trend of an increase in average particle size then continued with powder reuse.

Not every research group offered an explanation for the change in PSD. Slotwinski *et al.* (2014) believed the cause for the change was the formation of agglomerate particles (discussed in Chapter 2.3.3). Seyda *et al.* (2012) agreed that a high proportion of fine particles gives rise to agglomeration effects, but also hypothesised that small particles can be more easily thrown into the air during sieving and powder handling. Small particles vaporising from the laser during the build process could be another cause for the reduction in the number of small particles (Carroll *et al.*, 2006; Gasper *et al.*, 2018). Strondl *et al.* (2015) suggested two potential explanations for a reduction in small particles. It is possible that the smallest particles could be blown away and become trapped in filters by the inert gas stream during processing. Alternatively, the largest particles may be swept out the build chamber by the recoating arm, causing a higher volume of small particles to be used, whilst the larger particles are repeatedly unused. The latter hypothesis has been suggested by others (Slotwinski *et al.*, 2014;

Jacob *et al.*, 2017). Spatter particles ejected from the melt pool (further discussed in Chapter 2.3.4) were shown by Andani *et al.* (2018) to be larger than virgin powder, but often small enough to pass through a sieve, potentially shifting the PSD towards larger particles.

Not all literature reported an increase in PSD. Carroll *et al.* (2006) saw a great deal of variance in the mean particle size over ten powder reuses, making it difficult to determine if any significant change occurred with continual powder reuse. Only the mean particle size is measured, giving little information about the powder overall. Petrovic *et al.* (2015) used a similar blasting process with EBM-based powder as used by Ardila *et al.* (2014), finding that there was minimal change to the PSD with repeated powder reuse.

### 2.3.2 Packing density

The size of the particles in powder has a major impact on its usability, and has been identified as the most important property contributing to the powder layer quality (Karapatis, 2002). Within AM, it is highly undesirable to have each particle the same size. Figure 2-3 demonstrates how particles pack when they are of a uniform size, leaving numerous unfilled regions. The coverage of the particles over the background can be related to the packing density, as this demonstrates how well particles within a powder can occupy a space. Image analysis using ImageJ (Rasband, 1997-2018) shows that 79.2% coverage has been achieved. Figure 2-4 illustrates the packing of a range of particle sizes, capable of filling in many of the regions between larger particles. This achieves 84.6% coverage, showing the benefit of using a variety of particle sizes. These images represent the problem in 2-dimensional space. As powder occupies a 3-dimensional space, the magnitude of this 5.4% difference in coverage is significantly increased when multiple layers of powder particles are considered. Any uncovered region could lead to the formation of pores and reduced component density (see Chapter 2.4.2).

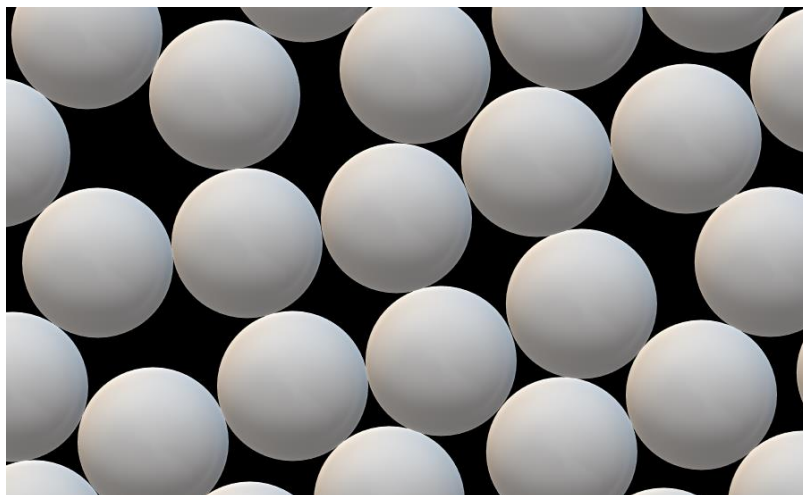


Figure 2-3 – Random packing of uniformly sized particles

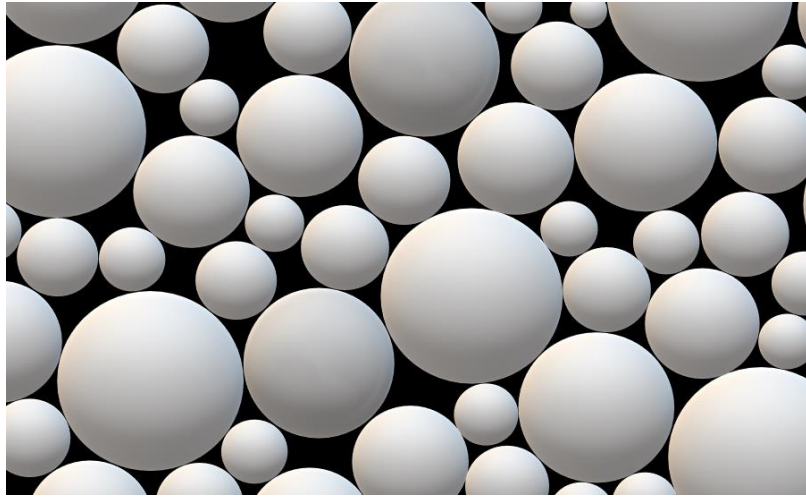


Figure 2-4 – Random packing of various sized particles

The formation of agglomerate particles is discussed in Chapter 2.3.3. These particles have an impact on the ability of particles to pack closely to one another and occupy space effectively. The principle of this is demonstrated in Figure 2-5 and Figure 2-6. The particles are completely spherical in Figure 2-5, achieving a coverage of 86.8%. However, when the agglomerate particles are added in Figure 2-6, the coverage reduces to 83.9%. Once again, this value of 2.9% decrease becomes far more significant when a 3-dimensional space is considered.

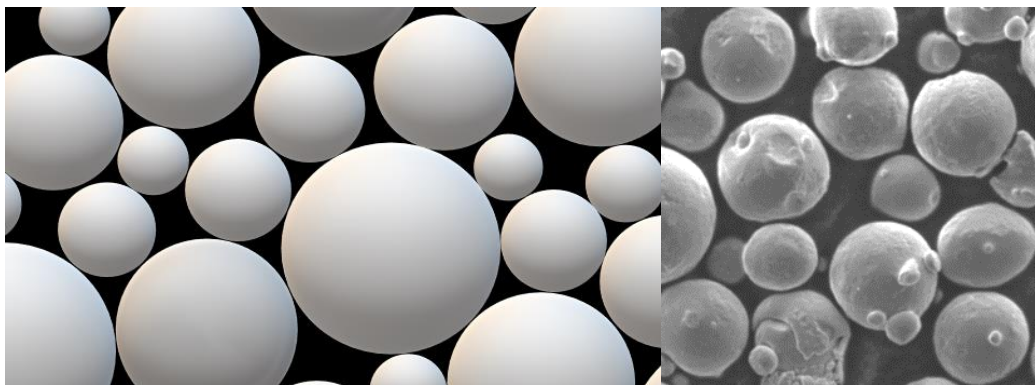


Figure 2-5 – Distribution of spherical particles (Left: model. Right: SEM image)

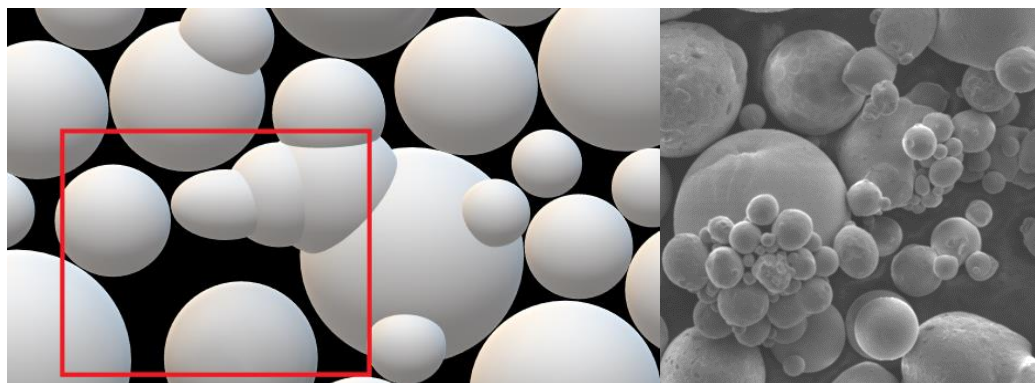


Figure 2-6 – Distribution of agglomerate particles (Left: model. Right: SEM image)

The rectangular outline on the model shows the region where, assuming the powder has been fed by gravity from the top of the diagram, the packing density is negatively influenced due to the agglomerates

Apparent density can be considered an indicator of particle packing in AM. To determine this, powder is allowed to flow freely to fill a vessel of a known size. Tap density is an alternative indicator of packing density, utilising mechanical action to move particles within a container to obtain an optimum packing state. As such, the tap density is typically denser than the apparent density. However, the tap density has been criticised as being an ill representation of the formation of the powder bed in AM by the spreading arm (Spierings *et al.*, 2011). Despite this, tap density can still give an indication of changes in the powder with continual reuse. Karapatis (2002) found that the packing density of powder beds was higher than the apparent density, owing to slight compaction during the powder bed formation process, suggesting that a combination of the apparent density and tap density are needed to predict the powder bed packing.

A study recording both apparent density and tap density with powder reuse with EBM found that whilst there was no change in the apparent density, the tap density gradually decreased in Ti-6Al-4V powder (Tang *et al.*, 2015). GranuTools (2018) found that recycled 316L stainless steel powder had both a reduced apparent density and tap density, although the number of uses is not stated. Del Re *et al.* (2018) found that the apparent and tap densities increased gradually with AlSi10Mg powder reuse in SLM, although the virgin powder used was not as typically spherical or high-quality as is used widely in the industry. The range of contradictory information makes it difficult to ascertain what happens to powder as it is recycled, possibly due to the various parameters the powder can be subjected to during its life.

### 2.3.3 Particle morphology

The shape of individual particles plays a role in the interactions with other particles within a powder. Each particle of powder interacts with the particles surrounding it, exerting forces on one another. The cumulative result of these forces causes powder to behave differently to just one individual particle. Understanding the particle morphology is therefore essential to understanding the bulk powder properties.

Whilst it is simple to visualise a particle as perfectly spherical, this is rarely the case. Particles will always have imperfections on their surfaces, referred to as surface roughness. The extent of this roughness influences how closely packed particles can be to one another; a rougher particle will pack less densely than a smoother one. This principle is demonstrated in Figure 2-7 and Figure 2-8. The shaded line around the particle represents the boundary around a particle where a force could be exerted on another object. As such, the region where the shaded lines overlap dictates where interparticle forces occur. As can be seen in Figure 2-7, smooth particles can form long regions of

interparticle bonding, owing to the gentle curvature of each particle. Figure 2-8 shows how the rough particle edges inhibits interparticle bonding, limiting them to a smaller region. This results in weaker forces holding the particles together.

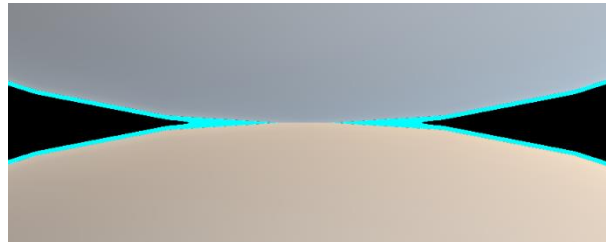


Figure 2-7 – Interparticle forces between two smooth particles

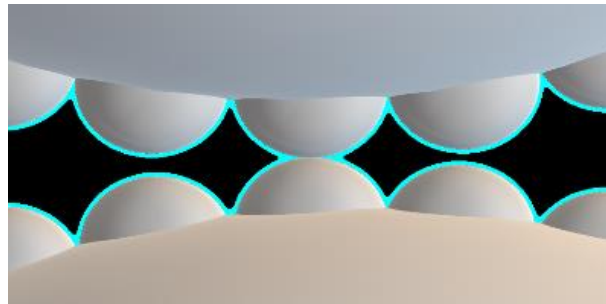


Figure 2-8 – Interparticle forces between two rough particles

In order to understand how particles may change in morphology, knowledge of the conditions the powder is subjected to is required. The build platform is housed within a controlled environment, flooded with inert gas and kept at a constant elevated temperature. During the build process, all particles become exposed to heat from the raised chamber temperature. Many particles may be further subjected to residual heat from the laser or melt pool when in proximity to the laser's targeted location. Smaller particles have an increased surface area and so absorb energy more efficiently from the laser (Gibson *et al.*, 2016; Simchi, 2006). This makes them more likely to melt or vaporise, whilst larger particles are less likely to fully melt.

Surface roughness occurs on a very small scale on a particle surface. A similar principle can be applied at a larger scale across an entire particle. There are two main types of morphological deformation that can occur in powder particles: satelliting and agglomeration. Partial melting, or "sintering" typically occurs at around two-thirds of the melting temperature of a metal (Slotwinski *et al.*, 2014) and is the mechanism by which these deformations occur. Satelliting occurs when a small powder particle adjoins to a larger particle through heating. An example can be seen in Figure 2-9. The large particle often does not show signs of melting or significant deformation from the spherical shape. Agglomerate particles form when two or more particles partially melt and fuse together, creating a deformed shape that can typically no longer be considered highly spherical. This is demonstrated in Figure 2-10. Agglomerates are likely to have more of an impact on interparticle forces than satellite particles due

to the significantly different shape of agglomerate particles, interfering with the ability of particles to fit next to one another and pack tightly.

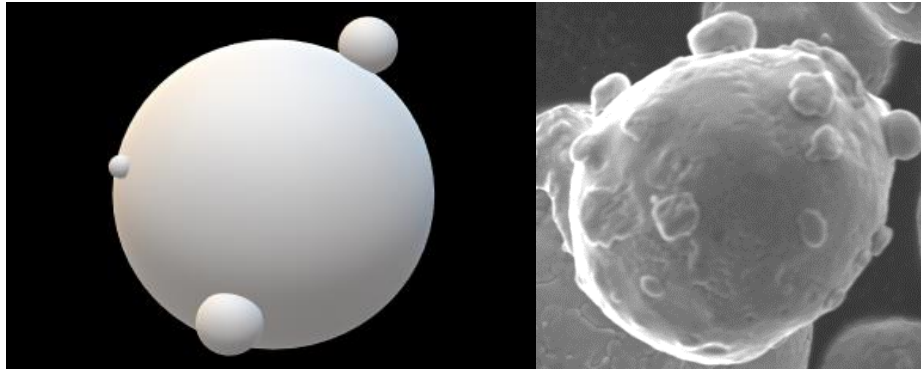


Figure 2-9 – A particle with satellites on it (Left: model. Right: SEM image)

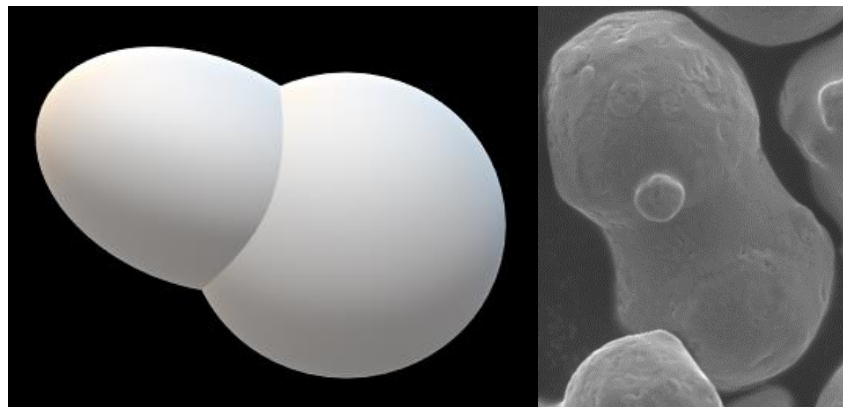


Figure 2-10 – An agglomerate particle made of two individual particles (Left: model. Right: SEM image)

Partial melting of individual particles can also occur, causing deformation that can look similar to particle agglomeration and have similar effects on powder properties. The difference is that agglomeration requires two or more particles to fuse together, whilst partial melting does not.

These individual particle deformations are known to influence the behaviour of the powder overall. As discussed in Chapter 2.3.1, the PSD can be influenced by the presence of these deformed particles, causing a shift towards larger particles (Slotwinski *et al.*, 2014; Seyda *et al.*, 2012). This indicates that any properties affected by a change in PSD are partially influenced by powder morphology. The particles are prevented from packing closely, demonstrated and discussed in Chapter 2.3.2, which would influence the density of the powder bed.

Sphericity is a measure of how round a particle is. Figure 2-5 and Figure 2-6 show that spherical particles are more desirable than deformed particles, allowing for a better packing density. It is therefore common to use the sphericity of particles as a measurement of the suitability of a powder for use within AM.

The morphology of particles has been observed to change with repeated reuse of metal powders in AM. Renishaw plc (2016) obtained SEM images of their Ti-6Al-4V powder used in SLM, observing an increase in the number of agglomerates present in recycled powder, but a reduction in the frequency of satellite particles. The majority of particles were still spherical. Another study using Ti-6Al-4V showed that repeated reuse led to the increased surface roughness of the particles, although the particles remained largely spherical with very few agglomerates or satellites forming (Tang *et al.*, 2015). Popov *et al.* (2018) found that there were a variety of defects present in recycled Ti-6Al-4V powders. Slotwinski *et al.* (2014) found that the sphericity of 17-4 stainless steel particles used in a PBF process began to decrease after multiple builds, although the reason for this was not stated.

Popov *et al.* (2018) suggest that deformation in particles occurs due to mechanical damage from the sieving process, but more importantly from exposure to heat during the AM process, causing particles to sinter. Gasper *et al.* (2018) observed a change in the morphology of the spatter particles (discussed in Chapter 2.3.4) that are inevitably produced in the AM process, suggesting that spatter particles falling back into the powder bed are likely the cause for the increase in deformed particles in recycled powders. Both of these hypotheses are supported by Renishaw plc (2016).

#### 2.3.4 Chemical composition

When AM is used in industrial applications, the chemical composition of the produced component can be of great importance. Whilst some chemical variation is expected between raw materials and produced components in any manufacturing process, the chemical composition of the input material can provide an indication of whether the produced component will be suitable for the intended application.

A change in chemical composition within the powder requires chemical reactions to take place. The presence of reactive agents in the air (such as oxygen, nitrogen and carbon) allow reactions to occur, either creating a stable oxide layer around particles, dissolving deeper into the particles or forming particulates on the surface of particles (Leicht, 2018). This is minimised during metallic AM processes by pumping inert gas into the build chamber. However, this does not eliminate all contaminants; there are still traces of these reagents present during the build process. Whilst this reduces the likelihood of chemical reactions occurring, two main factors contribute to the increased reactivity of metal powders in AM: surface area and temperature.

In traditional manufacturing methods, a slab of material occupying the same volume as that of the powder would have a significantly lower surface area exposed, and may also be kept in an inert environment where necessary. In AM, metal powders expose a large surface area, increasing reactivity

as there is a greater region over which reactions with contaminants can occur. Whilst this is mostly prevented by the inert gaseous environment, reactions are significantly more likely to occur during powder handling when an inert environment is not maintained.

During the build process, the build chamber is held at an elevated temperature. This reduces the dependency on the laser to melt the material and decreasing the thermal gradient between the melt pool and the surrounding powder, whilst causing minimal changes to the powder (Gibson *et al.*, 2016). EBM requires pre-sintering and thus typically preheats the powder to high temperatures (Swift and Booker, 2013), whilst SLM does not require as much preheating (Sames *et al.*, 2016). A rise in temperature increases the reactivity of particles, allowing chemical reactions to occur more easily.

The vast majority of reactions take place during the build process, owing to these raised temperatures. Oxides have been observed to form within the region where the laser/electron beam is focused, known as the melt pool (Gasper *et al.*, 2018). Renishaw plc (2016) confirm this finding, further suggesting that particles close to the weld pool that are heated but not melted also pick up impurities. When the melt pool forms, particles can be seen to “spark” off, dispersing themselves in the build chamber. This is referred to as spatter. Gasper *et al.* (2018), Andani *et al.* (2018), Sartin *et al.* (2017) and Liu *et al.* (2015) all demonstrated the potential for spatter to form partially or entirely oxidised particles. LPW Technology Ltd (2018a) stated that whilst many oversized spatter particles are removed during sieving, a “significant amount” of these contaminated spatter particles are small enough to pass through the sieve, becoming incorporated into future builds and changing the bulk powder chemical composition.

Further chemical changes can occur whilst the powder is being handled, such as during removal and sieving (Seyda *et al.*, 2012). Although this will typically be in cool and dry conditions to minimise reactivity, the absence of an inert gas increases the number of reactive particles coming into contact with the powder. Over an extended time, this could have an impact on the chemical composition of the particles. A similar problem can occur during storage of powder, although following standard practice by storing powder in an inert gas can minimise the potential for corrosion and contamination. Little information is available on the impact of powder storage on the AM process. Besides chemical changes, dust particles, fibres and other contaminants can also mix in with powder during the handling stages (Dawes, 2019).

Reused powder sees repeated long exposures to both the residual heat and heat from the melt pool. A study by Tang *et al.* (2015) on Ti-6Al-4V in EBM showed a gradual and constant increase in the oxygen content coupled with a decrease in the content of aluminium and vanadium within the powder over

21 uses. Renishaw plc (2016) had remarkably similar findings for the same material in SLM over 38 reuses, seeing a gradual increase in both the oxygen and nitrogen content that led to the powder being unacceptable for Grade 23 specifications. The pickup of oxygen in Ti-6Al-4V was seen across 69 rebuilds by Popov *et al.* (2018) during the EBM process, exceeding the maximum ASTM F2924-14 (2014) requirement of oxygen content by 68%.

The majority of spatter has been shown to fall back into the build area, and may thus become incorporated into the component being built at that time (Andani *et al.*, 2018). If this is avoided, it is likely the spatter will be cleaned out alongside the unused powder during the cleaning process. Although many spatter particles are oversized and will be removed during sieving, some spatter particles are small enough to pass through the sieve mesh (Harrison, 2019). This is one likely cause for the observed change in chemical composition as powder is recycled. LPW Technology Ltd has found that the accumulation of oxygen and nitrogen-rich spatter particles is proportional to the “laser on” time in Nickel-based powders, indicating that repeated reuse of powders will generate progressively more spatter particles and further changes to the chemical composition of a powder (Harrison, 2019).

Some sources have found a lack of change in the chemical composition as powder is recycled. Slotwinski *et al.* (2014) found no notable change in stainless steel powder used in SLM after the powder had been recycled eight times. Del Re *et al.* (2018) did not observe a notable change in AlSi10Mg powder over eight reuses in SLM, although they did not measure the presence of contaminants such as oxygen that may have been accumulating. Inconel 718 was found to have a virtually constant chemical composition after 14 reuses in the SLM process (Ardila *et al.*, 2014).

There is a disparity as to whether or not powder changes chemically over time. This seems to be divided by materials, with Ti-6Al-4V being widely observed to pick up oxygen, whilst other materials seem to maintain a constant chemical composition. Titanium is highly reactive and is held at high temperatures to overcome the high melting point, potentially explaining why it appears to pick up contaminants more than other materials. Further to this, the number of powder reuses in literature studying non-Ti-6Al-4V materials is significantly lower than that in the Ti-6Al-4V studies considered. A change in chemical composition may not be seen until the powder is further recycled. Further research is needed into the change in chemical composition of other materials used in AM to determine the chemical degradation of these powders.

The phase composition and microstructure of powder particles has not been considered, despite being shown to alter the melting point of a material (Liu and Shin, 2019). This decision was made as the influence of the phase composition of powder on the produced components within AM is considered

to be negligible; the melt pool is sufficiently hot to completely melt the metal, causing a change in phase composition of components produced through AM.

### 2.3.5 Flowability

Flowability is a measure of how easily particles move over one another within a powder. For AM, this affects the usability of the powder, influencing how easily powder can be fed into the build chamber from a hopper. In DED, good flowability ensures a constant feed rate of powder. In PBF, flowability can influence how well the powder bed is formed beneath the coating arm. Popov *et al.* (2018) showed that a lack of flowability could cause a lack of fusion in the manufactured components, influencing their properties. Flowability is therefore essential in ensuring the AM process functions as designed and has the desired outputs.

The International Standards Organisation (ISO) helped produce the ISO/ASTM Standard 52907 (2019), listing four factors that can affect the flowability of the powder. These are particle size distribution, inter-particle friction (affected by surface roughness and morphology), powder moisture content and electromagnetic forces (in ferrous materials). This can be simplified by stating that flowability is determined by the forces that hold particles together. Electromagnetic forces are not further discussed, as these forces are unlikely to change during the powder recycling process.

As particle size decreases, inter-particle frictional and electrostatic forces increase due to the increased surface area over which particles can interact, reducing flowability (Gibson *et al.*, 2016). Seyda *et al.* (2012) suggest that the presence of conglomerates reduces cohesive forces between particles, improving flowability. These principles can be inferred from Figure 2-3 and Figure 2-6; an increase in particle packing density allows for the formation of more interparticle forces, requiring more energy to overcome these forces to move, or “flow”.

An increased moisture content leads to the additional bonds forming between particles. Water increases cohesive forces by forming liquid bridges between particles (Crouter and Briens, 2013). The bonding between water is stronger than the interparticle bonds, and thus requires more energy to overcome, resulting in a reduction in powder flowability. Moisture content can also accelerate chemical degradation of powders, demonstrated by the increased oxidation of water atomised powders (Irrinki *et al.*, 2016).

It has been widely observed that the flowability of the powder increases with repeated use of metal powders (Tang *et al.*, 2015; Carroll *et al.*, 2006; Renishaw plc, 2016). Tang *et al.* (2015) found that the increase was most significant after the first six powder uses than the subsequent 15. Carroll *et al.* (2006) found similar results after ten powder reuses. Renishaw plc (2016) found the flowability to

gradually increase with no significant initial drop off, although there were sizeable fluctuations in results. The reasons suggested for these changes vary, but PSD, powder morphology and moisture content are all mentioned. A study by GranuTools (2018) showed that virgin powder exhibited better flow rates when the aperture size through which powder flowed was larger. Otherwise, little difference was observed between virgin and recycled powder.

## 2.4 Component properties

The review of literature thus far has demonstrated the changes that arise within reused powder. It is essential to understand the impact these particle and powder properties have on components produced through AM. Little work has been done to identify correlations between individual variables and the build properties, most likely due to the multiple property changes occurring simultaneously with powder reuse and being difficult to isolate. This makes it difficult to determine the true cause of any changes in component properties. All references cited used the same build parameters for both their virgin powder and reused powder builds, so all differences observed are likely to be due to changes in the powder quality.

### 2.4.1 Chemical composition

Industries such as the aerospace and medical sectors have highly specific requirements for the components produced. Changes in chemical composition can have an influence on the mechanical properties of the component (Dong *et al.*, 2019), causing these critical components to fail to function as designed.

The correlation between the chemical composition of the input powder and produced components was shown by Renderos *et al.* (2016). The difference in atomic composition of the Inconel 718 powder was found to be insignificant. Further recycling of the powder began to show an increasing change in chemical composition of the manufactured component when compared to the virgin powder. This was confirmed by Tang *et al.* (2015), seeing that the chemical composition of a tensile sample produced using Ti-6Al-4V powder changed gradually in line with changes in the powder chemical composition. A notable drop in aluminium content between the powder and tensile sample was observed, suggesting that for certain metals the powder chemical composition may only be indicative, but not representative, of the produced component's chemical composition. The same drop in aluminium in recycled Ti-6Al-4V was seen by Petrovic *et al.* (2015) as the build number increased, alongside a steady rise in the oxygen content.

#### 2.4.2 Density and porosity

Pores are regions where cracks initiate under stress (Wang *et al.*, 2012; LPW Technology Ltd, 2018b), and it is well known that increased porosity leads to a decrease in material properties in various materials (Wang *et al.*, 2017; Cherry *et al.* 2015). Pores close to the surface of a specimen lead to stress concentrations which could lead to component failure (Seyda *et al.*, 2012), whilst irregularly shaped pores with corners initiate microcracking, and thus failure, under loading (Pal *et al.*, 2020). Reduced density is indicative of increased porosity. As such, high density components are likely to be more predictable and therefore acceptable within demanding industries.

Spierings *et al.* (2011) stated that fine powders tend to lead to denser parts. Irrinki *et al.* (2016) confirms this finding, attributing this increased part density to an improved packing density. Dawes *et al.* (2015) reviewed other literature, concluding that irregular shaped particles cause lower part density, whilst fine particles with a wide PSD produced high-density components. Referring to Figure 2-3, the absence of differently sized and small particles prevents gaps being filled, resulting in a reduction in the packing volume of the powder bed. The shift in PSD towards larger particles observed in recycled powders may therefore contribute to a reduced part density.

Gaspar *et al.* (2018) discuss that oxygen-rich spatter particles (highlighted in Chapter 2.3.4) can be integrated into the current build by falling into the build chamber, often becoming reincorporated into future builds if they are not sieved out successfully. Andani *et al.* (2018) believe that the porosity seen in components could be explained by the presence and creation of these spatter particles, with Liu *et al.* (2015) also believing that increased porosity could be due to the inclusion of oversized spatter particles that do not fully melt. Extensive research into pore formation was offered by Pal *et al.* (2020), demonstrating how spatter particles can be large enough to disrupt powder spreading, in turn influencing the packing density and leading to the formation of pores. Regions of incomplete melting within the component caused by oversized spatter particles, interference from oxidised layers on spatter particles or unsuitable build parameters were also shown to cause pore formation and internal defects. As spatter particles accumulate as powder is recycled, the inclusion of an increased number of these particles could influence the density of components produced using recycled powder.

Tang *et al.* (2015) found that there was a slight reduction in the density of components produced by EBM using powder recycled 16 and 21 times when compared with less heavily used powders. This was coupled with a rise in the variation of the density. However, this was still 99.55% of the maximum theoretical density of the Ti-6Al-4V. McGeehan *et al.* (2018) found that virgin 316L stainless steel powder yielded dense components in SLM with little variation in results, but once the powder had

been reused six times the density reduced and became less predictable. Heavily used powder (number of uses unknown) was shown to produce components that were consistently less dense than virgin powder, but with a similar variance. Inconel 718 powder reused four times within a DMLD system was found to produce components with higher porosity than virgin powder, although the morphology of the pores is noted to remain consistent (Renderos *et al*, 2016). Ardila *et al.* (2014) observed a slight change in porosity between virgin and recycled Inconel 718 powder, with notably less variance in results as powder reuse increased. However, this change in porosity was not considered to be significant, even after 14 powder reuses.

Seyda *et al.* (2012) observed an increase in the density of SLM produced components after Ti-6Al-4V powder was recycled 12 times. Despite the reduced porosity, the size of the pores was noted to increase. This was believed to be due to a change in PSD causing more large particles to be present; any gaps in the powder bed would typically be larger than in virgin powder. Sartin *et al.* (2017) found that there was no consistent trend between density and powder reuse, putting any observed changes down to variations in the AM process.

#### 2.4.3 Tensile properties and hardness

The tensile properties of a material include Young's modulus, Yield Strength (YS), Ultimate Tensile Strength (UTS) and the elongation. Hardness indicates how well a material can resist scratching and permanent deformation. These are essential indicators of how a material will perform when subject to certain conditions. Being able to accurately predict these properties is essential to determine the suitability of a component to its function.

Tang *et al.* (2015) noted an increase in oxygen content led to increased YS and UTS in Ti-6Al-4V with a constant elongation at break. Using the same alloy, Renishaw plc (2016) showed that there was a general increase in Young's modulus and UTS as the powder was continually recycled, also attributing this to the increased presence of oxygen and nitrogen in the powder, although this was not considered to be significant. Similar findings were made by Seyda *et al.* (2012) with Ti-6Al-4V. An initial increase in UTS was followed by a small decrease, although the UTS was still higher in this recycled powder than in virgin powder. This change was put down to an increase in pore size. Studies by LPW Technology Ltd found a correlation between the UTS and YS of Ti-6Al-4V and the oxygen concentration of the built component, which increased as the powder was recycled (Harrison, 2019). Titanium alloys are known to become brittle with increases in oxygen and nitrogen concentrations (Donachic, 2000, cited in Sames *et al.*, 2016), so this is not representative of other materials.

Testing conducted by McGeehan *et al.* (2018) saw a reduction in the UTS in 316L stainless steel as the powder was reused alongside a reduction in Young's modulus. Different experimental data with 316L stainless steel showed a shift towards a higher percentage of larger particles has a significant negative effect on the UTS of the produced component, owing to an increased porosity creating weak points (Spierings *et al.*, 2011). This was studied and confirmed by Dong *et al.* (2019), alongside the finding of higher volumes of austenite (as opposed to ferrite) in low oxygen 12CrNi2 steel powders, explaining that austenite allows grains to slip over one another more easily, resulting in more ductile properties. Del Re *et al.* (2018) found that AlSi10Mg components made from recycled powder had a lower UTS and YS value when compared with virgin powder, with a general downwards trend being observed, although no significant change was observed in the elongation of tensile samples. Liu *et al.* (2015) found that the inclusion of spatter particles in a powder considered to be contaminated after five uses caused a reduction in the YS and UTS of produced components, although this was without sieving of the contaminated powder.

Sartin *et al.* (2017) found that there was no notable change in the UTS or ductility in components built from recycled powders versus virgin powder. The issue was noted that despite parameters being kept consistent, there is still a chance that other factors, such as laser muting from deposited material on the lens, could influence the quality of produced components, making it difficult to say with certainty that powder recycling rates are to blame for all observed changes.

Relatively little research has been conducted to investigate the hardness of components made from recycled powders. Seyda *et al.* (2012) found a slightly increased hardness in components built from recycled Ti-6Al-4V powder, explaining that this change was likely due to the increased oxygen content of the Ti-6Al-4V powder. Carroll *et al.* (2006) found that there was a reduction in hardness after just one powder reuse cycle with Inconel 718, with all subsequent builds remaining at this reduced hardness value.

There are notable differences with powder reuse between common AM alloys. Seemingly Ti-6Al-4V has increased material properties as the powder gets recycled, but the opposite is seen in other materials. Any deviation from the component properties produced when using recycled powder as opposed to virgin powder can cause difficulties when predicting component properties, demonstrating the potentially negative effect of powder recycling material properties.

#### 2.4.4 Surface roughness

Surface roughness is an indication of the build resolution and can thus indicate how accurately a part is being made. Further to this, polished components with a smoother surface can fail in various locations, with crack initiation happening anywhere in the metal, whereas as-printed builds crack along the rough edges between layers of the deposited material (Sames *et al.*, 2016). Polishing of components has been shown to improve fatigue resistance, most likely due to the absence of these rough edges allowing cracks to easily form and propagate (Wycisk *et al.*, 2014).

The roughness between layers can be visualised in Figure 2-11, where the edge of each layer is slightly rounded off. A rougher surface will require more post-processing to smooth the cracks between layers, as additional protruding material needs to be removed, seen in Figure 2-12. Additional post-processing to polish materials and increase their material properties can be both costly and time consuming, and is therefore undesirable.

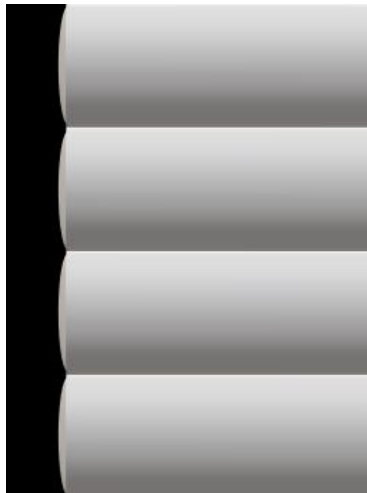


Figure 2-11 – An example of low surface roughness between layers

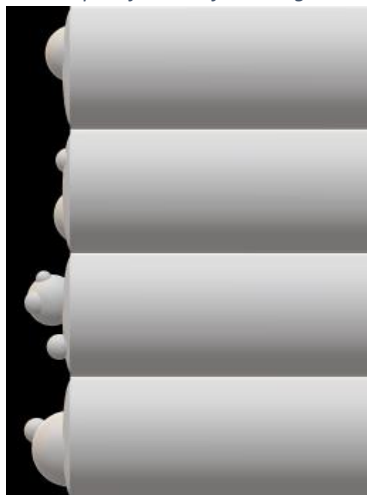


Figure 2-12 – An example of high surface roughness between layers

Surface roughness was negatively affected with repeated reuse of Ti-6Al-4V powder, showing a constant increase over 12 powder reuses, increasing in line with the increased presence of large particles in the PSD (Seyda *et al.*, 2012). It was suggested that the large particles begin to melt and attach to the surface of the exposed component, making it rougher. An increase in surface roughness in Inconel 718 components created through DED was also observed by Carroll *et al.* (2006), which saw an increase from 8.5 $\mu\text{m}$  to 19 $\mu\text{m}$  after ten reuses of the powder. A study conducted on 316L stainless steel SLM components showed that the surface roughness of components produced from virgin powder increased compared with powder recycled six times, although a large variation was seen in the results (McGeehan *et al.*, 2018). Spierings *et al.* (2011) showed that a powder with a PSD with more large particles produced rougher components than finer powders. It was further stated that the surface roughness can be improved by reducing the scan speed, giving larger particles more time to fully melt.

## 2.5 Combining virgin and recycled powder

It is common practice to extend the lifespan of used powder by mixing it with virgin powder. This can reduce the effect of the powder degradation seen in reused powders. All literature reviewed thus far focuses on the repeated recycling of powder, without the addition of new virgin powder. Comparatively little research has been carried out on the effect of combining powders of differing quality, despite being widely utilised within industry.

Research by Vock *et al.* (2018, cited in Vock *et al.*, 2019) saw that powder mixed equal parts virgin and recycled after each cycle in a PBF process saw no change in the PSD or flowability. Extrapolation of this indicates that other powder properties may not change either in this powder mixture. No work was done to test the impact of this powder recycling method on the component properties. However, as particle and powder properties have thus far been shown to affect the quality of components produced by AM, this could indicate that components produced through this powder reuse technique maintain constant with predictable properties.

Jacob *et al.* (2017) used a powder recycling technique in SLM with 17-4 stainless steel that introduced virgin powder to the build after five cycles and mixed the powder homogeneously. Apart from this, powder was predominantly recycled from the previous build, but also utilised some powder from older builds. This led to creation of components utilising a non-homogeneous blend of powders with various recycle rates.

Through this recycling process, powder properties had various changes. The morphology of particles remained constant whilst the PSD appeared to shift towards smaller particles. This shift was explained

as the PSD sample was taken using powder from the powder bed, which is known to sweep larger particles to the overflow bin, allowing more small particles from the virgin powder to be integrated into the powder bed.

The flow rate was seen to increase, as in other recycled powders. The apparent density steadily increased as the powder was repeatedly recycled, except when virgin powder was reintroduced after the fifth cycle, reducing the apparent density. Jacob *et al.* also recorded that the powder bed density increased in recycled powder combined with new virgin powder. The chemical composition was observed to stay constant.

Components produced during this study were observed to have relatively constant properties. The surface roughness showed a large variation between results, but the introduction of virgin powder after the fifth cycle caused a notable increase in roughness, contrary to expectation. The density of the component increased with a higher percentage of virgin powder present, but remained relatively constant throughout. Hardness values remained consistent, as did the UTS. The YS decreased as the quantity of virgin powder present decreased, indicating that virgin powder is preferable, but demonstrates the positive effect that mixing recycled powder with virgin powder can have.

More research needs to be done to investigate the effect of mixing virgin and recycled powders. Promising results have been seen, indicating that the impact of powder reuse is minimised through this technique. However, until these are tested on a range of materials under different conditions, AM users will be unable to achieve the maximum longevity and potential from their powders.

## 2.6 End of life powder

The difficulty of disposing of powders has been identified as an issue in AM (Ian Brooks 2019, personal communication). Minimising the waste produced reduces the need for companies to invest into safe disposal of their powders, saving them money whilst also reducing their environmental impact.

A combination of virgin and recycled powder has been demonstrated to improve powder longevity. Even through this practice, 12.5% of virgin powder ends up as waste, with potentially more produced in high-end industries (Louise Geekie 2018, personal communication). Sartin *et al.* (2017) found that 6.7% of the powder introduced to the build chamber in SLM was consumed. 2-3% was used to create components. Approximately 1% of powder per build was collected in the filtration system, and the remainder was consumed during the clean-out process. The remaining 93.3% of the powder was recovered and recycled repeatedly until it could no longer be reused, eventually creating the 12.5% of waste powder.

In order for combined virgin and used powder to be used effectively, careful logging of the usage history and build conditions of each powder is required, alongside the percentage of each powder used in the combination. However, this can only provide an indication of how the powder will behave. Technologies such as LPW Technology Ltd's PowderSolve provide this capability, allowing the component properties to be predicted, although this is in the early days of development and adoption. This can help to determine when powder could no longer be suitable for use in AM, thus needing a top up of virgin powder or removal from the AM cycle.

Besides mixing recycled powder, alternate avenues for EoL powder are not identified. If companies have identified solutions to give them a competitive edge in the AM market, this information would not likely be available in the public domain. Fine particles vaporise rather than melt (Carroll *et al.*, 2006; Gasper *et al.*, 2018), making the scrapping of powders difficult and unprofitable for recycling plants. Even if processes were identified to repurpose waste powder, the value of scrap metal is typically only 1-3% of the initial cost of virgin powder, making them unlikely to be profitable. As a result of this, companies in the AM industry do not have a means of upcycling their EoL powder, often sending waste powder to landfill or paying to have it removed safely (Ian Brooks 2019, personal communication).

The need for the safe removal of powders comes from the potential for metal powders to become combustible and ignite, causing an explosion and potentially severe damage. Investigation by Jacobson *et al.* (1964) shows that particles of stainless steel are in the "none" category of Relative Explosion Hazard Index, even with 100% of the powder smaller than 44 $\mu$ m. However, the report showed a serious risk with other metal powders, notably in titanium and aluminium alloys. These energetic powders often require safe, and sometimes costly, removal from site, hampering the profitability of the process.

The various rates of degradation in powders have been seen in Chapter 2.3, owing to different powder feedstocks, process parameters, builds and powder handling techniques. There are numerous factors affecting the quality of the produced component. As such, identifying the EoL point of powders is somewhat arbitrary. Standards in place, such as ASTM F3055 (2014) for AM using Inconel 718 in PBF, do not offer official guidelines on powder reuse or identification of EoL powders. This causes a large variation in what AM users consider "unusable" powder.

EoL powder has been an issue since the inception of metallic powder-based AM, and yet seemingly little research has been done to identify solutions to this. Research needs to be aimed at identifying methods to extend the lifespan of metal powders and prevent unusable powder from going to landfill.

### 3. Feasibility Analysis of Proposed Solutions<sup>2</sup>

The literature review in Chapter 2 provided a comprehensive understanding of the methods through which powder degrades and the life cycle of metal powder within the AM process. This background knowledge allows for effective analysis of the potential solutions that have been proposed by Croft AM, discussed in Chapter 3.1. The literature also identified alternative potential solutions that may be effective, outlined in Chapter 3.2. Conducting a feasibility analysis of each solution provides insight into their effectiveness, identifies potential barriers to success and ultimately can indicate which solutions to further pursue. The culmination of this discussion is seen in the concept-selection matrices in Chapter 3.3.

Any solution is likely to be environmentally preferable to sending powder to landfill. However, a solution needs to be economically viable for it to become adopted by the industry, as it may be cheaper to purchase new virgin powder than attempt to upcycle the EoL powder. This poses a significant challenge and may have inhibited research in this field to date.

#### 3.1 Proposed solutions by Croft AM

1. LARGER-DIAMETER PARTICLES CAN BE SIEVED INTO SIZE FRACTIONS. NEW SMALLER-DIAMETER POWDER FRACTIONS CAN BE PURCHASED AND THE POWDERS REMIXED INTO RELEVANT PROPORTIONS. THIS COULD THEN BE RESOLD OR REUSED AS SUITABLE FOR AM.

Most literature identified a small but gradual shift in PSD towards larger particles, notably within PBF techniques. This solution may reduce the absence of smaller particles in used powders, bringing the PSD of these mixed powders closer to that of virgin powders. If several sieves of decreasing mesh sizes were to be layered in a “sieve-stack”, the recycled powder could be fractioned out into various powder sizes. Virgin powder could then be mixed with the various size fractions to make up new powder with a suitable PSD for use in AM. This could potentially reduce the quantity of powder that is disposed, although it does not greatly reduce the quantity of virgin powder that needs to be purchased.

This solution would require the purchase of virgin powder with narrow and specific particle size ranges to fill in the gaps where small particles are absent. Such powders may be obtained through companies such as Tekna (n.d.), who offer powder with controlled grain sizes. However, higher specification of virgin powders would come at an increased cost to account for the increased complexity of obtaining

---

<sup>2</sup> This analysis was carried out in December 2018. As such, only potential solutions identified prior to this date are analysed. Research after December 2018 identified an alternative potential solution that is not discussed here (see Chapter 6.3). This new solution was analysed using the same approach as is in this chapter, but this analysis is not included within the present work.

these powders. This makes this solution unlikely to be appealing to AM users, as it would be cheaper to purchase new virgin powder made to specification for use in AM, without the need to blend powders together. However, if several kilograms of used powder could be reclaimed from the addition of one kilogram of small-particle virgin powder, this may become financially viable.

This solution does not take into account that recycled powder degrades in a multitude of ways. Whilst mixing a portion of virgin powder into the recycled powder could improve the PSD of the powder, it would not change the morphology or chemical composition of the recycled particles. As these deformed or oxidised particles have been shown to potentially cause defects in AM components, this solution may not greatly improve the quality of the end of life powder.

2. RE-SIZED FRACTIONS WITH LARGER PARTICLES MAY BE SUITABLE FOR USE IN OTHER AM TECHNOLOGIES. ALTERNATIVELY, THE POWDERS COULD BE USED IN OTHER POWDER-BASED INDUSTRIES.

The powder that Croft AM obtain from their supplier, LPW Technology Ltd, falls between 15µm and 45µm. They utilise a sieve mesh with 53µm aperture to remove oversized particles, maintaining this PSD as the powder is recycled. However, as the powder is continually reused, larger particles become more prevalent. Whilst the powder may become less suitable for use in SLM, it may be suitable in other AM processes or powder-based processes.

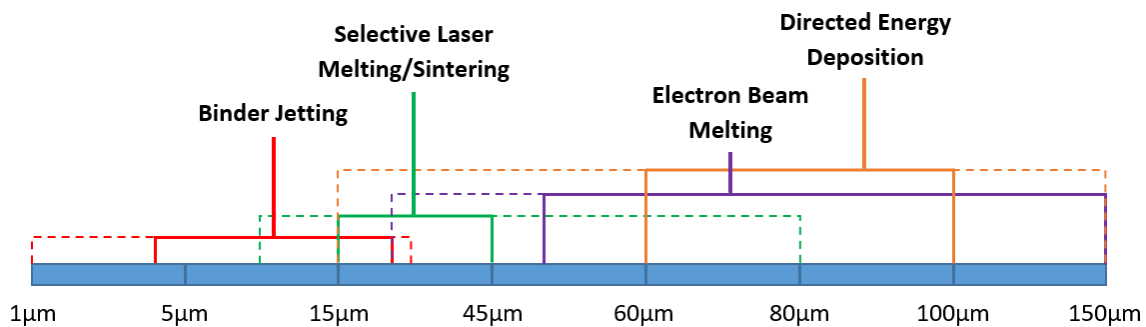


Figure 3-1 – Particle sizes used by the different metal powder based AM techniques. Thick lines indicate the desirable particle sizes for each process, whilst dashed lines indicate usable but less acceptable particle sizes.

A range of powder PSDs were seen to be used in SLM across the experiments in the sources cited in the literature review, as summarised in Figure 3-1. Vock *et al.* (2019) stated that, in general, particles between 10-60µm were used in the SLM process. Jacob *et al.* (2017) used 17-4 stainless steel powder in SLM with the majority of particles between 23.0-51.2µm, showing a variation to the PSD used by Croft for a similar metal. Seyda *et al.* (2012) used Ti-6-Al-4 particle sizes ranging from 1-80µm in the virgin powder used in SLM, with the upper bound increasing to over 100µm in recycled powder. It may therefore be possible for Croft AM and other powder users to pass on recycled metal powder to other companies utilising SLM with slightly larger particles.

Tang *et al.* (2015) found the particle distribution of Ti-6Al-4V used in EBM to be typically between 40-150 $\mu\text{m}$ , with Vock *et al.* (2019) stating that particles were used between 50-150 $\mu\text{m}$ . This demonstrates that different AM processes utilise different PSDs, allowing for the potential handing down of EoL powder. A study conducted by Karlsson *et al.* (2013) found that there was no notable change when powder with a PSD between 25-45 $\mu\text{m}$  was used in the EBM process. The hardness, chemical composition and microstructure of the produced component remained constant, with the surface roughness reducing. This suggests that the 15-45 $\mu\text{m}$  EoL powder used in SLM could be used in EBM to produce components with an improved surface finish that require less post-processing.

Renderos *et al.* (2016) noted that the DED process uses particles ranging from 15 $\mu\text{m}$  to 150 $\mu\text{m}$ , with the majority of particles being between 60-100 $\mu\text{m}$ . This finding is confirmed by Carroll *et al.* (2006), where the mean particle size was close to 100 $\mu\text{m}$  and ranges up to 150 $\mu\text{m}$ . The recycled powder from the SLM process may not be viable for use in DED, but recycled EBM powders may be. Larger particles or sieved out conglomerates from the SLM and EBM processes could also be used in DED.

Selective Laser Sintering (SLS) is a near-identical process to SLM. It can build components faster than SLM through the partial melting i.e. sintering of particles, although the built component has less reliable and weaker material properties (Santos *et al.*, 2006). More commonly used with polymers, SLS is often only used in metals where mechanical properties are not critical, such as rapid prototyping. However, there is also the potential for SLS to produce high-quality metal parts used in technologies such as dentistry (Shishkovsky, 2009), with the notable benefit of being highly porous from the nature of partial melting. Identifying new (and potentially porous) components and laser settings to enable Croft AM to utilise their Realizer 250 for SLS may permit them to continue to use EoL SLM powder to produce less critical components. Alternatively, other companies who are utilising SLS may be interested in EoL SLM powder.

BJ has been noted to use particles smaller than 25 $\mu\text{m}$  and as small as 1 $\mu\text{m}$  (Vock *et al.*, 2019). Do *et al.* (2017) used particles ranging from 4 $\mu\text{m}$  to 30 $\mu\text{m}$  in a series of BJ experiments. It has been noted that components produced through BJ are not applicable to many engineering scenarios, owing to their low density of typically 50-60% of the theoretical density (Do *et al.*, 2017). This would suggest that EoL SLM powders would be highly suitable in BJ, as mechanical properties wouldn't be of a concern, although only the finer particles used in SLM may be suitable.

Outside of the AM industry, thermal spray techniques such as plasma-transferred arc welding or high velocity oxygen fuel coating could utilise the EoL powder produced within the AM industry. Since the produced product from the metal powder is less mechanically critical in these industries, the main

considerations would be particle size and the material choice. For a material such as stainless steel, the powder is likely to be desirable due to the low cost, whereas expensive titanium-based alloys would be far less suitable. Thermal spray powders are typically between 50µm and 150µm (Sanwa Diamond Tools Pvt. Ltd., n.d.), indicating that some AM techniques may be able to direct their EoL powder to these industries.

Metal injection moulding sinters powder particles together, mass-producing complex components with material properties comparable to the wrought metal (Davies *et al.*, 2003). This process typically uses gas-atomised powders with particles no larger than 38µm, although most particles are smaller than 12µm (Murray *et al.*, 2011). Some EoL AM particles may be suitable for use in metal injection moulding, although it is unlikely that any SLM EoL powder would be suitable without first sieving the powder to remove particles over 38µm.

Whilst there is some promise with this redistribution concept, there are many difficulties to overcome. Much like Solution 1, this only considers the PSD to determine the suitability of a powder for AM. The EoL powder from one process may have a suitable PSD to be used in another process, but the chemical composition or morphology of the powder particles has also been shown to influence the suitability of a powder for use in AM.

The feasibility of this solution depends heavily upon the ease of delivery and other logistical considerations. Stephen Crownshaw from Renishaw plc (2018, personal communication) confirmed that this was a major challenge. He stated that trading of EoL powders does currently happen in the industry, but is normally between companies who have strong links. If these links were not well established, the difficulty of identifying a company that wish to purchase EoL powders and providing them with a regular supply of powder could be too much hassle.

A further complication is with the quality of powder that is supplied. Unless the company accepting the EoL powder has powder testing capabilities, they have no means of determining the quality of the powder they have been delivered. Companies may feel it would be more reliable to purchase virgin powder to mitigate this risk, even if it were more expensive.

3. THE POWDER MAY BE REMELTED INTO ANOTHER FORMAT FOR USE IN OTHER ADDITIVE PROCEDURES, SUCH AS WIRE, USABLE IN WIRE DEPOSITION METAL AM. ALTERNATIVELY, THE POWDER COULD BE FORMED INTO SOLID METAL MATERIALS FOR USE IN OTHER INDUSTRIES.

Metal ingots, sheets and wires are used widely in the manufacturing industry as raw materials, whilst metal powders are used for relatively few applications. A powder no longer suitable for use in AM due to chemical changes or particle morphology may be acceptable in other manufacturing processes. The

prevalence of the scrap metal industry is testament to the potential of this concept. This method has the potential to reduce the quantity of powder being sent to landfill.

As the metal powder is often fine enough to vaporise, it is difficult to melt metal powders into raw materials (Carroll *et al.*, 2006; Gasper *et al.*, 2018). Very little literature acknowledges this issue or addresses how metal powder could potentially be reformed into another format. A large amount of energy is required to melt metal (Jacobson & McKittrick, 1994). The energy required to melt and reform this EoL powder would likely be similar to the energy needed to melt the same mass of metal in the atomisation process. This is unlikely to be an environmentally friendly solution; the energy used to melt EoL powder may be better utilised producing a higher-grade metal powder through atomisation.

Dr Louise Geekie suggested that the powder could be heated at a lower temperature to sinter particles together. This could reduce the risk of powders vaporising whilst creating an ingot for use as scrap. The reduced energy required to heat the metal makes this sintering process more environmentally viable than remelting the powder. However, this is unlikely to be economically feasible; scrap stainless steel can be worth as little as £0.30 per kilogram (Louise Geekie 2018, personal communication).

#### 4. SOME METALLIC POWDERS BECOME MIXED. THESE POWDERS COULD BE SEPARATED INTO REPRESENTATIVE MATERIAL FRACTIONS FOR RECOMBINATION AS SINGLE MATERIAL, ALLOWING REUSE IN ANOTHER INDUSTRY.

It is possible for two or more different powders to mix together. This can occur through contamination picked up during powder handling or by other accidental means. There is potential to separate these into individual powders again. With ferrous materials, this could involve a solution as simple as magnetising a ferrous whisk-like device and stirring it through the powder, extracting the ferrous powder. However, when the mixed powders are non-ferrous, more elaborate techniques may need to be utilised.

An air jig may allow powders to be easily separated. Air jigs force air upwards into a chamber, providing enough force to suspend the particles in the air (Sampaio *et al.*, 2016). The downwards force, weight, is a function of the particle volume, whereas the upwards force (upthrust) acting on the particle is a function of the exposed surface area. Both of these are dependent on the radius,  $r$ , of the particle. However, the weight is dependent on  $r^3$ , whilst the surface area is dependent on  $r^2$ . As a particle increases in radius, the particle will have a larger increase in weight than in upthrust. This results in larger particles achieving equilibrium and stabilising lower down in the stream of air (closer to the air source) whilst smaller particles will stabilise higher up in the air flow.

With this principle in mind, it could be possible to separate and collect particles in various size fractions. Denser powders would stabilise closer to the air source, whilst less dense powders would stabilise further away, as seen in Figure 3-2. In mixed powders, the differing densities of various materials would cause less dense but larger particles to stabilise in a similar region to smaller but denser particles. However, these larger particles of one material could then be separated from the smaller particles of another material by sieving this mixture.

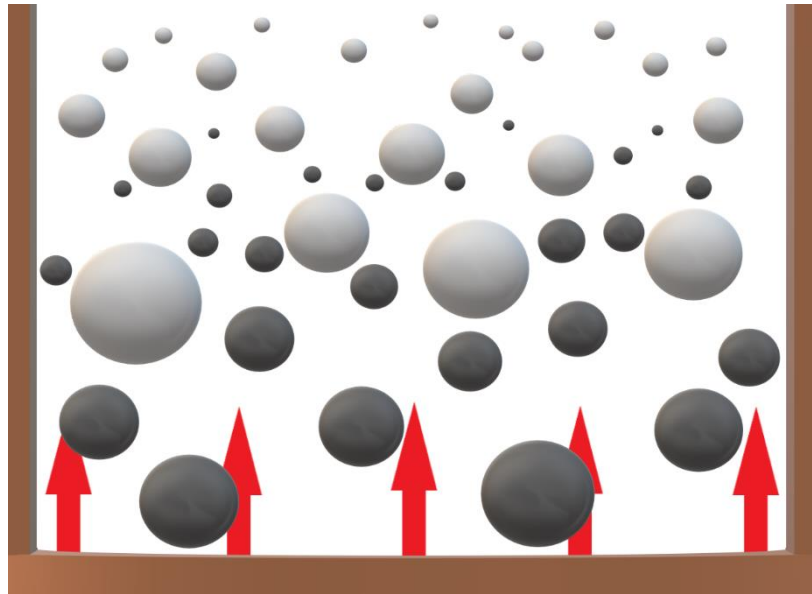


*Figure 3-2 – Representation of the air jiggling principle with a mixed powder. Air flows from the bottom of the chamber upwards. Denser particles are presented by darker grey, whilst less dense particles are lighter grey.*

Whilst there is potential for powder contamination, it is infrequent within the AM industry; strict powder handling can easily prevent such a mistake. This casts doubt on the necessity of this practice being further investigated, as it is unlikely to be a common problem. Whilst the solution may be inexpensive, it may be used so rarely that it is not worthwhile.

### 3.2 Further proposed solutions

5. LARGE CONGLOMERATES, SIEVED OUT REJECTS AND SUPPORT STRUCTURES COULD BE REGROUND THROUGH BALL MILLING TO PRODUCE A METAL POWDER SUITABLE FOR USE IN AM.

Ball milling uses kinetic energy in large balls with high hardness to break down comparatively small pieces of a softer material. Over several hours, a drum is rotated (often at high speeds) to allow the balls to repeatedly impact the milled material, breaking the material into smaller pieces. This process can be seen in Figure 3-3.

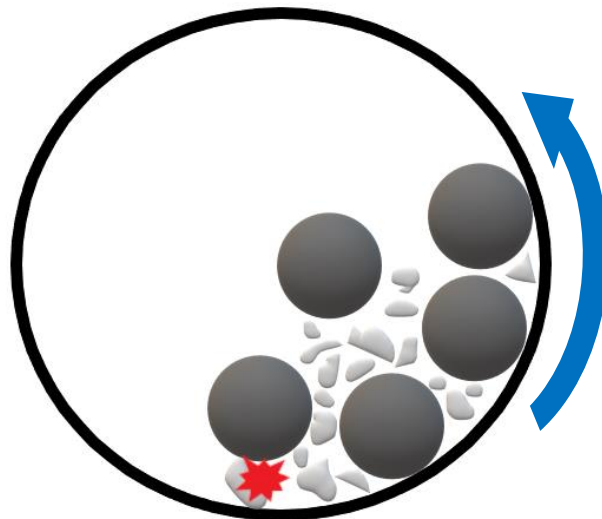


Figure 3-3 – An example of ball milling

When considering metal powders, ball milling is typically used to further reduce the size of metal micron-sized powders from to nanoparticles (Rane *et al.*, 2018). However, a study conducted by Fullenwider *et al.* (2019) investigated the production of metal powder for use in AM through the mechanical ball milling of recycled machining chips. This reused waste material whilst also reducing the necessity for virgin powder to be purchased. As mechanical milling is carried out at room temperature, the necessity to melt metal in the atomisation processes is eliminated, making this a potentially less energy demanding process (Fullenwider *et al.*, 2019). The support structure in builds is currently considered waste material and is thrown away or scrapped. Conglomerates formed from both residual heat and spatter that are sieved out are also waste by-products. The formation of these reduces the possible yield from the powder. If this mechanical milling technique could be utilised to create a metal powder from these waste products, this powder could be reintroduced into future builds.

A limitation of this method would be the potential for oxidised particles to be reincorporated into future builds, negatively impact the produced component. It has been shown that conglomerates and spatter particles show increased signs of oxide compounds on the particle surfaces. To counter this, the powder produced by milling could be mixed with virgin powder to minimise any negative effects the milled powder may have on the AM process.

A further limitation is the size and shape of particles produced by this method. The particles studied by Fullenwider *et al.* (2019) were not found to be as spherical as the particles produced by gas atomisation, and were notably rougher. They were also larger than the particles used in many SLM processes, although they were shown to be usable in DED. Irrinki *et al.* (2016) dispels concerns

regarding the rougher and less spherical particles, demonstrating that the particles produced by water atomisation are similar in quality to those produced by ball milling.

The findings by Fullenwider *et al.* (2019) would need to be adapted for use with conglomerates and support structures. If they were capable of producing particles suitable for use in AM, this would find a use for this otherwise wasted metal. This solution could improve the yield of the powder by minimising waste, whilst also reducing the need to produce more virgin powder. This solution does not, however, prevent EoL powders from being sent to landfill. On a large scale, this solution may be economically viable, although this is hard to gauge without extensive research.

#### 6. END OF LIFE METAL POWDER COULD BE SOLD ON AND EMBEDDED WITHIN A POLYMER MATRIX TO ENHANCE THE MATERIAL PROPERTIES, IN EITHER AM OR OTHER INDUSTRIES.

Work by Singh *et al.* (2016) discusses the concept of embedding metal powder within a polymer matrix to produce filament wire for use within structural engineering applications. This was done with iron powder and waste polymer, indicating that this method could also reduce waste in other industries beyond AM. The matrix resulted in a variety of property changes, dependent on the parameters of the manufacturing method. Many desirable changes such as increased tensile strength and hardness were obtained.

Singh *et al.* (2016) explored a very specific use of a polymer-powder matrix. This could be adapted for use in various industries which require tough, non-recyclable polymers. The benefit of this solution is that it requires little work beyond proof of concept; through demonstrating the benefits of embedding metal powder in polymers, potential buyers for EoL powder can further investigate and tweak the matrix composition and manufacturing parameters themselves.

A challenge with this method is the wear that hard components in matrices can cause on machinery. Gerard Shields of Lancaster University (2018, personal communication) observed that using a glass fibre matrix in a wire-deposition AM process caused deposition nozzles to wear out significantly faster than if only a polymer was used. This caused the part to rapidly fall outside of acceptable tolerances and thus resulted in build problems. It was suggested that this could be mitigated by using suitably hard materials, such as rubies, within nozzles.

It can be assumed that a similar issue would arise with metallic powder based matrices. Injection moulding is a common polymer manufacturing method that uses nozzles to feed material into a mould. There could be negative consequences of using metal-polymer matrices within this process; moulds could gradually be worn down, machines may be difficult to clean and feed rates may be

affected by nozzle wear. The requirement of specialist tooling and equipment to overcome these issues could act as a barrier to the adoption of this practice.

It may be possible for the metal powder to be mixed within a polymer and used in a polymer-based AM process. Aluminium powder can be mixed with polyamide powder to create Alumide for use in the SLS process. Alumide has a considerably higher stiffness than polyamide and can be easily post-processed, resulting in its use in several applications that neither aluminium nor polyamide may have been suitable for (de Beer *et al.*, 2019). As Alumide is sintered by energy from the laser, there is no damage caused to the manufacturing equipment through wear from the aluminium powder.

Whilst the success of this technique has been demonstrated, other metal-polymer composites for use in AM are not as widely researched. Other metal-polymer powder blends for use in SLS may exhibit favourable properties. Metal powder could alternatively be suspended within a resin for use in stereolithography, offering another means of forming composite materials through AM with enhanced properties. The main challenge posed by combining two materials is achieving homogeneity of the matrix, especially within a resin. However, if this could be achieved, this would be a progressive change in the AM industry.

One kilogram of powder may be able to enhance the properties of several kilograms of polymer, making this economically viable to polymer manufacturers. However, as part of the appeal of polymers is that they are cheap, this solution may not be economically feasible when using highly expensive metal such as Ti-6Al-4V, limiting the potential impact of this solution on the wider AM community outside of Croft AM. Whilst this method would reduce the quantity of EoL powder sent to landfill, it would not reduce the purchasing of new virgin powder.

#### 7. POWDERS COULD BE SIMPLY GRADED THROUGH MEASURING THEIR FLOWABILITY TO PREDICT THE COMPONENT PROPERTIES, BASED UPON THE CORRELATION BETWEEN THESE PROPERTIES.

A simple method to grade powder could be to measure its flowability, as literature identified a common correlation between increased powder flowability versus powder reuse. A correlation between powder reuse and the produced component properties was also observed. If a correlation between flowability and component properties could be shown to be consistent, flowability could be used to predict the quality of the produced component. Sames *et al.* (2016) noted that the effect of flowability on processability is not well published, despite it being critical to many AM processes.

Vock *et al.* (2019) showed that there are a variety of methods employed to determine the flowability of powders, although the ASTM Standard 52907 only accepts Hall and Carney funnel tests as standard

practices. However, a rotating cylinder is also considered feasible. The Hall flow test can be indicative of powder flowability, but literature showed a wide variance in the results of this test. As such, alternative flowability methods may need to be considered for this solution to be effective.

Work has already been carried out by GranuTools into simply measuring the flowability of powders in a rotating cylinder. The GranuDrum acts as a powder rheometer, allowing a small quantity of powder (10-50ml) to be placed inside a drum and rotated (GranuTools, 2016). The more cohesive the particles of powder are to one-another, the higher the dynamic angle of repose will be, indicative of the powder flowability. Measurements of this angle could be obtained for a variety of angular velocities from 2-60 rpm and correlated to powder flowability. If this can be shown to be a reliable indicator of flowability, it may be capable of accurately predicting the properties of the produced component.

This solution relies heavily on a strong, reliable and quantifiable correlation being found between powder flowability and component properties. Preliminary research suggests that the correlation is present, but the strength of this is unknown. This would require large data sets to determine the validity of this solution, which may prove to be fruitless. Data would need to be obtained for various powders in order for this research to have an impact on the wider AM community beyond Croft AM. Without a guarantee of the powder history, such as poor powder handling introducing contaminants, there is no guarantee that powder can be graded solely on flowability.

Determining effectively when a powder is no longer suitable for use in AM will extend powder life through ensuring powder is used until the last possible cycle. This would reduce the quantity of virgin powder purchased. There would be minimal costs associated with this solution, with potentially huge savings in virgin powder costs in expensive powders. However, the solution does not find a use for EoL powders.

#### 8. THE LASER SETTINGS AND COATING ARM SPEED COULD BE ADJUSTED WHEN UTILISING RECYCLED POWDERS TO REDUCE THE NEGATIVE EFFECTS ASSOCIATED WITH POWDER REUSE.

Porosity has been shown to increase as powder is recycled and has been shown to negatively impact component properties. Spierings *et al.* (2011) theorised that increasing the laser power (or similarly, decreasing the laser speed) may improve part density when using recycled powder with more large particles in the PSD. This is confirmed by Pal *et al.* (2020). Reducing the laser speed slows down manufacture, potentially reducing the AM process throughput. Increasing the laser power requires more electrical power, and thus costs more money per build. However, with the knowledge that the powder flowability increases with powder usage, the build settings could be modified to offset these issues. The coating blade will be able to operate faster due to the increased flowability, partially

compensating for the reduced laser speed or increased power output. The optimum coating speed can be established utilising the GranuDrum technology, as discussed in Solution 7.

Research has already been carried out by Andani *et al.* (2018) demonstrating that increased laser power reduces porosity. A change in the build parameters could therefore reduce the porosity of components built using recycled powder, where porosity is more likely to occur. Contrary to this, higher energy input into the melt pool creates more spatter, which has been shown to negatively impact component properties. As such, this method could seemingly have both positive and negative effects, but the available evidence is inconclusive. Further research into this could extend the point at which powder become unusable, preventing the need to purchase more virgin powder. The cost would be fairly minimal to the AM user; no further equipment would need to be purchased. However, this solution does not identify a method of preventing EoL powders of being sent to landfill.

9. POWDER COULD BE RETURNED TO THE SUPPLIER FOR REGRADING AFTER IT HAS BEEN USED, THEN REDISTRIBUTED BY THE SUPPLIER.

Stephen Crownshaw, Renishaw plc (2018, personal communication) revealed that many AM companies would not have access to their own material testing labs. In the case of SMEs where money isn't plentiful, an expensive solution to EoL powder disposal involving investing in new equipment may not be feasible. This could limit the impact this research could have on the AM industry and prevent small businesses from easily accessing AM.

Encouraging powder suppliers with access to powder testing facilities to purchase EoL powders from AM users may prevent powder being sent to landfill. Chapter 2.5 demonstrated that mixing virgin powder with used powder prevented powder degradation, in turn having a positive impact on the properties of components produced using this powder mixture. Powder suppliers could combine virgin and used powder together and utilise their powder testing facilities to ensure the produced powder is suitable for use in AM. This would reduce the quantity of virgin powder that is produced whilst preventing EoL powder being sent to landfill.

This solution negates the need for SMEs and other AM users to invest in potentially expensive equipment. The powder suppliers would be able to resell regraded EoL powders at a higher value, allowing for a circular economy to be established. This would financially benefit the entire AM community, whilst reducing the quantity of waste produced by the AM process.

In order to implement this, the industry as a whole would need to see a change in the powder supply process, which may take a long time to see or encounter heavy resistance. Many consumers believe

that virgin powder is the best powder, and may not want to purchase these lower-quality powder mixtures. Powder manufacturers would also be receiving powder from various consumers with different standards of powder handling or machine set ups, influencing the quality of the powder sent back to them; some powder may be in an irrecoverable state.

10. PLASMA SPHEROIDISATION CAN BE UTILISED TO UPCYCLE POOR QUALITY POWDERS INTO POWDERS SUITABLE FOR USE IN AM.

General Electric Co (GE) are developing a technique called plasma spheroidisation, capable of improving the properties of powders that are used as feedstock (Kelkar, 2018). The basic principle is shown in Figure 3-4. By melting the outmost layers of the particle, the size of particles decreases to within acceptable parameters for use in SLM, whilst the particles become more spherical. The oxygen, nitrogen and hydrogen content reduced between the powder feedstock and the powder output significantly, forming powders similar to gas atomised powder from a water atomised feedstock. These claims are supported by Boulos (2012), claiming that spheroidisation could improve flowability, packing density, particle porosity, surface morphology and powder purity.

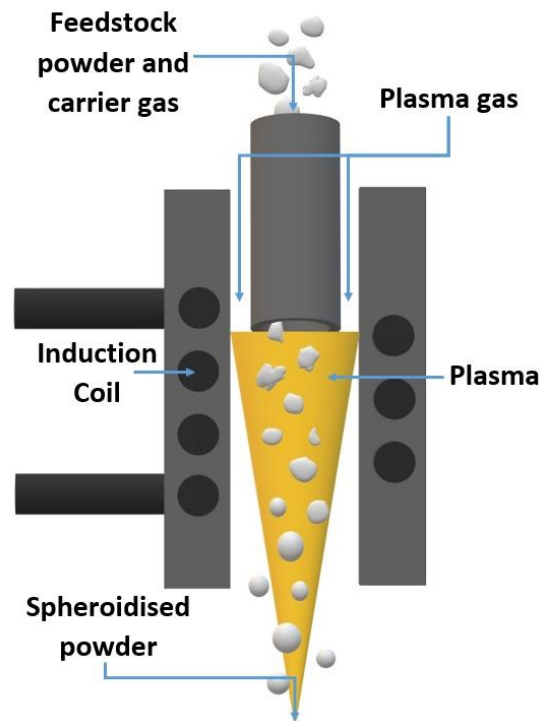


Figure 3-4 – An overview of plasma spheroidisation

Further to this, GE state that alloying elements can be mixed into the feedstock powder to change the chemical composition of the output powder, allowing a powder to be chemically altered to fall within a specification. This was demonstrated by O'Dell *et al.* (2004), showing that a composite powder of pure molybdenum and rhenium could produce a powder alloy of these constituent elements when

fed into a plasma spheroidiser. In this same experiment, the oxygen content was also seen to decrease by 97%. This significant result demonstrates that feedstock powder could be chemically altered to match or surpass the quality of virgin powder produced through the widely accepted gas atomisation process.

Plasma spheroidisation has also been investigated by other major powder suppliers. LPW Technology Ltd (2016) found that particles produced using a spheroidiser were highly spherical, although the reduction in size seen in the study by GE was not reproduced. Particle sizes remained constant in two materials and increased in size in a third. It was believed that tweaking the parameters used in plasma spheroidisation caused these changes. This was confirmed by Kobiela *et al.* (2015), finding that both the quality of the feedstock material and process conditions heavily influenced the output of the spheroidised material. Despite allegedly optimising the process, small cracks and pores were seen on the surface of spheroidised tungsten powder.

Studies of the spheroidisation process tend to use heavily misshapen non-spherical powders as their feedstock, produced from water atomisation, chemical reactions or mechanical processes. These powders are typically in a worse state than the EoL powders that are being considered as a feedstock for the plasma spheroidisation process. Therefore, it is highly probable that using EoL powder as a feedstock material will produce particles of a similar or higher quality than those used in the reviewed literature.

Sartin *et al.* (2017) reported that of the 93.3% of powder recovered for recycling per build (see Chapter 2.6), a further 3% of this powder was removed during the sieving process. Sieved out particles therefore represent a portion of the waste in AM, on top of the 12.5% of waste powder produced. Approximately one kilogram of unusable powder is created per kilogram of components produced through AM (Sartin *et al.*, 2017). If a sufficient quantity of these particles could be collected, it is likely that they could also be used as a feedstock powder for the spheroidisation process, further reducing the waste produced by the AM industry.

The potential energy savings of this technology can be demonstrated through data provided by Tekna (n.d.) on their TekSphero-200 spheroidisation system. A throughput of 5-50kg of powder can be achieved per hour, utilising up to 200kW of power. Boulos (2012) showed that a lower powder throughput rate dramatically increased the tap density of the produced powder, representative of increased sphericity of particles. However, as the feedstock powder is already highly spherical, it can be assumed the maximum throughput can be utilised. If this were combined with the highest machine power setting, one kilogram of powder would require 4kWh to produce. This equates to 14.4MJ of

energy per kilogram of powder produced, utilising only 81.7% of the energy required in the direct atomisation process of steel powders. The resultant reductions in CO<sub>2</sub> emissions from this are analysed in Appendix B – Carbon Reductions Calculations. It is highly probable that steel would not require this much energy to spheroidise; Boulos (2012) used only 100kW to spheroidise molybdenum, which has a melting point 1200°K higher than steel. Therefore, this value may be further reduced. This powder upcycling method is therefore likely to be preferable to produce high-quality powders for AM than atomisation, both reducing EoL powder waste and reducing energy consumption in the creation of new powders.

### 3.3 Matrix analysis

With many potential research options to consider within a limited timeframe, the best solutions needed to be identified and pursued at an early stage. A concept-scoring matrix provided the best means of achieving this, as laid out by Ulrich and Eppinger (2012). An outline of the process followed is detailed below:

Key criteria to score each concept against were initially identified. Typically, one of the proposed solutions is selected as a datum to compare all other solutions with. In this matrix, the datum was to “do nothing”, quantifying how any concept would improve upon the current industry practice. Whilst this was the overall datum concept, it did not represent the average performance of every criteria. Where this is the case, an alternative datum was identified (represented by a bold rating value in Table 3-2 to 3-4) to prevent scale compression. Table 3-1 outlines the scoring system used.

*Table 3-1 – Scoring system breakdown used in the concept-scoring matrix*

<b>Comparative performance</b>	<b>Rating</b>
Significantly worse than datum	1
Worse than datum	2
Little-to-no change from datum	3
Better than datum	4
Significantly better than datum	5

Each criteria identified was assigned a “weight” value. This was determined by the importance of certain criteria, based on information provided by Croft AM, the wider AM community and the Centre for Global Eco-Innovation (CGE). The product of the rating given and criterion weighting was recorded, with the sum of these collected for each concept. Potential solutions with the highest scores could then be considered for further investigation.

The selection matrix is highly subjective. The final scores are dependent upon how important an individual considers each criteria to be and how well they believe a solution will perform. In order to achieve a non-biased score for each concept, the matrix was designed by the author and approved by beneficiaries of this project<sup>3</sup>. As this work was commercially sensitive, only three beneficiaries from the project could complete the questionnaire.

A sensitivity analysis could be conducted if the rating or weighting was debatable. Using a spreadsheet, these values can be changed, automatically updating the final score. This allowed assessment as to whether this uncertainty had a notable impact on the chosen solution(s). This method cannot be presented within this thesis. However, it was applied to assess the concept-scoring matrices.

---

<sup>3</sup>The matrices were filled in based on a literature review and feasibility analysis document provided to each respondent in December 2018. This differs the updated versions seen in Chapters 2 and 3. These matrices are therefore provided to demonstrate the methodology used to identify and justify the research avenues that were pursued.

Table 3-2 – Concept-scoring matrix filled in by Respondent 1

Concept-scoring Matrix - Respondent 1		0 - Do nothing		1 - Separate into size fractions		2 - Repurpose for other AM technologies		3 - Reform into an alternative format		4 - Separation of different metal powders		5 - Reuse of conglomerates and support structures		6 - Embedding powder within a matrix		7 - Grading powders through flowability		8 - Adjustment of laser settings and coating arm speed		9 - Regrading by powder supplier	
		Rating	Weighted Score	Rating	Weighted Score	Rating	Weighted Score	Rating	Weighted Score	Rating	Weighted Score	Rating	Weighted Score	Rating	Weighted Score	Rating	Weighted Score	Rating	Weighted Score	Rating	Weighted Score
Reduces virgin powder purchasing	<b>0.100</b>	1	0.1	3	0.3	3	0.3	2	0.2	3	0.3	4	0.4	1	0.1	3	0.3	3	0.3	2	0.2
Improves longevity of powder	<b>0.150</b>	1	0.15	3	0.45	3	0.45	2	0.3	5	0.75	3	0.45	3	0.45	3	0.45	4	0.6	3	0.45
Maintains quality of produced component	<b>0.125</b>	3	0.375	2	0.25	1	0.125	3	0.375	5	0.625	2	0.25	3	0.375	4	0.5	4	0.5	5	0.625
Identifies use for EoL powder	<b>0.175</b>	1	0.175	2	0.35	4	0.7	5	0.875	2	0.35	3	0.525	5	0.875	2	0.35	2	0.35	3	0.525
Improves yield/reduces scrap	<b>0.100</b>	1	0.1	3	0.3	4	0.4	5	0.5	4	0.4	5	0.5	5	0.5	4	0.4	3	0.3	4	0.4
Energy savings	<b>0.075</b>	3	0.225	4	0.3	3	0.225	1	0.075	2	0.15	4	0.3	3	0.225	3	0.225	2	0.15	1	0.075
Ease to establish/set up	<b>0.050</b>	5	0.25	4	0.2	1	0.05	3	0.15	2	0.1	3	0.15	2	0.1	4	0.2	4	0.2	1	0.05
Expected cost of solution	<b>0.050</b>	5	0.25	2	0.1	5	0.25	4	0.2	2	0.1	3	0.15	4	0.2	3	0.15	4	0.2	2	0.1
Monetary savings/profit once established	<b>0.050</b>	3	0.15	3	0.15	3	0.15	4	0.2	4	0.2	4	0.2	3	0.15	4	0.2	4	0.2	2	0.1
Risk of powder contamination and oxidisation	<b>0.075</b>	3	0.225	2	0.15	3	0.225	4	0.3	2	0.15	3	0.225	5	0.375	2	0.15	3	0.225	5	0.375
Powder risk assessment	<b>0.050</b>	5	0.25	2	0.1	3	0.15	4	0.2	2	0.1	3	0.15	2	0.1	3	0.15	4	0.2	5	0.25
Final score	-	2.25		2.65		3.025		3.375		3.225		3.3		3.45		3.075		3.225		3.15	
Ranking	-	<b>10</b>		<b>9</b>		<b>8</b>		<b>2</b>		<b>4=</b>		<b>3</b>		<b>1</b>		<b>7</b>		<b>4=</b>		<b>6</b>	

Table 3-3 – Concept-scoring matrix filled in by Respondent 2

Concept-scoring Matrix - Respondent 2		0 - Do nothing		1 - Separate into size fractions		2 - Repurpose for other AM technologies		3 - Reform into an alternative format		4 - Separation of different metal powders		5 - Reuse of conglomerates and support structures		6 - Embedding powder within a matrix		7 - Grading powders through flowability		8 - Adjustment of laser settings and coating arm speed		9 - Regrading by powder supplier	
		Rating	Weighted Score	Rating	Weighted Score	Rating	Weighted Score	Rating	Weighted Score	Rating	Weighted Score	Rating	Weighted Score	Rating	Weighted Score	Rating	Weighted Score	Rating	Weighted Score	Rating	Weighted Score
Reduces virgin powder purchasing	0.050	1	0.05	4	0.2	3	0.15	4	0.2	1	0.05	2	0.1	1	0.05	4	0.2	4	0.2	2	0.1
Improves longevity of powder	0.250	1	0.25	5	1.25	4	1	3	0.75	2	0.5	2	0.5	2	0.5	4	1	4	1	3	0.75
Maintains quality of produced component	0.100	3	0.3	4	0.4	3	0.3	3	0.3	2	0.2	2	0.2	3	0.3	2	0.2	4	0.4	4	0.4
Identifies use for EoL powder	0.280	1	0.28	3	0.84	4	1.12	4	1.12	3	0.84	1	0.28	4	1.12	2	0.56	1	0.28	3	0.84
Improves yield/reduces scrap	0.050	1	0.05	4	0.2	4	0.2	4	0.2	3	0.15	4	0.2	4	0.2	3	0.15	4	0.2	3	0.15
Energy savings	0.050	2	0.1	3	0.15	4	0.2	3	0.15	3	0.15	4	0.2	3	0.15	3	0.15	3	0.15	3	0.15
Ease to establish/set up	0.050	5	0.25	1	0.05	2	0.1	2	0.1	1	0.05	3	0.15	3	0.15	2	0.1	4	0.2	2	0.1
Expected cost of solution	0.010	1	0.01	3	0.03	3	0.03	3	0.03	1	0.01	2	0.02	3	0.03	3	0.03	3	0.03	2	0.02
Monetary savings/profit once established	0.100	1	0.1	4	0.4	4	0.4	4	0.4	3	0.3	3	0.3	4	0.4	2	0.2	4	0.4	2	0.2
Risk of powder contamination and oxidisation	0.010	1	0.01	1	0.01	2	0.02	2	0.02	1	0.01	2	0.02	4	0.04	1	0.01	3	0.03	3	0.03
Powder risk assessment	0.050	1	0.05	3	0.15	1	0.05	2	0.1	1	0.05	1	0.05	1	0.05	1	0.05	2	0.1	3	0.15
Final score	-	1.45		3.68		3.57		3.37		2.31		2.02		2.99		2.65		2.99		2.89	
Ranking	-	10		1		2		3		8		9		4=		7		4=		6	

Table 3-4 – Concept-scoring matrix filled in by Respondent 3

# Concept-scoring Matrix - Respondent 3

Selection Criteria		0 - Do nothing		1 - Separate into size fractions		2 - Repurpose for other AM technologies		3 - Reform into an alternative format		4 - Separation of different metal powders		5 - Reuse of conglomerates and support structures		6 - Embedding powder within a matrix		7 - Grading powders through flowability		8 - Adjustment of laser settings and coating arm speed		9 - Regrading by powder supplier	
		Rating	Weighted Score	Rating	Weighted Score	Rating	Weighted Score	Rating	Weighted Score	Rating	Weighted Score	Rating	Weighted Score	Rating	Weighted Score	Rating	Weighted Score	Rating	Weighted Score	Rating	Weighted Score
Reduces virgin powder purchasing	0.100	1	0.1	2	0.2	2	0.2	2	0.2	3	0.3	4	0.4	2	0.2	3	0.3	3	0.3	2	0.2
Improves longevity of powder	0.150	1	0.15	3	0.45	4	0.6	2	0.3	4	0.6	3	0.45	3	0.45	3	0.45	4	0.6	3	0.45
Maintains quality of produced component	0.125	3	0.375	2	0.25	3	0.375	3	0.375	2	0.25	2	0.25	4	0.5	2	0.25	4	0.5	5	0.625
Identifies use for EoL powder	0.175	1	0.175	1	0.175	5	0.875	5	0.875	2	0.35	3	0.525	5	0.875	2	0.35	1	0.175	4	0.7
Improves yield/reduces scrap	0.100	1	0.1	3	0.3	4	0.4	4	0.4	4	0.4	5	0.5	5	0.5	2	0.2	3	0.3	4	0.4
Energy savings	0.075	3	0.225	3	0.225	3	0.225	2	0.15	3	0.225	4	0.3	3	0.225	3	0.225	2	0.15	1	0.075
Ease to establish/set up	0.050	5	0.25	4	0.2	1	0.05	4	0.2	4	0.2	3	0.15	3	0.15	3	0.15	4	0.2	1	0.05
Expected cost of solution	0.050	5	0.25	2	0.1	4	0.2	4	0.2	5	0.25	3	0.15	4	0.2	3	0.15	4	0.2	2	0.1
Monetary savings/profit once established	0.050	3	0.15	3	0.15	3	0.15	4	0.2	3	0.15	4	0.2	3	0.15	4	0.2	3	0.15	2	0.1
Risk of powder contamination and oxidisation	0.075	3	0.225	3	0.225	2	0.15	3	0.225	4	0.3	2	0.15	4	0.3	3	0.225	3	0.225	1	0.075
Powder risk assessment	0.050	5	0.25	3	0.15	2	0.1	3	0.15	3	0.15	2	0.1	2	0.1	3	0.15	3	0.15	1	0.05
Final score	-	2.25		2.425		3.325		3.275		3.175		3.175		3.65		2.65		2.95		2.825	
Ranking	-	10		9		2		3		4=		4=		1		8		6		7	

Respondent 1 completed the matrix analysis in the early stages of the project. Respondent 2 and Respondent 3 completed their versions after Respondent 1. This led to the initial direction of the project being determined by Table 3-2 (see Chapter 3.4), allowing continuation of work whilst the later matrices were completed. Table 3-2 shows the necessity for something to be done about the current practice of doing nothing with EoL powder, as this scored 21% lower than the weakest alternative and 36% lower than the strongest solution. The three highest scoring solutions scored well in different areas, indicating that no one solution will achieve all the desired outcomes, but in fact several solutions combined may yield the best result.

The later provision of matrices by Respondent 2 and Respondent 3 provided a different perspective on the optimal solutions. The highest scoring solutions highlighted by Respondent 3 identified uses for EoL powder and reduced waste. Embedding the metal powder within a matrix was identified as the favoured solution, confirming the initial findings by Respondent 1. Reusing support structures and conglomerate particles, the solution that had already been carried forward, ranked fourth. Respondent 2 had very different weightings to the other respondents, possibly explaining the difference in their identified best solutions. Separating the powder into size fractions scored highest, with some of the other solutions proposed by Croft AM also scoring highly. Reuse of support structures and conglomerates scored lowest of all the new solutions. Completion of these matrices gave insight into which of the multiple project objectives were the most important to Croft AM.

*Table 3-5 – Average scores and rankings based on the completed concept-scoring matrices*

Average scores	0 - Do nothing	1 - Separate into size fractions	2 - Repurpose for other AM technologies	3 - Reform into an alternative format	4 - Separation of different metal powders	5 - Reuse of conglomerates and support structures	6 - Embedding powder within a matrix	7 - Grading powders through flowability	8 - Adjustment of laser settings and coating arm speed	9 - Regrading by powder supplier
Respondent 1	2.25	2.65	3.025	3.375	3.225	3.3	3.45	3.075	3.225	3.15
Respondent 2	1.45	3.68	3.57	3.37	2.31	2.02	2.99	2.65	2.99	2.89
Respondent 3	2.25	2.425	3.325	3.275	3.175	3.175	3.65	2.65	2.95	2.825
Average scores	1.98	2.92	3.31	3.34	2.90	2.83	3.36	2.79	3.06	2.96
Ranking	<b>10</b>	<b>6</b>	<b>3</b>	<b>2</b>	<b>7</b>	<b>8</b>	<b>1</b>	<b>9</b>	<b>4</b>	<b>5</b>

Table 3-2, Table 3-3 and Table 3-4 led to the creation of Table 3-5, showing the average scores for each solution. The top three solutions scored remarkably closely to one another and were a comfortable margin ahead of the other suggested solutions. All three solutions identified a use for the EoL powder, indicating that this was the most important objective of the current research.

The matrices simply identified which solutions were most likely, at an early stage, to yield the desired results for Croft AM and the AM industry. Some concepts are not developed in this work due to time constraints or low matrix scores, but should not be discounted in future research. The foundations have been laid in Chapters 3.1 and 3.2 to allow others to explore the viability of any proposed solution.

The concept-scoring matrix was only an indication of potential and was not to be rigidly followed. New findings throughout the research could prompt changes to the matrices, identify a solution not currently assessed in the matrix, or a seemingly viable solution may prove to be ineffective. The concept-scoring matrix and feasibility analysis could be continually referred to throughout the project to identify which solutions may be useful, should a dead end be reached.

#### 3.4 Concepts carried forwards

Until Respondent 2 and Respondent 3 had completed the concept-scoring matrix, it was decided that project resources should not be spent. The decision of which solution to further investigate at the early stages was therefore governed by the ability to perform initial experiments with the resources already available to both Croft AM and Lancaster University at minimal cost. Should this solution show promise, it was to be further investigated using project resources.

Table 3-2 identified embedding powders within a matrix as the strongest solution by Respondent 1. Despite only being beneficial to AM users utilising low-cost powders, it fulfilled many of the objectives defined by Croft AM. However, testing of this solution would have required equipment that was not available to Croft AM or Lancaster University, so was not pursued at an early stage.

Reforming metal powders into alternative feedstocks was the next strongest solution identified in Table 3-2. This prevented powders from going to waste and reduced the raw material consumption needed to produce components through other manufacturing processes. Neither Croft AM nor Lancaster University had facilities that would have melted the 316L stainless steel powder used by Croft AM. The difficulty of testing this solution led to it being rejected at the early stages.

The reuse of conglomerates and support structures to create a powder was identified as another strong solution by Respondent 1. Despite not identifying a use for EoL powder, there was potential for a large reduction in waste, as almost every single build used in SLM requires support structures or

heat sinks that are then scrapped. As the initial breakdown of support structures could be done with tools already available to Croft AM, this solution was carried forwards and further developed.

Plasma spheroidisation was identified as a solution after feasibility analysis of each prior solution had been conducted and the matrices completed. However, it was considered to be suitably similar to the “reforming metal powders into alternative feedstocks” concept, which scored highly in the concept-scoring matrices, indicating the potential in this solution. Following a meeting with Croft AM, it was decided that plasma spheroidisation was likely to be a good solution to prevent EoL powder from going to waste, whilst also reducing the necessity to produce new virgin powders. Regrettably, the timeframe of the project did not allow for this research avenue to be pursued, although experiments were set up to be continued independently by Croft AM.

## 4. Powder Analysis

The literature review in Chapter 2 confirmed that powder degradation occurs widely in the AM community. Croft AM had identified this in their own 316L stainless steel powders, noting that the reduced powder quality can affect the properties of the built component. Thorough understanding of the powder was necessary to understand when powder is no longer suitable for use by Croft AM's own standards, establishing a benchmark against which further research can be compared against.

### 4.1 Introduction

Many factors can influence the powder quality after each build. These may include the AM hardware used, percentage of the build chamber volume utilised, powder handling techniques and build parameters (LPW Technology Ltd, 2018a). This explains the variation in the rate of powder degradation within research, as these numerous factors are inconsistent. As such, there is reason to doubt that the findings in these papers will be representative of Croft AM's own powder degradation.

Croft AM do not currently know how their 316L stainless steel powder degrades using their own specific build parameters with the Realizer 250. There is limited information available within literature focusing on stainless steel powders within AM, making it hard to draw reliable inferences about how Croft AM's 316L stainless steel powder will degrade with continual reuse. It is therefore essential to analyse the powder properties of both the new and used powders that Croft AM utilise, establishing criterion that other powders can be compared against.

Analysis of other SLM users' powders gives Croft AM insight into how effective their current build parameters are at maintaining powder quality versus their competitors. Further to this, evaluation of these powders can show that this issue is not just internal to Croft AM, but impacts the wider AM community, validating the value of any research carried out to extend powder longevity and maintaining powder quality.

Currently, powder collected in the overflow region of the build chamber is of a questionable quality. Croft AM would like to determine if sieving this overflow powder and subsequent reintroduction to builds should be standard practice, as they are unsure if this affects build quality through a change in chemical composition. Further to this, it is currently unknown what can be done with the sieved out rejects from the overflow region. If they can be shown to be chemically similar to virgin powder, these particles could still be used in other manufacturing processes.

Croft AM have also observed that a “black powder” residue can form during the build process and have been unable to identify the cause of this. As this is seemingly unavoidable at this time, analysis of the black powder is essential to ensure that it is not impacting the quality of built components.

Croft AM provided ten different 316L stainless steel samples for analysis. Information about each sample can be seen in Table 4-1. Definitions of the descriptors used can be found in Table 4-2.

Table 4-1 – Powder details

Powder number	Powder details	Powder user
Powder 1	Virgin powder - UK83898 - produced by LPW	Croft AM
Powder 2	Used but “acceptable” powder	Croft AM
Powder 3	Heavily used powder	Croft AM / Liverpool John Moores University
Powder 4	Used – 1 cycle	Croft AM
Powder 5	Used – x cycles	EOS
Powder 6	Used – y cycles	LPW Technology Ltd
Powder 7	Single overflow powder	Croft AM
Powder 8	Double overflow powder	Croft AM
Powder 9	Re-sieved overflow powder	Croft AM
Powder 10	Black powder	Croft AM

Table 4-2 – Powder descriptors

Powder label	Description
Virgin	Directly from the manufacturer, as sold; has never been used in the AM process
Used	Has been put through the SLM process a number of times, as indicated
Heavily used	Highly unlikely to be suitable for further use in SLM
Acceptable	Suitable for use in the SLM process
Single overflow	Taken from the excess powder that accumulates at the sides of build chamber as powder is spread by the recoating arm
Double overflow	Particles from the single overflow powder that did not pass through the 53µm sieve
Re-sieved overflow powder	Particles from the single overflow powder that have successfully passed through the 53µm sieve
Black powder	Powder taken from sooty-coloured deposits that are seen in the Realizer 250 operated by Croft, near the build region

Powder 5 and Powder 6 are from an alternative supplier. These powders were used an unknown number of times prior to being analysed. As they were not produced for Croft AM directly, the powder could have been manufactured to a different specification, such as a different PSD or sphericity of the virgin powder. Without knowledge of these samples as virgin powder, there is no way to ascertain how many builds this powder has been run through.

Powder 2 and Powder 3 have been through an unknown number of builds, making the rate of degradation of Croft AM's powder difficult to discern. Instead, it is possible to use these powders as benchmarks for other powders to be compared against, indicating their suitability for use within AM.

No information has been provided regarding the number of uses of Powders 7-10. The interest in these powders was to determine the properties of Powder 8 and Powder 9 as a derivative from Powder 7, with Powder 9 being considered for use in AM. Powder 10 is a standalone interest.

In order to compare these powder properties, procedures were taken from ASTM Standard 52907, 2019. This identified several powder properties that required measuring for a complete analysis of the powder. However, time constraints mean that only PSD, chemical composition and particle morphology were measured. The impact of each of these within the AM procedure is discussed in Chapter 2.3.

As metal powders used in SLM typically contain particles between 15µm to 45µm, they cannot be easily visualised using standard light microscopes. Inspection of the powders with the naked eye gives a general idea of the powder quality, but only when gross changes are observed between two powders. This can be seen in Figure 4-1. Coarser particles are seen in the double overflow powder, indicating poorer quality powder, but it is impossible to discern the particle size distribution, particle morphology or chemical composition from visual inspection alone.



*Figure 4-1 – Visual comparison of 316L stainless steel metal powders. Left: virgin powder. Right: double overflow powder*

Scanning electron microscopy (SEM) allows images of particles as small as microns to be obtained and visually analysed. Electrons are fired at the sample, producing signals that are detected and interpreted in the form of images. This makes SEM the optimum tool to visualise AM powders, giving an overview of the PSD and particle morphology at low magnifications. SEM images at higher magnifications can indicate sphericity and more detailed particle morphology. Quantitative analysis of the PSD can be carried out using specific imaging software.

Energy-Dispersive x-ray Spectroscopy (EDS) measures x-rays emitted from atoms when hit by charged particles, producing a histogram of the wavelengths detected. As each atom emits characteristic wavelengths, analysis of an EDS spectrum gives insight into the chemical composition of a specimen. This can be used in tandem with SEM, choosing a specific site on the sample using the SEM image and carrying out EDS analysis of that location, giving the chemical composition of the selected site.

## 4.2 Methodology

SEM imaging was carried out using a JEOL JSM-7800F Schottky Field Emission Scanning Electron Microscope with an acceleration voltage of 15kV. Samples were prepared in a clean environment, adhering a single layer of metal powder to a stub using a carbon adhesive pad. Any excess powder was blown away with a gas gun filled with inert gas. During SEM analysis, at least two random sites of each sample were chosen and imaged, starting at x60 magnification and progressing through x140, x400 and x1000 magnification. Sites of interest were typically magnified, such as conglomerates, contaminated particles or partially melted particles. These images were visually inspected, qualitatively analysing the PSD, sphericity and presence of deformations/impurities of the particles. The morphology of particles was compared to Figure 4-2 to quantify these qualitative observations. This has been written in the format [roundness, sphericity] in text.

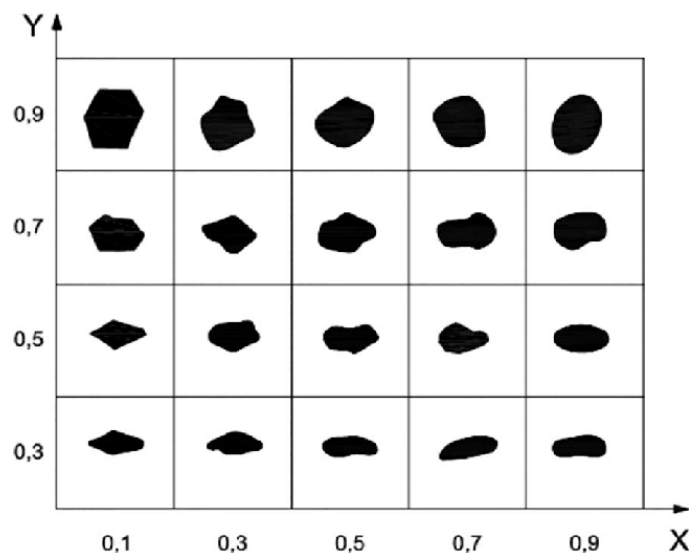


Figure 4-2 – Quantified particles to allow visual analysis of roundness (x) and sphericity (y) and (Krumbein and Sloss 1963)

EDS analysis was carried out alongside SEM imaging using an X-Max50, large area 50 mm<sup>2</sup> Silicon Drift Detector with an acceleration voltage of 15kV. EDS analysis of an entire image could not be carried out accurately due to the presence of the adhesive carbon pad the powder was secured with, as this would have shown an unnaturally high carbon peak. Instead, individual sites were analysed on images at x1000 magnification, intending to give a peak for “typical” particles in the sample, as well as any “atypical” particles. This made accurate analysis of the chemical composition of the powder sample difficult to achieve, as the definition of a “typical” particle is subjective. Further to this, only a small number of particles could be selected for analysis, making the results less representative of the entire sample. However, the chemical composition of individual sites could be compared against one another within the same powder with more certainty. Due to the sterile environment in which the samples were prepared, only the essential chemical constituents in 316L stainless steel were detected, removing the likelihood of the software misinterpreting peaks as similar elements that would almost certainly not be present.

Once the SEM images had been obtained, the image-processing software ImageJ (Rasband, 1997-2018) was used to determine the particle sizes from x140 magnification images. The only exception is for Powders 9 and 10, where the particles were too large, resulting in x60 magnification images being used. The data was imported to an Excel spreadsheet, where it was further manipulated. This was capable of analysing approximately 300 particles per image taken, giving a fair estimation of the PSD of the powder, which could be verified by visually comparing the results against the SEM image. Where several images were available, all images were analysed to improve the accuracy of the PSD curve obtained.

Once all the individual results had been collected, comparison was made between the various powders. Most powder samples were compared against Powder 1 to provide a benchmark, as virgin powder is typically considered preferable within the AM industry to recycled powder. Powder 2 was considered to be towards the bottom-end of acceptable powders. As such, the suitability of many lower-quality powders was assessed through comparison to Powder 2.

## 4.3 Results

### 4.3.1 SEM Imaging

#### Powder 1

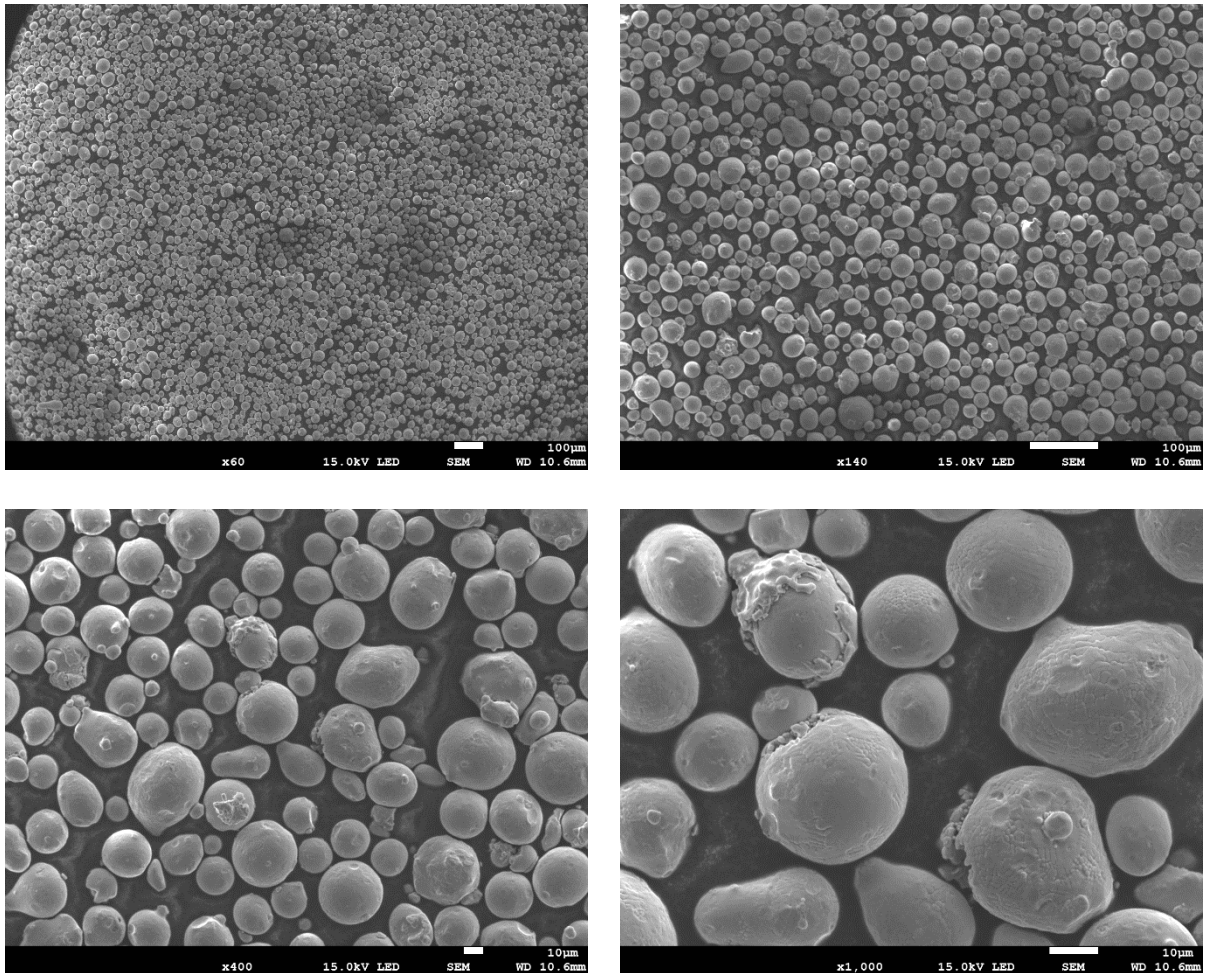


*Figure 4-3a (top left), Figure 4-3b (top right), Figure 4-3c (bottom left) & Figure 4-3d (bottom right) – x60, x140, x400 and x1,000 magnifications of Powder 1 (respectively)*

The virgin powder looks as expected from the SEM imagery. Figure 4-3a and Figure 4-3b show that particles are typically very spherical and round [0.9, 0.9], with a consistent size distribution. Figure 4-3c and Figure 4-3d show that some particles have satellite particles on them, amongst some other deformations such as partial melting. The majority of particles are, however, approximately spherical and have relatively few minor defects.

## Powder 2

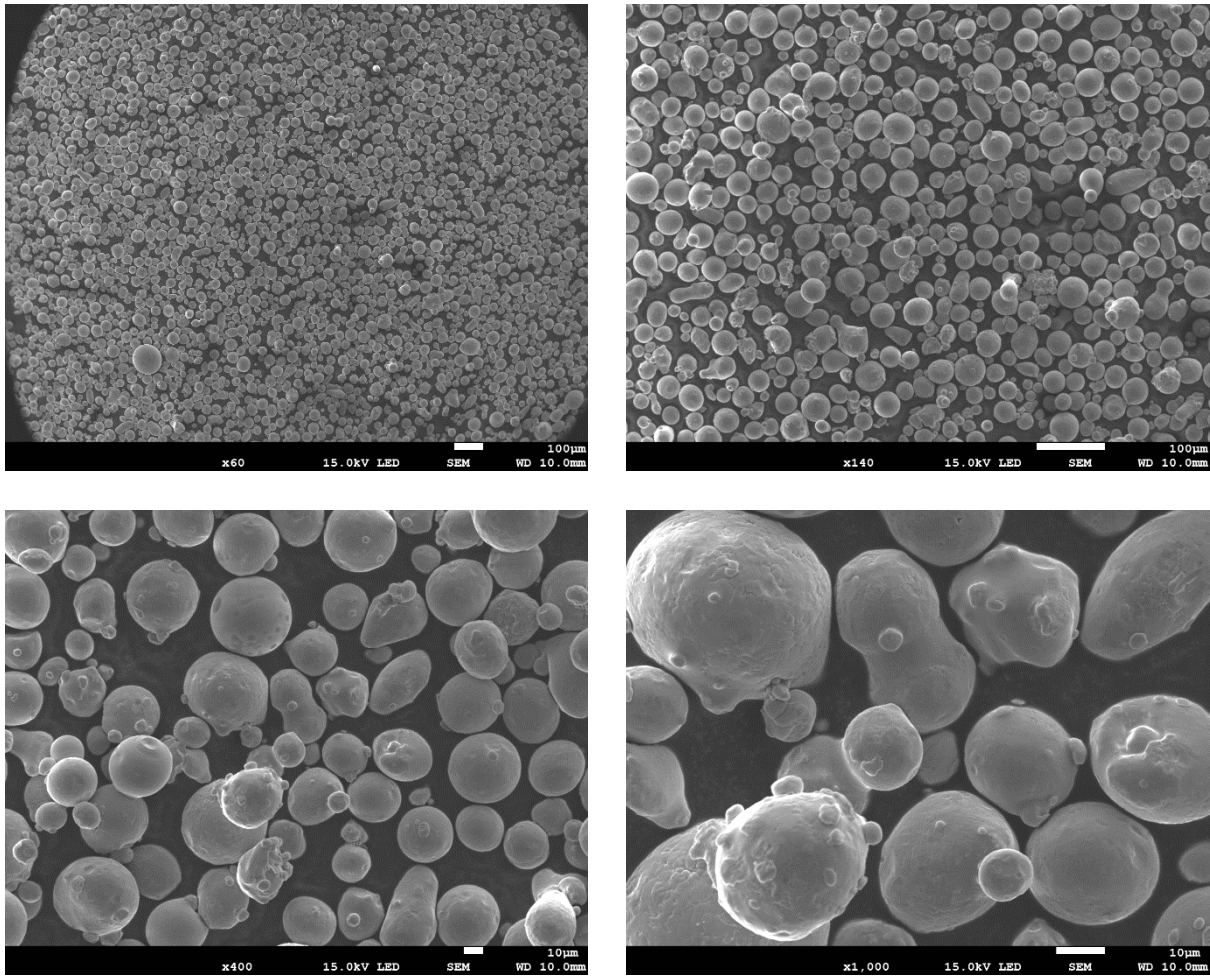


*Figure 4-4a (top left), Figure 4-4b (top right), Figure 4-4c (bottom left) & Figure 4-4d (bottom right) – x60, x140, x400 and x1,000 magnifications of Powder 2 (respectively)*

Powder that was deemed acceptable by Croft AM was observed to have similar particle sizings, albeit with a slightly higher number of oversized particles present, seen clearly in Figure 4-4a and Figure 4-4b. The vast majority of particles appear spherical [0.9, 0.9] and within the expected size range. Figure 4-4c and Figure 4-4d show that partially melted particles are increasingly common, causing larger and misshapen particles [0.7, 0.7], with the presence of satellite particles becoming more common.

## Powder 3

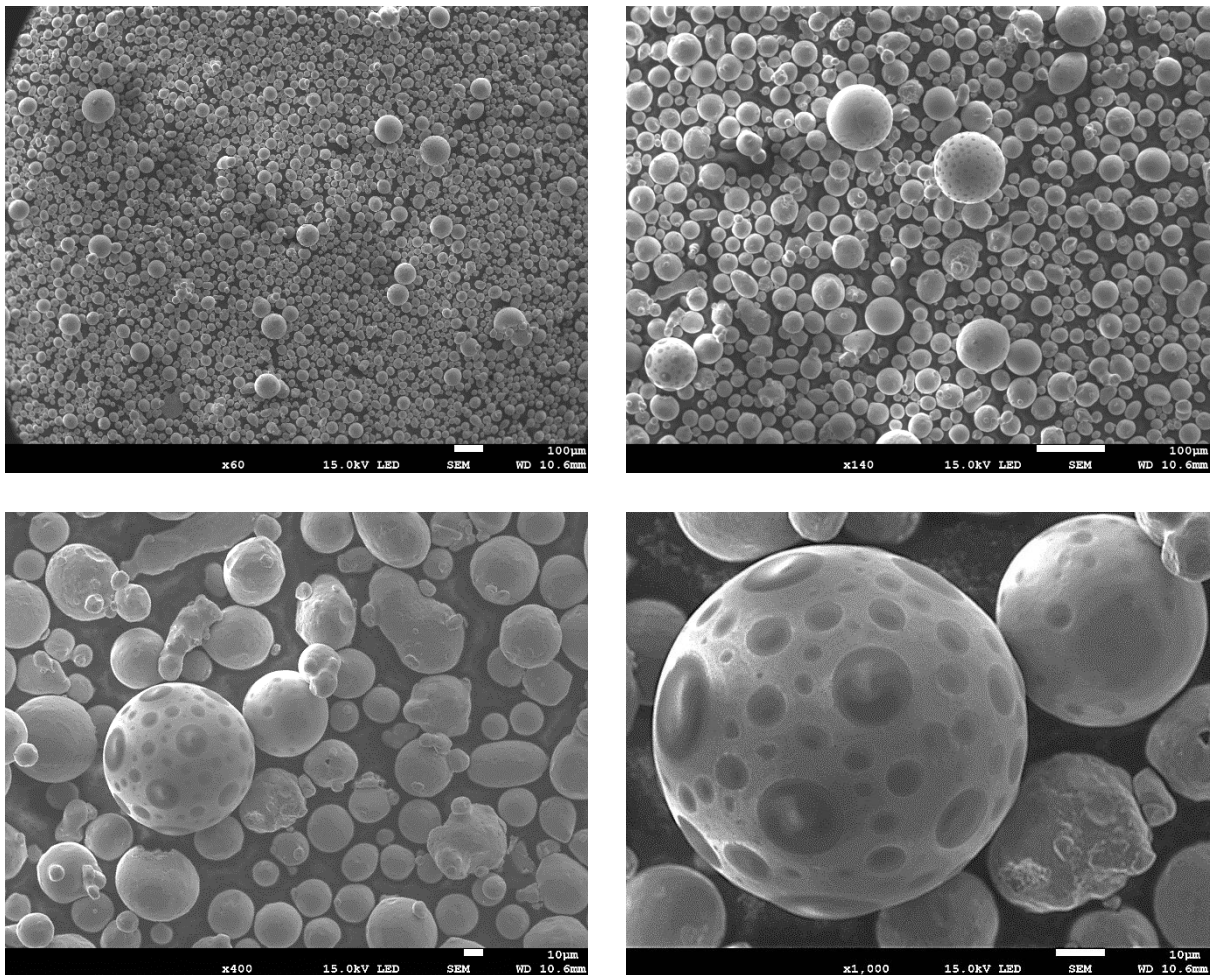


*Figure 4-5a (top left), Figure 4-5b (top right), Figure 4-5c (bottom left) & Figure 4-5d (bottom right) – x60, x140, x400 and x1,000 magnifications of Powder 3 (respectively)*

Figure 4-5a and Figure 4-5b immediately show that there are significantly more oversized particles within heavily used powder when compared with virgin powder or acceptable powder. Figure 4-5a and Figure 4-5b suggest that particles are still mostly spherical [0.9, 0.9], with few exceptions [0.9, 0.5]. Figure 4-5c and Figure 4-5d show that more particles are partially melted than in virgin or used but acceptable powder, with an increased presence of satellite particles on both partially melted and normal particles.

An effect that shall be referred to as “dotting” can be observed in this powder, seen in Figure 4-5d. Blister-like blackened marks appear on the surface of some particles, although the particle is still spherical and has no other notable deformations. This was seen on several particles within the sample across a range of SEM images.

## Powder 4

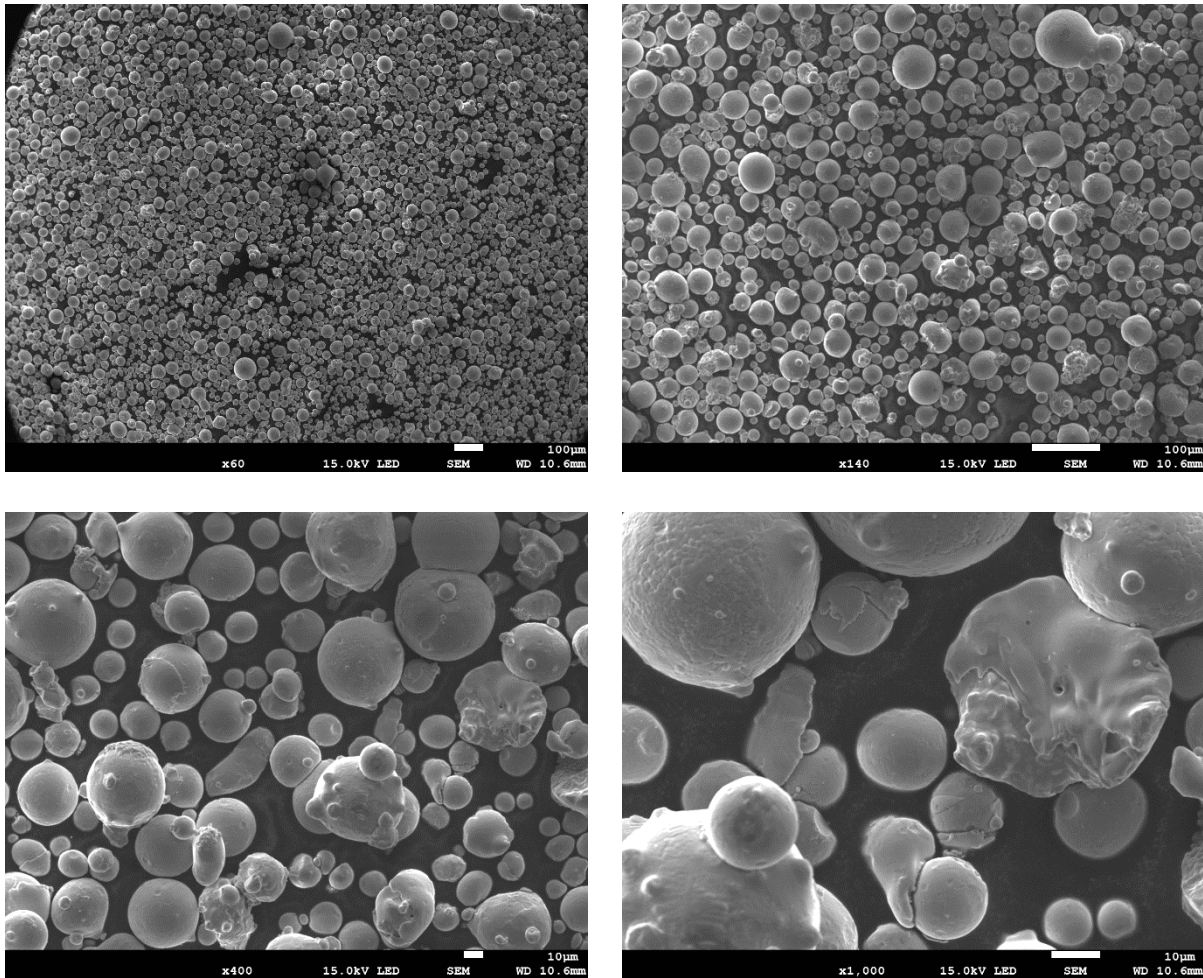


Figure 4-6a (top left), Figure 4-6b (top right), Figure 4-6c (bottom left) & Figure 4-6d (bottom right) – x60, x140, x400 and x1,000 magnifications of Powder 4 (respectively)

Powder that had only been used once by Croft AM looks remarkably similar to virgin powder in Figure 4-6a, with particles exhibiting a similar sphericity [0.9, 0.9] and only a few larger particles present. As the magnification increases, it becomes evident that many of the particles are generally larger than virgin powder, with misshapen particles becoming increasingly common [0.5, 0.7] and satellites occurring more frequently, seen in Figure 4-6b, Figure 4-6c and Figure 4-6d. The number of partially melted particles is higher than that of virgin powder, contributing to the reduced sphericity of particles.

Powder 5

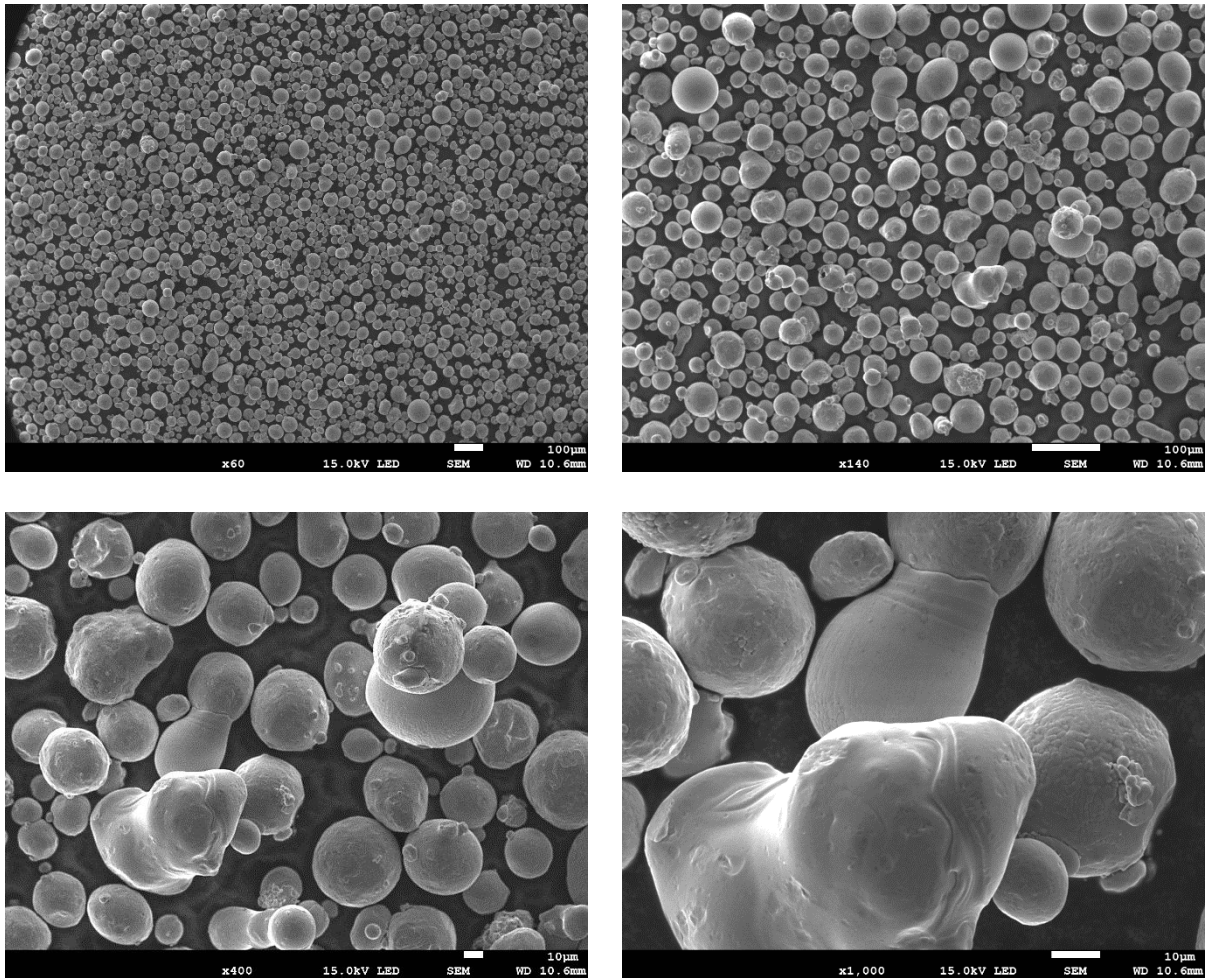
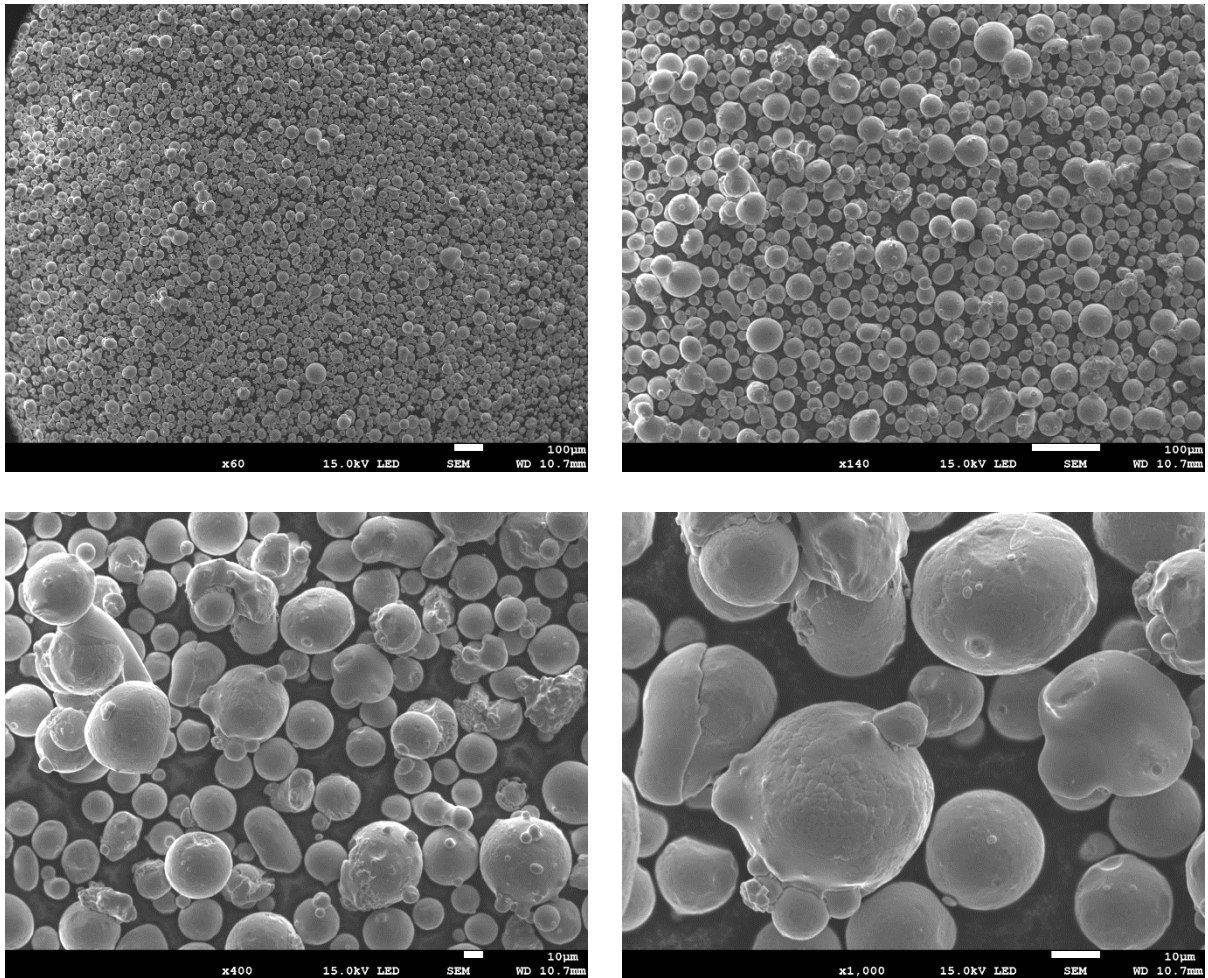


Figure 4-7a (top left), Figure 4-7b (top right), Figure 4-7c (bottom left) & Figure 4-7d (bottom right) – x60, x140, x400 and x1,000 magnifications of Powder 7 (respectively)

The powder sample supplied by Electro Optical Systems (EOS) was used an undisclosed number of times. In Figure 4-7a and Figure 4-7b, particles are seen to be similar in size to those in Powder 2, with few oversized particles. Figure 4-7c and Figure 4-7d reveal that particles are typically slightly larger than particles in Powder 2, with a similar number of partially melted and agglomerate particles adhering to satellite particles. Few particles are seen in the pristine spherical condition as would be expected from virgin powder, with many being deformed or partially melted [0.7, 0.7].

## Powder 6



*Figure 4-8a (top left), Figure 4-8b (top right), Figure 4-8c (bottom left) & Figure 4-8d (bottom right) – x60, x140, x400 and x1,000 magnifications of Powder 8 (respectively)*

The powder sample supplied by LPW Technology Ltd was also used an undisclosed number of times. Figure 4-8a and Figure 4-8b seem to indicate generally spherical particles [0.9, 0.9], with a slightly increased number of large particles when compared with Powder 2. Figure 4-8c and Figure 4-8d reveal many large partially melted and agglomerated particles [0.7, 0.7], seemingly more so than in Powder 5. An increased number of small sized particles can be seen when compared to that of Powder 2 and Powder 5.

## Powder 7

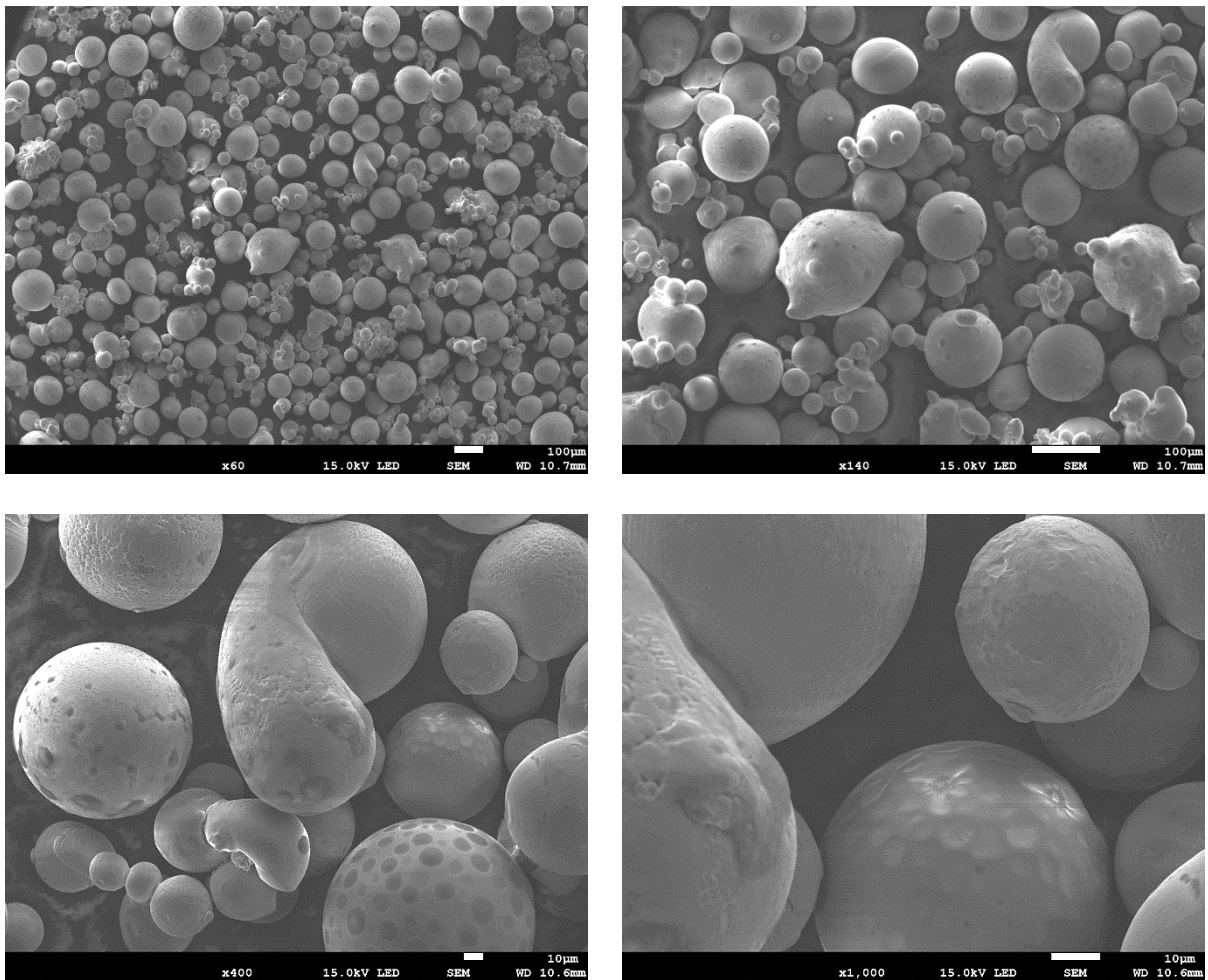


*Figure 4-9a (top left), Figure 4-9b (top right), Figure 4-9c (bottom left) & Figure 4-9d (bottom right) – x60, x140, x400 and x1,000 magnifications of Powder 9 (respectively)*

The single overflow powder seems to show a large variety of particle sizes, shapes and levels of deformation. Figure 4-9a and Figure 4-9b show that the majority of particles are significantly larger than Powder 2 and all other powders observed thus far, with various non-spherical shapes seen frequently [0.5, 0.7]. Figure 4-9c and Figure 4-9d further demonstrate this, showing highly agglomerated particles alongside misshapen particles. However, it can also be seen that there are a number of smaller and largely spherical particles dispersed amongst these large, misshapen particles. Dotting is observed in some of the particles in this powder, notably in Figure 4-9c, as seen previously in Powder 3. It can be seen at various stages of development, from half a particle through to the entire visible surface of a particle being covered.

## Powder 8

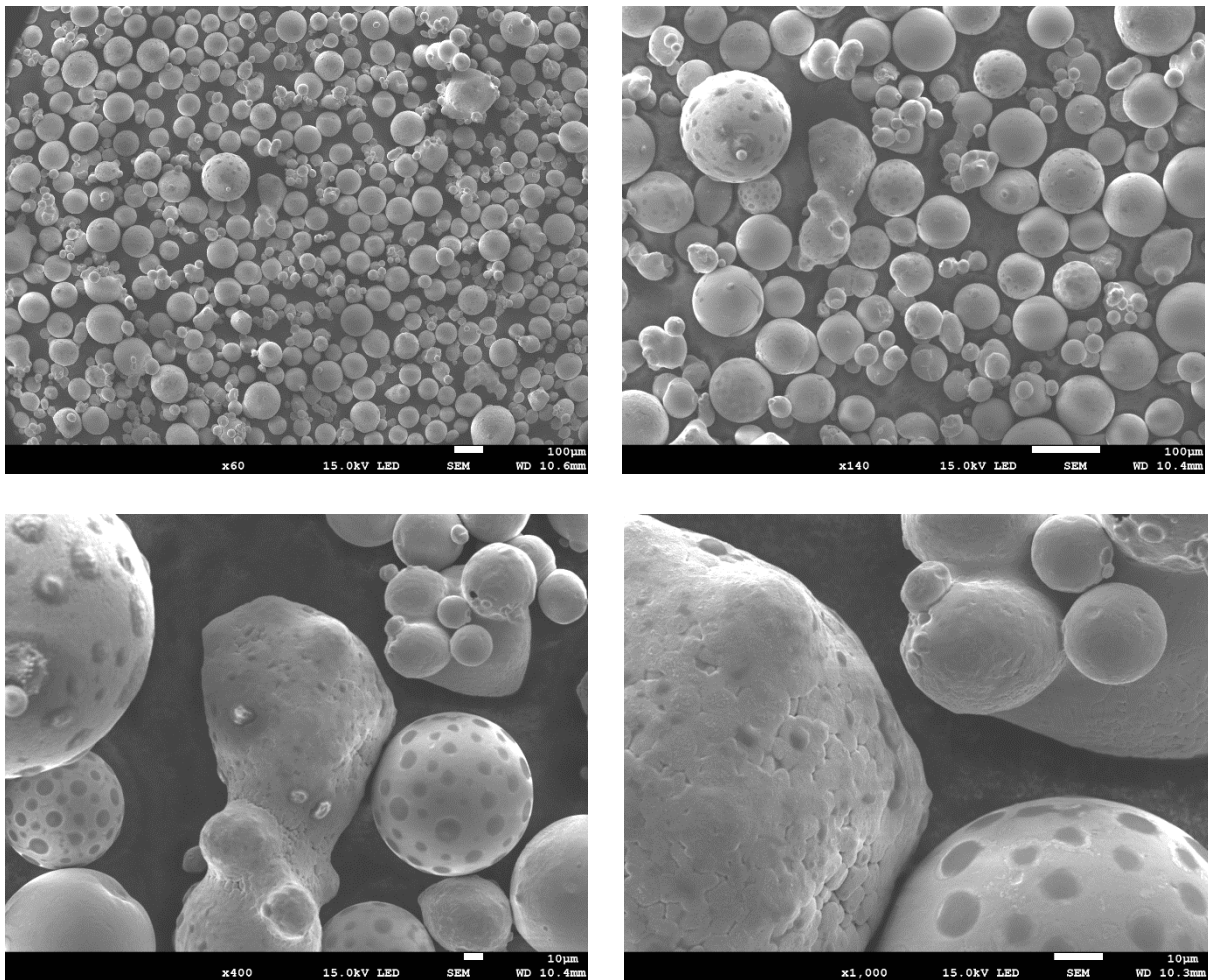


*Figure 4-10a (top left), Figure 4-10b (top right), Figure 4-10c (bottom left) & Figure 4-10d (bottom right) – x60, x140, x400 and x1,000 magnifications of Powder 10 (respectively)*

Powder 8 appears to be similar to Powder 7. The main difference is the reduction in the number of small particles dispersed between the larger and often misshapen particles, easily visualised in Figure 4-10a. Whilst some small particles are still present, they typically are part of an agglomerate particle, seen in Figure 4-10b. The majority of particles are noticeably larger than the 53 $\mu$ m sieve used. Partially melted and agglomerate particles are plentiful. Figure 4-10c shows that dotting can be witnessed in several particles in this powder sample, with slightly different blistering effects to the dotting seen previously, further shown in Figure 4-10d

## Powder 9

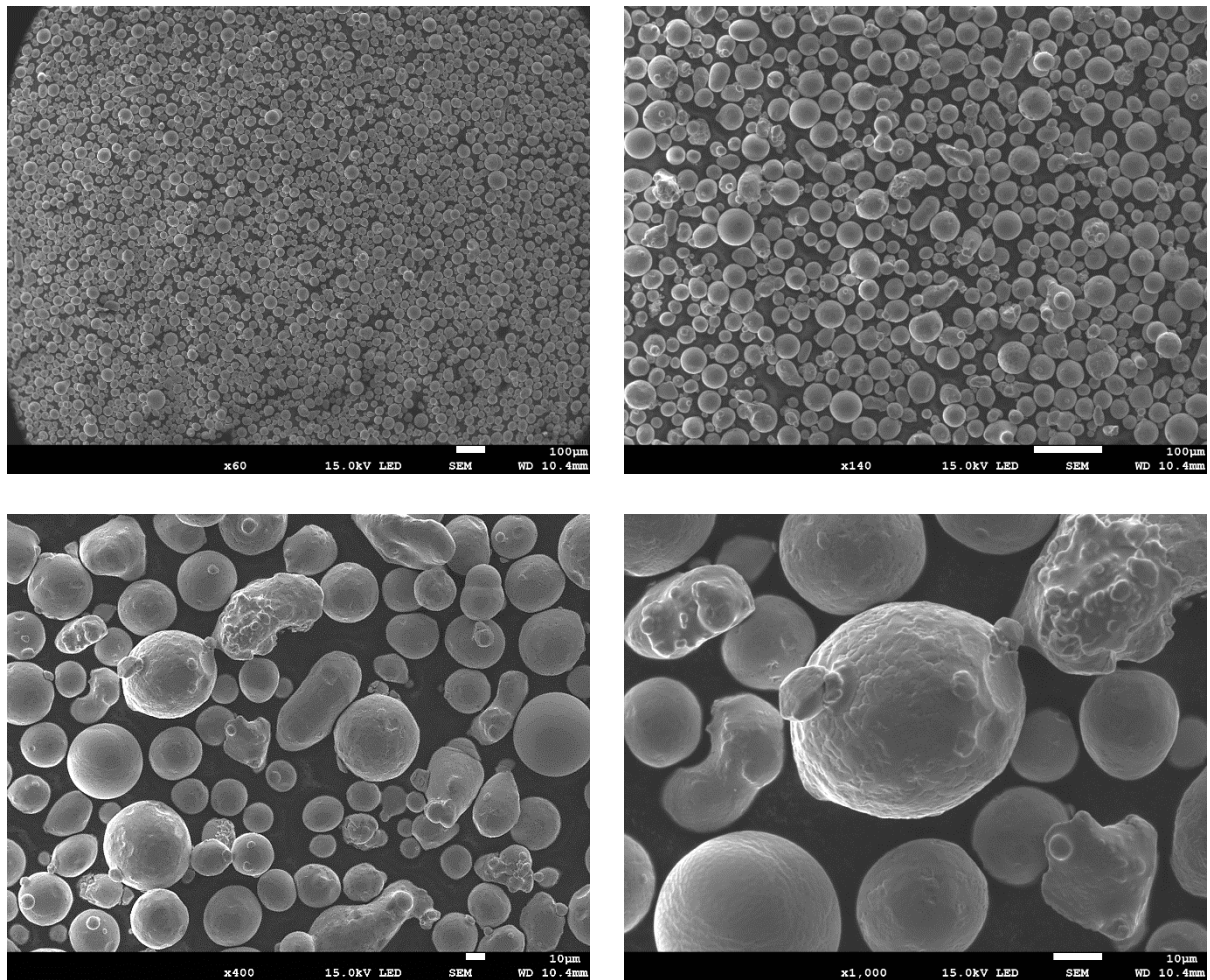


*Figure 4-11a (top left), Figure 4-11b (top right), Figure 4-11c (bottom left) & Figure 4-11d (bottom right) – x60, x140, x400 and x1,000 magnifications of Powder 11 (respectively)*

Figure 4-11a and Figure 4-11b indicate that the re-sieved overflow powder has a slightly increased number of larger particles than Powder 2. However, the particle size distribution seems to be otherwise similar to Powder 2 with similar quantities of misshapen particles, although these particles appear both rounder and more spherical [0.5, 0.9]. These misshapen particles, seen in Figure 4-11c and more closely in Figure 4-11d, are largely due to partial melting of the particles with some satelliting occurring, much like Powder 2, although the particles are seemingly less spherical in this powder. No particles that showed dotting were observed in this re-sieved overflow powder.

## Powder 10

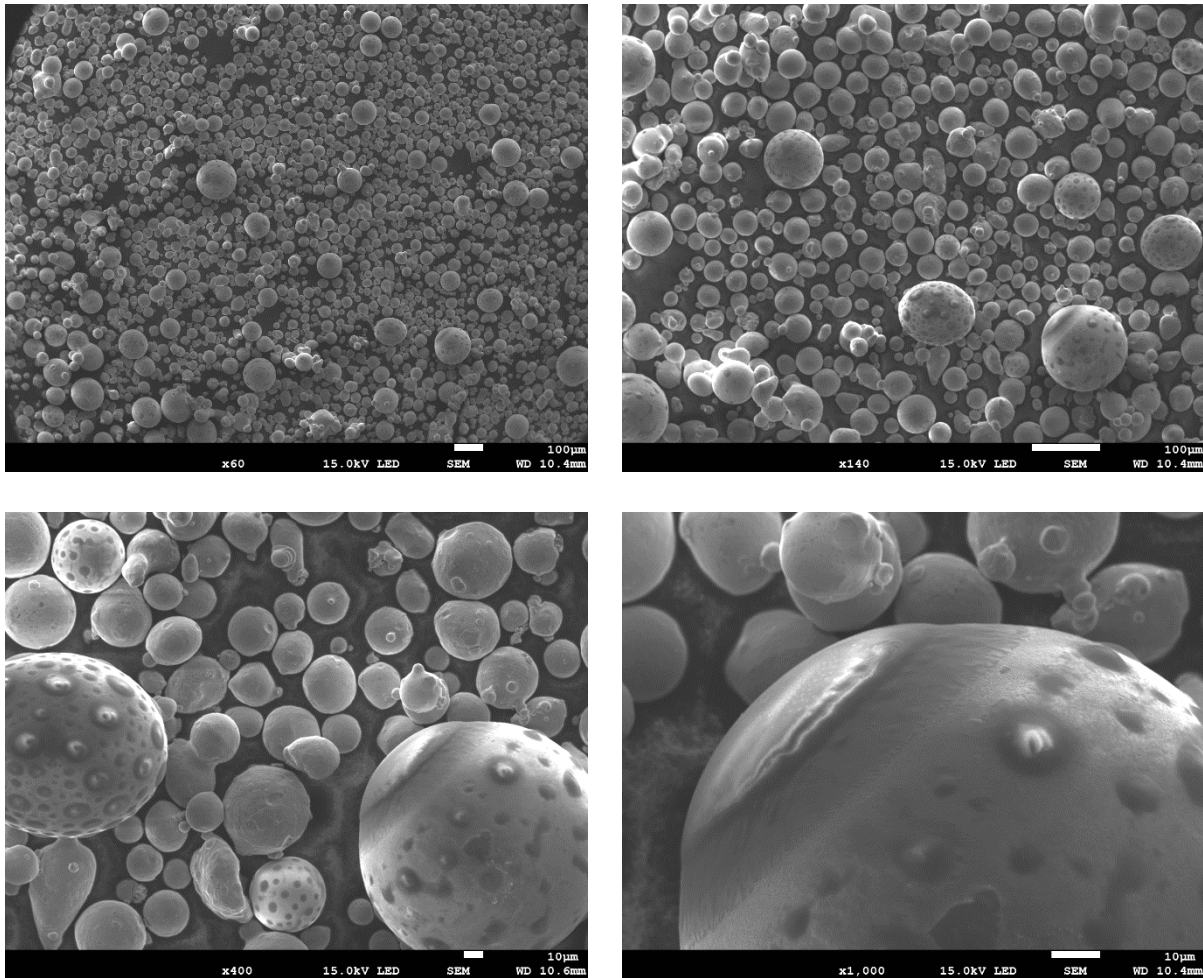


*Figure 4-12a (top left), Figure 4-12b (top right), Figure 4-12c (bottom left) & Figure 4-12d (bottom right) – x60, x140, x400 and x1,000 magnifications of Powder 12 (respectively)*

The black powder demonstrated a high volume of dotted particles, with some blisters observable from magnifications as low as x60, as in Figure 4-12a. Figure 4-12a and Figure 4-12b show that the majority of particles were round [0.9, 0.9] and, minus the relatively few large or deformed particles, the powder was similar in size range and level of deformation to Powder 2. Almost all of the large, spherical particles displayed dotting; it was not observed on any agglomerates or small particles. Different blistering effects can be seen in Figure 4-12c and Figure 4-12d when compared to the blisters observed in Powder 3.

### 4.3.2 EDS Analysis

Inconsistencies between results were observed in the EDS analysis of the powder samples. The expected atomic composition of 316L stainless steel was not always detected automatically by the software used. As such, where the element was “forced” to be displayed, the results are highlighted.

In some instances, there was a great deal of variation between the chemical composition of the same powder particles. EDS analysis was therefore deemed to be more appropriate to analyse the difference between regions of contamination within the powder and normal powder particles, rather than determining the bulk powder chemical composition, which could be obtained more reliably from Inductively Coupled Plasma - Optical Emission Spectrometry (ICP-OES). An indication of one powder when compared to another can be determined, but more reliable testing methods are required to compare powders with certainty.

Figure 4-13 through to Figure 4-22 show the sites where EDS analysis took place for all analysed powders. Table 4-3 through to Table 4-12 display the %Wt of each element analysed at each of these sites.

Powder 1

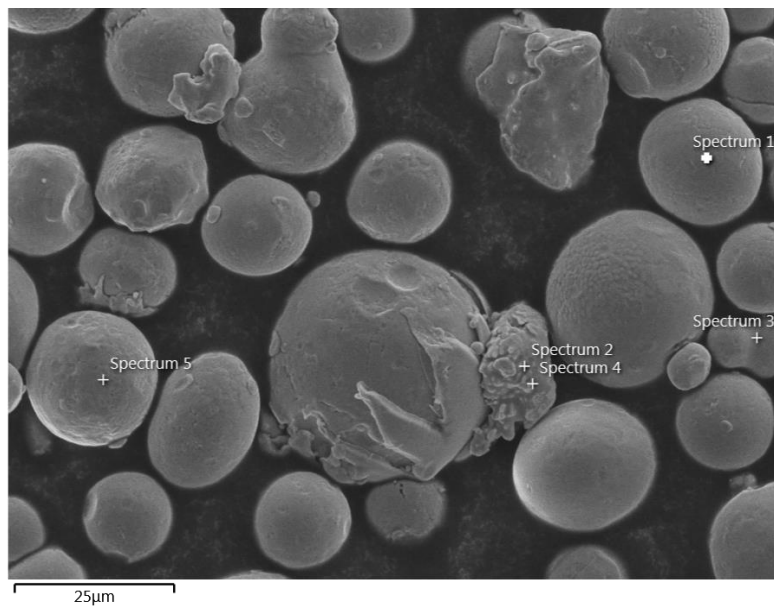


Figure 4-13 – EDS site locations for Powder 1

Table 4-3 – Chemical composition of each site in Figure 4-13

Spectrum #	1	2	3	4	5
Description	Normal	Agglomerate	Partly fused	Agglomerate	Normal
Wt%					
Fe	61.8	48.6	60.4	63.8	59.3
Cr	17.4	13.8	17.0	18.7	19.0
Ni	12.5	9.3	12.0	11.6	12.7
C	4.3	24.0	6.2	3.0	4.1
Mo	2.0	1.8	2.2	1.4	3.0
Si	0.7	0.5	0.7	0.2	0.8
O	0.7	1.5	0.9	0.5	0.7
Mn	0.6	0.4	0.6	0.8	0.4

The chemical composition of the virgin powder was recorded and analysed to set a benchmark for all results to be compared against. The chemical composition of “normal” particles is largely as expected, falling within specification for 316L stainless steel, with the notable exception of carbon, which is higher than expected. Readings for the chemical composition of agglomerate particles seemed to vary greatly, making it hard to reliably make inferences from Spectra 2 and 4.

Powder 2

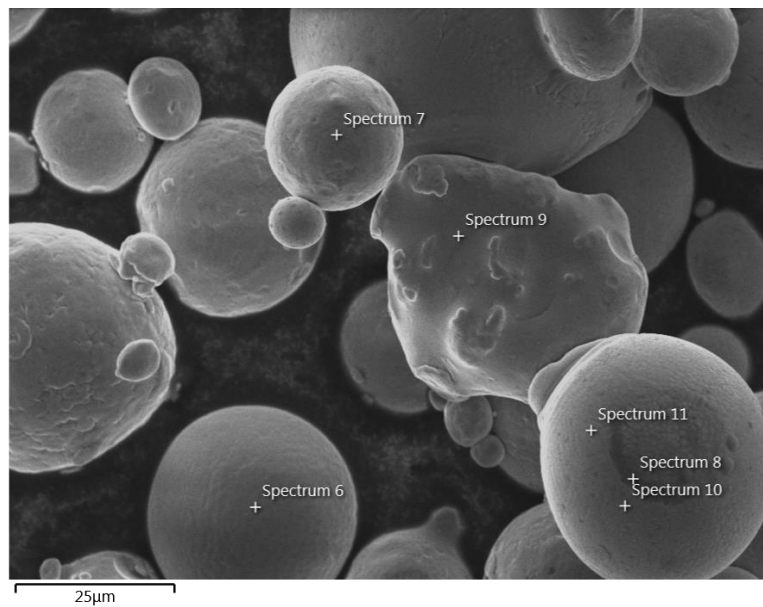


Figure 4-14 – EDS site locations for Powder 2

Table 4-4 – Chemical composition of each site in Figure 4-14

Spectrum #	6	7	8	9	10	11
Description	Normal	Normal	Darker patch	Partially melted particle	Outside dark patch - normal	Outside dark patch - normal
Wt%						
Fe	61.3	58.0	44.8	61.5	63.4	58.2
Cr	17.1	17.2	13.9	17.5	18.2	17.3
Ni	11.3	13.7	8.3	11.5	11.6	11.5
C	5.2	4.9	27.0	3.3	2.0	6.1
Mo	2.3	2.7	1.8	2.0	1.5	2.7
Si	1.1	0.6	0.5	0.7	0.3	0.8
O	1.4	1.6	2.6	1.8	1.5	2.1
Mn	0.4	1.3	1.1	1.8	1.4	1.2

An SEM image of Powder 2 showed the presence of a darker patch on a particle when compared to the rest of the particle. This dark patch was found to have a significantly increased carbon composition, increased oxygen content and a large reduction in iron, chromium and nickel. Normal particles were found to be similar to that of virgin powder, but had a consistently higher percentage of oxygen present.

Powder 3

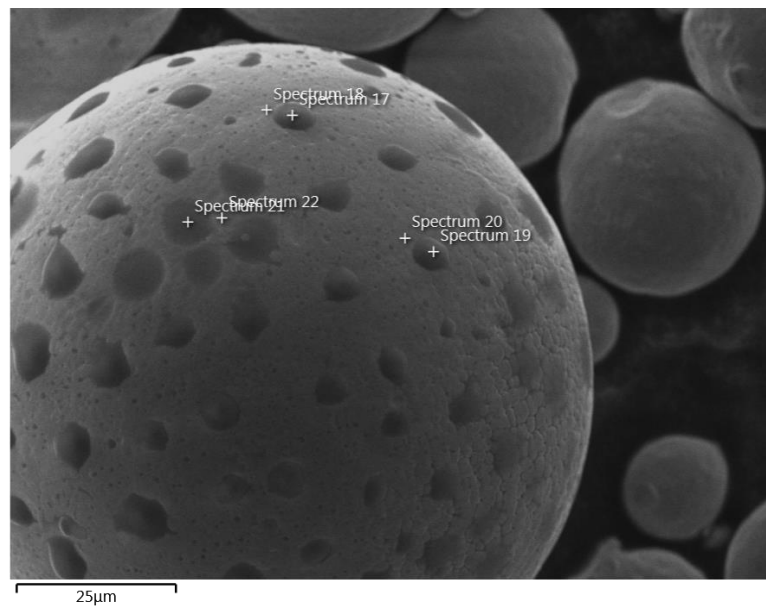


Figure 4-15 – EDS site locations for Powder 3

Table 4-5 – Chemical composition of each site in Figure 4-15

Spectrum #	17	18	19	20	21	22
Description	Dot	Non-dotted region	Dot	Non-dotted region	Dot	Non-dotted region
Wt%						
Fe	2.9	53.7	3.2	57.1	22.5	58.3
Cr	12.3	16.4	12.7	16.6	13.6	17.0
Ni	0.5	12.7	0.4	11.7	3.5	11.6
C	6.7	9.6	5.7	7.3	5.7	7.9
Mo	0.2	2.8	0.3	2.6	1.0	2.6
Si	16.1	0.9	16.6	0.8	11.2	0.7
O	43.2	2.9	41.2	2.7	29.8	1.1
Mn	18.1	1.0	19.8	1.3	12.6	0.9

EDS analysis of dotting in Powder 3 indicated that the blisters are almost devoid of iron, nickel and molybdenum. Instead, a grossly different chemical composition comprising of largely oxygen, followed by similar levels of silicon and manganese, formed at these blisters. Carbon content is also seen to decrease alongside the level of chromium. The non-blistered region of the particle seems to have picked up notable levels of oxygen and carbon when compared to that of Powder 1 and 2, with a similar decrease observed in iron.

Powder 4

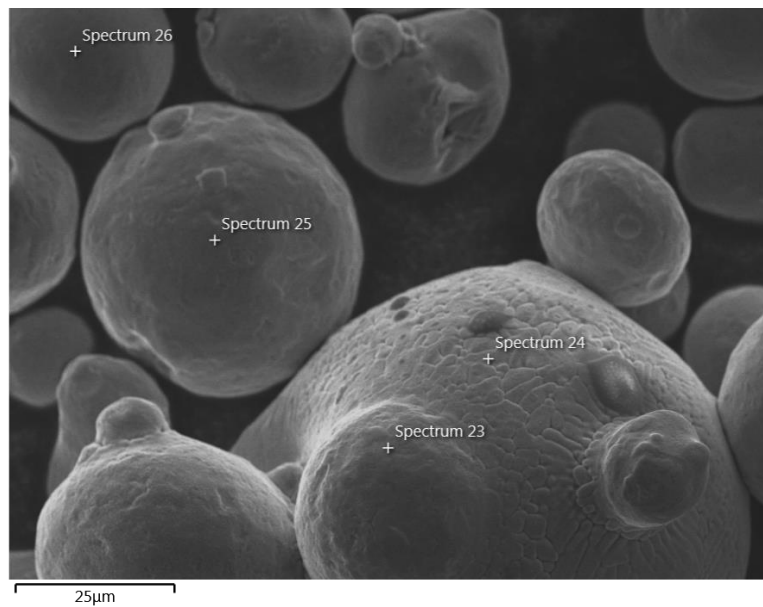


Figure 4-16 – EDS site locations for Powder 4

Table 4-6 – Chemical composition of each site in Figure 4-16

Spectrum #	23	24	25	26
Description	Partially melted	Partially melted	Fairly normal	Normal
Wt%				
Fe	50.1	50.5	61.1	61.1
Cr	15.9	16.1	17.7	17.2
Ni	9.8	9.6	11.0	11.9
C	9.5	9.4	4.7	5.0
Mo	2.2	2.1	2.3	2.1
Si	1.0	1.1	0.9	0.6
O	9.8	9.4	1.0	0.9
Mn	1.7	1.8	1.3	1.1

Where the powder has only been used once, no significant change is observed in the normal particles. EDS analysis does indicate that the partially melted particles can have large increases in the percentage of carbon and oxygen present, whilst iron, chromium and nickel levels decrease in these particles. This may not be the case for all agglomerate particles; the small data set makes it difficult to verify this indication.

Powder 5

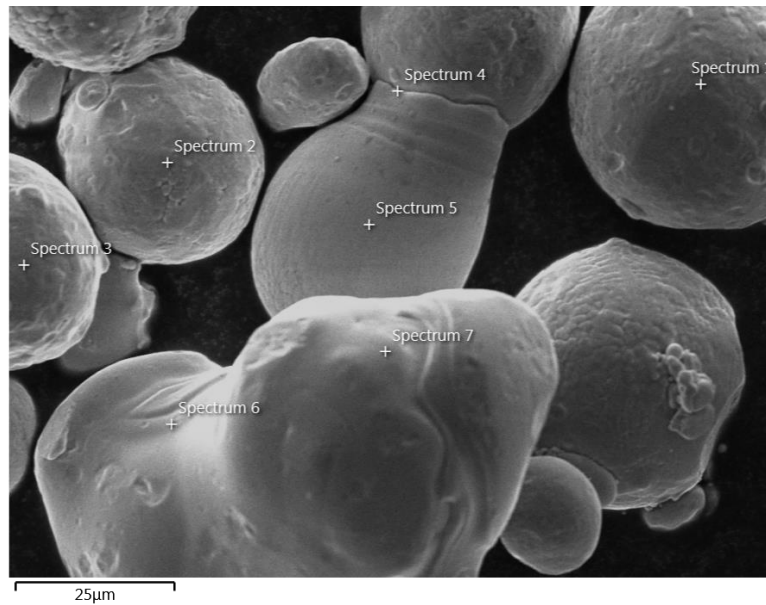


Figure 4-17 – EDS site locations for Powder 5

Table 4-7 – Chemical composition of each site in Figure 4-17

Spectrum #	1	2	3	4	5	6	7
Description	Normal	Fairly Normal	Fairly Normal	Fused, at point of fusion	Fused, on normal region of particle	Large melted particle	Large melted particle
Wt%							
Fe	58.4	59.4	58.3	54.7	58.0	55.2	54.6
Cr	17.8	18.0	17.6	16.9	17.7	17.0	17.2
Ni	13.5	13.2	13.6	10.3	11.9	12.0	12.4
C	4.5	3.7	4.7	9.6	5.5	8.7	9.6
Mo	2.6	2.7	2.7	2.1	2.2	3.2	3.0
Si	0.5	0.6	0.5	0.5	0.7	0.7	0.7
O	0.8	1.0	1.0	4.0	2.3	1.3	1.0
Mn	1.9	1.4	1.5	1.9	1.7	1.9	1.4

Powder supplied by EOS is best compared against Powder 2 used by Croft AM, as the number of uses is unknown and thus comparison against acceptable powder provides a reasonable benchmark. Iron levels are lower than in Powder 2, whilst nickel percentages appear higher. Otherwise, normal particles seem to have a similar composition to Powder 2.

Powder 6

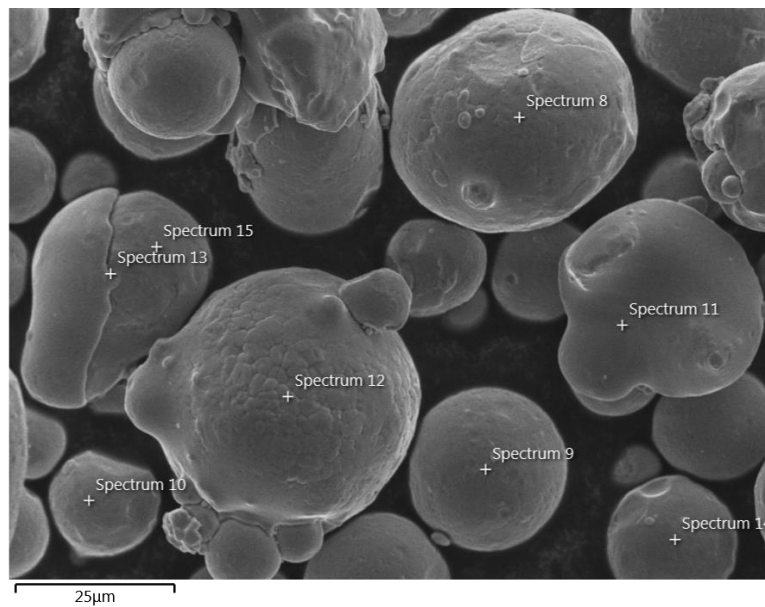


Figure 4-18 – EDS site locations for Powder 6

Table 4-8 – Chemical composition of each site in Figure 4-18

Spectrum #	8	9	10	11	12	14
Description	Normal, some satelliting	Normal	Fairly normal	Fairly normal, slightly deformed	Partially melted with agglomerates	Fairly normal
Wt%						
Fe	61.4	63.7	62.0	66.7	60.0	58.3
Cr	17.0	16.8	16.8	18.4	16.4	16.3
Ni	10.7	11.1	11.2	10.0	11.0	13.8
C	5.2	3.6	4.4	1.6	6.8	5.7
Mo	2.8	2.6	2.7	1.0	2.7	3.0
Si	0.5	0.4	0.5	0.2	0.6	0.7
O	1.1	0.7	0.9	0.3	1.2	0.8
Mn	1.4	1.2	1.5	1.8	1.2	1.4

Powder supplied by LPW Technology Ltd is also compared against Powder 2 used by Croft AM, as once again the number of uses is unknown. The chemical composition is highly similar to that of Powder 2 in all regards. This can be expected, as LPW Technology Ltd supply Croft AM with their metal powder.

Powder 7

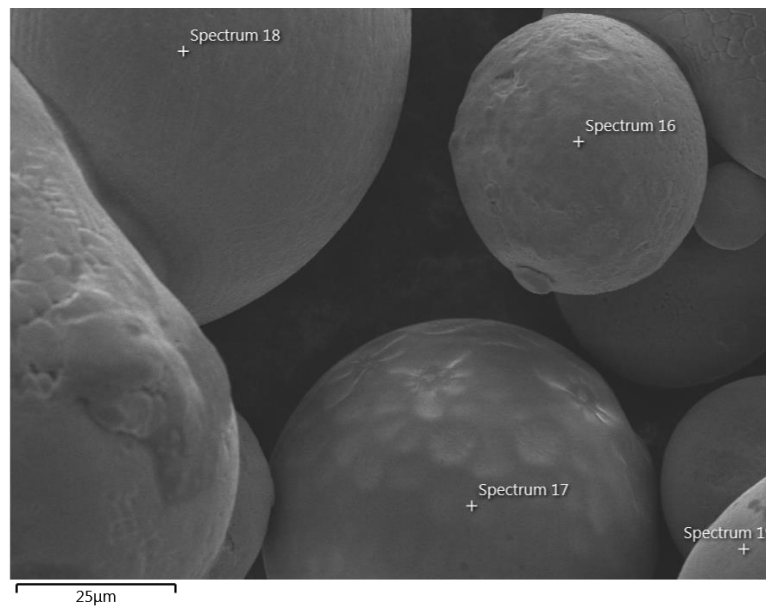


Figure 4-19 – EDS site locations for Powder 7

Table 4-9 – Chemical composition of each site in Figure 4-19

Spectrum #	16	17	18	19
Description	Normal, slightly cratered	Cratered particle	Normal large particle	Normal, slightly cratered
Wt%				
Fe	55.8	57.5	58.3	53.5
Cr	17.8	16.9	17.3	16.5
Ni	10.1	10.3	11.3	10.5
C	5.5	4.5	4.1	9.5
Mo	1.9	2.3	2.3	2.7
Si	1.0	2.8	0.6	1.2
O	5.7	4.9	5.1	4.5
Mn	2.4	0.8	1.1	1.7

Powder 7 does not seem to have many significant changes from Powder 1 and Powder 2, except that there is a significantly higher oxygen content, with a small reduction in the percentage of iron and nickel in the powder. The manganese content may be different, but the results vary too much to ascertain this. Whilst dotted particles were observed in the SEM images, they were not further analysed, as enough dotted particles had been analysed elsewhere.

Powder 8

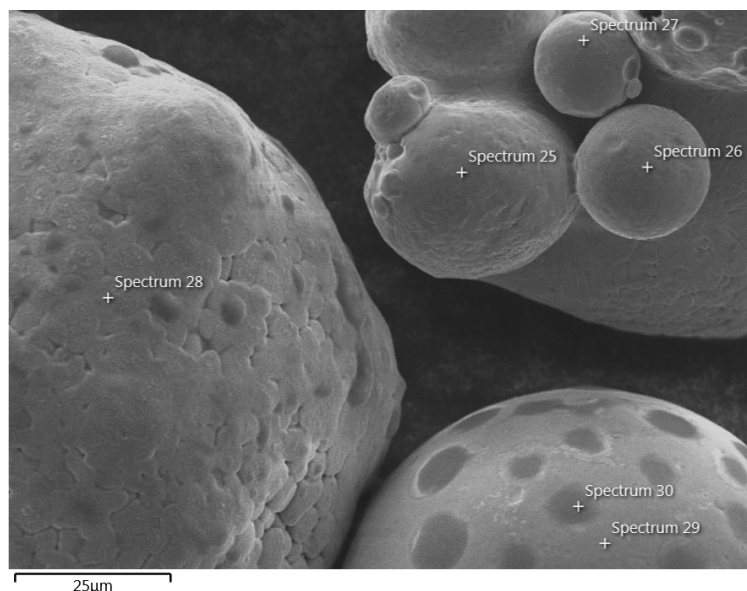


Figure 4-20 – EDS site locations for Powder 8

Table 4-10 – Chemical composition of each site in Figure 4-20

Spectrum #	25	26	27	28	29	30
Description	Agglomerate, partially melted fused satellite	Satellite, non-melted	satellite, non-melted	Partially melted particle	Dotted particle, not on dot	Dotted particle, dot
Wt%						
Fe	59.4	60.7	59.2	59.9	53.9	17.9
Cr	17.7	17.2	16.9	15.8	15.7	12.6
Ni	11.4	11.5	11.2	11.3	10.5	3.0
C	3.7	4.7	6.3	3.6	6.8	6.6
Mo	2.1	2.5	2.8	1.8	2.4	1.2
Si	0.8	0.8	0.9	0.7	2.9	11.8
O	3	1.6	1.2	5.7	6.6	33.4
Mn	1.8	1.0	1.5	1.2	1.3	13.4

EDS analysis of Powder 8 did not analyse any “normal” particles, as these were hard to identify. It was possible to determine the chemical composition of blisters in particles, confirming that oxygen is the most prevalent element present, causing vast reductions in the percentage of iron present. The quantity of silicon and manganese also rises in the blisters, whilst chromium and nickel become less prevalent. This behaviour was similar to Spectrum 22 in Powder 3 (see Table 4-5), suggesting these results are reliable. Besides the dotted particle, the chemical composition of the double overflow powder was similar to that of Powder 2. A slight reduction in the percentage of iron was coupled with a slight increase in manganese, whilst oxygen and carbon fluctuate too much to comment upon reliably. However, since this particle was not “normal”, it is hard to state that this is representative of the rest of the powder particles.

Powder 9

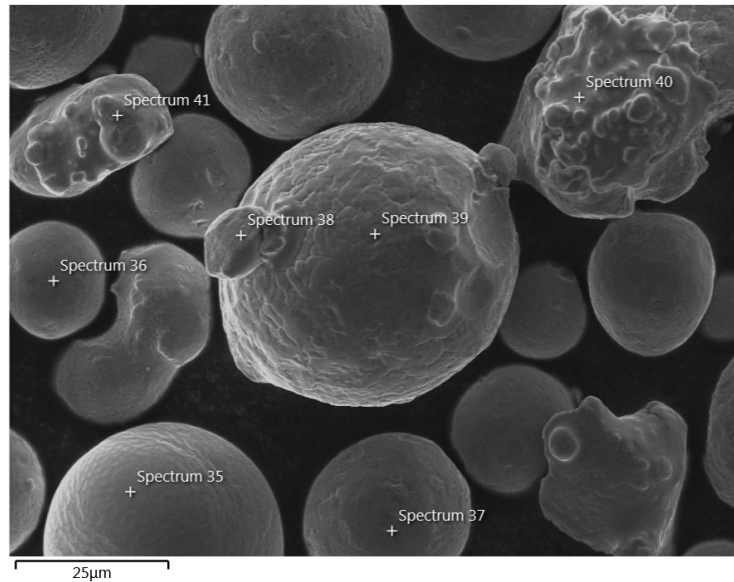


Figure 4-21 – EDS site locations for Powder 9

Table 4-11 – Chemical composition of each site in Figure 4-21

Spectrum #	35	36	37	38	39	40	41
Description	Normal	Normal	Normal, slightly rough	Satellite on rough agglomerate	Main body of rough agglomerate	Partially melted particle, x	Partially melted particle, y
Wt%							
Fe	56.8	58.4	62.1	57.3	59.6	56.6	60.3
Cr	16.5	17.5	19.6	16.7	17.8	17.1	17.3
Ni	11.1	13.0	10.6	11.3	12.3	12.0	11.5
C	7.8	5.3	3.4	8.4	5.5	8.1	6.0
Mo	2.6	2.4	1.4	2.6	2.1	2.7	2.3
Si	1.7	0.8	0.5	0.8	0.8	0.8	0.7
O	2.5	1.0	0.7	1.6	0.8	1.0	1.0
Mn	0.9	1.6	1.8	1.1	1.1	1.6	0.9

Re-sieved overflow powder had a similar composition to that of Powder 8. The exception is that the carbon percentage is notably higher in this powder compared to Powder 8. This similarity was unexpected, as the larger particles typically exhibited higher levels of light elements, such as oxygen and carbon. By removing these large particles in the sieving process, there was the expectation that the powder composition would be more similar to Powder 2, rather than Powder 7.

As there is intent to reuse Powder 9 particles in the SLM process, it is best to compare this powder against the acceptable Powder 2. The level of iron is below that of Powder 2, with carbon levels seeming to have increased. However, oxygen content in Powder 9 seems to be closer to the levels seen in Powder 1, indicating that this chemical composition of this powder lies in a region between virgin and used but acceptable powder.

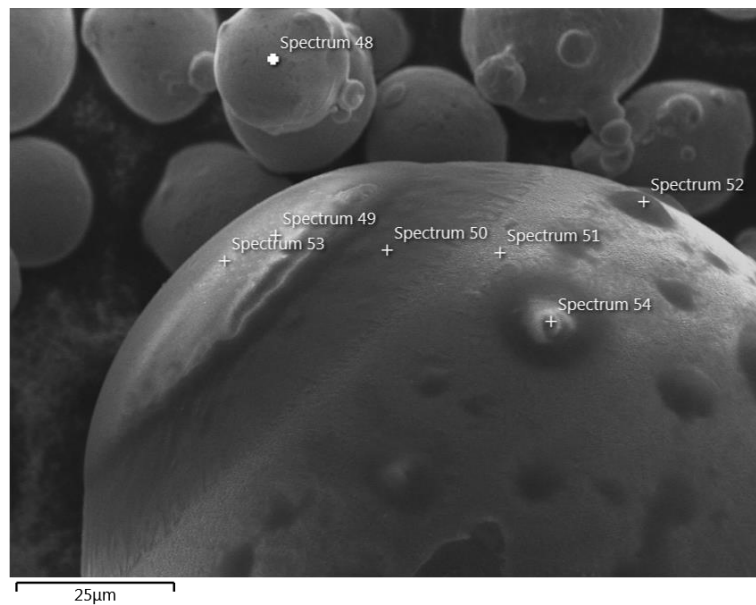


Figure 4-22 – EDS site locations for Powder 10

Table 4-12 – Chemical composition of each site in Figure 4-22

Spectrum #	48	49	50	51	52	53	54
Description	Fairly normal, satellite	Highly glazed region of large dot	Region between blister and rest of particle	Normal region of particle	Dark dot on particle	Highly glazed region of large dot	Light dot on particle
Wt%							
Fe	59.0	5.0	35.6	52.0	4.5	6.9	2.4
Cr	17.4	16.0	15.5	15.4	10.6	15.3	14.7
Ni	11.6	0.8	7.2	9.8	0.4	1.0	0.3
C	5.6	11.6	9.4	11.0	10.8	12.1	6.6
Mo	2.1	0.2	2.0	2.4	0.1	0.1	0.1
Si	1.0	12.5	5.6	0.4	14.0	12.3	15.6
O	1.4	44.7	20.1	7.9	42.7	43.0	43.9
Mn	1.8	9.2	4.7	1.0	16.9	9.2	16.3

The black powder had many irregular particles and dotted particles, as seen in Figure 4-12b, but one particularly large blister was analysed. The chemical composition of this large blister was found to be similar to that of other blisters, seen by comparing Spectra 49 and 53 with Spectrum 54. Oxygen levels were greatly increased, as seen in Powder 3 on the blisters, with iron, nickel and molybdenum almost completely absent. Silicon levels were also higher than previously seen. A particular region of interest in this EDS analysis was the region between the blister and the rest of the particle, shown by Spectrum

50. This showed the chemical composition of this region was somewhere between the chemical composition of the blistered region and that of the normal region of the particle, as expected.

It is of particular note that the chemical composition of the “normal” particle was similar to that of Powder 2. This indicates that the changes in the black powder seem to result from the blistered and dotted particles, which exhibit significantly higher carbon levels in Powder 10 than blisters in other powders. The small particles may therefore be suitable for reuse in the SLM process if they could be separated from these contaminated particles.

### 4.3.3 Particle Size Distribution

#### *Powders used by Croft AM*

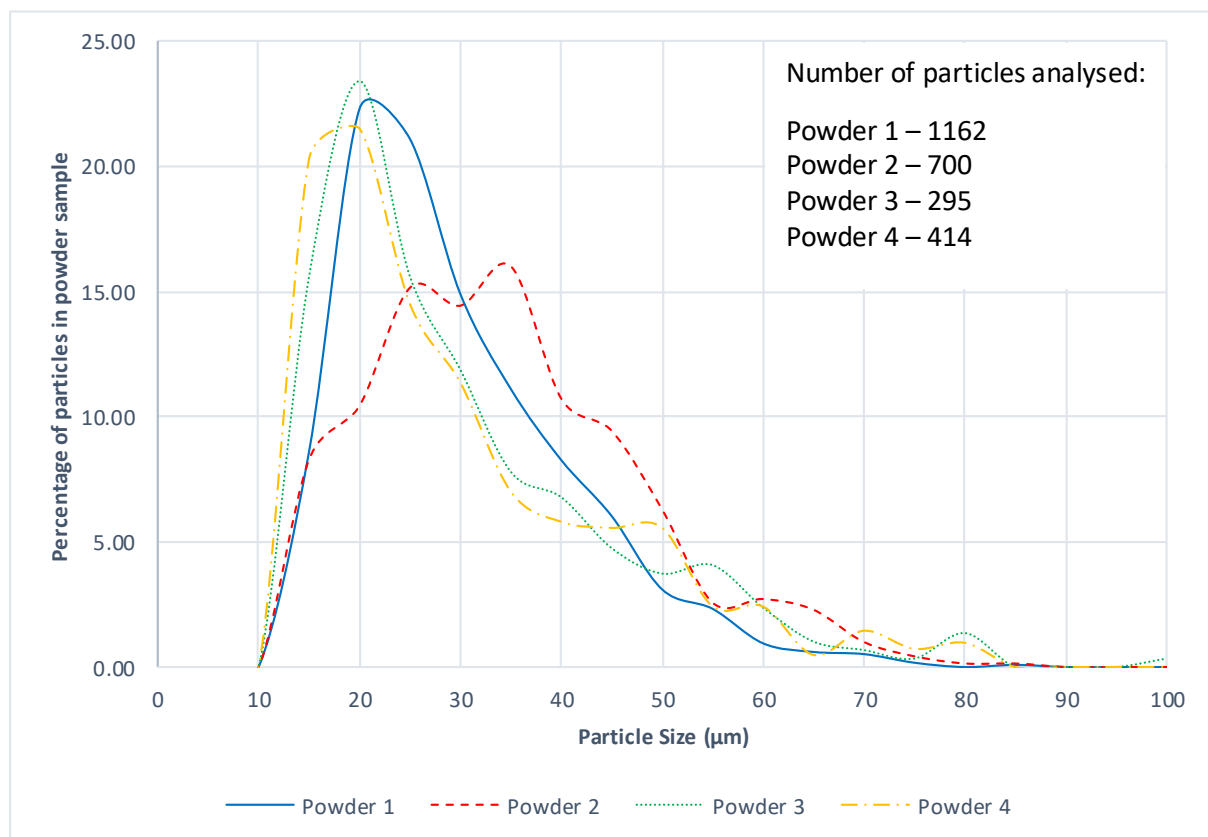


Figure 4-23 – PSDs of powders used by Croft AM at various stages of reuse

Table 4-13 – d10, d50, d90 and mean particle sizes for powders used by Croft AM at various stages of reuse

<i>Powder #</i>	<i>d10 (µm)</i>	<i>d50 (µm)</i>	<i>d90 (µm)</i>	<i>Mean (µm)</i>
<i>Powder 1</i>	15.3	24.5	42.7	27.3
<i>Powder 2</i>	15.9	30.6	49.4	32.0
<i>Powder 3</i>	13.9	23.7	50.1	28.4
<i>Powder 4</i>	13.4	22.3	48.9	27.4

Figure 4-23 and Table 4-13 yield some information regarding the degradation of PSD within powder with reuse. Powder 4, which has been reused just once, shows a very similar PSD curve to Powder 1 (virgin powder), with an even higher percentage of finer particles. This is confirmed by the d10 value for Powder 4, but the d90 value also indicates that Powder 4 is likely to have more large particles than virgin powder. Powder 3 shows that heavily used powder has similar d10, d50 and d90 values to that of Powder 4. Combined with a similar PSD curve, this indicates that the PSD of the powder does not change significantly over time, and that Croft AM do not see notable degradation in their powder PSD over time. This is most likely due to the sieving process. It is hard to compare Powder 2 in the same way, as it is unknown how many times this powder has been used.

Figure 4-23 gives insight into an acceptable PSD for use in SLM AM. The PSD of a powder can be considered as acceptable if it is similar enough to Powder 1 and/or Powder 2 (i.e. virgin powder and acceptable powder). As the presence of finer particles has been shown to increase component density through improved packing, smaller particles are desirable amongst the PSD. Powder still deemed to be acceptable does not have such a high concentration of finer particles, as seen by the curve for Powder 2. 84% of particles were found to be within the typical specification range of 15-45 $\mu$ m in the acceptable powder, when compared to the 92% of particles within this range in virgin powder, suggesting that up to 16% of particles can be larger than specification and still be acceptable. This establishes a benchmark against which other powders can be compared.

*Powders used by other companies*

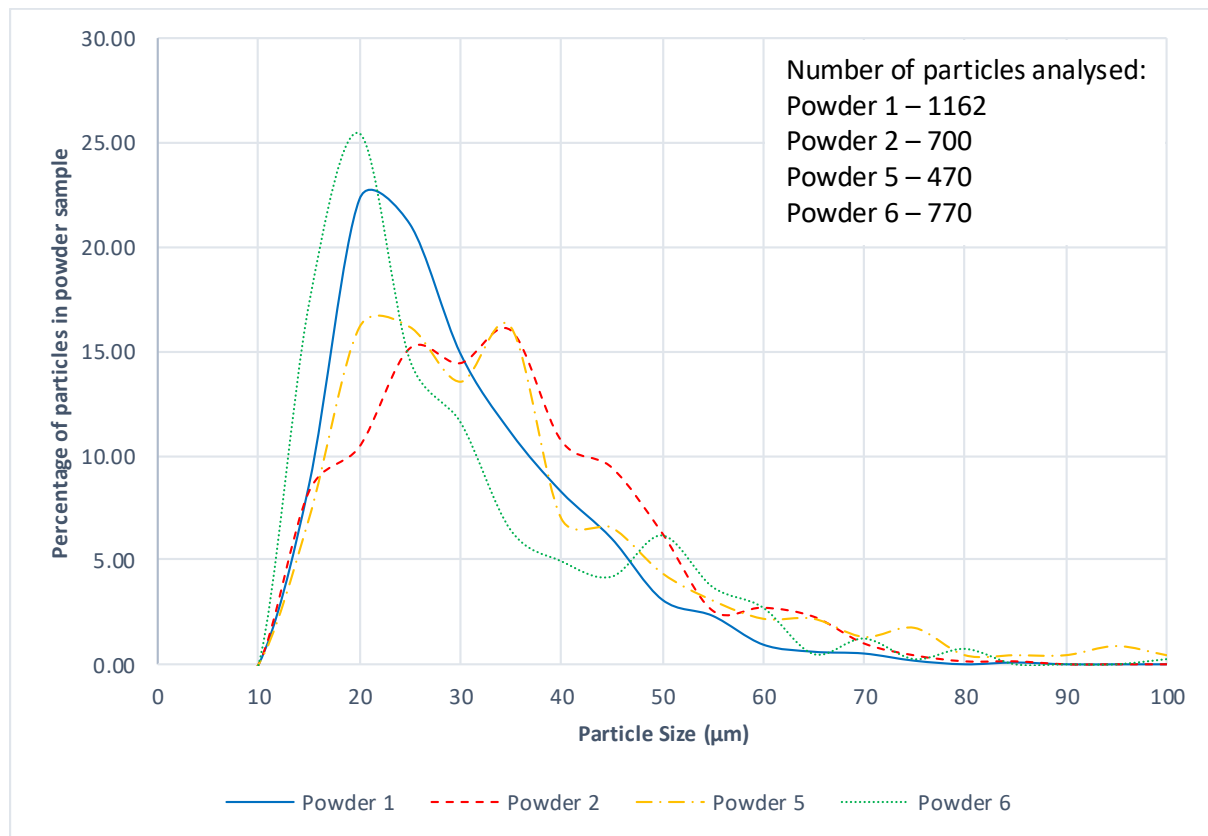


Figure 4-24 – PSDs of powders from different companies compared to virgin powder and acceptable powder used by Craft AM

Table 4-14 – d10, d50, d90 and mean particle sizes for powders from different companies with numerous reuses compared to virgin powder and acceptable powder

<i>Powder #</i>	<i>d10 (µm)</i>	<i>d50 (µm)</i>	<i>d90 (µm)</i>	<i>Mean (µm)</i>
<i>Powder 1</i>	15.3	24.5	42.7	27.3
<i>Powder 2</i>	15.9	30.6	49.4	32.0
<i>Powder 5</i>	16.1	29.3	53.9	32.5
<i>Powder 6</i>	13.8	22.1	49.4	27.4

As highlighted already, the number of uses of Powders 5 and 6 is unknown, making it difficult to know which powder to compare them to. The PSD curve shown in Figure 4-24 of Powder 5 is seemingly more like Powder 2. This is confirmed by Table 4-14, showing similarities in the d10, d50 and d90 values, whilst Powder 6 is more similar to Powder 1. Powder 6 does have a higher presence of oversized particles, shown by the higher d90 value, suggesting that it may have been used, but not as much as Powder 2 has been used. However, Powder 6 also has lower d10 and d50 values than seen in Powder 1, indicative of a broader PSD with many finer particles.

The expectation would be that Powder 6 lies within the PSDs exhibited by Powder 1 and Powder 2, as LPW Technology Ltd supply Croft AM with their powder. This is true for this powder. Powder 5 is likely to have been manufactured to different specification, and therefore it is unsurprising that the PSD does not match that of the virgin powder produced by LPW Technology Ltd in Powder 1. Given that Powder 5 and 6 are both designed for use within SLM, the large disparity between the two demonstrates the range of what can be considered “acceptable for use” within the AM industry.

### Overflow powders

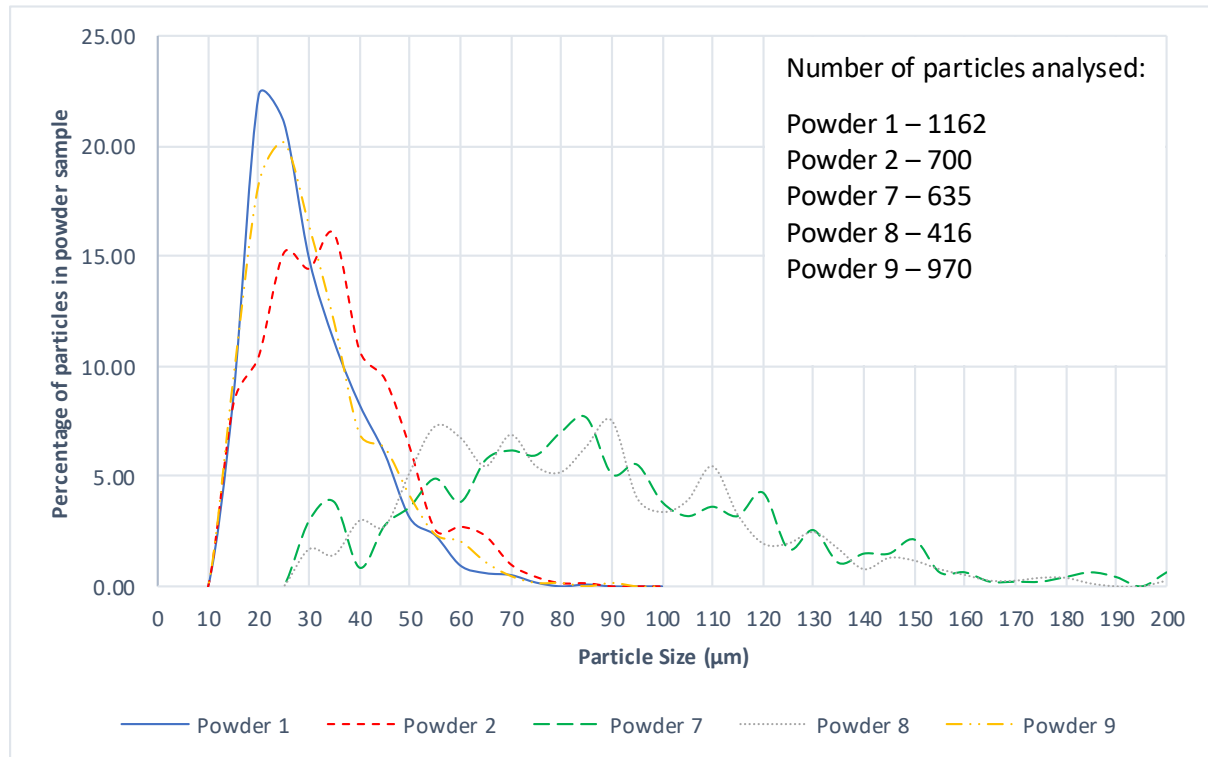


Figure 4-25 – PSDs of overflow powders compared with virgin and acceptable powder

Table 4-15 – d10, d50, d90 and mean particle sizes for overflow powder and derivatives compared to virgin powder and acceptable powder

Powder #	d10 (µm)	d50 (µm)	d90 (µm)	Mean (µm)
Powder 1	15.3	24.5	42.7	27.3
Powder 2	15.9	30.6	49.4	32.0
Powder 7	43.8	81.7	136.8	87.1
Powder 8	45.7	72.8	128.1	83.3
Powder 9	15.0	25.6	45.4	28.1

Figure 4-25 and Table 4-15 give clear indications of how unsuitable the overflow powder is for use in AM, as Powder 7 has less than 8% of particles in the 15-45 $\mu$ m range. Powder 8, representing the rejected particles in the sieving process, has a similar PSD to Powder 7. Powder 9 appears to have an acceptable PSD, closer to that of virgin powder than acceptable powder. This suggests that powder sieved from overflow powder could be suitable for reuse in SLM when considering PSD.

Interestingly, Powder 7 does not show any particles in the 10-25 $\mu$ m range, but when sieved through and turned into Powder 9, 48% of the particles are in this band. This indicates that PSD analysis through SEM may not be an accurate measure of PSD, most likely due to the overlapping of particles in the image causing the image analysis software to consider this as one large particle. The lack of particles seen in this range could also be due to the x60 magnification images analysed for Powders 7 and 8, as opposed to the x140 magnification images analysed in all other samples, making it harder for the software to detect small particles.

#### Black powder

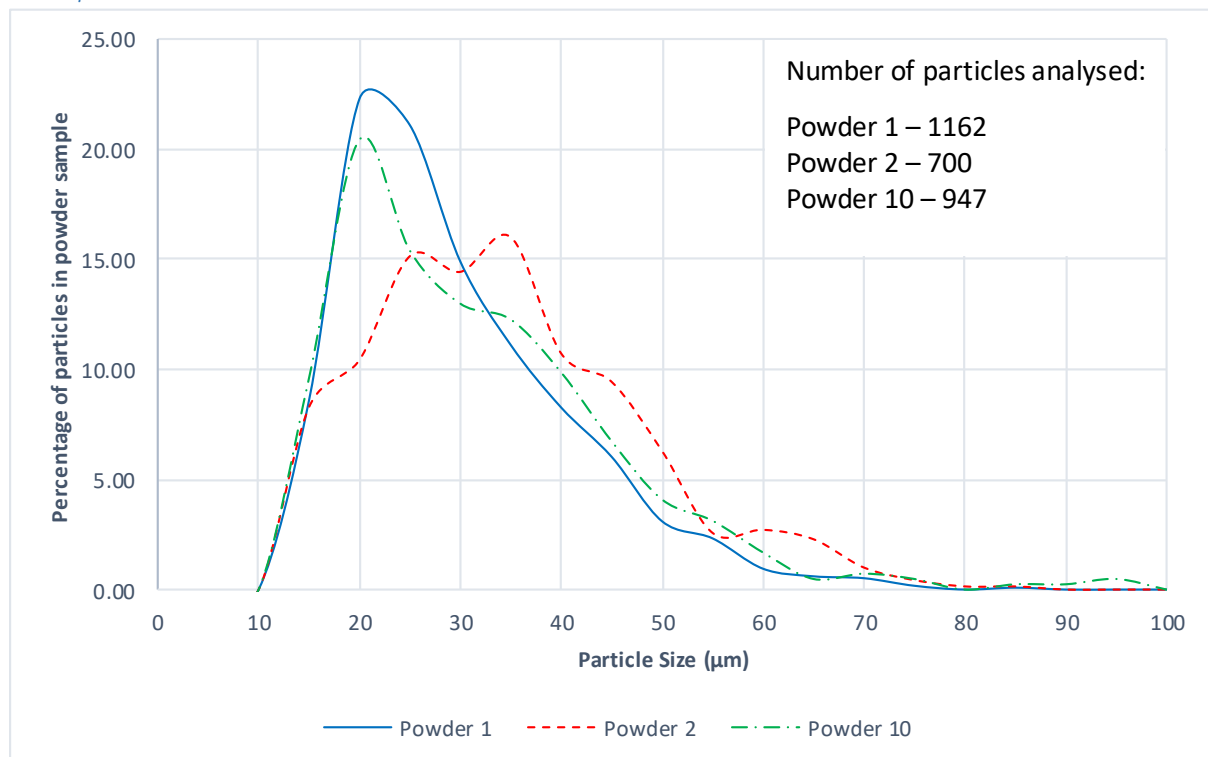


Figure 4-26 – PSD of black powder compared with virgin and acceptable powder

Table 4-16 – d10, d50, d90 and mean particle sizes for black powder compared to virgin powder and acceptable powder

Powder #	d10 ( $\mu$ m)	d50 ( $\mu$ m)	d90 ( $\mu$ m)	Mean ( $\mu$ m)
Powder 1	15.3	24.5	42.7	27.3
Powder 2	15.9	30.6	49.4	32.0
Powder 12	15.0	26.1	47.5	30.3

Figure 4-26 and Table 4-16 indicate that the PSD of black powder, seen in Powder 10, is in the region between Powder 1 and Powder 2. Despite the SEM indicating that there were many oversized particles, much of this powder would not be removed in the sieving process, and would therefore be reincorporated into future builds. However, SEM and EDS analysis suggested that the larger particles were typically the particles with dotting and an altered chemical composition, so it is likely that these particles would be sieved out, lessening the risk of contamination.

## 4.4 Discussion

### *Error Analysis*

It is difficult to draw conclusions with certainty from the results obtained for the following reasons:

The SEM images provide an accurate visualisation of the powder, but require a degree of qualitative analysis to interpret these images. The potential for variation in this analysis has been reduced by having the same person interpret each image, using a standardised list of powder qualities to comment upon for each powder. The SEM images are therefore the most reliable out of the results, but yield no quantitative data to easily compare powders with.

Despite being relatively consistent, the EDS data shows a notable variation between results for the same powder particles. This indicates that each of the spectra have a fairly large error margin, suggesting that these results are best interpreted as a ball-park figure for the chemical composition of the particle. Further to this, it is unreasonable to claim that analysis of a few sites per powder sample is truly representative of the entire powder; bulk sample analysis is more appropriate for such comparisons. However, if these potential errors are considered, the comparison of the EDS analysis of each powder can be inferred. Sites within the same powder sample can be compared to one another more reliably, as there is no need to assume these sites represent the entire powder, causing less room for error.

The PSD graphs obtained indicate the number of particles in each size region, but this is not representative of the volume that these particles would occupy. 100 small particles may only occupy the same volume as one large particle. This limits the usage of these graphs, although for the purpose of comparison the graphs produced are acceptable, as they indicate if there is a change in the number of particles of various sizes. Manipulation of the data to produce volume occupation PSD graphs was considered to be too time consuming and unnecessary, with Malvern testing being recommended if more accurate results were needed in the future.

The PSD analysis software, ImageJ, had several limitations in determining the PSD of particles. Figure 4-27a, Figure 4-27b, Figure 4-27c and Figure 4-27d give an indication of how accurately ImageJ can determine particle size. Inclusion parameters such as sphericity and particle size were defined to minimise the inclusion of anomalous particles by the software, removing many large particles and agglomerates that would have given inaccurate results. However, in some instances, as seen in Figure 4-27a, this excluded oversized but spherical particles, which would lead to an inaccurate PSD being calculated. To minimise the error this would have caused, the inclusion parameters were modified to produce another image. Any newly included particles in the second image that had been evidently omitted previously were included in the PSD analysis, whilst any other particles created were ignored. Despite this correction, Figure 4-27a, Figure 4-27b, Figure 4-27c and Figure 4-27d show that not all particles were included, causing inaccuracies in the PSD calculation. To further minimise this error, it was ensured that at least 250 particles were analysed in each sample.

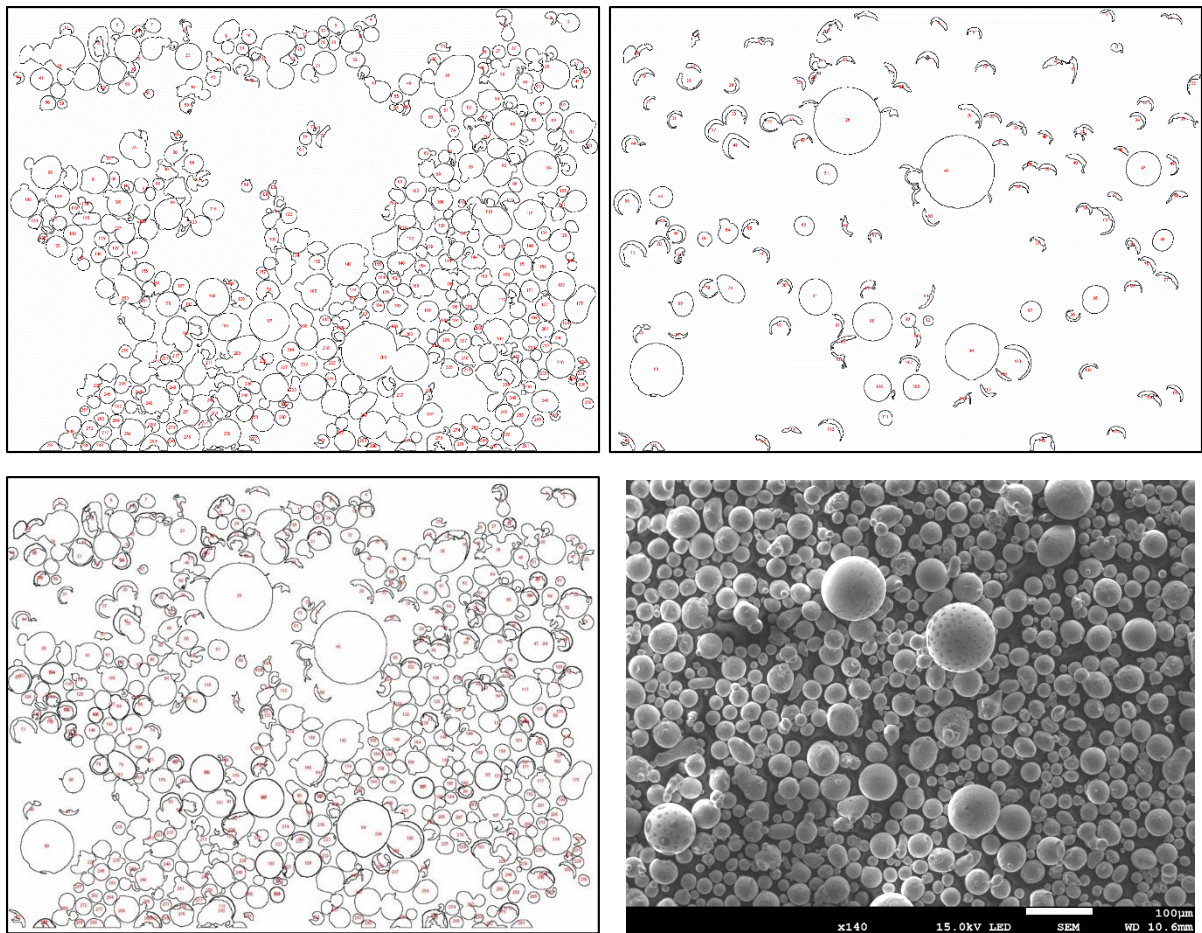


*Figure 4-27a (top left) – Initial particle size analysis image*

*Figure 4-27b (top right) – Adjusted particle size image analysis to include larger particles*

*Figure 4-27c (bottom left) – Overlaid image of Figure 4-27a and Figure 4-27b*

*Figure 4-27d (bottom right) – SEM image of Powder 3 at x140 magnification, from which Figure 4-27a and Figure 4-27b were derived*

The images used to gather information on the PSDs were either at x60 or x140 magnifications. This could exclude some smaller particles from being observed, as some tiny particles can be seen in the x400 images that may not have been picked up by the ImageJ software. A further source of error is seen where particles overlap, making it difficult for the software to determine if two particles are separate or not. This caused many smaller particles to be obscured, considered to be agglomerates by the software. PSDs calculated through ImageJ would therefore tend towards larger PSDs, excluding very small particles.

All particles were assumed to be perfectly spherical by the software. From a 2D SEM image, this is impossible to see, so may be an inaccurate assumption. Some partially melted particles or agglomerates were seen to be significantly distorted, causing long obloid particles that may have been oversized in one dimension. However, ImageJ would record the area of these particles, which would then be assumed to be a circle, potentially indicating that some irregularly-shaped oversized particles were smaller than they were. However, many of these particles were removed by the software parameters, minimising this risk. Therefore, ImageJ can be deemed to give an accurate enough representation of PSD to compare results with confidence, although further PSD analysis through Malvern testing is recommended.

#### *Powders used by Croft AM*

Croft AM were interested in understanding how their powder degraded over time with continual reuse, as this would set a benchmark for any further research and development to be compared against. Virgin powder consists of very spherical and round particles with relatively few defects, displaying a chemical composition with very small quantities of carbon and oxygen. The recorded PSD has 92% of particles within the 15-45  $\mu\text{m}$  range.

Used powder still deemed acceptable for use in AM was seen to have more misshapen particles, with an increase in the percentage of oxygen present in the powder compared to virgin powder and the beginnings of particle contamination seen in Figure 4-14. The prevalence of larger particles, seen by the PSD graphs in Figure 4-23, further suggests this powder can be considered less optimal than virgin powder, as expected.

Heavily used powder shows notable differences to virgin powder. Misshapen and agglomerate particles were equally, if not more, prevalent than in the used but acceptable powder, with dotting observed in many of the larger particles. These particles had a significantly different chemical composition to the other particles in the powder, showing their unsuitability for use in AM and thus the unsuitability of this powder. The non-dotted regions of the particle analysed exhibited higher

quantities of both oxygen and carbon, suggesting that this had gradually increased from virgin powder between every build. The PSD of smaller particles was remarkably similar to that of virgin powder, but there are more large particles above 50µm in diameter in the heavily used powder.

Powder 4, having only been used once, seems to show instant degradation compared to virgin powder, with notably more deformed and oversized particles. This indicates that the particles are affected as early as one build in, although they largely seem to remain high-quality particles with low oxygen content. The number of oversized particles increases, but the numerous small particles still present are likely to cancel out any resultant negative effects.

From the discussion above, it is evident that powder used by Croft AM degrades over time. The change in chemical composition is the most important change observed, as this is likely to cause built components to no longer fall within specification and exhibit different mechanical properties (see Chapter 2.4). Unfortunately, the rate of degradation cannot be determined, as the number of uses of Powders 2 and 3 is unknown.

#### *Powders used by other companies*

Powders from other companies could give Croft AM insight into how their powder compared to competitors, indicating any major differences observed between powders considered to be similar.

Powders 5 and 6 were used an unknown number of times. Further to this, nothing is known about the powder properties when they were in a virgin state, making it difficult to ascertain how many builds these powders have been through. However, Powder 5 shows Croft AM that their powder varies compared to other AM users in both chemical composition and PSD. Seemingly, Croft AM's own powder is of an even higher quality than other metal powders considered to be competitors, owing to the increased frequency of larger particles in powder supplied by EOS. However, this could be due to repeated reuse of this powder.

Powder 6, supplied by LPW Technology Ltd, is remarkably similar to that of Croft AM's own powders in all aspects. This provides a useful indication to Croft AM that they are using and handling their powder in a similar way to the manufacturer, confirming that they are following good powder handling practice and using typical build parameters.

#### *Overflow powders*

Overflow powder is a potential cause for waste in the AM industry, as this powder is often considered unsuitable for reuse. Analysis therefore helps to identify appropriate alternative uses for this powder.

There were many particles with dotting present in the larger particles in the overflow powders. These particles were found to have grossly different chemical compositions, suggesting that they are unsuitable for use within AM, and unlikely to be desirable in other industries either. It is reassuring to see that oversized and dotted particles are in the overflow powder, as this indicates that these particles are not being included within the powder-bed. In turn, this prevents these particles from being integrated into the build, minimising their potential impact on the produced component.

Sieving of Powder 7 separated the oversized particles in Powder 8 from the particles suitable for use in AM in Powder 9. Powder 9 seems to have a PSD similar to that of virgin powder, with a chemical composition lying between that of Powder 1 and Powder 2. Particle morphology is similar to that of used but acceptable powder. Further to this, SEM images suggest that the dotted particles have been removed. This indicates that sieved particles from overflow powder are suitable for use in AM, reducing the waste from overflow powder.

SEM images from Powder 8 show that there are still many small particles that could be suitable for use in AM, suggesting that a more rigorous sieving process may be required to maximise the reclamation process from overflow powders. If it were possible to isolate or remove the dotted particles, the overflow powder may be considered more useable by other powder based AM processes, such as laser metal deposition, utilising particles as large as 150 $\mu$ m (see Chapter 3.1). This would further reduce waste within the SLM process.

#### *Black powder*

Understanding the nature of the black powder may assist Croft AM in identifying the cause of these defects. If the cause cannot be identified, insight into the properties of the black powder could give an indication of the impact on the build quality of black powder particles.

The presence of dotted particles causes a powder to be less suitable for use in AM, as the chemical composition is grossly different; a reduced iron content is replaced almost entirely by oxygen and silicon. Powder 10 showed that there were many oversized and dotted particles mixed amongst seemingly normal particles, seen in both the SEM images and from the PSD compared with virgin powder. EDS analysis of a normal particle confirms this. This could imply that the blackened trait of the powder may only be resulting from the dotted particles. Separation of these dotted particles from the remaining powder, followed by bulk chemical analysis, could confirm this. This may prevent waste, as the non-contaminated regions of black powder could be reincorporated into future builds.

It is possible that every instance of dotting seen in the powder samples is caused by black powder residue that was not removed during the sieving process. If this is the case, the impact of the black

powder on build quality is far-reaching. This could be a viable avenue for further research to minimise or mitigate this issue, as it could be impacting powder longevity.

#### 4.5 Conclusions

The powders were analysed for several different purposes, but most importantly provide a benchmark against which any future powder reclamation solutions can be compared against. This has been achieved. As such, future methods of powder production and reclamation will be analysed using the same techniques, enabling direct comparison to the powders analysed here. Powder degradation has been demonstrated, although it was impossible to determine the rate of degradation with the samples available. Overflow powders have been shown to be suitable for use in AM once sieved, whilst black powder has been found to be potentially damaging to builds if not removed.

Whilst the analysis led to insightful and useful inferences being made, several improvements to the powder analysis methodology have been identified. To ensure the reliability of the results obtained, ICP-OES is recommended for bulk analysis of the chemical compositions of the powder. There is a limitation, as oxygen content cannot be recorded from this method. Since oxygen has been shown to be a contributing factor to the degradation of component quality in the literature review, this process may miss some important information in the chemical analysis of the powder. Initial testing of ICP-OES is suggested to determine how useful these results could be.

Alternative non-carbon methods of particle adhesion may allow bulk EDS analysis to be carried out, preventing an erroneously high carbon content being seen in entire-image EDS scans. This would allow accurate comparison of samples to one another. If no solutions can be found, bulk analysis of an image could still be performed, instead removing the carbon content from measurements. This would quantify the changes in all other elements of stainless steel, which may be of interest.

PSD could be more reliably analysed by a Malvern particle size analyser, yielding results for thousands of particles as opposed to hundreds, without the limitations of ImageJ outlined in Chapter 4.4. As this is a simple test and not time consuming, this is suggested as a standard in future powder analysis.

Once a suitable method of bulk chemical composition analysis has been tested and identified, either through ICP-OES or another method, it would be desirable to show the rate of degradation of the powder. This could be achieved by taking a sample for analysis after every third build Croft AM complete, provided they have not introduced virgin powder to the hopper.

Attempting to separate the dotted particles from the remainder of the powder could allow for an improvement of powder quality, thus impacting powder longevity. No suggestions are made at this stage as to a methodology for this.

The analysis of these powders provides Croft AM with information on 316L stainless steel powders that they did not have access to before. This information can be further analysed in a commercial environment, assisting the company to understand how best to utilise their powders. It also gives further direction to any upcoming research and development work Croft AM have planned.

## 5. Breakdown of Support Structures into Metal Powder <sup>4</sup>

The first concept-scoring matrix completed (see Table 3-2) identified the reuse of support structures, sieved out rejects and agglomerates as a strong solution, achieving many of the essential aims of the project. The resources to carry out experimental testing of this solution were readily available, resulting in this solution being investigated first. It was noted that the amount of waste produced by sieved out rejects and agglomerates was negligible compared with that of support structures (Ian Brooks 2019, personal communication). Combined with the knowledge that sieved out rejects can often be heavily oxidised (Slotwinski *et al.*, 2014; Jacob *et al.*, 2017), it was decided that these rejects would not be further considered for breakdown to metal powder. Support structures were instead considered for repurposing to produce metal powder suitable for AM. A stronger understanding of support structures was developed, allowing for subsequent identification of suitable breakdown solutions.

### 5.1 Establishing further understanding of support structures

Support structures are necessary in all metal components produced by AM. Where components have overhanging features or tall, thin parts, support structures are used to hold the component shape as it forms, whilst also providing support against deformation from the sweeping arm (Zelinski, 2015; Hussein *et al.*, 2013). Furthermore, supports allow dissipation of residual heat from the melt pool, which would otherwise cause stress and deformation of a component mid-build (Zelinski, 2015; Hussein *et al.*, 2013; Jiang *et al.*, 2018). Small support structures are used in virtually all builds to prevent the component being built directly onto the build platform, allowing easy removal of the component. Some processes, such as directed energy deposition, can only deposit material on existing surfaces in previous layers, requiring support structures as a platform to build upon (Jiang *et al.*, 2018).

Support structures create potential issues, and are thus avoided or minimised when possible. Piller *et al.* (2018) reported that 19% of the entire build time can be used in creating support structures, whilst Zelinski (2015) found that this time building supports could be up to 50% of the entire build time. Supports therefore prolong the manufacturing time of components, increasing production costs through power consumption whilst lowering component output. Expensive virgin metal powder is consumed creating this soon-to-be waste structure, incurring further costs.

---

<sup>4</sup> The following chapter constitutes the entirety of a paper published in the RDPM conference proceedings 2019 (Powell *et al.*, 2019). This paper has therefore not been included as an appendix to reduce paper consumption, in line with the environmental focus of this thesis.

Components are separated from the build plate initially using a bandsaw, pneumatic saw or wire erosion, dependent on the accuracy required and facilities available. Support structures are then snipped away from the component by hand one at a time, requiring a lot of time and precision, or can be milled using Computer Numerical Control, requiring expensive and complex equipment. Zelinski (2015) noted that the removal of supports without causing damage to the component in small or delicate components can be difficult. When removed, the component requires further processing to polish off any resultant burrs on the surface, further demonstrating the issues associated with support structures.

A summary of papers investigating supports in AM conducted by Jiang *et al.* (2018) found that minimising the volume of supports is the typical academic focus, intending to reduce raw material usage. Other papers investigate how orientation of the component can reduce the number of required supports, but show how this can negatively influence part accuracy and build times (Strano *et al.*, 2012). With much of the academic research within the AM industry aiming to improve the process efficiency, seemingly little research has been undertaken to consider recycling within the industry. Current industry practice is to scrap the unwanted support structures where possible; alternatively they are discarded.

Croft AM has stated that it is common for only 1-3% of the cost of one kilogram of virgin powder to be regained per kilogram of uncontaminated scrap metal sold, with this being confirmed by Ian Brooks (2019). Frank Cooper (2019, personal communication) showed that in the precious metal industry, the value of the gold, silver or platinum “waste” is significantly higher. Support structures are returned to the supplier and swapped, gram for gram, for replacement powder, with an adjustment charge to cover their costs and variations in price. The result is a significantly higher return on investment from the precious metal powder, and the scrap precious metal can be repurposed.

Ball milling consumes significantly less energy than atomisation, as it does not require the energy-intensive process of melting the metal, making it environmentally preferable to producing virgin powder from remelted support scrap (Fullenwider *et al.*, 2019). As metal powder is more valuable than support structure scrap, identifying a method to convert support structures to a feedstock for ball milling can provide an economic benefit to AM users and powder manufacturers alike, whilst also reducing the carbon footprint of the AM industry.

## 5.2 Proposed breakdown techniques

As discussed in Chapter 3.2, Fullenwider *et al.* (2019) demonstrated that small machining chips of 304L Stainless Steel could be broken down into metal powder, comparable to particles produced by water atomisation. Others have also demonstrated that ball milling can produce powder in other metals, although not for use within AM (Liang *et al.*, 2014). In order to ball mill metal, the typical feed size must not exceed 3mm (Tencan, n.d.). The chips used Fullenwider *et al.* (2019) were between 5-20mm in length, although typically less than 1mm thick. A chip is therefore likely to be “suitably small” for use as ball milling feedstock if it is <3mm in width and thickness, provided it is <20mm in length.

To make support structures viable for ball milling, they need to be broken down into smaller chips. This could be possible using a slow speed shear shredder. Shredding waste metals is not uncommon practice in the production of metal scrap, providing a simple method of breaking apart long chains of support structure. The feasibility of this would vary for different metals depending on their mechanical properties, as the typical 4140 HT steel cutter material may not always be harder than the support structure material (SSI Shredding Systems, n.d.). Further to this, many AM users are likely to find shear shredders and ball mills on the market to be too loud for workshop use and too expensive compared with the powder savings.

To overcome these issues, a change in the current AM industry may be required. If large powder suppliers invested in this equipment, they could accept waste support structures produced from AM users, converting this into powder that they could then sell back to AM users at a reduced rate. This would save the AM user money as they get useable, cheaper powder from their low-value scrap, whilst the powder supplier gets money-for-nothing. This would be especially viable with high-value alloys such as Ti6Al4V.

It is worth noting that the size range of particles produced through ball milling would not be suitable for any one AM process, due to the small particle sizes required (Sames *et al.*, 2016). The powder produced may also have an altered chemical composition when compared with virgin powder, as some materials have been shown to exhibit notable chemical changes between the powder used and the produced component (Tang *et al.*, 2015). In order to overcome this issue, the produced powder could be sieved into size fractions and remixed with virgin powder of similar sizes. This could be done by either the AM user or by the powder supplier, with the latter being preferable due to the powder testing facilities available. Previous work has demonstrated the viability of this concept. Reused powder and virgin powder were mixed in several different percentage fractions, finding that the mechanical and chemical properties of produced components were continually within specification

(Jacob *et al.*, 2017). Frequent analysis and monitoring of this powder would be required to make this feasible.

### 5.3 Experimental Procedure

Due to the promise shown by this breakdown technique, an experimental procedure was designed, aiming to investigate the feasibility of this experiment at a rudimentary level. Four different designs of support structure were broken down, based on the typical supports used for commercial builds by Croft AM. They are referred to as light border supports, dense border supports, light hatches and dense hatches. These were built using 316L stainless steel powder. Results could therefore be compared to the machining chips used in previous work, due to the near-identical mechanical properties of 316L and 304L stainless steels. The supports used were considered to be scrap from commercial builds in a Realizer 250. Figure 5-1 provides visual representation of these supports. The removal of support structures often causes damage to the supports; as such, the supports seen are not in the condition they would be in on the build plate.

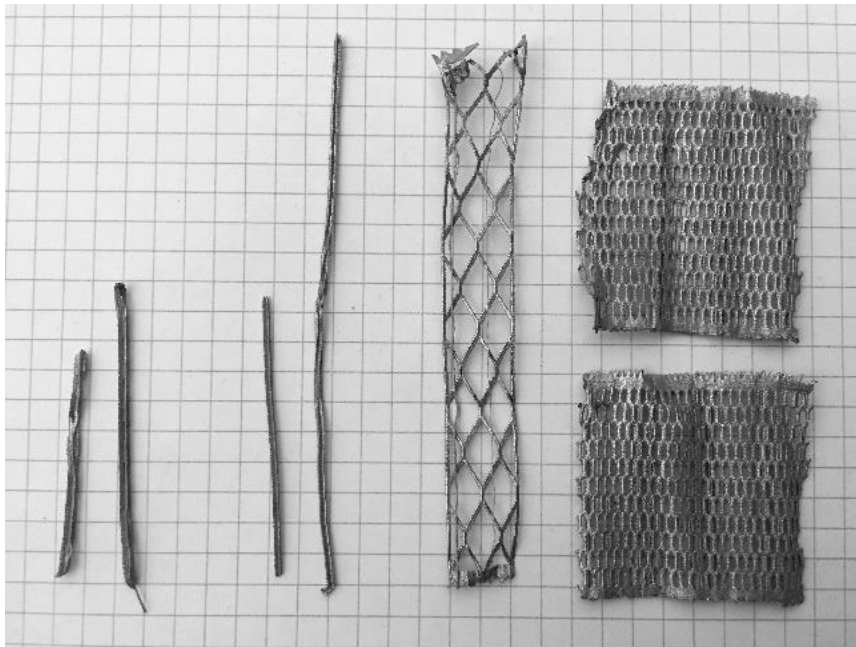


*Figure 5-1 – Supports used for breakdown analysis, overlaid on a 5x5mm grid. From left to right: light hatch, dense hatch, light border support, dense border support.*

Table 5-1 gives further information on the uses of each of the support structures that were broken down. It can be assumed that these various supports will always be separated from one another when cut away from the component post-build. As such, there is unlikely to be an event when a block support (a combination of both borders and hatches) will need to be broken down, preventing the need for analysis of this.

A guillotine was used as a representation of the slow speed shear shredding process, operating similarly to a shredder by using shear force to break down the supports. A Gabro Shear Notcher 3M2 was used to cut strips approximately 4.5mm wide, producing 250g of chips from the various support structures in two hours. These strips were then measured and analysed visually, assessing them for the success of their breakdown and usability in ball milling procedures.

*Table 5-1 – A summary of the four support structures used for breakdown analysis*

<b>Name</b>	<b>Description</b>	<b>Use</b>
<b>Light Hatches</b>	1.8mm wide, plus shaped, regular 3mm slits along the length of the central axis. 0.27mm thick	Found within the light border supports, forming the bulk of the “block” support structure. Lighter, more dispersed and use minimal material.
<b>Dense Hatches</b>	1.4mm wide, plus shaped, fully filled in, 0.23mm thick	Found within the dense border supports, forming the bulk of the “block” support structure. Stronger, tightly packed and better at heat sinking.
<b>Light Border Supports</b>	10x5.5mm diamonds interconnected and supported by external beams	Border the hatch supports on surfaces in less need of support.
<b>Dense Border Supports</b>	2.5x0.5mm irregular hexagons interconnected and supported by external beams	Border the hatch supports on surfaces in greater need of anchoring or heat sinking.

## 5.4 Results

The breakdown process took approximately two hours to complete. The type of support structure caused significant variation in the size of the chip produced, as seen in Figure 5-2.

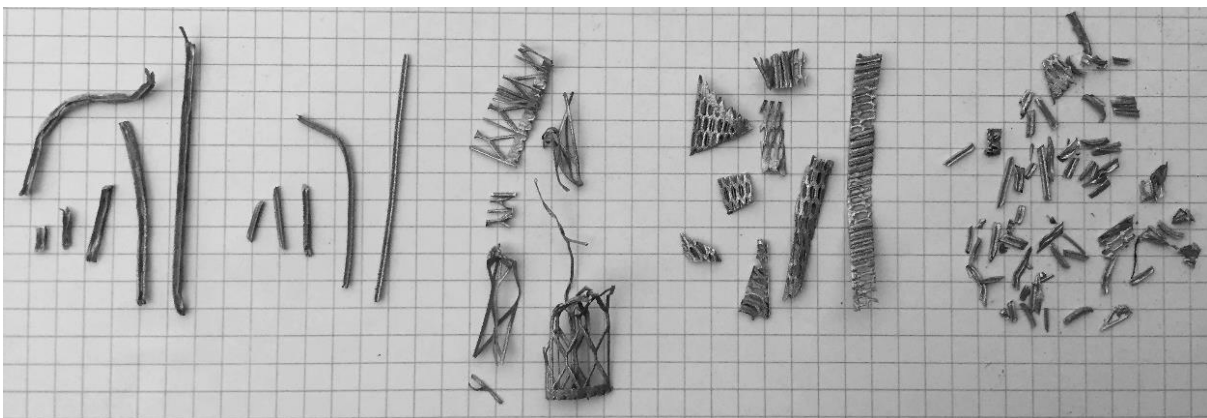


*Figure 5-2 – Broken down support structures, overlaid on a 5x5mm grid. From left to right: light hatch, dense hatch, light border support, dense border support, variety of chips from all support types*

Both light and dense hatches seemed often bend instead of shearing, as seen in Figure 5-2. When hatches broke down successfully, small chips were produced, often between 3-10mm. Bent chips and other hatches that were not broken down were, on average, 40mm long.

Similar behaviour was exhibited by light border supports. These supports tended to bend slightly, but typically were able to be broken down into strips between 15-30mm long. Some light border supports were found to fold upon themselves, becoming stronger at these thicker regions. Where this did not occur, these supports were noted to be significantly weaker and easily deformed by hand compared with other supports.

Dense border supports formed strips of consistent size, no wider than 5mm typically, breaking down as expected from the guillotine. They did not bend or deform like other supports, and were found to break apart at various angles to the guillotine. This can be seen in Figure 5-2, where the supports have evidently been cut in multiple directions to the lattice.

Various small chips and finer particles were also produced, shown in Figure 5-2. Whilst some of the finest particles were likely to be residual powder from the build process, there is no doubt that small chips, no larger than 5mm long, were produced from the guillotine process.

## 5.5 Discussion

Hatches did not break down as easily as expected, which is concerning given they are the most common supports. This is most likely due to the ductile nature of 316L stainless steel, resisting breakage by deforming plastically. However, this deformation would cause subsequent work hardening of the metal. A second attempt to break it down would likely have more success, indicating that the repeated shear action of shear shredding may be suitable to break these supports down. Different materials used in AM are often brittle, such as Ti6Al4V, and would be unlikely to have this problem with bending (Tang *et al.*, 2015). Where they did break down, chips were found to be of a suitably small size. A potential issue could arise with broken down dense hatches, as they have no natural weak points where breakage is likely to occur. This could require notably higher forces from ball milling to break them apart.

Light border supports were unable to be broken down into chips of less than 5mm, thus would be too large for ball milling. However, with these supports being particularly thin and weak, continual shear action is likely to break them down further. When successfully broken down, the thin nature of these supports would make them similar to machining chips, indicating that these would be suitable as a feedstock in ball milling.

The most successful breakdown was observed in the dense border support. The latticed structure ensured the supports had enough strength to resist bending and deformation, whilst providing natural weak breaking points. The breakdown was tested at different angles, as would be the case in shear

shredding, and proven to be equally as effective. Combined with the thin nature of these supports, the chips produced would likely be useable as ball milling feedstock.

Whilst the mass of chips small enough to be useable immediately in ball milling was estimated to only be between 10-15% of the 250g of broken down supports, this result is the most promising. The shear action of the guillotine was evidently capable of producing chips small enough for use in ball milling. Through the random and repeated shearing of shear shredding, any larger chips produced would be broken down further, until they were suitably small.

## 5.6 Conclusion

It is highly likely that support structures used in AM can be broken down through shear shredding into suitably small chips for use in ball milling. This process would be significantly less energy intensive than the current recycling procedure, especially in metals with high melting points. Having demonstrated the viability of this process using 316L stainless steel, a highly ductile material, suggests that the other less ductile materials used in AM will yield equally as promising, if not better, results.

However, it is improbable that metal AM manufacturers would have enough support structure waste to warrant investing in equipment such as shear shredders and ball mills, as they would be unlikely to see a return on investment. To see this practice adopted in the AM industry, the onus would fall upon powder suppliers to invest in this equipment, utilising their powder testing facilities to ensure the powder produced is of a suitable quality.

Following these promising results, further research should be carried out into the effects of mixing lower-grade powder with virgin powder on the AM process, as this practice has been highlighted as a gap in knowledge (see Chapter 2.5). Designing and testing a specialised-for-AM shear shredder would be desirable, aiming to reduce both its size and cost, whilst also investigating materials hard enough to break down harder metals than 316L stainless steel. Alternative mechanical breakdown methods, such as hammer milling, should also be investigated and compared to current findings.

Machining chips may behave differently to support structure chips in ball milling for unforeseen reasons. The broken down support structures produced in this experiment should therefore be subjected to ball milling to ensure the suitability of this practice, following a similar procedure to that carried out by Fullenwider *et al.* (2019). A harder material is suggested to increase the rate of particle formation, attempting to improve upon the previous ball milling procedure.

## 6. Continuation of support structure breakdown through ball milling

Further breakdown of support structure chips through ball milling had been identified as a future research avenue in Chapter 5, using a process similar to the methodology used by Fullenwider *et al.* (2019). This was considered the most logical next step as the background knowledge had already been established. Ball milling would also require minimal resources compared to the other solutions identified in Chapter 3.

### 6.1 Environmental justification

The suggestion by Fullenwider *et al.* (2019) that ball milling was less energy intensive than scrapping metal was unsubstantiated. To affirm this claim a rudimentary investigation was carried out, aiming to demonstrate a reduction in power consumption when compared to current powder production methods, such as atomisation. If this could not be shown, then ball milling would not be further pursued, as the objectives of research state that environmentally friendly solutions are required.

Morrow *et al.* (2007) showed that 32.81MJ is required to atomise 1kg of powder that has been recycled from scrap steel, remelting the material and forming a plate for use in atomisation. The Pulverisette 5/4 (the proposed ball mill for use in potential experimentation) draws up to 1.73kW of power, equating to 6.23MJ per hour of run time. The machine is capable of milling four 225ml samples (i.e. 900ml of material) at once (Fritsch, n.d.). Assuming the density of the 316L stainless steel to be 7.99g/cm<sup>3</sup>, 900ml of stainless steel equates to 7.19kg. Assuming that it will take 24 hours of “machine-on” time to break down the chips, this will use 149.52MJ of energy. This suggests that 20.80MJ of energy would be needed per kilogram of powder produced if the milling bowls were fully loaded. This is 63.4% of the energy consumption used in the current scrapping process to recreate steel powders, justifying further investigation of ball milling.

The above example is an estimation and only considers steel. Harder materials, such as Ti-6Al-4V, will take longer to break down, requiring longer machine-on times and thus consuming more energy. Materials with lower melting points, such as aluminium, may require less energy to remelt and atomise, potentially resulting in ball milling becoming a less effective alternative solution. Experimental work may not be representative of upscaled powder production, and thus the 900ml sample size used in the above calculations may need be reduced, further reducing the efficiency of the process. Alternatively, ball milling may take less than 24 hours, in which case the energy efficiency may increase.

As resource efficiency becomes increasingly critical and renewable energy becomes more abundant, it may prove more important to reduce waste material than reduce power consumption. Research into the production of powder from waste is therefore likely to become valuable to the AM community, even if found to be more energy intensive than initially estimated.

## 6.2 Initial experimentation

### 6.2.1 Methodology

Through the N8 Research Partnership<sup>5</sup>, a suitable testing facility was identified at the Dalton Cumbrian Facility, affiliated with Manchester University. The established procedure followed a similar approach to that used by Fullenwider *et al.* (2019), although some notable changes were made, justifying the necessity for experimental work. These changes are highlighted where appropriate.

The 316L stainless steel support structure chips detailed in Chapter 5 were used as the feedstock for the ball milling procedure. Two samples of approximately 15ml were measured out and each sample was weighed, shown in Table 6-1. Examples of each sample shown in Figure 6-1, whilst a sided-by-side example is seen in Figure 6-2. The “standard” sample included small chips typically no longer than 5mm and no wider or deeper than 2mm, more often from hatches or light border supports (see Table 5-1). These chips were considered to be similar to those used by Fullenwider *et al.* (2019). The “oversized” sample mostly comprised of chips from dense border supports that would likely be considered too large for typical breakdown. However, due to the naturally occurring weak points in their design, it was believed these chips may still break down through ball milling.



Figure 6-1 – Examples of the chips included in each sample, overlaid on a 5x5mm grid. Left: standard chips. Right: oversized chips

---

<sup>5</sup> The N8 Research Partnership is a collaboration of the eight most research intensive Universities in the North of England: Durham, Lancaster, Leeds, Liverpool, Manchester, Newcastle, Sheffield and York. Website available here: <https://www.n8research.org.uk/>

Table 6-1 – The composition of standard and oversized samples

Chips	Description	Mass
Standard	Small chips (<5mm) predominantly from hatches and light border supports	18.7g
Oversized	Large chips (>5mm) predominantly from dense border supports	11.1g



Figure 6-2 – Side-by-side comparison of the 15ml samples of standard (left) and oversized (right) chips, occupying the same volume

The chips were milled using a Pulverisette 5/4 Planetary Ball Mill system using two 80ml tungsten carbide bowls, one for each sample. Budget limitations only permitted  $\varnothing 20\text{mm}$  tungsten carbide balls to be used, preventing the methodology established by Fullenwider *et al.* (2019) from being entirely replicated. However, it was believed that  $\varnothing 20\text{mm}$  balls would be capable of reducing the support structure chips down to particles of 30-70 $\mu\text{m}$  in diameter (Matt Gye 2019, personal communication). Five  $\varnothing 20\text{mm}$  tungsten carbide balls were added to each bowl, filling approximately 60% of the bowl with the milling media. Tungsten carbide is significantly harder than 316L stainless steel and other commonly used alloys in the AM industry, making it suitable for the breakdown of these materials and likely to achieve faster breakdown than the stainless steel balls used by Fullenwider *et al.* (2019). The maximum rotation speed of 400rpm was used to achieve the highest energy transfer rate possible. The equipment was used on cycles of 15 minutes on / five minutes off, keeping an hour break after the fourth repetition to avoid excessive temperature build up in the bowls. The bowls were filled with a nitrogen atmosphere to minimise changes in chemical composition during milling, achieving <1ppm of both  $\text{O}_2$  and  $\text{H}_2\text{O}$ .

Ball milling was carried out for seven hours of machine-on time before the bowls were opened. Random powder samples from each bowl were removed and prepared for SEM analysis, mounted upon stubs using acetone. SEM images of each sample were obtained using an FEI Quanta 250 ESEM with an acceleration voltage of 10kV. Both secondary electron (SE) and back-scattered electron (BSE) images were taken at x200 magnification. SE images allowed for visualisation of the powder whilst BSE images simplified the quantitative analysis using ImageJ (Rasband, 1997-2018), an image-

processing software, to determine the PSD of the powder. Particles were compared to Figure 4-2 to allow quantitative comparison of particle morphology to the powders tested in Chapter 4, using the same in-text format [roundness, sphericity]. EDS analysis was also carried out using an Oxford Instruments XMax 80 detector to determine the chemical composition of the powder. The chemical composition was determined at individual sites rather than across the entire image, as the acetone background would have caused erroneous levels of oxygen and carbon to be seen.

## 6.2.2 Results

### *Physical Inspection*

Based on findings by Fullenwider *et al.* (2019), the breakdown of the support structures was expected to take 24 hours or longer. The opening of the bowls after seven hours of milling was intended to be an initial viability check, to ensure that the chips were breaking down as intended. However, after the initial seven hours, a powder was found to have been formed from both the standard and oversized chips, as seen in Figure 6-3 and Figure 6-4. Further milling of the chips was therefore ceased.



Figure 6-3 – Powder formed from standard chips in the ball milling process



Figure 6-4 – Powder formed from oversized chips in the ball milling process

The standard chips produced noticeably larger particles than the oversized chips, resulting in a coarser and loose powder, henceforth referred to as “standard” powder. The oversized chips milled much faster than the standard chips, creating a finer powder henceforth referred to as “oversized” powder. Some of the powder adhered to the side of the bowl, seen in both Figure 6-3 and Figure 6-4, although the adhesion is more severe in the oversized powder. The powder also adhered to the balls. Both powders contaminated the milling balls and bowls irreversibly due to powder becoming fused with the tungsten carbide surfaces.

*Table 6-2 – Mass comparison of input support structure and output powder*

<b>Chips</b>	<b>Initial mass</b>	<b>Powder mass</b>	<b>Percentage of initial mass</b>
<b>Standard</b>	18.7g	25.36g	135.6%
<b>Oversized</b>	11.1g	6.99g	63.0%

Table 6-2 shows the mass of loose powder that was recoverable from each bowl. Considerably more powder was recovered than the mass of standard chips input to the bowl. This can be explained by heavy tungsten carbide contamination, caused by the tungsten carbide-tungsten carbide collisions between the balls and the bowl. Tungsten carbide has a density of 15.63g/cm<sup>3</sup>, almost twice that of stainless steel. Assuming that the increase in mass of 35.6% is entirely due to tungsten carbide and that all 316L stainless steel powder was recovered, this represents an increase in powder volume of 18.2%. Therefore, approximately 1/6<sup>th</sup> of the volume of powder collected will be tungsten carbide contaminant. However, as much of the powder adhered to the side of the bowl, the volume of contaminant is likely to be higher than this estimate.

A decrease in mass of 37% is seen in the oversized powder sample. This is due to a sizeable quantity of the powder becoming fused with both the bowl and balls, shown in Figure 6-5. This is typical behaviour of powders smaller than 20µm (Gyorgyi Glodan 2019, personal communication), further indicating that a fine powder was created. Tungsten carbide contamination was still present in the oversized powder, although the quantity of contaminant cannot be determined from the data obtained.



*Figure 6-5 – Powder adhered to both the mixing bowl and balls*

Although it has not been quantified, the volume of powder produced was considerably less than the volume of support structure input to the mill. This is due to the empty regions left in each individual support structure, as well as the inability of support structures to pack densely. This is evidenced in Figure 6-2 and Table 6-1; the support structures each occupied 15ml of space, but the relatively small standard chips weighed 70.3% more than the larger oversized chips .

SEM Imaging

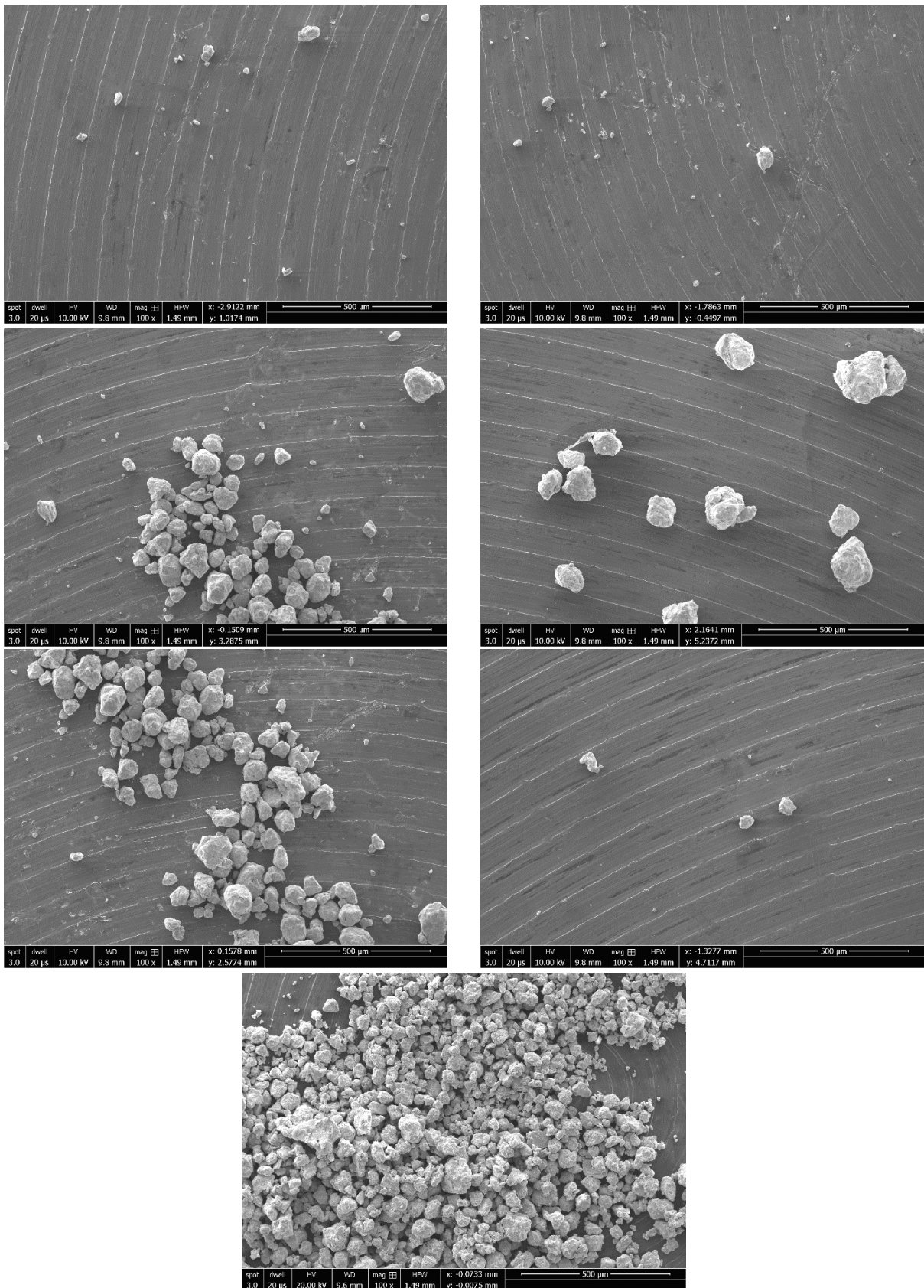


Figure 6-6a (top left), Figure 6-6b (top right), Figure 6-6c (middle left), Figure 6-6d (middle right), Figure 6-6e (bottom left), Figure 6-6f (bottom right) & Figure 6-6g (bottom centre) – x200 magnification SEM images of the powder produced from standard chips

Figure 6-6a-g show the powder produced from the standard chips. The particles are large, typically ranging in diameter from 50-150 $\mu\text{m}$ , although there are some particles as small as 10 $\mu\text{m}$  and as large as 200 $\mu\text{m}$ . The majority of the particles seem to be in the range of 50-100 $\mu\text{m}$ . The particles are considered to be spherical, although they have rough surfaces with many facets [0.3, 0.9]. Few particles appear to be non-spherical. The impact of the faceted edges on particle packing can be seen in Figure 6-6g, where smaller particles are unable to easily fill the regions between larger particles.

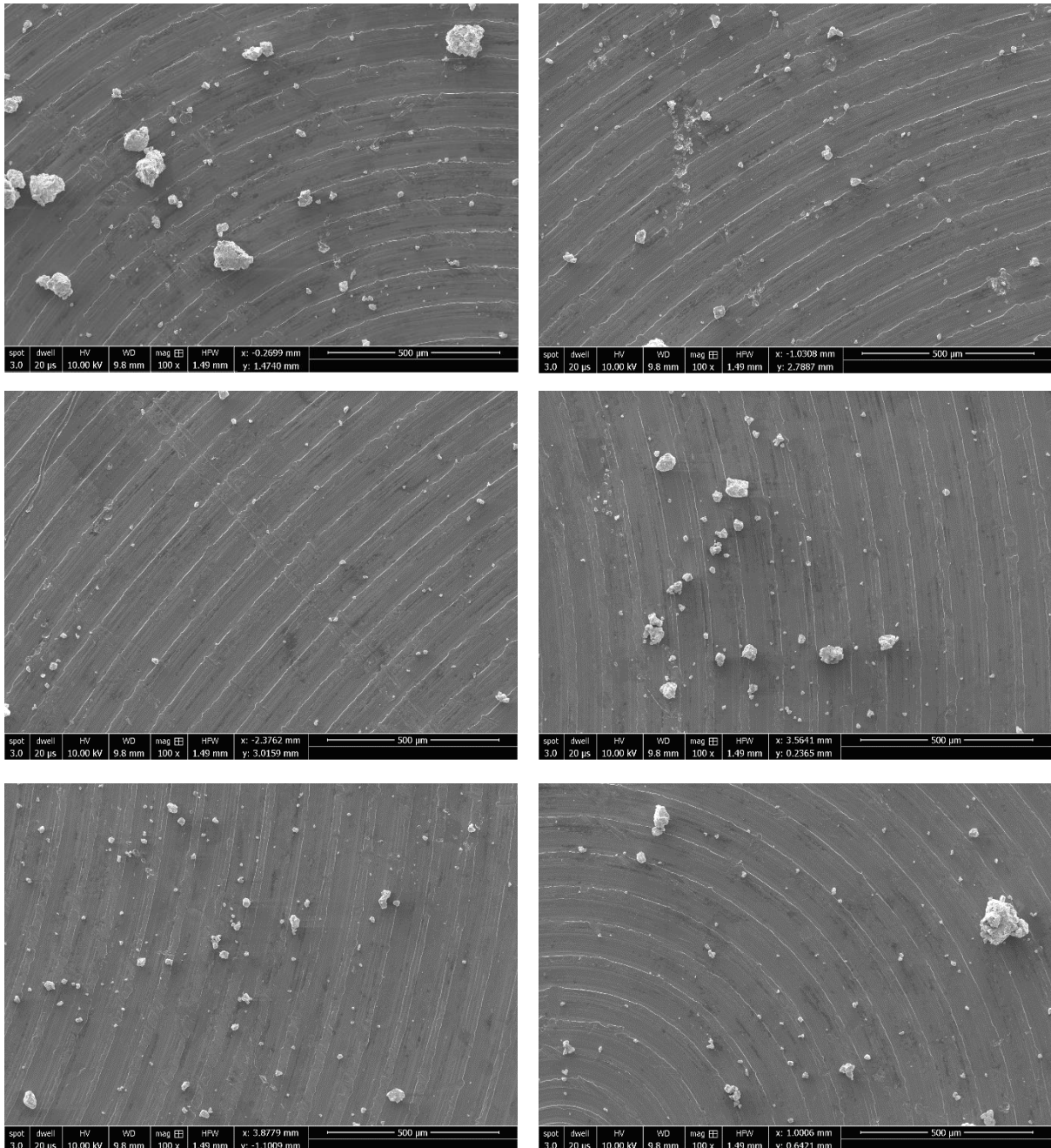


Figure 6-7a (top left), Figure 6-7b (top right), Figure 6-7c (middle left), Figure 6-7d (middle right), Figure 6-7e (bottom left) & Figure 6-7f (bottom right) – x200 magnification SEM images of the powder produced from oversized chips

Figure 6-7a-f show the powder produced from oversized chips. The particles in this powder are considerably smaller, with the largest particles reaching approximately 100µm in size. The majority of particles created range between 10-50µm in diameter. The morphology of the particles is similar to that of the standard powder [0.3, 0.9], with rough-faced spherical chips being produced, although the larger particles appear to be slightly less spherical than seen in the standard sample [0.3, 0.7].

From visual inspection, it is impossible to discern tungsten carbide particles from 316L stainless steel. Tungsten carbide chips would have been generated through brittle fracture, possibly resulting in large rough particles. To confirm this hypothesis, EDS analysis would need to be carried out on larger chips. However, these chips may have broken down into smaller particles, making identification difficult.

### Particle Size Distribution

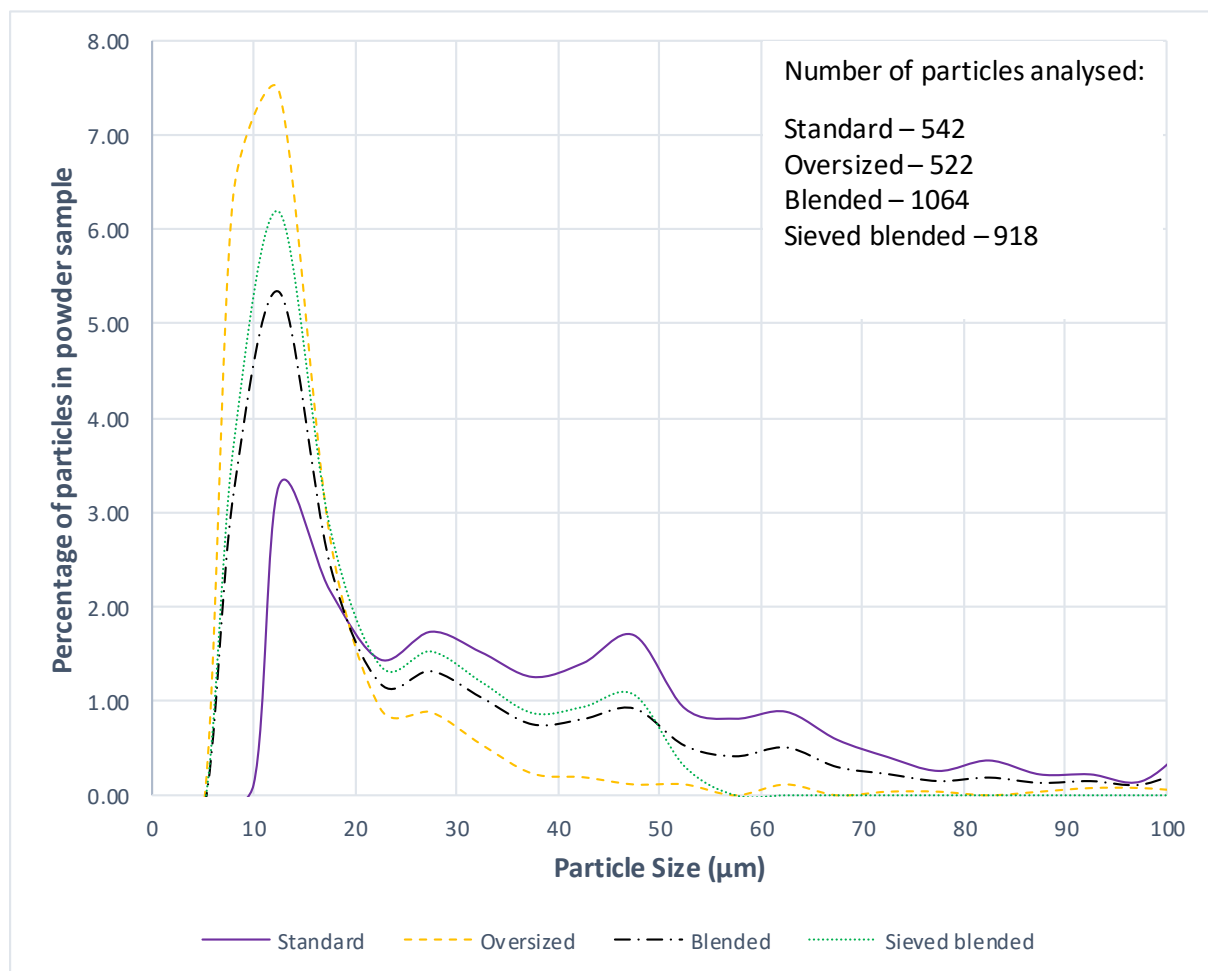


Figure 6-8 – PSDs of the powders created from ball milling and the theoretical blended powders they could create

Table 6-3 – d10, d50, d90 and mean particle sizes for powders created from ball milling and the theoretical blended powders they could create

<i>Powder type</i>	<i>d10 (μm)</i>	<i>d50 (μm)</i>	<i>d90 (μm)</i>	<i>Mean (μm)</i>
<i>Standard</i>	12.7	34.3	72.1	39.5
<i>Oversized</i>	8.5	11.6	27.6	16.0
<i>Blended</i>	9.1	17.9	61.0	20.6
<i>Sieved blended</i>	8.9	15.3	41.3	20.4

BSE images of the same sites seen in Figure 6-6a-g and Figure 6-7a-g provided data for PSD graphs to be produced and d10, d50, d90 and mean particle sizes to be found. These results are manifested in Figure 6-8 and Table 6-3. “Blended” powder is a combination of the particles produced in both the standard and oversized powders. “Sieved blended” powder assumes that the theoretically-generated blended powder has been passed through a 53μm sieve, and that all particles larger than 53μm were removed from the powder, replicating the procedure that all powder would be subjected to prior to being used in AM.

The PSD curve and d10, d50 and d90 values show that the powder produced from the standard chips is substantially larger than the powder created by the oversized chips, indicative of a faster breakdown in the oversized chips. In all powders, there is a significant bias towards very fine particles. Table 6-4 gives an indication of how many particles are suitable for use in the standard SLM range of 15-45μm. Whilst Figure 6-8 suggests that the standard powder has many oversized particles, Table 6-4 shows that standard powder has the most particles that are suitable for use in AM. Based on data in Chapter 4.3.3, virgin powder only has 8.61% of particles smaller than 15μm, with 92.25% of particles being smaller than 45μm, suggesting that much of the powder created through ball milling is likely to be too fine for use in AM.

Table 6-4 – Percentage of particles smaller than 15μm and 45μm for powders created from ball milling and the theoretical blended powders they could create

<i>Powder type</i>	<i>% of particles &lt;15μm</i>	<i>% of particles &lt;45μm</i>	<i>% of particles between 15-45μm</i>
<i>Standard</i>	16.97	64.58	47.61
<i>Oversized</i>	69.16	96.74	27.55
<i>Blended</i>	42.58	80.36	37.78
<i>Sieved blended</i>	49.35	93.14	43.79

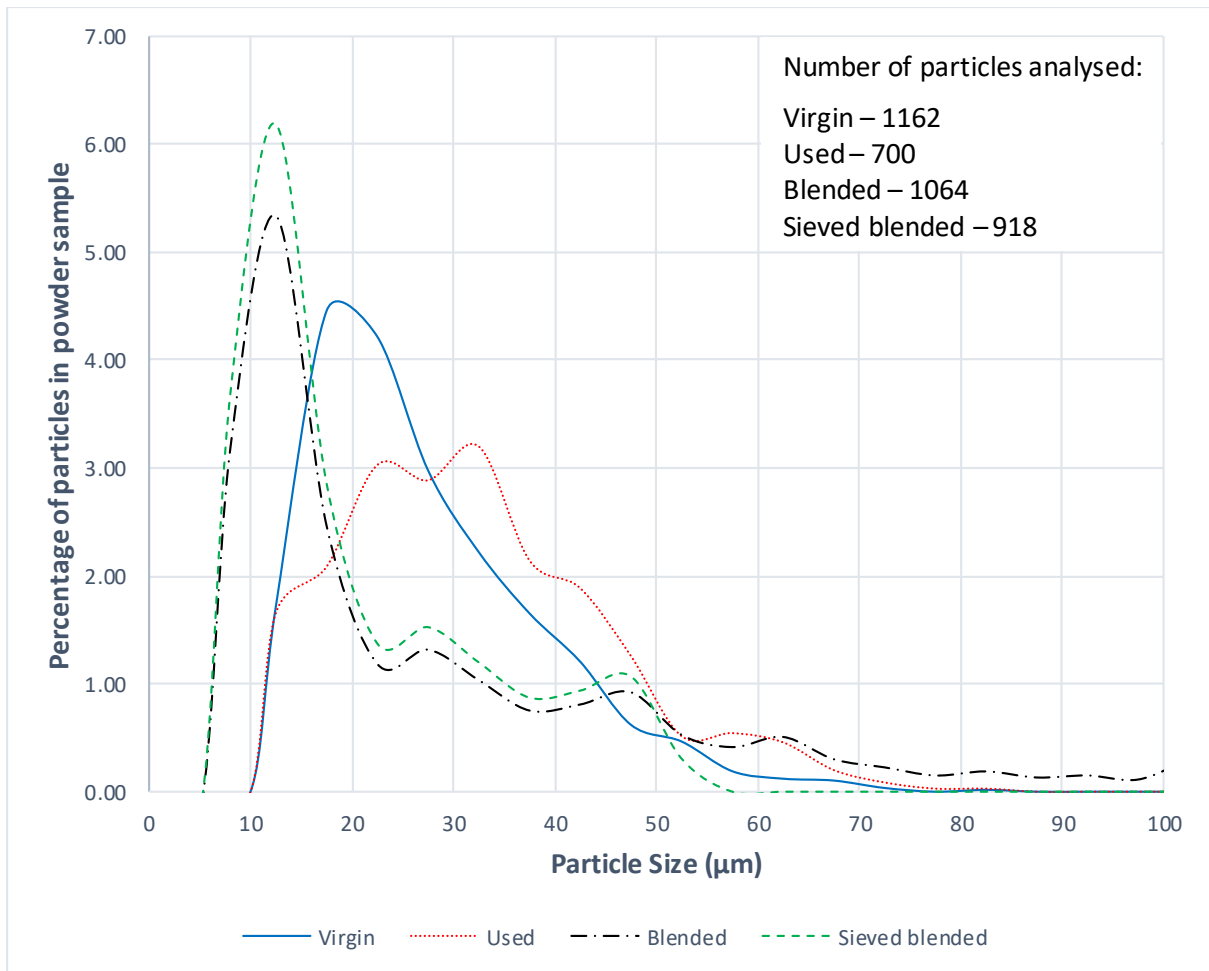


Figure 6-9 – PSDs of the theoretical blended powders compared with virgin and used powders

Table 6-5 –  $d_{10}$ ,  $d_{50}$ ,  $d_{90}$  and mean particle sizes for the theoretical blended powders created from ball milling compared with virgin and used powders

Powder type	$d_{10}$ ( $\mu\text{m}$ )	$d_{50}$ ( $\mu\text{m}$ )	$d_{90}$ ( $\mu\text{m}$ )	Mean ( $\mu\text{m}$ )
Virgin	15.3	24.5	42.7	27.3
Used	15.9	30.6	49.4	32.0
Blended	9.1	17.9	61.0	20.6
Sieved blended	8.9	15.3	41.3	20.4

Figure 6-9 and Table 6-5 compare the blended and sieved blended powders with virgin and used powders from the previous powder analysis completed in Chapter 4.3.3. It is clear that the particles in the ball milled powders are finer than virgin powder, which could lead to complications in the AM process if utilised. The theoretical sieving of the blended powder had the intended effect, reducing the number of oversized particles and creating a PSD that is closer to virgin powder between 15 $\mu\text{m}$  and 45 $\mu\text{m}$ . Used but acceptable powder has an increased number of larger particles within the range

of 30-70 $\mu\text{m}$ , indicating that the powders produced through ball milling can be larger than the powders produced in this experiment, yet still be suitable for use in SLM.

Not all particles could be detected by the image processing software, although they could be seen in the images by qualitative analysis. To prevent lightly-coloured marks on the background of the SEM from being perceived as particles, no particles with a surface area smaller than 50 $\mu\text{m}^2$  were analysed, excluding a small number of the smallest powder particles produced. However, as the sample size was sufficiently large, the statistical significance of the omitted particles is deemed to be negligible. A further source of erroneous results could stem from the lack of a thorough cleaning process used on the chips prior to milling, which may have had residual powder from the AM process adhered to their surface. However, the mass of these particles would be negligible, and thus is also unlikely to significantly influence any results.

### EDS Analysis

Inconsistencies between results were observed in the EDS analysis of the powder samples. The expected atomic composition of 316L stainless steel was not always detected automatically by the software used. As such, where the element was “forced” to be displayed, the results are highlighted. Due to the likely presence of tungsten carbide in the powder, tungsten and carbon have not been shown on the results below. Only the chemical constituents of 316L stainless steel have been detected by the software. This gives a better understanding of the composition of the 316L stainless steel powder being produced.

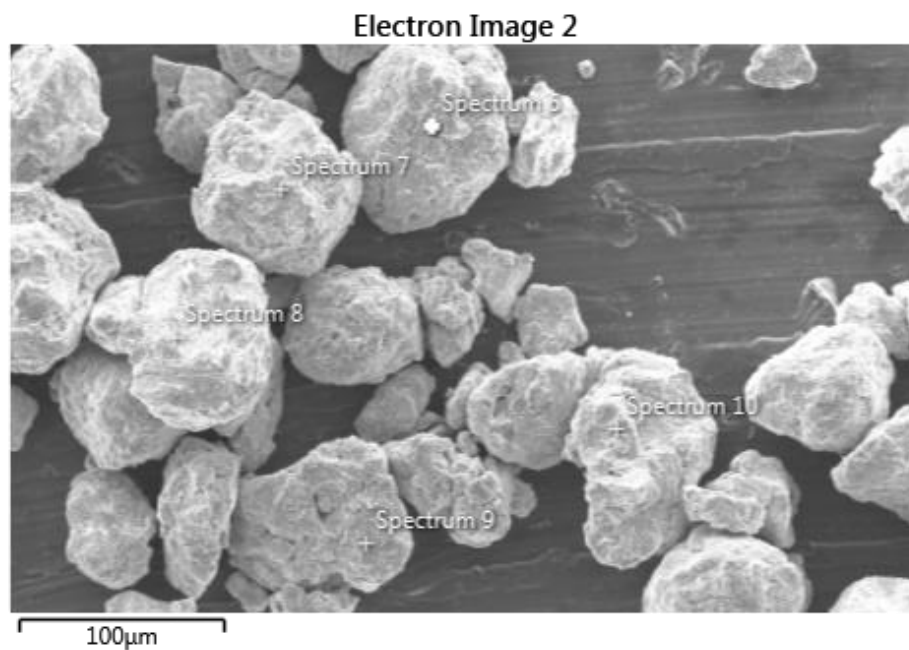


Figure 6-10 – EDS site locations for powder produced from standard chips

Table 6-6 – Chemical composition of each site in Figure 6-10

Spectrum #	6	7	8	9	10
Wt%					
Fe	69.3	57.8	53.3	54.7	67.6
Cr	16.3	15.7	14.4	14.5	16.4
Ni	10.1	10.8	9.3	9.3	10.5
Mo	0.2	1.5	1.5	1.2	0.3
Si	1.9	8.8	13.6	15.2	2.3
O	0.5	4.2	6.7	3.8	1.5
Mn	1.8	1.2	1.1	1.3	1.4

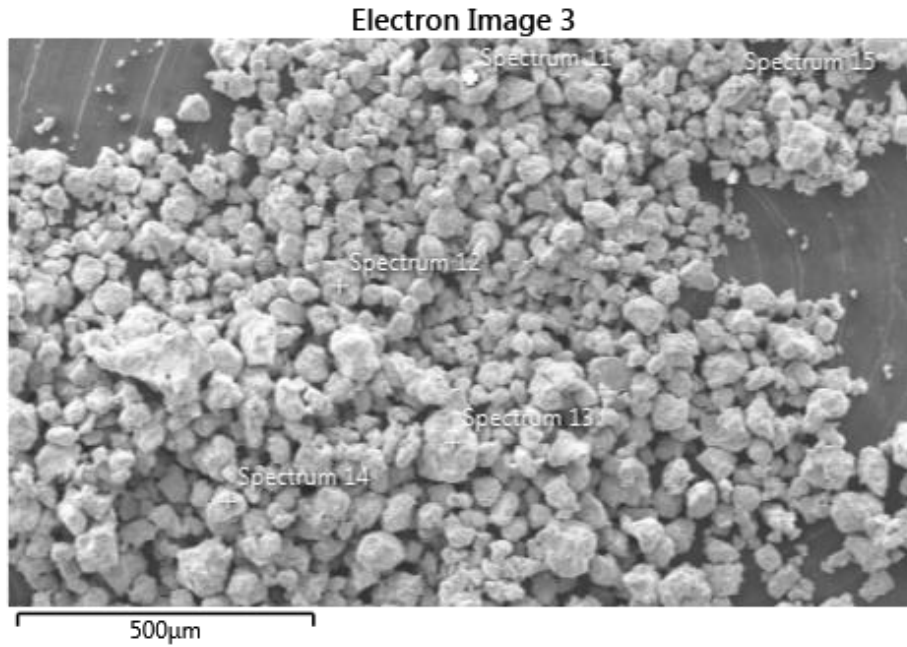


Figure 6-11 – EDS site locations for powder produced from oversized chips

Table 6-7 – Chemical composition of each site in Figure 6-11

Spectrum #	11	12	13	14	15
Wt%					
Fe	44.9	45.1	41.6	46.8	38.6
Cr	12.6	12.2	11.6	12.4	10.9
Ni	8.4	8.3	7.4	8.9	6.7
Mo	1.8	1.6	1.5	1.0	1.8
Si	25.8	25.1	32.6	26.9	33.9
O	5.7	6.9	4.1	3.1	7.7
Mn	0.8	0.8	1.2	0.9	0.5

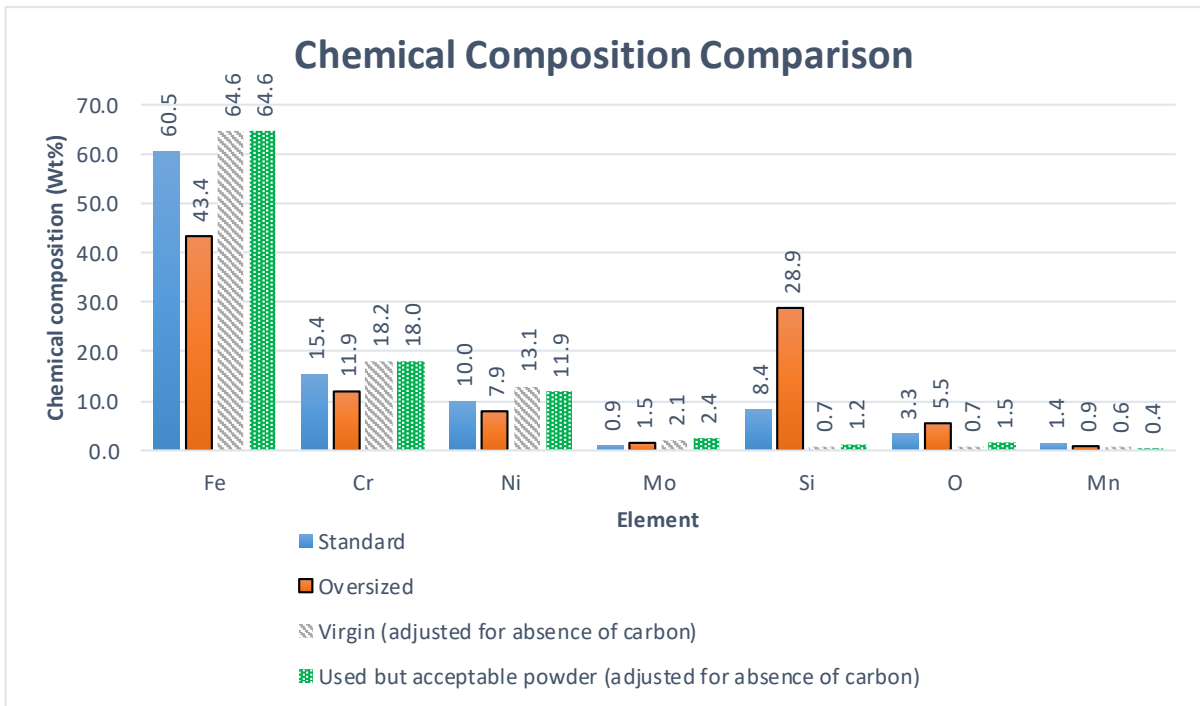


Figure 6-12 – Comparison of the average chemical composition of powders formed from standard and oversized chips with virgin powder (see Table 4-3) and used but acceptable powder (see Table 4-4)

Figure 6-10 and Figure 6-11 show the sites that yield the results seen in Table 6-6 and Table 6-7, in turn giving rise to Figure 6-12. Figure 6-12 allows the difference between both produced powders to be easily seen and compared with powders that are currently used by Croft AM. A significant difference is observed between the standard and oversized powders, where the silicon content is recorded to be over three times larger than that of standard powder, whilst both powders' silicon contents are significantly higher than the levels seen in powders currently used by Croft AM. The presence of this silicon in the oversized powder reduces the quantity of almost all other elements by a considerable margin, with the exception of molybdenum and oxygen. The increased presence of silicon in the standard powder may account for the slighter lower elemental content of iron, chromium, nickel and molybdenum when compared to the virgin or used but acceptable powders.

Standard powder is more similar to the powders used by Croft AM than the oversized powder, although the raised oxygen content and significantly raised silicon content are indicative of a substantial change after ball milling takes place. It is possible that some contaminants were present due to the previous use of the bowls with other materials. As the chips were not thoroughly cleaned prior to being placed in the mill, contaminants may have been picked up in the mechanical workshop in which they originated, or at any point between coming out of the Realizer 250 and being placed in the mill. It is also possible that the chemical composition changes during the SLM process, resulting in the support structures having a different chemical composition to the powders used to create them, although this was not identified in 316L stainless steel during the literature review in Chapter 2.4.1.

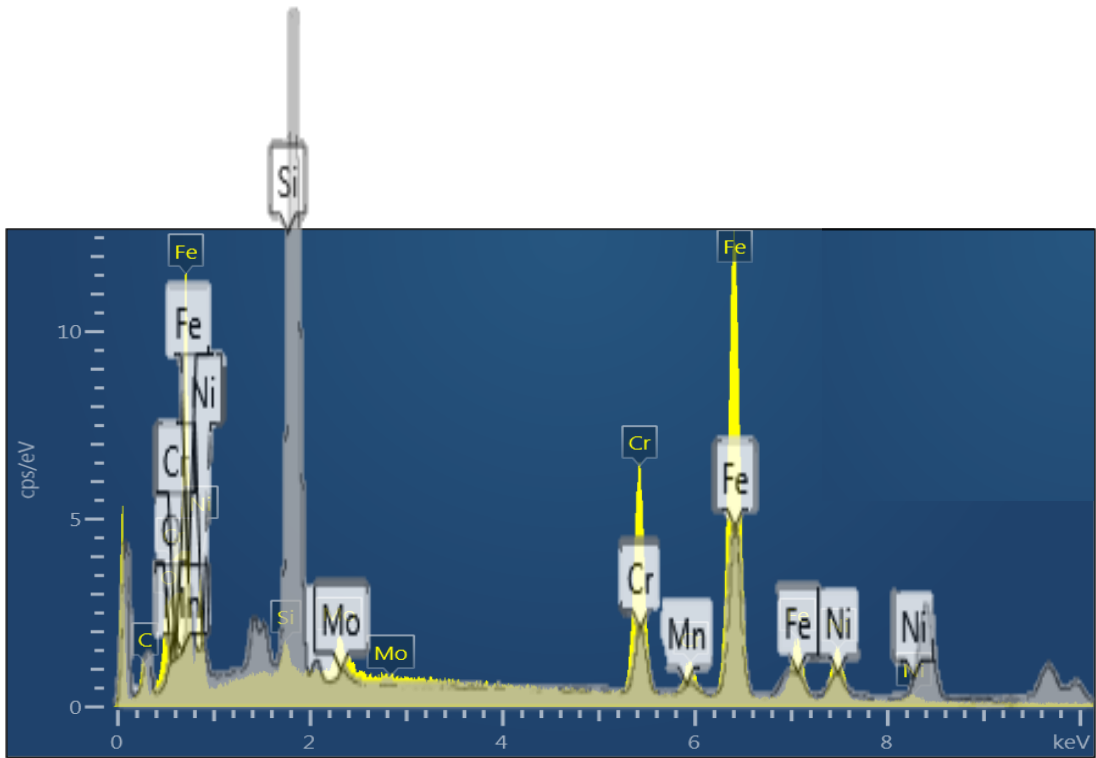


Figure 6-13 – EDS peaks produced for analysis, detecting only the main constituent elements of 316L stainless steel. Yellow regions = a typical particle from virgin powder. Grey regions = a typical particle from oversized powder (minus carbon).

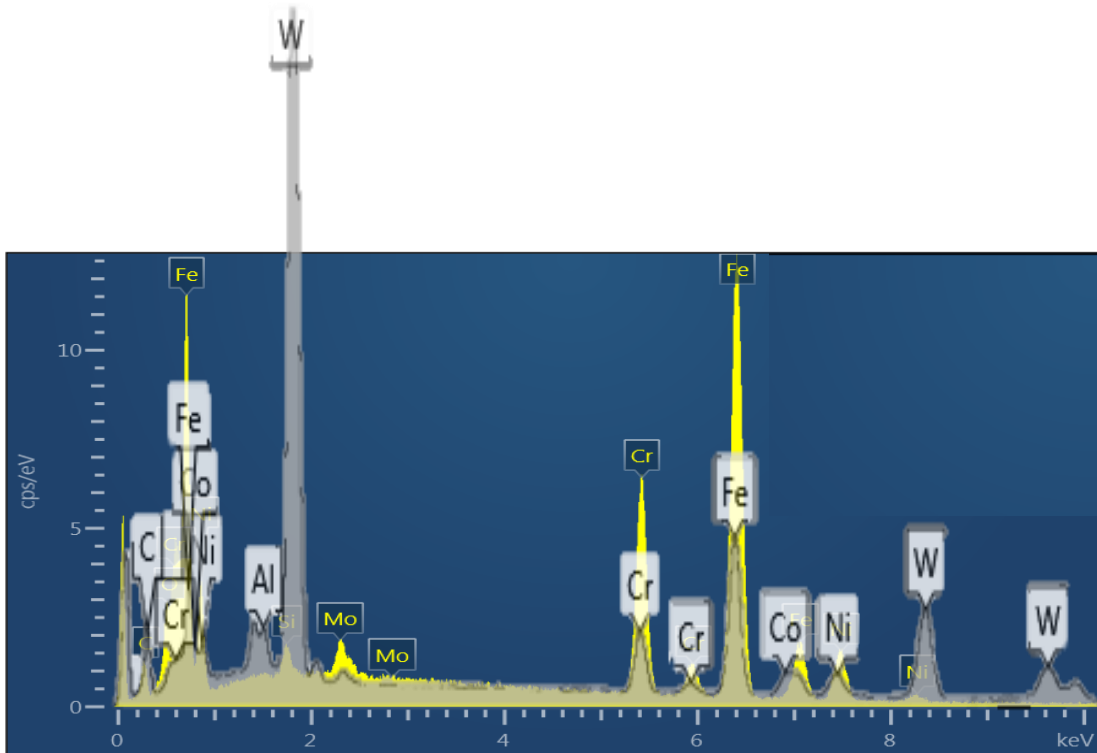


Figure 6-14 – EDS peaks produced for analysis, allowing the software to pair peaks to the most likely element detected. Yellow regions = a typical particle from virgin powder. Grey regions = a typical particle from oversized powder (minus carbon).

The comparison between Figure 6-13 and Figure 6-14 provides a more probable explanation for the increased quantity of silicon detected in the oversized powder. It is far more likely that the largest peak, detected as silicon in Figure 6-13, is tungsten from tungsten carbide contamination. This explains the considerable difference seen between powders in Figure 6-12, illustrating the challenge associated with accurately determining the chemical composition of 316L stainless steel powders.

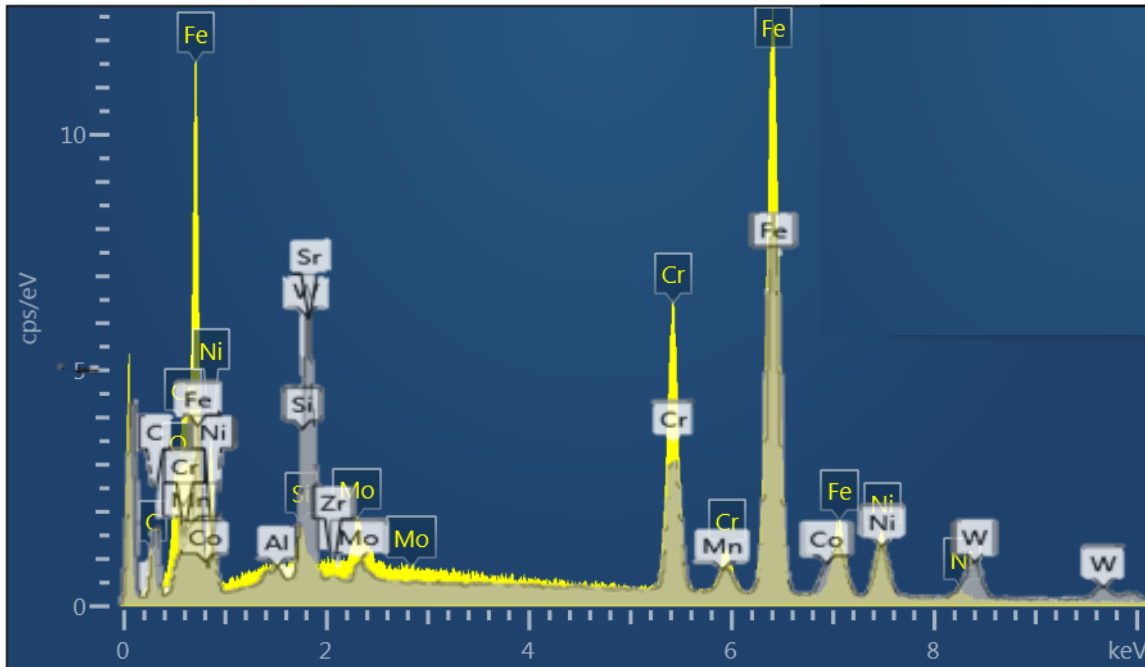


Figure 6-15 – EDS peaks produced before analysis, allowing the software to pair peaks to the most likely element detected. Yellow regions = a typical particle from virgin powder. Grey regions = a typical particle from standard powder (minus carbon).

The level of contamination inferred from Figure 6-14 is unacceptably high, rendering the powder produced through ball milling of oversized chips unusable in AM. However, Figure 6-15 indicates that the powder produced from standard sized chips contained less tungsten carbide contamination. This may have occurred due to the oversized chips occupying a smaller volume once they had begun to break down (evidenced by the reduced initial mass of oversized chips), resulting in more frequent tungsten carbide-tungsten carbide collisions. This would result in more tungsten carbide chips forming and breaking down, mixing in with the 316L stainless steel powder, and thus high levels of contaminants. As there was a higher volume of powder once the standard chips had begun to break down than in the oversized chips, there would be less tungsten carbide-tungsten carbide collisions, resulting in less tungsten carbide contamination within the standard powder.

Whilst this conflicts with the data in Table 6-2, an unknown mass of produced powder fused with the balls and bowls, making it difficult to ascertain information from mass measurements alone. The data in Figure 6-14 and Figure 6-15 suggests that filling bowls with more milling media may reduce the level

of contamination from tungsten carbide during ball milling. Currently, the volume of chips does not represent the volume of powder that is formed from ball milling; 15ml of perfectly packed stainless steel powder should weigh 119.85g, whilst 15ml of support structure only weighed 18.7g and 11.1g. This equates to 15.6% and 9.3% of the theoretical mass that could have been input to the mill. It is therefore possible that the bowls were underfilled in the present experiment, resulting in more tungsten carbide-tungsten carbide collisions, and thus a higher level of contamination in the produced powders.

Whilst Figure 6-15 shows the typical levels of contamination in an average powder particle, Site 6 and Site 10 in Table 6-6 show remarkably similar chemical compositions to that of the powders currently used by Croft AM, with considerably less silicon than seen in other standard particles, indicating that they are less contaminated by the presence of tungsten causing this erroneous silicon reading. This suggests that contamination does not always occur in the ball milling process and that there may be a means of producing powder particles that are considerably less contaminated, and, therefore, more useable in AM.

### 6.2.3 Discussion

The breakdown of chips produced from support structures into powder through ball milling with tungsten carbide occurred at an unexpectedly rapid rate; it was initially considered to take upwards of 24 hours. This led to the production of an unnecessarily fine powder that may not be suitable for use in AM, and is likely to have contributed to the excessive wear and breakdown of the tungsten carbide balls and bowls, resulting in the presence of tungsten carbide contamination within the produced powder. This further reduces the viability of this powder for use in AM.

The 316L stainless steel powder could be considered to be of a similar quality to water-atomised powder. Fullenwider *et al.* (2019) had already demonstrated that 316L stainless steel powder produced using ball milling could be utilised in DED AM methods, although the powder produced in the present experiment was considerably finer and therefore has potential to be utilised in other AM technologies, such as SLM. The powder produced was considerably different in morphology and chemical composition to that of the powders currently used in SLM, although further processing could make the powder more suitable for use. Figure 3-4 considers a method of powder reclamation, plasma spheroidisation, which has already seen success in converting water-atomised powders into high-quality spherical powders (Kelkar, 2019).

The objective of creating this powder was to demonstrate that there may be an environmentally-friendly alternative to virgin powder production through atomisation of waste support structures. The initial calculations of the energy efficiency of the process laid out in Chapter 6.1 can now be modified to improve their accuracy.

*Table 6-8 – Energy consumption calculations based on the data collected*

<b>Chips</b>	<b>Mass of 15ml sample</b>	<b>Mass of 900ml sample</b>	<b>Machine-on time</b>	<b>Machine energy consumption</b>	<b>Energy consumption per kilogram</b>
<b>Standard</b>	18.7g	1.122kg	7 hours	43.61MJ	38.87MJ/kg
<b>Oversized</b>	11.1g	0.666kg			65.48MJ/kg
<b>Blended</b>	14.9g	0.894kg			48.78MJ/kg

Table 6-8 shows the overall energy consumption required to produce powders from both standard and oversized chips, alongside a theoretical blended sample of both types of chip. The maximum sample size of 900ml per machine is used to assume the work has been upscaled to be carried out at a medium-sized facility. The calculations are based on the assumption that the methodology is refined through future experiments, allowing all of the powder produced to be reclaimed. The production of chips from support structures (see Chapter 5) is expected to consume a negligible quantity of energy in comparison to ball milling, and is therefore not considered in these calculations.

Standard chips would provide the best output of powder per unit of energy, although this was still found to be 18.5% higher than the 32.81MJ of energy required to produce 1kg of powder from scrap stainless steel. 35.42% of particles produced in the standard powder were larger than 45µm (see Table 6-4), potentially resulting in much of this powder being sieved out if it were to be used for AM, negatively influencing this energy consumption value. Ball milling of oversized chips would require 99.6% more energy per gram of powder produced than the atomisation of scrap steel. However, the powder produced was much finer, with only 3.25% of particles being over 45µm in diameter (see Table 6-4), resulting in a significantly higher potential usage rate of this powder. Assuming that the standard chips and oversized chips were mixed in equal quantities in the milling process, the blended powder produced would use 48.7% more energy per gram of powder produced than the current recycling method. This powder would likely produce fewer oversized particles, creating a PSD that would be usable in SLM.

This data suggests that ball milling may not be a viable green avenue to further pursue for the creation of powders suitable for use in AM. However, the particles that were created were unnecessarily fine. If it could be demonstrated that less time is needed to produce larger particles that were more suitable

for use in SLM through ball milling, then this value could be substantially reduced; if only three hours of milling was required, blended chips would use 36.3% less energy than the current method to produce powder from scrap steel. Despite this potential reduction, if the powder requires reclamation to ensure it is suitably spherical for use in SLM, the upcycling process would certainly require more energy than the current recycling process. As such, ball milling may only be a more sustainable method to create low-quality, larger powders for use in EBM or DED at this stage (see Figure 3-1).

#### 6.2.4 Conclusions

The powder produced from ball milling broken-down support structures is not as high-quality as powders produced by the typically-used gas atomisation process. The particles produced have a rough surface and lack of regularity in shape, although they are typically spherical. Using the current methodology, many of the particles produced were found to be overly fine for use in AM. The chemical composition of some of the powder particles produced was found to be suitable to 316L stainless steel powders currently used in AM, although the presence of tungsten carbide contamination in the majority of the produced powder particles is a challenge that needs to be overcome.

Whilst the powder produced by ball milling in this experimental setup seems to be unusable in SLM in its current state, the results are promising. By reducing the duration of milling, it may be possible to produce powders with fewer fine particles, aligning more closely with the PSD of virgin powders utilised in SLM. The use of a grinding aid may assist in accelerating the breakdown of chips, in turn reducing the tungsten carbide contamination level in the powder through further reduction in the required duration of ball milling. The volume and type of chips used as feedstock material appeared to have a large impact on the success of the breakdown procedure. It has been hypothesised that using a mixture of chip sizes as input material may further assist in producing powder that has a suitable PSD for use in AM processes. Filling the bowls with an increased mass of chips may also assist in reducing contamination from tungsten carbide whilst increasing the yield of powder produced per MJ consumed. Future experimentation with a reduced ball milling duration, grinding aid and a greater mass of assorted chips is therefore recommended.

Once a larger volume of sample powder has been collected, plasma spheroidisation of the produced powders should be carried out, determining if the powder can be effectively upcycled (see Figure 3-4). If this is found to be unfeasible, then alternative uses for the powder should be identified, such as using it in other powder-dependent industries, or within the less-demanding DED process.

## 6.3 Further experimentation

### 6.3.1 Methodology

Based on the findings in Chapter 6.2, further ball milling experiments were carried out at the Dalton Cumbrian Facility. The objective was to validate the conclusions previously drawn in Chapter 6.2.4. As such, the experimental procedure was kept the same, with the following changes implemented:

The chip samples input to the bowls were comprised of a random mix of variously shaped and sized chips from different support structure designs, as produced in Chapter 5 and shown in Figure 6-16. This decision was made as Chapter 6.2 demonstrated that the size of the chips had seemingly little effect on how well they broke down into powder. By using a broad range of chip sizes, a wider PSD may be achieved, whilst less time would be needed separating chips prior to ball milling. This led to the inclusion of some “thick chips”, highlighted in Figure 6-16. These chips formed when several dense border support structures compressed in the guillotine, interlacing multiple layers together, and were presumed to be significantly harder to break down.



Figure 6-16 – Examples of the chips included in each sample, overlaid on a 5x5mm grid. Left: assorted chips. Right: overfilled assorted chips. Circled regions show example of thick chips

Two samples were measured out. The “assorted” sample comprised of approximately 15ml of randomly chosen chips, whilst the “overfilled” sample contained approximately 30ml of randomly chosen chips. A comparison of the two samples can be seen in Figure 6-17. Measuring the mass was considered to be a more important and accurate method of representing the volume of powder that would be produced, with the mass and theoretical powder volume of each sample being shown in Table 6-9. It was hypothesised that increasing the volume of chips in the bowl may reduce the level of tungsten carbide contamination in the produced powder through reduced tungsten carbide – tungsten carbide interactions.



Figure 6-17 – Side-by-side comparison of the samples of assorted (left) and overfilled assorted (right) chips

Table 6-9 – The volume of chips, mass and theoretical volume of powder for each sample

Chips	Approximate volume of chips	Mass	Theoretical volume of powder
Assorted	15ml	16.9g	2.11ml
Overfilled	30ml	30.3g	3.79ml

The bowls were thoroughly scraped and cleaned using a chisel prior to the new samples being added to minimise the effect of the previous samples on this experiment, although some solidified powder remained. Ball milling was carried out for 270 minutes of machine-on time. Milling was paused after every 30 minutes of machine-on time to allow a random powder sample to be taken for analysis by SEM and EDS. This would allow the rate of breakdown to be determined, as the seven hours of ball milling gave no indication of this in Chapter 6.2. When the machine was stopped, the bowls were opened before the mill could cool down in an attempt to prevent the solidification and adhesion of the powder seen in Chapter 6.2.2. Any powder that had begun to adhere to the bowl was scraped off using a stainless steel spoon as best possible. As much of the remaining powder was reclaimed as possible after 270 minutes.

### 6.3.2 Results

#### *Physical Inspection*

The regular sampling of the powder allowed for visual inspection of the samples and breakdown process over time. The assorted powder began to break down faster than the overfilled powder and was fine enough to start sticking to the ball milling equipment after 150 minutes of ball milling. The overfilled powder was fine enough to exhibit the same behaviour after 210 minutes. Figure 6-18 compares the two powders created after 270 minutes of ball milling with virgin powder.



Figure 6-18 – The powders formed from assorted chips (top left) and the overfilled chip sample (top right) compared with virgin powder (bottom)

The powders created after 270 minutes of ball milling were considerably coarser than the virgin powder used by Croft AM. The overfilled powder produced a larger quantity of powder, but to the naked eye has more large particles than the assorted powder. The virgin powder is fine enough to stick to the Ziploc bag when moved, whilst this behaviour is not seen in either of the powders created after 270 minutes of ball milling.

Table 6-10 – The mass of powder produced after 270 minutes of ball milling

<b>Chips</b>	<b>Initial mass</b>	<b>90mins</b>	<b>Initial variation</b>	<b>180mins</b>	<b>Midpoint variation</b>	<b>270mins</b>	<b>Final variation</b>
<b>Assorted</b>	16.9g	21.72g	+ 4.82g	21.95g	+ 5.05g	22.55g	+ 5.65g
<b>Overfilled</b>	30.3g	35.61g	+ 5.31g	35.85g	+ 5.55g	35.50g	+ 5.20g

The mass of each sample was weighed every 90 minutes, displayed in Table 6-10. There is a notable difference between the initial masses of the samples weighed and the masses of the powders recorded from both assorted and overfilled chips. This change in mass is likely to be contamination from the previous ball milling experiment, where powder had adhered to the bowls and balls. As much of the adhered powder was removed as possible with a chisel, but some powder may have subsequently become loose once ball milling began and the stuck powder was impacted upon. This powder would have loosened at an early stage and become mixed with the rest of the powder, explaining the initial increase in mass. As such, this error is likely to be systematic, with the initial

variation indicating the mass of old powder that has contaminated each sample. Whilst this contaminated the resultant powder, the mass of contaminant is similar in both samples. However, as there was a smaller mass of assorted chips to begin with by approximately half, the impact of this contamination is likely to have nearly twice the effect on the assorted chips.

The more important data is the change in mass over time. The mass appears fairly consistent in the overfilled sample, whereas a small and constant increase is seen in the assorted sample. This is potentially indicative the accumulation of tungsten carbide fragments as the mechanical breakdown of chips reduces as the powder becomes smaller, increasing ball-to-ball and ball-to-bowl interactions. These results may be indicative of increased contamination in the assorted chips when compared to the overfilled chips. Despite this, the relative consistency of the powder mass demonstrates a considerable improvement in experimental procedure over the initial ball milling experimentation carried out in Chapter 6.2.

SEM Imaging

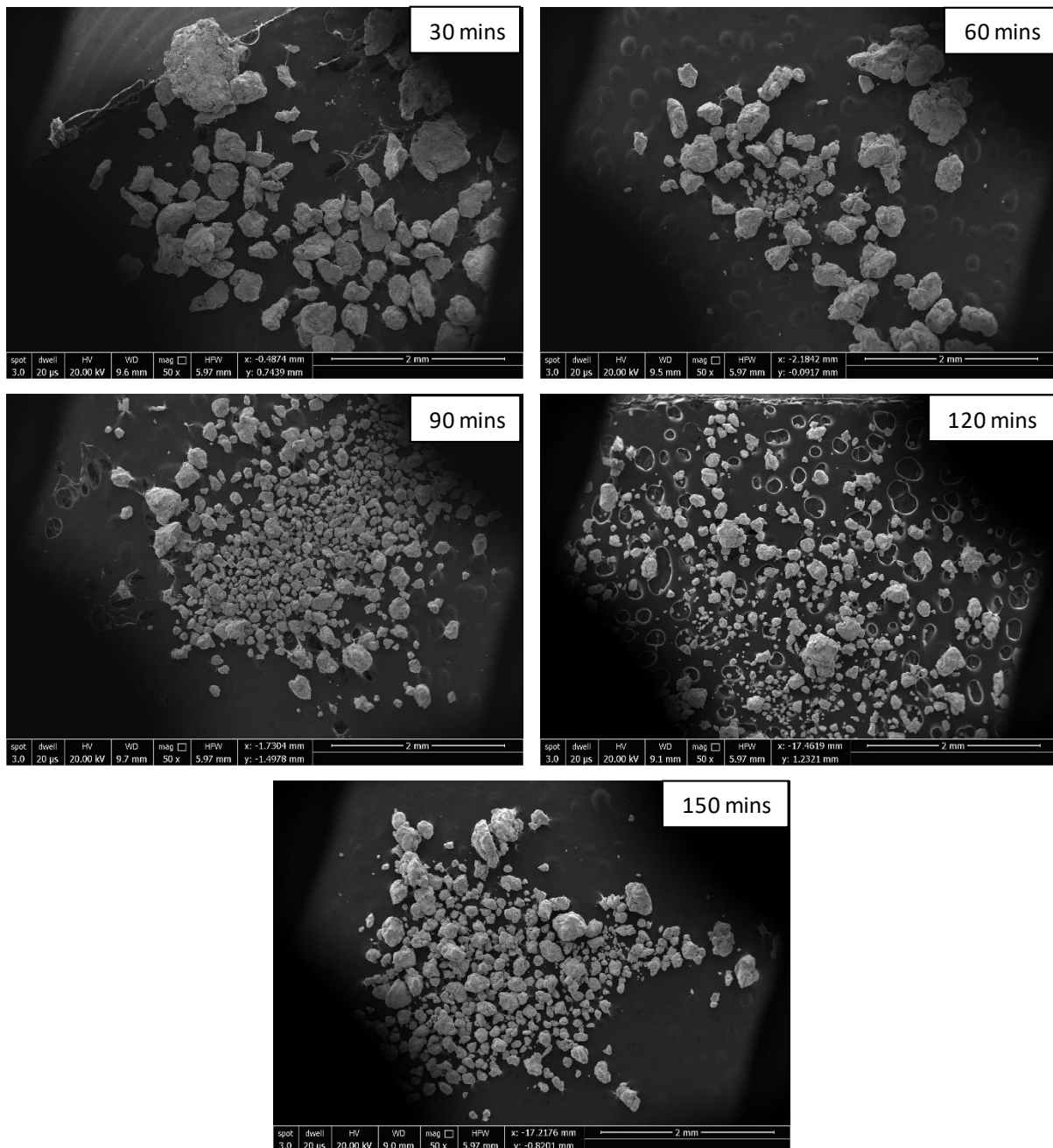


Figure 6-19a (top left), Figure 6-19b (top right), Figure 6-19c (middle left), Figure 6-19d (middle right) and Figure 6-19e (centre bottom) – x50 magnification SEM images of the powder produced from the assorted sample after 30, 60, 90, 120 and 150 minutes respectively

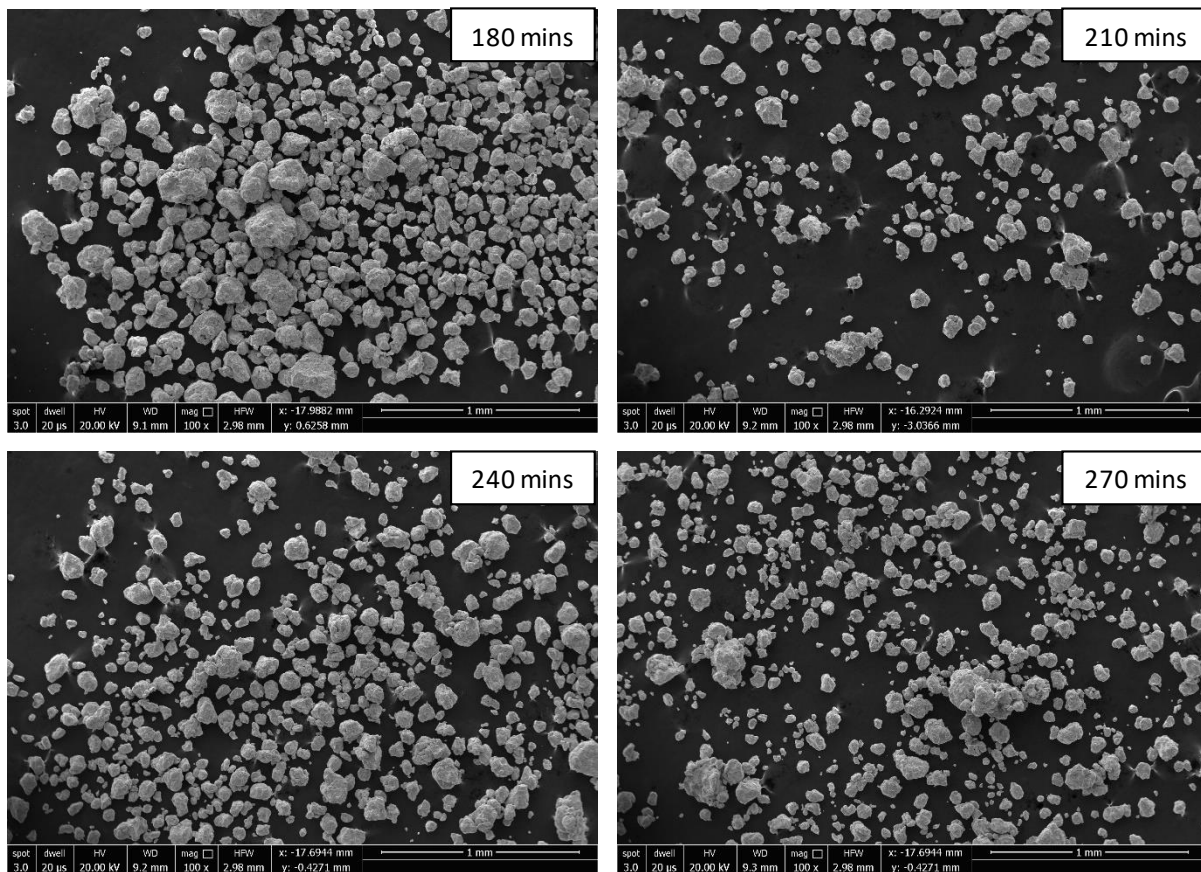


Figure 6-19f (top left), Figure 6-19g (top right), Figure 6-19h (bottom left) and Figure 6-19i (bottom right) – x100 magnification SEM images of the powder produced from the assorted sample after 180, 210, 240 and 270 minutes respectively

Figure 6-19a through to Figure 6-19i demonstrate the rate of powder formation from the assorted sample. At the early stages most particles are over 300µm, although some particles are already as small as 75µm, with most particles having been flattened and very rough [0.1, 0.3]. After 90 minutes many of the particles appear to be suitably small for use in AM, typically between 50-100µm, although a considerable number of oversized particles remain. The particles are smoother and considerably more spherical [0.3, 0.7]. This is still the case after 150 minutes. After 210 minutes most particles appear to be suitably small for AM, ranging between 15-100µm, although other particles are as large as 300µm. The particles remain rough but become highly spherical at this stage [0.3, 0.9], making them similar in morphology to the powder produced by the ball milling procedure in Chapter 6.2. This suggests there is unlikely to be a change in particle morphology after 210 minutes of ball milling, despite further particle size reductions. Oversized particles remain present even after 270 minutes, although these particles could be easily separated through sieving prior to use in AM.

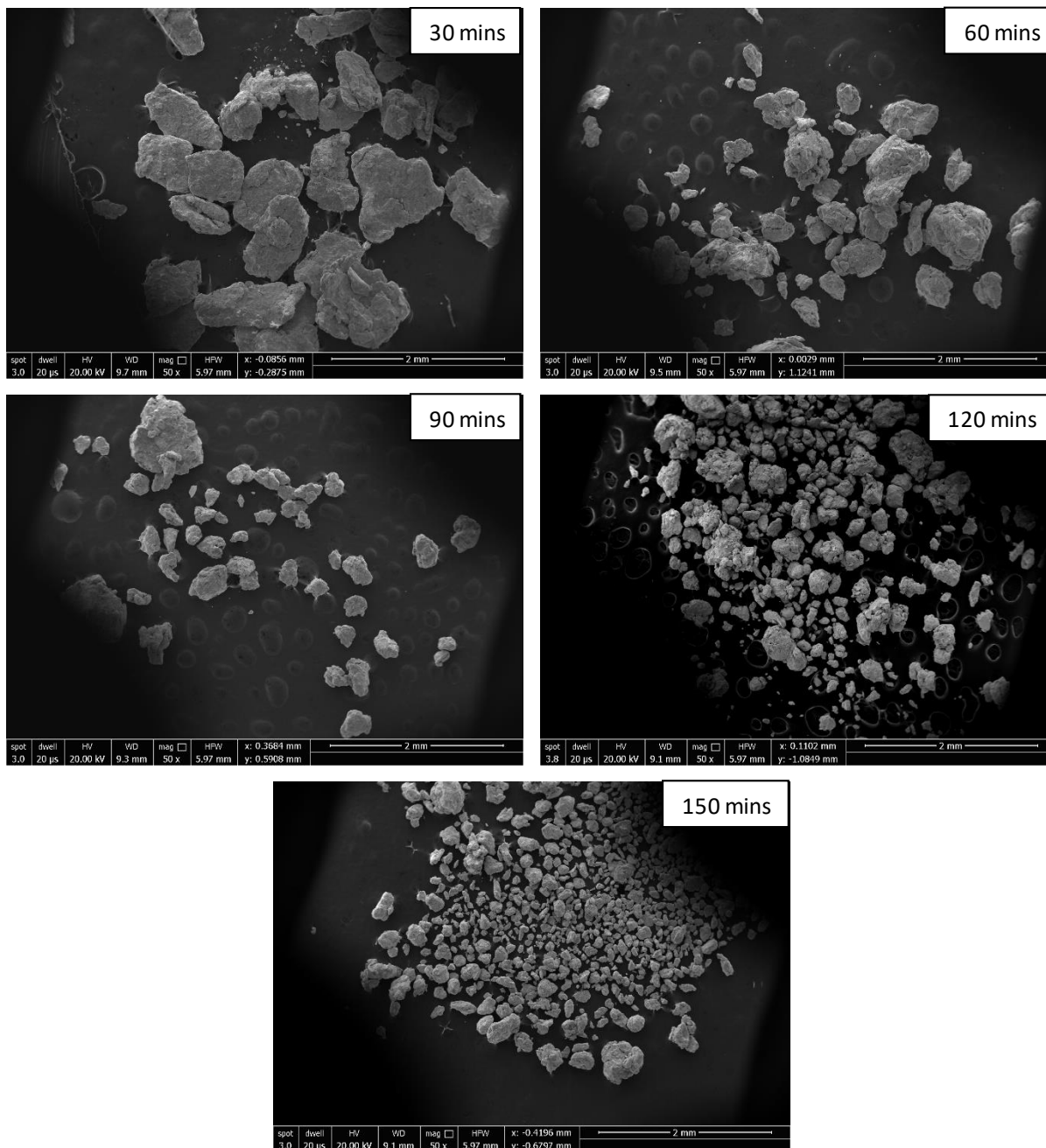


Figure 6-20a (top left), Figure 6-20b (top right), Figure 6-20c (middle left), Figure 6-20d (middle right) and Figure 6-20e (centre bottom) – x50 magnification SEM images of the powder produced from the overfilled sample after 30, 60, 90, 120 and 150 minutes respectively

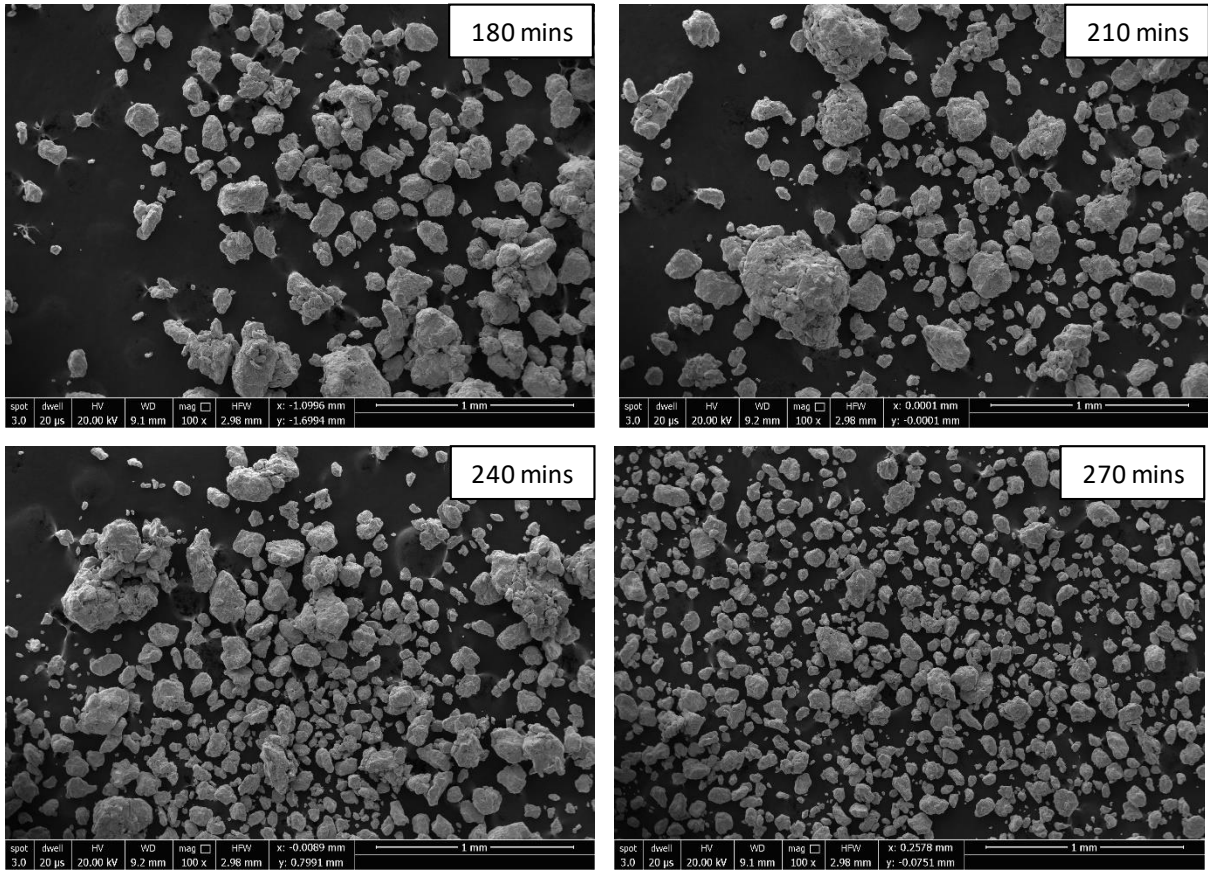


Figure 6-20f (top left), Figure 6-20g (top right), Figure 6-20h (bottom left) and Figure 6-20i (bottom right) – x100 magnification SEM images of the powder produced from the overfilled sample after 180, 210, 240 and 270 minutes respectively

Figure 6-20a through to Figure 6-20i demonstrate the rate of powder formation from the overfilled chips. The particles appear to take longer to break down when compared to the assorted chips. After 30 minutes of ball milling, almost all particles are still larger than 750 $\mu$ m, highly flat and rough [0.1, 0.3]. The overfilled powder particles after 150 minutes of ball milling are similar to those produced after only 90 minutes in the assorted sample; many particles are between 50-100 $\mu$ m, although many are larger than this, and the particles become smoother and more spherical [0.3, 0.7]. After 210 minutes the powder seems to have similar morphologies to the other powders produced from ball milling, with most particles that are not oversized appearing spherical [0.3, 0.9]. Considerably less oversized particles are seen when the powder is milled for 270 minutes. Throughout the process there appear to be consistently more oversized particles than seen in the assorted powder after the same duration of ball milling.

### Particle Size Distribution

By comparing the PSD of the powder at various stages, it is possible to identify when ball milling can be ceased. If the powder is suitably similar to that of acceptable powders in use by Croft AM currently, there would be no further benefit in continuing to mill the powder. This assists in ensuring the power consumption estimates in Chapter 6.3.3 are accurate, and thus helps determine if overfilling bowls is beneficial environmentally.

Many of the SEM images in the powder samples before 150 minutes did not contain enough particles to accurately perform PSD analysis using ImageJ. As such, PSD analysis was only carried out on the powder samples taken after 150, 210 and 270 minutes.

It is possible that the potential contamination from the balls and bowls used in the previous experiment reduced the average particle size in both the assorted and overfilled powders. This should therefore be considered when conclusions are drawn from PSD analysis of these powders.

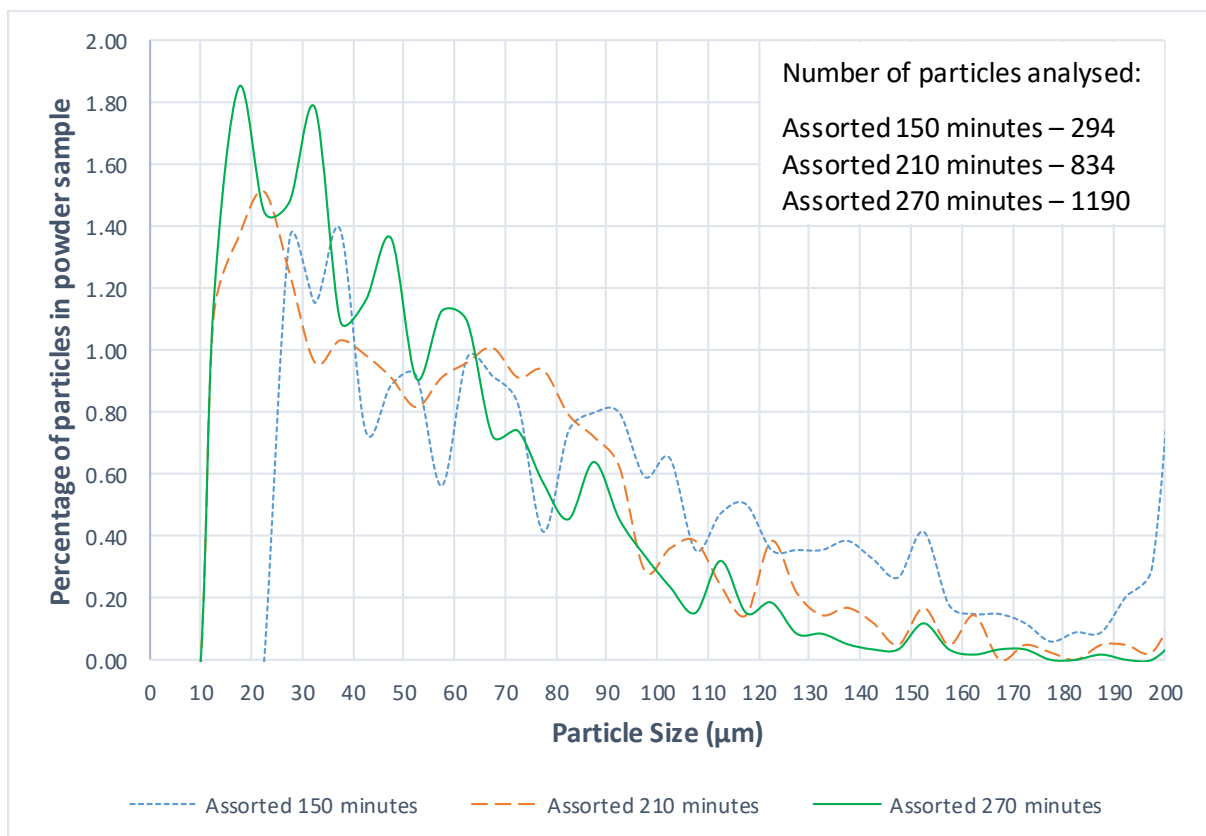


Figure 6-21 – PSD of the powder produced from assorted chips after various durations of ball milling

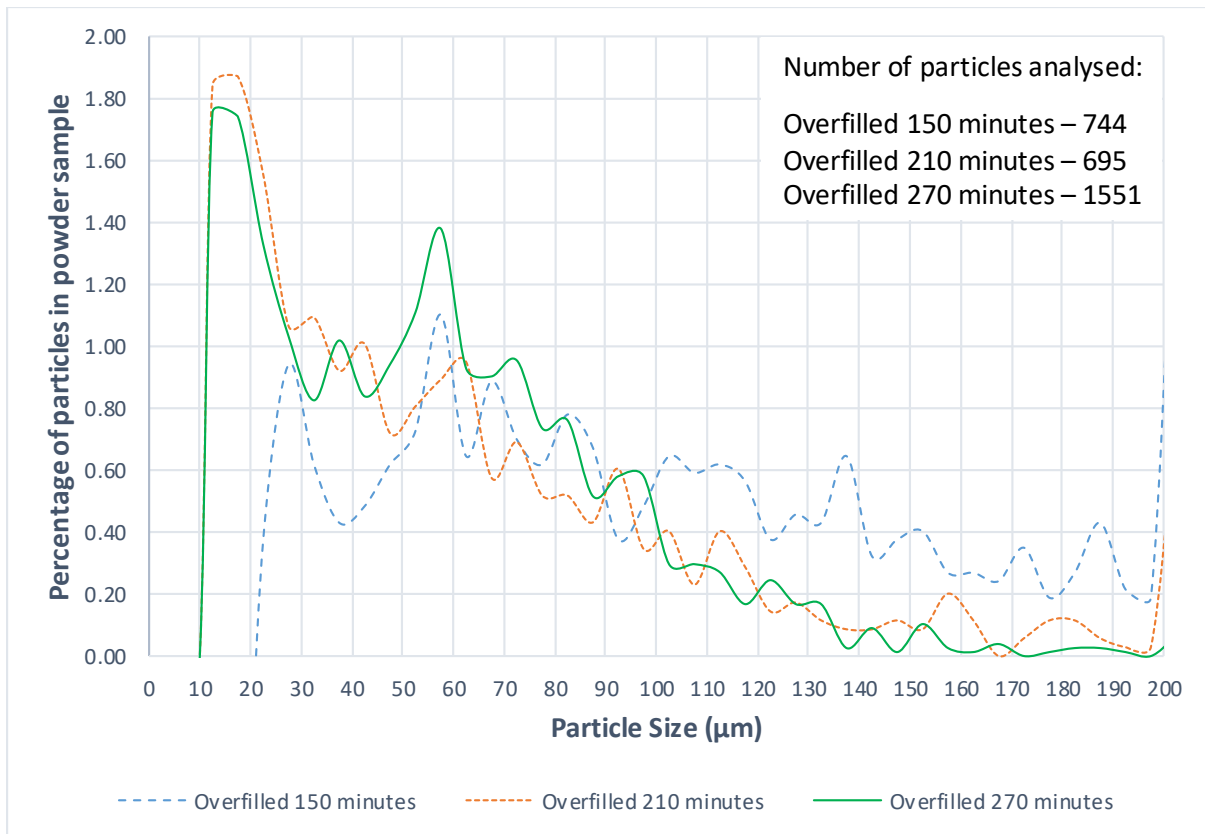


Figure 6-22 – PSD of the powder produced from the overfilled chip sample after various durations of ball milling

Table 6-11 – d10, d50, d90 and mean values of the powder produced from assorted and overfilled chip samples after various durations of ball milling

	d10 (µm)	d50 (µm)	d90 (µm)	Mean (µm)
<i>Assorted 150 mins</i>	32.6	105.9	212.6	114.9
<i>Assorted 210 mins</i>	18	55.4	112.8	61.8
<i>Assorted 270 mins</i>	16.9	45.2	94.6	51.9
<i>Overfilled 150 mins</i>	35.9	95.3	192.6	109.3
<i>Overfilled 210 mins</i>	15.4	58	126.1	64.5
<i>Overfilled 270 mins</i>	15.7	52.3	101.1	56

Figure 6-21, Figure 6-22 and Table 6-11 show how the PSD of the powders changed as ball milling continued. Longer durations of ball milling reduced the average particle size, as expected, increasing the number of small particles and reducing the number of larger particles. The reductions in particle size are close to 50% between the 150 and 210 minute samples, although the reduction in size between 210 and 270 minutes is no greater than 20%. This indicates that the rate of breakdown begins to decline as ball milling continues, requiring an exponential increase in power consumption to achieve a smaller particle size.

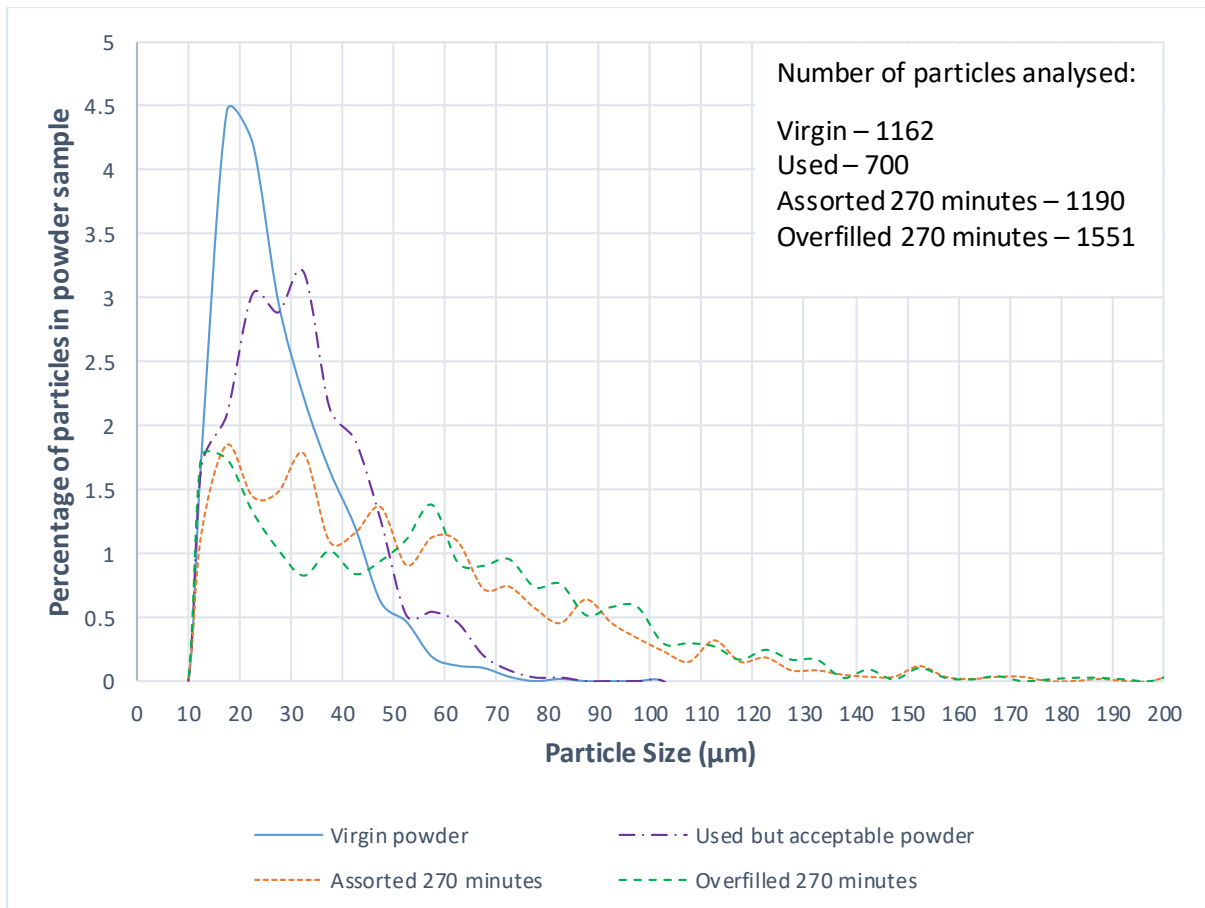


Figure 6-23 – PSD curves of the powders produced from ball milling compared with powders used by Croft AM

Table 6-12 – Percentage of particles within various size ranges for powders created from 270 minutes of ball milling

Powder type	% of particles <15µm	% of particles between 15-45µm	% of particles between 45-150µm	% of useful particles
Assorted 270 minutes	5.71	38.32	48.66	86.98
Overfilled 270 minutes	8.77	33.91	55.64	89.55

Figure 6-23 shows that the powders produced by the shortened duration of ball milling were not as suitable for use in SLM as the powders produced in Chapter 6.2. From Table 6-12, it can be discerned that 56.0% and 57.3% of particles in the powders produced from assorted chips and overfilled chips respectively were larger than 45µm and therefore unlikely to be suitable for use in SLM. Table 6-12 further considers the percentage of particles produced that are oversized or undersized, yielding a “useful particle” percentage. This represents the number of particles that can be confidently used in AM processes. In both the assorted and overfilled powder samples, these values are above 86%, although further refining of the ball milling procedure could improve this.

Although the percentage of particles between 15-45 $\mu\text{m}$  is above a third of the total number of particles produced, the volume of powder produced at these particle sizes is considerably less than a third of the total volume of powder produced; larger particles will occupy more volume, but are still only considered to be one particle in these calculations. As such, there is likely to be a very small mass of powder between 15-45 $\mu\text{m}$  produced compared to the mass of powder generated between 45-150 $\mu\text{m}$ . This indicates that the powder generated through shorter durations of ball milling is unlikely to be suitable to produce the quantity of powder necessary for SLM, although it may be capable of producing enough powder for other AM processes such as DED and EBM.

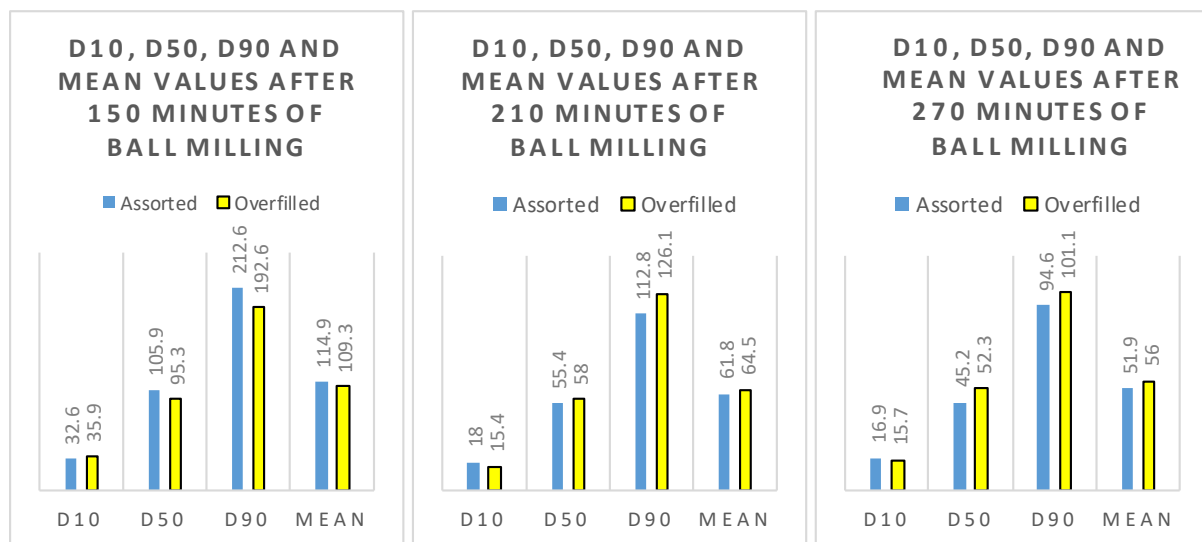


Figure 6-24a (left), Figure 6-24b (centre) and Figure 6-24c (right) – Comparison of d10, d50, d90 and mean values for the powder produced at various stages by both the assorted and overfilled chips

Figure 6-24a, Figure 6-24b and Figure 6-24c show the similarity of the two powders produced by ball milling. After 150 minutes, the assorted powder particles are larger than the overfilled powder particles, although the d10 value is lower in the assorted powder. At 210 minutes the d10 value of the overfilled powder drops below that of the assorted powder, whilst the d50, d90 and mean values are all lower in the assorted powder. After 270 minutes the overfilled powder continues to have a lower d10 value. The difference in the d50 and mean values between the two powders increases, whilst the difference in d90 values decreases. After 270 minutes of milling, the largest difference is 15.7% between the d50 values, whilst the difference between the remaining values is less than 8%. These results show that there is not a large difference in the rate of powder production when the milling bowl is overfilled.

### *EDS Analysis*

Whilst the expected atomic composition of 316L stainless steel was not always detected automatically by the software used in Chapter 6.2, all expected elements were forced in this round of EDS analysis. As such, there is no way to determine if an element was “forced” to be displayed. Previously tungsten and carbon were not included in the spectrum in order to determine if the stainless steel had changed in chemical composition. As the chemical composition of each particle has been demonstrated to not change during ball milling, tungsten has been included in the following EDS results in an attempt to determine the level of tungsten carbide contamination. Carbon has not been included as it would be impossible to discern if the carbon levels were from the stainless steel, tungsten carbide contamination or the acetone upon which the powder was mounted.

Figure 6-25 through to Figure 6-32 show the sites where EDS analysis took place for both assorted and overfilled powders after various durations of ball milling. Table 6-13 through to Table 6-20 display the %Wt of each element analysed at each of these sites.

### Electron Image 1

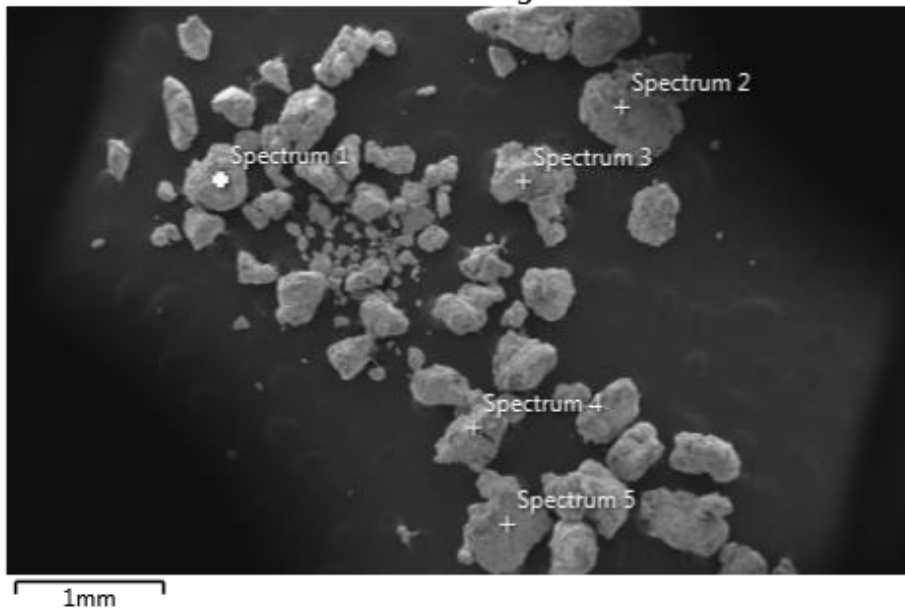


Figure 6-25 – EDS site locations for powder produced from assorted chips after 60 minutes of ball milling

Table 6-13 – Chemical composition of each site in Figure 6-25

Spectrum #	1	2	3	4	5
Wt%					
Fe	60.04	58.39	61.28	64.94	60.25
Cr	17.99	21.58	17.4	17.83	18.4
Ni	10.68	7.74	11.18	10.93	11.14
Mo	1	0.9	1.27	0.61	1.53
Si	0.27	0	0.63	0.54	0.75
O	2.28	5.72	3.78	0.87	1.86
Mn	1.37	1.87	1.35	1.61	1.36
W	6.37	3.8	3.11	2.66	4.71

### Electron Image 3

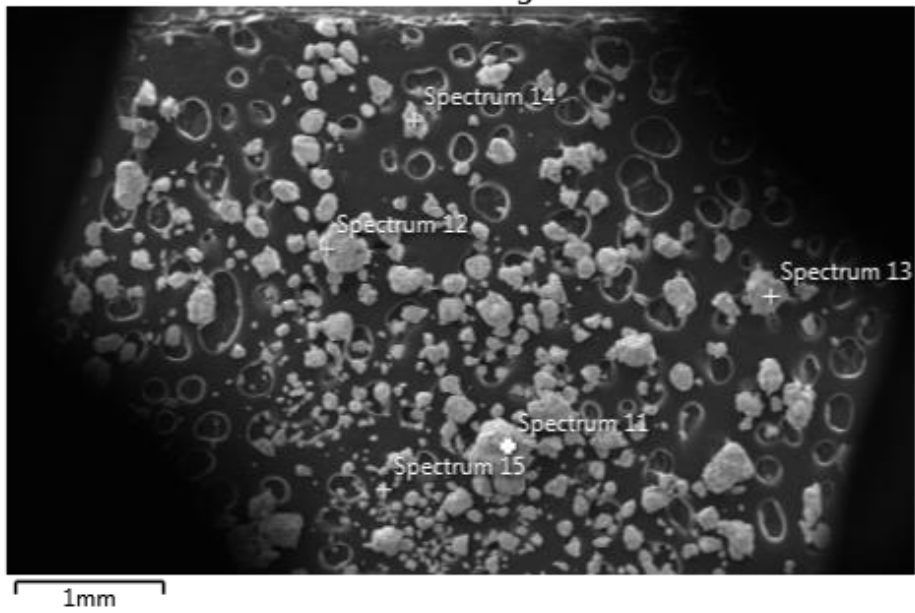


Figure 6-26 – EDS site locations for powder produced from assorted chips after 120 minutes of ball milling

Table 6-14 – Chemical composition of each site in Figure 6-26

Spectrum #	11	12	13	14	15
Wt%					
Fe	53.92	47.05	51.22	58.46	49.23
Cr	17.17	14.39	16.11	18.33	15.39
Ni	9.38	7.49	8.1	9.46	8.32
Mo	1.63	0.79	0.72	0.89	1.29
Si	0	0	0	0.23	0
O	6.65	5.25	4.01	3.94	12.31
Mn	1.14	1.23	1.21	1.32	1.09
W	10.11	23.8	18.65	7.36	12.37

### Electron Image 5

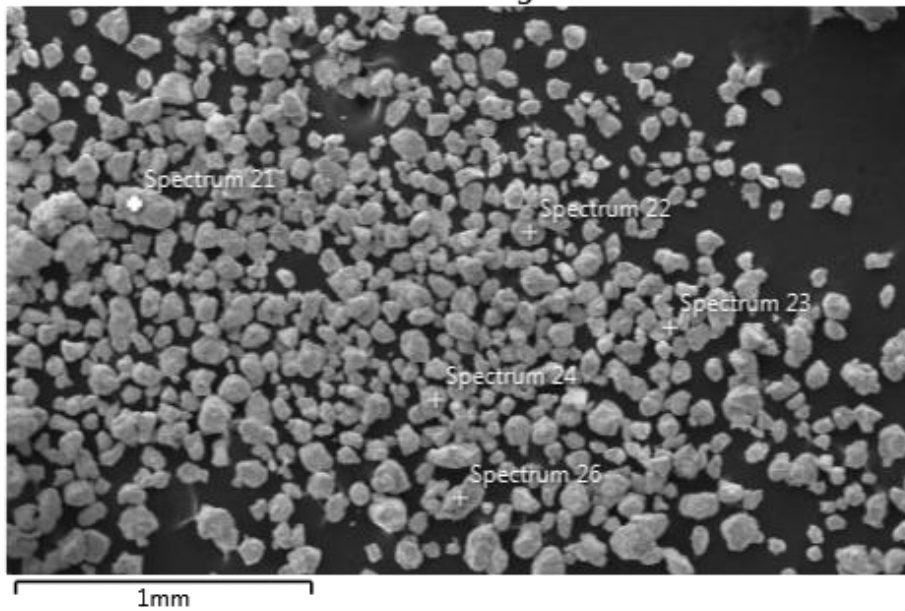


Figure 6-27 – EDS site locations for powder produced from assorted chips after 180 minutes of ball milling

Table 6-15 – Chemical composition of each site in Figure 6-27

Spectrum #	21	22	23	24	26
Wt%					
Fe	58.44	53.80	61.27	56.02	58.62
Cr	17.04	17.09	18.66	17.10	17.55
Ni	9.37	9.21	7.75	10.71	10.93
Mo	0.91	1.31	0.33	1.55	1.71
Si	0.21	0	0.36	0	0.56
O	5.35	5.42	2.81	6.75	5.37
Mn	1.58	1.08	2.12	0.99	1.18
W	7.09	12.10	6.69	6.87	4.08

### Electron Image 8

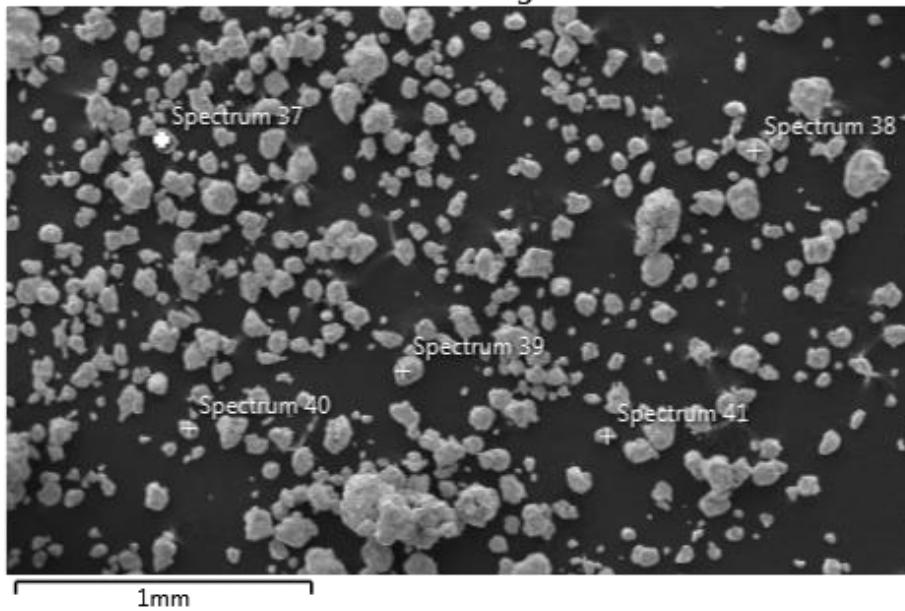


Figure 6-28 – EDS site locations for powder produced from assorted chips after 270 minutes of ball milling

Table 6-16 – Chemical composition of each site in Figure 6-28

Spectrum #	37	38	39	40	41
Wt%					
Fe	55.55	59.3	54.18	53.75	56.61
Cr	16.86	17.98	14.81	16.45	16.49
Ni	9.98	9.03	8.24	9.76	8.72
Mo	1.28	0.39	0.19	1.53	0.73
Si	0	0.02	0.12	0	0
O	7.76	1.35	6.64	7.59	8.56
Mn	1.12	1.39	1.45	1.1	1.33
W	7.44	10.54	14.35	9.82	7.55

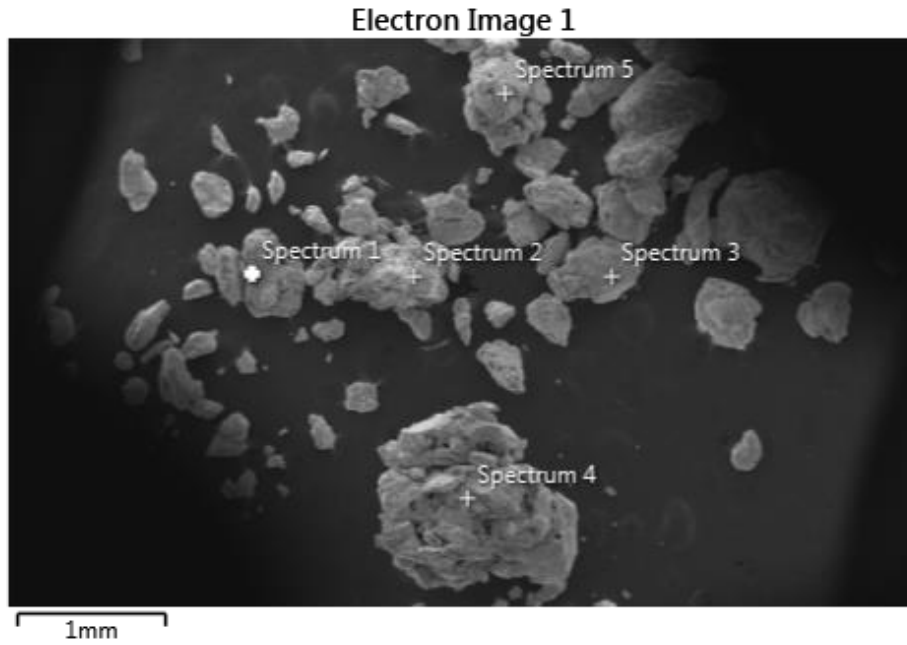


Figure 6-29 – EDS site locations for powder produced from the overfilled sample after 60 minutes of ball milling

Table 6-17 – Chemical composition of each site in Figure 6-29

Spectrum #	1	2	3	4	5
Wt%					
Fe	61.64	60.37	60.9	64.14	62.69
Cr	19.22	18.95	18.86	20.22	18.54
Ni	11.17	10.62	9.63	9.54	6.9
Mo	1.58	1.28	0.99	0.57	0.39
Si	1.49	0.73	0.8	0.38	0
O	3.31	3.12	4.51	0.52	2.35
Mn	1.26	1.31	1.66	1.72	1.97
W	0.33	3.62	2.65	2.9	7.17

### Electron Image 3

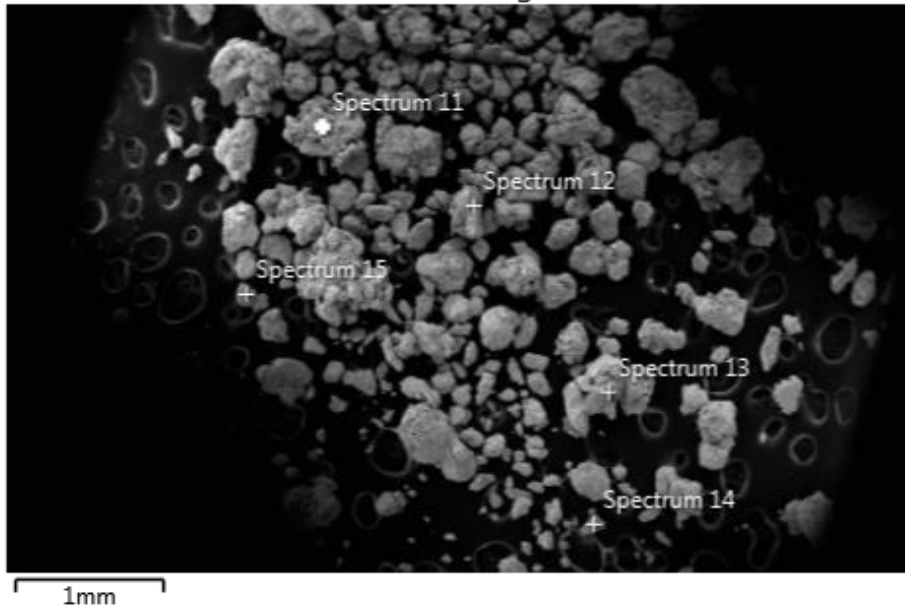


Figure 6-30 – EDS site locations for powder produced from the overfilled sample after 120 minutes of ball milling

Table 6-18 – Chemical composition of each site in Figure 6-30

Spectrum #	11	12	13	14	15
Wt%					
Fe	55.07	54.07	60.74	48.45	59.14
Cr	17.42	17.5	17.96	15.16	18.4
Ni	9.81	9.76	10.83	7.03	10.67
Mo	1.2	1.64	1.29	0.71	1.55
Si	0	0	0.74	0	0.93
O	4.23	8.09	3.6	10.94	5.21
Mn	1.16	1.16	1.26	1.29	1.21
W	11.1	7.78	3.57	16.41	2.89

### Electron Image 5

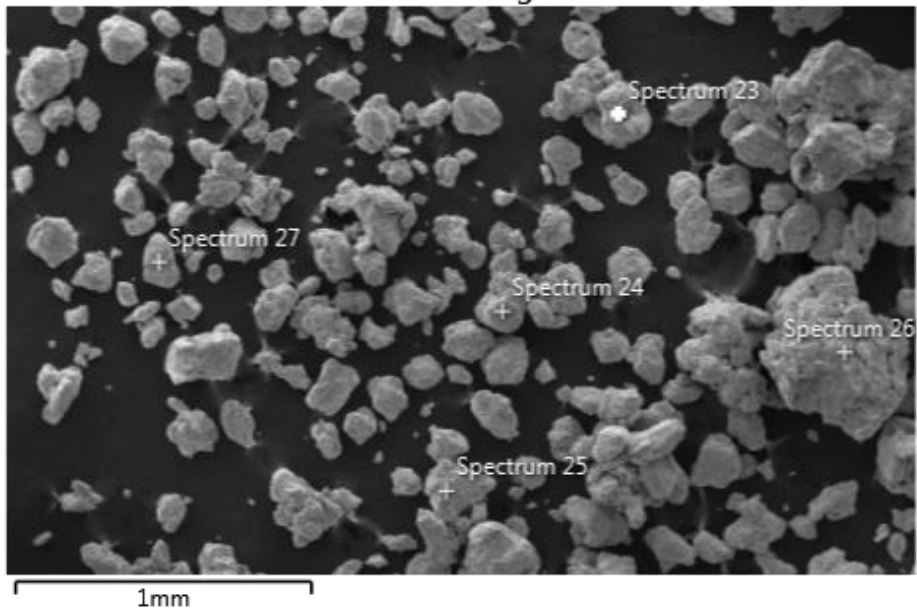


Figure 6-31 – EDS site locations for powder produced from the overfilled sample after 180 minutes of ball milling

Table 6-19 – Chemical composition of each site in Figure 6-31

Spectrum #	23	24	25	26	27
Wt%					
Fe	58.43	65.46	60.73	53.54	62.7
Cr	17.72	20.65	18.1	17.02	18.39
Ni	10.85	4.39	11.09	9.75	10.02
Mo	1.56	0.22	1.36	1.58	0.75
Si	1.26	0.42	1.41	1.54	0.42
O	6.49	4.06	4.72	10.89	2.89
Mn	1.12	3.2	1.31	1.09	1.54
W	2.57	1.6	1.28	4.58	3.32

### Electron Image 8

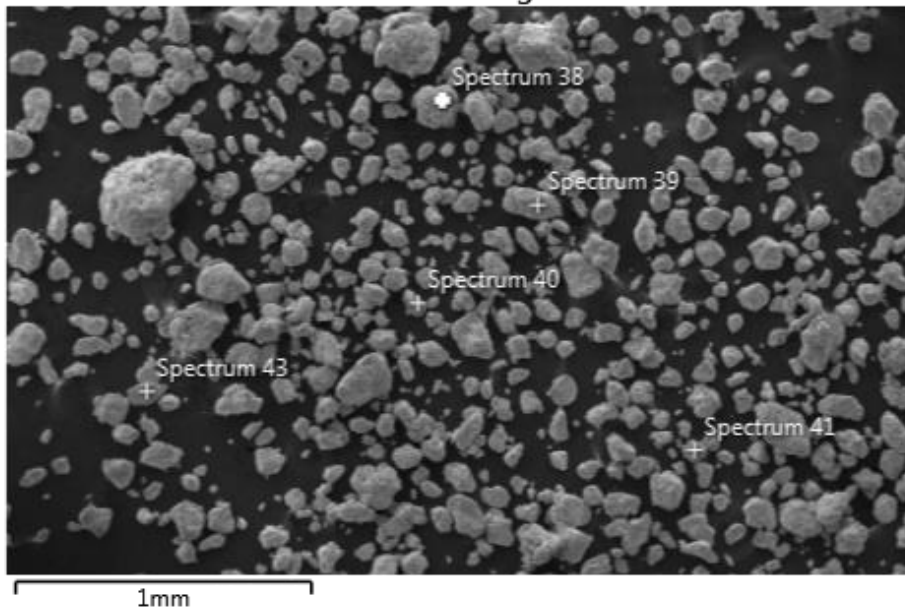


Figure 6-32 – EDS site locations for powder produced from the overfilled sample after 270 minutes of ball milling

Table 6-20 – Chemical composition of each site in Figure 6-32

Spectrum #	38	39	40	41	42
Wt%					
Fe	59.81	63.65	50.44	60.57	59.02
Cr	18.07	19.24	15.18	18.83	17.87
Ni	10.78	7.73	9.29	10.26	9.91
Mo	1.51	0.28	1.32	0.98	1.06
Si	1.28	0.9	4.66	0.76	0.59
O	5.65	2.95	16.59	3.71	5.51
Mn	1.26	1.83	1.01	1.46	1.45
W	1.65	3.42	1.51	3.43	4.6

Table 6-21 – Average Wt% of tungsten present at all sites in each powder sample

<i>Wt% Tungsten</i>	<i>60 mins</i>	<i>120 mins</i>	<i>180 mins</i>	<i>270 mins</i>
<i>Assorted</i>	4.13	14.46	7.37	9.94
<i>Overfilled</i>	3.33	8.35	2.67	2.92

Table 6-13 through to Table 6-20 give rise to the data in Table 6-21. Table 6-21 shows that there is a consistent and considerably lower level of tungsten present in the overfilled powder samples throughout the entire ball milling process. The unusual spikes seen after 120 minutes of ball milling cannot be considered erroneous as the Wt% values are consistently high in Table 6-14 and Table 6-18. However, as there is no known reason for this, these results shall not be considered at present. There is a steady increase in the Wt% of tungsten in the powder produced from assorted chips, whilst the powder produced from overfilled chips exhibits a stable level of tungsten. This is likely due to the reduction of ball-to-ball and ball-to-bowl interactions caused by the increased volume of powder present in the overfilled samples, reducing the level of tungsten carbide that forms inside the bowl. This confirms the hypothesis that overfilling milling bowls can help to reduce contamination in the powder.

### 6.3.3 Discussion

The powders produced in this experiment did not produce particles as fine as those seen in Chapter 6.2. The particles produced were considerably larger, with less than 50% of particles being suitable for use in SLM. This was to be expected with a reduced ball milling duration, although the particles were larger than expected after 270 minutes of ball milling. As the reduction in particle size appeared to exponentially decrease, the effectiveness of ball milling to produce powders suitable for use in SLM is put into question. The PSD of the produced powders are, however, suitable for other AM processes, such as DED and EBM (see Figure 3-1), which often do not require high-quality powders like SLM. This confirms a conclusion drawn in Chapter 6.2.3; ball milling may be more effectively used to generate low-quality powder feedstock for less demanding AM processes as an alternative to water atomisation.

Comparison of the assorted powder with standard and oversized powders was not possible due to the difference in ball milling duration used to create these powders. However, mixing standard and oversized support structures did not appear to have a negative impact on the creation of particles suitable for use in AM at lower ball milling durations. This practice should be continued for simplicity in the future when carrying out ball milling of chips.

Overfilling the bowl seemed to have a small effect on the PSD, with the particles tending to be larger and breaking down slower than in the normally filled bowl. However, this difference was negligible when compared to the potential power savings that result from overfilling the bowl (see Table 6-22). This practice is therefore recommended to be carried forwards.

Contamination of the produced powder continues to be an issue. It is believed that powder from the experiments in Chapter 6.2 contaminated the produced powder, influencing the results. The potential contamination makes it impossible to determine the level of contamination reduction with any certainty. However, it seems that the level of tungsten carbide contamination may be greatly reduced when the milling bowls are overfilled, with little negative impact on the rate of powder formation.

*Table 6-22 – Energy consumption calculations based on the data collected (see Chapter 6.2)*

<b>Chips</b>	<b>Mass of sample</b>	<b>Mass of 900ml bowl sample</b>	<b>Machine-on time</b>	<b>Machine energy consumption</b>	<b>Energy consumption per kilogram</b>
<b>Standard</b>	18.7g	1.122kg	7 hours	43.61MJ	38.87MJ/kg
<b>Oversized</b>	11.1g	0.666kg			65.48MJ/kg
<b>Blended</b>	14.9g	0.894kg			48.78MJ/kg
<b>Assorted</b>	16.9g	1.014kg	4.5 hours	28.04MJ	27.65MJ/kg
<b>Overfilled</b>	30.3g	1.818kg			14.42MJ/kg

The objective of creating these powders was to refine the environmentally-friendly alternative of metal powder creation from waste support structures demonstrated in Chapter 6.2. This can be seen in Table 6-22, allowing comparison of the energy consumption required to create powders from all ball milling experimentation carried out. Once again, the maximum sample size of 900ml per machine is used, assuming the work has been upscaled to be carried out at a medium-sized facility. The overfilled sample is assumed to be scaled up and overfilled to the same extent in the theoretical 900ml bowl calculation.

The powder generated by both the assorted and overfilled chips was not suitable for use in SLM, whereas the powder produced from standard and blended chips was suitably small. As such, the comparison is currently biased towards the assorted and overfilled chips. However, when the bowl is overfilled, the production of coarser, low-quality powders through ball milling uses only 43.9% of the 32.81MJ/kg of energy required to make the powder through atomisation. For EBM or DED, almost all of the particles produced from the overfilled sample would be usable, resulting in a higher process efficiency.

This data is considerably more promising than the results in Chapter 6.2. A reduction is seen the energy consumption required to create the powder, and all particles formed are within the size range needed for DED or EBM. This suggests that ball milling, when optimised, can reduce waste from scrap support structures whilst reducing the consumption of raw materials and energy by reducing the production of virgin water atomised powders.

It may be possible to further increase these energy savings. Table 6-10 showed that the theoretical powder volume of 30ml of chips was only 3.79ml. As the bowl could be filled with 15ml of powder, more chips could have been added, maximising the potential bowl capacity. Given that the chips reduced in size rapidly after just 30 minutes of milling, it may be possible to top up the bowls with another 30ml of chips at regular intervals, increasing the volume of powder present within the bowls. Whilst this may reduce the rate at which the powder decreases in size, it may minimise tungsten carbide-tungsten carbide interactions within the bowls, potentially reducing tungsten contamination in the produced powder. If the rate of powder breakdown was unaffected, adding another 30ml of chips after 30 minutes would reduce the energy consumption per kilogram of powder produced to 7.21MJ/kg, only 22.0% of the energy required to make virgin powder through atomisation.

#### 6.3.4 Conclusion

The hypotheses formed in Chapter 6.2 were tested in the present experiment. The milling time was reduced, allowing for the determination of the rate at which the powder formed and preventing the powder from becoming excessively small. Chips were selected randomly, assessing how this affected the breakdown, intending to prevent the necessity of manually sorting through chips in future procedures. One milling bowl was overfilled in an attempt to improve the efficiency of the AM process whilst also aiming to reduce the level of tungsten carbide contamination in the powder.

The powder produced from ball milling assorted chips and overfilling the milling bowl were similar in morphology than the powder produced when milling for seven hours, but the average particle size was considerably larger. The level of tungsten carbide contamination is believed to have been reduced through the overfilling of the milling bowls, although further research is needed to confirm this hypothesis. It is believed that producing powder purely for SLM from ball milling will not be environmentally justifiable due to the length of time required to create a suitably small powder. The particles produced from ball milling are better suited to EBM and DED, which often do not require high-quality feedstock. The generation of powder through ball milling for EBM or DED could only use 43.9% of the energy used to create virgin powder. As such, further research into ball milling of chips

generated from support structures should be continued, aiming to produce powders for use in EBM and DED.

Testing of DED using a similar powder generated by ball milling has been shown to be successful by Fullenwider *et al.* (2019). The powders created through the present ball milling process should be tested in both DED and EBM processes to confirm their suitability. This would require the generation of more powder through ball milling, allowing the experimental procedure to be further refined. Acquiring new balls and bowls that have not been irreversibly contaminated is essential to determine how contaminated the powders are, allowing solutions to be found if this issue persists. Topping up the bowls with additional chips during the early hours of ball milling should be considered, attempting to produce more powder per ball milling cycle.

With the process having been further optimised, assessment of ball milling on a larger scale should be conducted to prove that this process is less energy intensive than the current and well-established recycling procedure. This would permit unforeseen complications to be addressed in the research and development phase of this procedure. This testing may require the use of alternative equipment with larger bowl capacities. Utilising alternative materials as feedstock in the milling process could then be investigated, widening the impact of this research beyond 316L stainless steel AM users.

## 7. Conclusions

AM is finding its feet in the manufacturing industry. Both the understanding of AM and hardware continue to be developed in tandem, creating a rapidly expanding body of knowledge. The technology is excelling in resource efficiency and the reduction of waste whilst continuing to produce high-quality components that can compete with other manufacturing processes. However, the work within this thesis has affirmed the belief that more can be done to further enhance the efficiency of the AM supply chain, reducing both waste and the necessity for new powder to be created.

The aims of the project were left intentionally open-ended, enabling unexplored, innovative or uncommon solutions to be considered. This allowed the feasibility of several potential solutions to be investigated, narrowing down the initially-wide project aims and focusing the objectives of the project onto reducing waste and maximising resource efficiency.

A method of quickly and simply determining the quality of powder was not found. Numerous complex particle and powder properties were found to impact the AM process, making it unlikely that any one variable could be measured in order to accurately represent the powder quality. The most effective means of determining powder suitability for use in AM was believed to be building tensile and hardness specimens and testing their performance. Many AM users would not have access to such testing facilities, limiting the effectiveness of this suggestion.

Interaction with a number of AM users throughout the project highlighted that many SMEs do not have access to extensive powder testing facilities. Universities are also unlikely to possess the numerous specialist technologies required to extensively analyse metal AM powders. This places much of the onus for powder-based research on the powder manufacturers who have access to such technologies; they will be able to test and develop methods to prevent powder waste and improve the resource efficiency of the entire AM process. Most importantly, powder suppliers have the influence in the AM product lifecycle to make disruptive changes to the industry.

Perhaps the most important finding in this research is the untapped potential of plasma spheroidisation. Plasma spheroidisation was shown to upcycle low-quality powders, creating feedstock suitable for use in AM from powders that would have been previously unsuitable. However, this is a new technology with only one machine available in the UK to date. Should this technology become mainstream, waste and resource efficiency would be greatly reduced in the AM community. EoL powders would no longer be disposed of, accompanied by a reduced necessity to produce virgin powders, achieving the main objectives set out by this research.

The multiple ball milling experiments demonstrated the potential to create metal AM powders using less energy than current alternative production methods. Ball milling is not a tool that is typically considered in AM for powder creation, offering an innovative solution to reduce waste. This method is likely to have economic benefits, potentially creating powder with a market value 100 times greater than the support structure scrap.

The project was unable to develop any solutions to a stage of readiness for use in industry. Ball milling was validated in a laboratory environment as an environmentally friendly means to create powder, whilst plasma spheroidisation experimentation methodology was considered, allowing future work to be carried out. In an academic environment with a broad set of project aims, it is unlikely that any identified solutions could be developed beyond this point, as the identification and analysis of potential solutions is more important. This allowed the project aims to be refined for future experimentation to take place. As such, given the time constraints of the present research, the outcomes of this project are considered to be successful.

## 8. Further Work

Demonstrating economic feasibility is of high importance when attempting to disrupt the current practices of an industry; there is little benefit in generating perfect procedures if they will not be adopted due to non-profitability. It is difficult to determine the economic feasibility of many solutions in an academic environment. This can be overcome by working closely alongside AM users in any future work that develops concepts investigated or reported upon within this thesis. It is recommended that the cost of equipment should be understood to allow initial return on investment calculations to take place. However, profitability should not be the only consideration. To achieve sustainability in the AM industry, profit at the expense of environmental benefit is unacceptable.

The powders produced by ball milling should be utilised in DED to determine their suitability as feedstock powder. Alternatively, the powders produced could be plasma spheroidised to produce higher-quality spherical powders that may be more suitable in EBM. This may improve the value of the powders even further. Ball milling experimentation should be scaled up and further refined, eventually allowing a business case to be formed.

Budget and time constraints prevented experimentation on powders at various stages of reuse to be analysed using a GranuDrum. It was believed that there is a correlation between powder reuse and the flowability of the powder, which may be identified through the use of a GranuDrum. This may therefore indicate powder quality with minimal cost to the AM user. Links with GranuTools have been established, allowing this experimentation to take place in the future.

Additional funding for experimental work to be carried out using plasma spheroidisation was secured through the Henry Royce Institute's PhD Equipment Access Scheme. An experimental procedure was established, but unexpected delays to the equipment setup prevented the experimentation being completed within the timeframe of this research. The experimental procedure established has been included as Appendix C – Programme of work for plasma spheroidisation.

Once the equipment is fully set up, further experimentation into the ability to add alloying elements into the powder and the use of reduction gases to reduce impurities should be investigated. Experimentation using different powders should be considered once the process has been well established with 316L stainless steel, demonstrating the wider impact of this technology. Powders produced through spheroidisation should be used in AM builds to confirm their suitability.

Without the support of the wider AM industry, any solution identified will not become widely adopted. It is therefore of the utmost importance that successful results and solutions are well marketed to the

community through the use of academic papers, advertising and open-source information. This needs to be done alongside any further research, ensuring that economic and environmental benefits are shared across the ever-growing AM community.

## References

- Additive Manufacturing UK (2017) "National Strategy 2018-25" [online] Available here: [http://am-uk.org/wp-content/uploads/2017/11/AM-UK\\_Strategy\\_Publication\\_Amendments\\_November\\_Digital.pdf](http://am-uk.org/wp-content/uploads/2017/11/AM-UK_Strategy_Publication_Amendments_November_Digital.pdf) (Accessed: August 23, 2019)
- Andani, M.T., Dehghani, R., Karamooz-Ravari, M.R., Mirzaeifar, R. and Ni, J. (2018) "A study on the effect of energy input on spatter particles creation during selective laser melting process" *Additive Manufacturing*, 20, pp. 33–43. <https://doi.org/10.1016/j.addma.2017.12.009>
- AP&C (2014) "Designed for additive manufacturing", Available at <http://advancedpowders.com/our-plasma-atomized-powders/designed-for-additive-manufacturing/>
- Ardila, L., Garciandia, F., González-Díaz, J., Álvarez, P., Echeverria, A., Petite, M., Deffley, R. and Ochoa, J. (2014) "Effect of IN718 Recycled Powder Reuse on Properties of Parts Manufactured by Means of Selective Laser Melting" *Physics Procedia*, 56, pp. 99–107. <https://doi.org/10.1016/j.phpro.2014.08.152>
- ASTM F2924-14 (2014) "Standard Specification for Additive Manufacturing Titanium-6 Aluminum-4 Vanadium with Powder Bed Fusion" ASTM International, West Conshohocken, PA
- ASTM F3055-14a (2014) "Standard Specification for Additive Manufacturing Nickel Alloy (UNS N07718) with Powder Bed Fusion" ASTM International, West Conshohocken, PA
- ASTM Standard 52900 (2015) "Standard Terminology for Additive Manufacturing – General Principles – Terminology", ASTM International, West Conshohocken, PA, 2015
- ASTM Standard 52907 (2019) "Additive manufacturing – Feedstock materials – Methods to characterize metal powders" ASTM International, West Conshohocken, PA
- Atlas Speciality Metals (2002) "Stainless Steel – Cryogenic Properties", [online] Available at: <https://www.azom.com/article.aspx?ArticleID=1176> (Accessed: March 11, 2019).
- Boulos, M. (2012) "New frontiers in thermal plasmas from space to nanomaterials" *Nuclear Engineering and Technology*, 44(1) <https://doi.org/10.5516/NET.77.2012.001>
- Bourhis, F.L., Kerbrat, O., Dembinski, L., Hascoet, J.Y. and Mognol, P. (2014) "Predictive Model for Environmental Assessment in Additive Manufacturing Process" *Procedia CIRP*, 15, pp. 26–31. <https://doi.org/10.1016/j.procir.2014.06.031>
- Campbell, T., Williams, C., Ivanova and O., Garrett, B. (2011) "Could 3D Printing Change the World?" Washington DC: Atlantic Council.
- Carroll, P.A., Brown, P., Ng, G., Scudamore, R., Pinkerton, A.J., Syed, W., Sezer, H., Li, L. and Allen, J. (2006) "The Effect of Powder Recycling in Direct Metal Laser Deposition on Powder and Manufactured Part Characteristics", RTO-MP-AVT-139.
- Cherdo, L. (2019) "The best Metal 3D printers in 2019" [online], Available at: <https://www.aniwaa.com/best-of/3d-printers/best-metal-3d-printer/> (Accessed: August 23, 2019)
- Cherry, J. A., Davies, H. M., Mehmood, S.N., Lavery, P., Brown, S. G. R., and Sienz, J. (2015) "Investigation into the effect of process parameters on microstructural and physical properties of 316L stainless steel parts by selective laser melting" *International Journal of Advanced Manufacturing Technology*, 76, pp. 869–879. <https://doi.org/10.1007/s00170-014-6297-2>
- Crouter, A. and Briens, L. (2013) "The Effect of Moisture on the Flowability of Pharmaceutical Excipients" *AAPS PharmSciTech*, 15(1), pp. 65-74 <https://doi.org/10.1208/s12249-013-0036-0>

- Davies, P.A., Dunstan, G.R., Hayward, A.C., Howells, R.I.L., Lane, M.I.M.L.D. and Altrincham, C. (2003) "Metal Injection Moulding of Heat Treated Alloy 718 Master Alloy" *Advances In Powder Metallurgy and Particulate Materials*, 8, pp. 8-12.
- Dawes, J. (2019) "Powder Management in Additive Manufacturing" *Mastering AM: Sharing User Experience*, 27th March, Coventry, United Kingdom
- Dawes, J., Bowerman, R. and Trepleton, R. (2015) "Introduction to the Additive Manufacturing Powder Metallurgy Supply Chain" *Johnson Matthey Technology Review*, 2015, 59, (3), pp. 243-256. <https://doi.org/10.1595/205651315x688686>
- de Beer, D.J., Becker, L., van der Walt, P., Mauchline, D., Campbell, R.I. and Dean, L.T. (2019) "Additive manufacturing of alumide jewellery" [online] Available from: <https://hdl.handle.net/2134/11196> [Accessed 6/12/2019]
- Del Re, F., Contaldi, V., Astarita, A., Palumbo, B., Squillace, A., Corrado, P. and Di Petta, P. (2018) "Statistical approach for assessing the effect of powder reuse on the final quality of AlSi10Mg parts produced by laser powder bed fusion additive manufacturing" *International Journal of Advanced Manufacturing Technology*, 97(5-8), pp. 2231-2240 <https://doi.org/10.1007/s00170-018-2090-y>
- Do, T., Kwon, P. and Shin, C.S. (2017) "Process development toward full-density stainless steel parts with binder jetting printing", *International Journal of Machine Tools and Manufacture*, 121, pp. 50–60.
- Dong, Z., Kang, H., Xie, Y., Chi, C. and Peng, X. (2019) "Effect of powder oxygen content on microstructure and mechanical properties of a laser additively-manufactured 12CrNi2 alloy steel" *Materials Letters*, 236, pp. 214–217. <https://doi.org/10.1016/j.matlet.2018.10.091>
- Duthil, P. (n.d.) "Material Properties at Low Temperature", Université de Paris Sud, Available at: <https://arxiv.org/ftp/arxiv/papers/1501/1501.07100.pdf> (Accessed: March 11, 2019)
- Faludi, J., Baumers, M., Maskery, I. and Hague, R. (2016) "Environmental Impacts of Selective Laser Melting: Do Printer, Powder, Or Power Dominate?" *Journal of Industrial Ecology*, 21(S1). <https://doi.org/10.1111/jiec.12528>
- Fritsch (n.d.) "Planetary Mill - PULVERISETTE 5/4" [online] Available here: <https://www.fritsch-international.com/sample-preparation/milling/planetary-mills/details/product/pulverisette-54-classic-line/technical-details/> (Accessed: September 4, 2019)
- Fullenwider, B., Kiani, P., Schoenung, J.M. and Ma, K. (2019) "Two-stage ball milling of recycled machining chips to create an alternative feedstock powder for metal additive manufacturing", *Powder Technology*, 342, pp. 562–571.
- Gasper, A., Szost, B., Wang, X., Johns, D., Sharma, S., Clare, A. and Ashcroft, I. (2018) "Spatter and oxide formation in laser powder bed fusion of Inconel 718" *Additive Manufacturing*, 24, pp. 446–456. <https://doi.org/10.1016/j.addma.2018.09.032>
- Gibson, I., Rosen, D.W. and Stucker, B. (2016) "Additive manufacturing technologies: 3D printing, rapid prototyping, and direct digital manufacturing" New York: Springer.
- Gökelma, M., Celik, D., Tazegul, O., Cimenoglu, H. and Friedrich, B. (2018) "Characteristics of Ti6Al4V Powders Recycled from Turnings via the HDH Technique" *Metals*, 8(5), pp. 336-346.
- Grand View Research (2019) "3D Printing Metal Market Size, Share & Trends Analysis Report By Form (Filament, Powder), By Product (Steel, Titanium, Nickel), By Application (Medical, Aerospace & Defense), And Segment Forecasts, 2019 – 2025" [online], Available here: <https://www.grandviewresearch.com/industry-analysis/3d-metal-printing-market> (Accessed: September 10, 2019)

- GranuTools (2016) "GranuDrum", Available at: <https://granutools.com/products/granudrum/> (Accessed: August 23, 2019)
- GranuTools (2018) "Investigation of Powders ageing for Additive Manufacturing Process" [online], Available at: <https://granutools.com/references/application-notes/highlighting-reproducibility-powders-ageing/> (Accessed: August 23, 2019)
- Harrison, N. (2019) "Powder specification workshop" *Mastering AM: Sharing User Experience*, 27th March, Coventry, United Kingdom
- Herzog, D., Seyda, V., Wycisk, E. and Emmelmann, C. (2016), "Additive manufacturing of metals" *Acta Materialia*, 117, pp. 371-392. <https://doi.org/10.1016/j.actamat.2016.07.019>
- Hopkinson, N., Hague, R. and Dickens, P. (2006) "Rapid manufacturing: an industrial revolution for the digital age", Somerset, NJ: John Wiley & Sons.
- Hussein, A., Hao, L., Yan, C., Everson R. and Young, P., (2013) "Advanced lattice support structures for metal additive manufacturing" *Journal of Materials Processing Technology*, 213 (7), pp. 1019–1026.
- Irrinki, H., Dexter, M., Barmore, B., Enneti, R., Pasebani, S., Badwe, S., Stitzel, J., Malhotra, R. and Atre, S.V. (2016) "Effects of Powder Attributes and Laser Powder Bed Fusion (L-PBF) Process Conditions on the Densification and Mechanical Properties of 17-4 PH Stainless Steel" *Journal of the Minerals, Metals & Materials Society*, 68(3), pp. 860–868. <https://doi.org/10.1007/s11837-015-1770-4>
- ISO/ASTM 52907 (2019) "Additive manufacturing — Feedstock materials — Methods to characterize metal powders" ASTM International, West Conshohocken, PA
- Jacob, G., Brown, C., Donmez, M., Watson, S. and Slotwinski, J. (2017) "Effects of powder recycling on stainless steel powder and built material properties in metal powder bed fusion processes" National Institute of Standards and Technology. <https://doi.org/10.6028/NIST.AMS.100-6>
- Jacobson, L. A. and McKittrick, J. (1994) "Rapid solidification processing", *Material Science Engineering: R: Reports*, 11, pp. 355-408.
- Jacobson, M., Cooper, A.R. and Nagy, J. (1964) "Explosibility of metal powders" [online], Available here: <https://apps.dtic.mil/dtic/tr/fulltext/u2/b270510.pdf> (Accessed: August 23, 2019)
- Javidrad, H. Erfan, A., Larky, M. and Riahi, M. (2018) "Investigation in environmental and safety aspects of additive manufacturing (AM)" *5th International Reliability and Safety Engineering Conference*, 9<sup>th</sup>-11<sup>th</sup> May, Shiraz, Iran
- Jiang, J., Xu, X. and Stringer, J. (2018) "Support Structures for Additive Manufacturing: A Review," *Journal of Manufacturing and Materials Processing*, 2 (4), p. 64.
- Karapatis P. (2002) "A sub-process approach of selective laser sintering" Doctoral thesis, EPFL, Lausanne, Switzerland <https://doi.org/10.5075/epfl-thesis-2506>
- Karlsson, J., Snis, A., Engqvist H. and Lausmaa, J. (2013) "Characterization and comparison of materials produced by Electron Beam Melting (EBM) of two different Ti–6Al–4V powder fractions", *Journal of Materials Processing Technology*, 213, pp. 2109–2118.
- Kelkar, R. M. (2018) "High Quality Spherical Powders for Additive Manufacturing Processes Along With Methods of Their Formation" US20190061005A1
- Kobiela, K., Smolina, I., Frankiewicz, M. and Chlebus, E (2015) "Plasma spheroidisation of high melt point materials on example of tungsten" *Welding Technology Review*, 87, pp. 31-34. <https://doi.org/10.26628/ps.v87i11.526>
- Krumbein, W. and Sloss, L. (1963) "Stratigraphy and Sedimentation" W.H. Freeman and Co., San Francisco, pp. 660 .

- Lawley, A. (2001) "Atomization", *Encyclopedia of Materials: Science and Technology*, 2<sup>nd</sup> ed., Drexel University, Philadelphia, Pennsylvania USA, pp. 387-392
- Leicht, A. (2018) "Aspects of building geometry and powder characteristics in powder bed fusion" Licentiate Thesis, Chalmers University of Technology, Gothenburg, Sweden
- Li, J., Wu, B. and Myant, C. (2016) "The Current Landscape for Additive Manufacturing Research" Imperial College London, London [online] Available here: <https://core.ac.uk/download/pdf/77018324.pdf> (Accessed: August 23, 2019)
- Li, R., Shi, Y., Wang, Z., Wang, L., Liu, J. and Jiang, W. (2010) "Densification behavior of gas and water atomized 316L stainless steel powder during selective laser melting," *Applied Surface Science*, 256(13), pp. 4350–4356. <https://doi.org/10.1016/j.apsusc.2010.02.030>
- Liang, J., Jia, M., Guo, X. and Zhang, D. (2014) "Microstructural evolution and microhardness change of Al–7wt%Si–0.3wt%Mg alloy granules/powder particles during high energy ball milling" *Materials Science and Engineering: A*. 590. pp. 307-313.
- Liu, B., Wildman, R., Tuck, C., Ashcroft I. and Hague, R. (2011) "Investigation the effect of particle size distribution on processing parameters optimization in selective laser melting process", Presented at the 'Solid Freeform Fabrication Symposium', Austin, Texas
- Liu, S. and Shin, Y.C. (2018) "Additive manufacturing of Ti6Al4V alloy: a review" *Materials & Design*, 164, <https://doi.org/10.1016/j.matdes.2018.107552>
- Liu, Y., Yang, Y., Mai, S., Wang, D. and Song, C. (2015) "Investigation into spatter behavior during selective laser melting of AISI 316L stainless steel powder" *Materials & Design*, 87, pp. 797-806. <https://doi.org/10.1016/j.matdes.2015.08.086>
- LPW Technology Ltd (2016) "Case Study 07: Plasma Spheroidisation" [online] Available here: <https://carpenteradditive.com/wp-content/uploads/2016/09/LPW-Case-Study-07.pdf> (Accessed: August 23, 2019)
- LPW Technology Ltd (2018a) "Metal powder reuse regimes and impact on part reproducibility – Part I" [online] Available here: <http://maschinetech.com/wp-content/uploads/2018/06/Powder-Degradation-in-Serial-Production-Pt-I.pdf> (Accessed: August 23, 2019)
- LPW Technology Ltd (2018b) "The impact of powder variability on Additive Manufacturing build quality" [online] Available here: <https://www.carpenteradditive.com/news/impact-of-metal-powder-variability-on-build-quality/> (Accessed: 10th September 2019)
- McGeehan, O., Oldfield, S., Wilks, J., Mawby, J. and Linaker, L. (2018) "Testing and Analysis of Additive Manufactured Parts from Partially Recycled Powder" MEng thesis, Liverpool John Moores University, Liverpool.
- Mindt, H.W., Megahed, M., Lavery, N.P., Holmes, M.A. and Brown, S.G.R. (2016) "Powder Bed Layer Characteristics: The Overseen First-Order Process Input", *Metallurgical and Materials Transactions A*, 47(8), pp. 3811–3822.
- Morrow, W.R., Qi, H., Kim, I., Mazumder, J. and Skerlos, S.J. (2007) "Environmental aspects of laser-based and conventional tool and die manufacturing", *Journal of Cleaner Production*, 15 (10), pp. 932-943. <https://doi.org/10.1016/j.jclepro.2005.11.030>
- Murray, K., Coleman, A. J., Tingskog T. and Whychell, D. (2011) "Effect of Particle Size Distribution on Processing & Properties of MIM 17-4PH" *International Journal of Powder Metallurgy*, 47(4), pp. 21-28.
- Nagai, K., Yuri, T., Ogata, T., Umezawa, O., Ishikawa, K., Nishimura, T., Mizoguchi, T. and Ito, Y. (1991) "Cryogenic Mechanical Properties of Ti-6Al-4V Alloys with Three Levels of Oxygen Content" *ISIJ International*, 31(8), pp. 882–889.

- O'Dell, J.S., Schofield, E.C., McKechnie, T.N. and Fulmer, A. (2004) "Plasma Alloying and Spheroidization Process and Development" *Journal of Materials Engineering and Performance*, 13(4), pp. 461-467. <https://doi.org/10.1361/10599490419946>
- Pal, S., Lojen, G., Gubelj, N., Kokol, V. and Drstvensek, I. (2020) "Melting, fusion and solidification behaviors of Ti-6Al-4V alloy in Selective Laser Melting at different scanning speeds", *Rapid Prototyping Journal*, Accepted (in Press)
- Petrovic, V. and Niñerola, R. (2015) "Powder recyclability in electron beam melting for aeronautical use" *Aircraft Engineering and Aerospace Technology*, 87(2), pp. 147–155
- Petrovic, V., Gonzalez, J.V.H., Ferrando, O.J., Gordillo, J.D., Puchades, J.R.B. and Griñan, L.P. (2010) "Additive layered manufacturing: sectors of industrial application shown through case studies" *International Journal of Production Research*, 49(4), pp. 1061–1079. <https://doi.org/10.1080/00207540903479786>
- Piller, F.T., Poprawe, R., Schleifenbaum, H.J., Schuh, G., Barg, S., Dolle, C., Hinke, C., Jank, M.-H., Jiang, R., Meiners, W., Riesener, M., Schrage, J. and Ziegler, S. (2018) "Introducing a Holistic Profitability Model for Additive Manufacturing: An Analysis of Laser-powder Bed Fusion," *2018 IEEE International Conference on Industrial Engineering and Engineering Management (IEEM)*, pp.1730-1735. <https://doi.org/10.1109/IEEM.2018.8607729>
- Popov, V. V., Katz-Demyanetz, A., Garkun, A. and Bamberger, M. (2018) "The effect of powder recycling on the mechanical properties and microstructure of electron beam melted Ti-6Al-4V specimens" *Additive Manufacturing*, 22, pp. 834-843 <https://doi.org/10.1016/j.addma.2018.06.003>
- Powell, D., Rennie, A. E. W., Molyneux, A., Burns, N. & Geekie, L. (2019) "Repurposing of metal support structures to form powder for use in additive manufacturing" *Proceedings of the 16<sup>th</sup> Rapid Design, Prototyping and Manufacturing Conference (RDPM 2019)*, Uxbridge, UK, 4<sup>th</sup>-5<sup>th</sup> April, ISBN: 978-1-5272-5164-9
- Rane, A.V., Kanny, K., Abitha, V.K. and Thomas, S. (2018) "Methods for synthesis of nanoparticles and fabrication of nanocomposites" In *Synthesis of inorganic nanomaterials* (pp. 121-139). Woodhead Publishing.
- Rasband, W.S. (1997-2018) "ImageJ" U. S. National Institutes of Health, Bethesda, Maryland, USA, <https://imagej.nih.gov/ij/>
- Renderos, M., Girot, F., Lamikiz, A., Torregaray, A. and Saintier, N. (2016) "Ni Based Powder Reconditioning and Reuse for LMD Process" *Physics Procedia*, 83, pp. 769–777. <https://doi.org/10.1016/j.phpro.2016.08.079>
- Renishaw plc (2016) "Investigating the effects of multiple re-use of Ti6Al4V powder in additive manufacturing (AM)" [online] Available here: <https://resources.renishaw.com/en/details/white-paper-investigating-the-effects-of-multiple-powder-re-use-in-am--83164> (Accessed: August 23, 2019)
- Rushton, J. (2019) "Powder management in Additive Manufacturing" *Mastering AM: Sharing User Experience*, 27th March, Coventry, United Kingdom
- Sames, W. J., List, F. A., Pannala, S., Dehoff, R. R. and Babu, S. S. (2016) "The metallurgy and processing science of metal additive manufacturing" *International Materials Reviews*, 61(5), pp. 315-360. <https://doi.org/10.1080/09506608.2015.1116649>
- Sampaio, C., Cazacliu, B., Miltzarek, G., Huchet, F., le Guen, L., Petter, C., Paranhos, R., Ambrós, W. and Oliveira, M. (2016) "Stratification in air jigs of concrete/brick/gypsum particles" *Construction and Building Materials*, 109, pp. 63-72.
- Santos, E. C., Shiomi, M. Osakada, K, Laoui, T. (2006) "Rapid manufacturing of metal components by laser forming" *International Journal of Machine Tools and Manufacture*, 46 (12), pp. 1459-1468

- Sanwa Diamond Tools Pvt. Ltd. (n.d.) "Thermal Spray Powders" Available at: <http://www.atomizedpowders.com/thermal-spray-powders.htm> (Accessed: December 14, 2018).
- Sartin, B., Pond, T., Griffith, B., Everhart, W., Elder, L., Wenski, E., Cook, C., Wieliczka, D., King, W., Rubenchik, A., Wu, S., Brown, B., Johnson, C. and Crow, J. (2017) "316L Powder Reuse For Metal Additive Manufacturing" *28th Annual International Solid Freeform Fabrication Symposium – An Additive Manufacturing Conference*, 7<sup>th</sup>-8<sup>th</sup> August, Austin, Texas
- Seyda, V., Kaufmann, N. and Emmelmann, C. (2012) "Investigation of Aging Processes of Ti-6Al-4V Powder Material in Laser Melting" *Physics Procedia*, 39, pp. 425–431. <https://doi.org/10.1016/j.phpro.2012.10.057>
- Shishkovsky, I. (2009) "Stress–strain analysis of porous scaffolds made from titanium alloys synthesized via SLS method", *Applied Surface Science*, 255(24), pp. 9902–9905.
- Simchi, A. (2006) "Direct laser sintering of metal powders: Mechanism, kinetics and microstructural features" *Materials Science and Engineering: A*, 428(1-2), pp. 148–158. <https://doi.org/10.1016/j.msea.2006.04.117>
- Singh, R., Singh, N., Fabbrocino, F., Fraternali, F. and Ahuja, I.P.S. (2016) "Waste management by recycling of polymers with reinforcement of metal powder", *Composites Part B: Engineering*, 105, pp. 23-29.
- Slotwinski, J. A., Garboczi, E. J., Stutzman, P. E., Ferraris, C. F., Watson, S. S., and Peltz, M. A. (2014) "Characterization of Metal Powders Used for Additive Manufacturing" *Journal of research of the National Institute of Standards and Technology*, 119, pp. 460-93. <https://doi.org/10.6028/jres.119.018>
- Spierings, A., Herres, N. and Levy, G. (2011) "Influence of the particle size distribution on surface quality and mechanical properties in AM steel parts" *Rapid Prototyping Journal*, 17(3), pp. 195–202. <https://doi.org/10.1108/13552541111124770>
- SSI Shredding Systems (n.d.) "M45 two-shaft shredder", [online], Available at: <https://www.ssiworld.com/en/products/two shaft shredders/dual shear m45> (Accessed 31/01/2019)
- Strano, G., Hao, L., Everson, R.M. and Evans, K.E. (2012) "A new approach to the design and optimisation of support structures in additive manufacturing," *The International Journal of Advanced Manufacturing Technology*, 66 (9-12), pp. 1247–1254.
- Strondl, A., Lyckfeldt, O., Brodin, H., Ackelid, U. (2015), "Characterization and Control of Powder Properties for Additive Manufacturing" *The Journal of Minerals, Metals & Materials Society*, 67 (3), pp 549–554. <https://doi.org/10.1007/s11837-015-1304-0>
- Swift, K.G., Booker, J.D. (2013) "Manufacturing Process Selection Handbook" Butterworth-Heinemann, pp. 227-241.
- Takemura, S., Koike, R., Kakinuma, Y., Sato, Y. & Oda, Y. (2019) "Design of powder nozzle for high resource efficiency in directed energy deposition based on computational fluid dynamics simulation" *The International Journal of Advanced Manufacturing Technology*, pp. 1-15. <https://doi.org/10.1007/s00170-019-03552-1>
- Tang, H.P., Qian, M., Liu, N., Zhang, X.Z., Yang, G.Y. and Wang, J. (2015) "Effect of Powder Reuse Times on Additive Manufacturing of Ti-6Al-4V by Selective Electron Beam Melting", *Journal of the Minerals, Metals & Materials Society*, 67(3), pp 555-563.
- Tang, Y., Zhou, Y., Hoff, T., Garon, M. and Zhao, Y.F. (2016) "Elastic modulus of 316 stainless steel lattice structure fabricated via binder jetting process" *Materials Science and Technology*, 32(7), pp. 648–656. <https://doi.org/10.1179/1743284715Y.0000000084>

- Tekna (n.d) "Spherical powders" [online] Available at: <http://www.tekna.com/spherical-powders> (Accessed: July 29, 2019)
- Tekna (n.d.) "TekSphero-200 – Plasma Powder Spherodization" [online] Available here: <http://www.tekna.com/landing-page/teksphero-200> (Accessed: 1st August 2019)
- Tencan, (no date) "Horizontal Planetary Ball Mill", [online]. Available at: <http://www.lab-mills.com/planetary/horizontal.html>, [Accessed 30/01/2019]
- The Economist (2011) "The printed world" [online] Available here: <https://www.economist.com/briefing/2011/02/10/the-printed-world> (Accessed August 23rd, 2019)
- Total Materia (2001) "Stress Corrosion Cracking of Aluminum Alloys", [online] Available at: <http://www.totalmateria.com/Article23.htm>, [Accessed: March 11, 2019]
- Ulrich, K.T. and Eppinger, S.D. (2012) "Product Design and Development", 5<sup>th</sup> ed., New York: McGraw-Hill, pp. 154-159.
- Vock, S., Härtel, M., Maiwald-Immer, T., Wendt, F., Burghardt, K. *et al.* (2018) "Powder assessment for powder bed based additive manufacturing" *Proceedings of Fraunhofer direct digital manufacturing conference*
- Vock, S., Klöden, B., Kirchner, A., Weißgärber, T. and Kieback, B (2019) "Powders for powder bed fusion: a review" *Progress in Additive Manufacturing*, pp. 1-15. <https://doi.org/10.1007/s40964-019-00078-6>
- Wang, F., Williams, S., Colegrove, P. and Antonysamy, A.A. (2012) "Microstructure and Mechanical Properties of Wire and Arc Additive Manufactured Ti-6Al-4V" *Metallurgical and Materials Transactions A*, 44(2), pp. 968–977. <https://doi.org/10.1007/s11661-012-1444-6>
- Wang, Y., Shi, J., Lu, S. and Xiao, W. (2017) "Investigation of Porosity and Mechanical Properties of Graphene Nanoplatelets-Reinforced AlSi10 Mg by Selective Laser Melting" *Journal of Micro Nano-Manufacture*, 6(1). <https://doi.org/10.1115/MSEC2017-2911>
- Wohlers, T., Campbell, I., Diegel, O., Huff, R. and Kowen, J. (2019) "Wohlers Report 2019: 3D Printing and Additive Manufacturing: State of the Industry" Wohlers Associates
- Wycisk, E., Solbach, A., Siddique, S., Herzog, D., Walther, F., and Emmelmann, C. (2014) "Effects of defects in laser additive manufactured Ti-6Al-4V on fatigue properties" *Physics Procedia*, 56, pp. 371–378. <https://doi.org/10.1016/j.phpro.2014.08.120>
- Zelinski, P. (2015) "Additive's Idiosyncrasies", [blog] Additive Manufacturing, Available at: <https://www.additivemanufacturing.media/blog/post/additives-idiosyncrasies> [Accessed 30/01/2019]

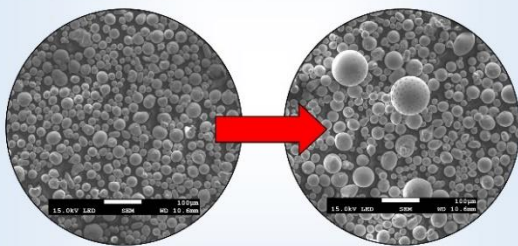
## REDUCING WASTE IN ADDITIVE MANUFACTURING: THE POWDER PROBLEM

Daniel Powell

MSc Engineering (by Research), Engineering Department  
Supervisor: Dr Allan Rennie

### Introduction

Additive Manufacturing is being increasingly used to produce high-quality, ready-to-use metal products in industrial applications, such as the aerospace, medical and filtration sectors. To make metallic additive manufacturing economically viable, metal powder needs to be repeatedly reused. However, repeated reuse causes powder degradation; particles pick up reactive contaminants from the air, change in morphology and get larger<sup>1</sup>.



Type of powder	Iron content	Carbon content	Oxygen content
Virgin	58.8 %	4.40 %	0.86 %
Used	57.9 %	4.88 %	1.83 %
Heavily used	55.7 %	7.15 %	5.28 %

### The problem

Powder degradation has been shown to negatively impact the quality of manufactured components<sup>1</sup>. Eventually, metal powder can no longer be used within additive manufacturing. This “end-of-life” powder is often sent to landfill, currently resulting in approximately 12.5% of powder produced going to waste<sup>2</sup>. The production of metal powders to replace this end-of-life powder consumes electrical power, contributing to carbon emissions.

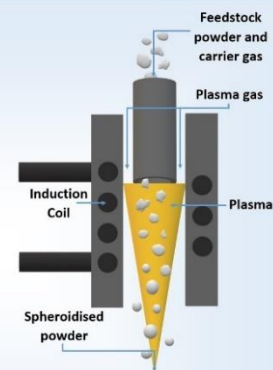
### The objectives

1. Prevent end-of-life metal powders going to landfill
2. Find a cost-effective solution to improve the longevity of metal powders
3. Find alternative ‘green’ methods of powder production
4. Demonstrate a reduction in carbon emissions

### The solution

Plasma spheroidisation has been shown to remove contaminants from particles, restore sphericity and reduce particle size<sup>3</sup>.

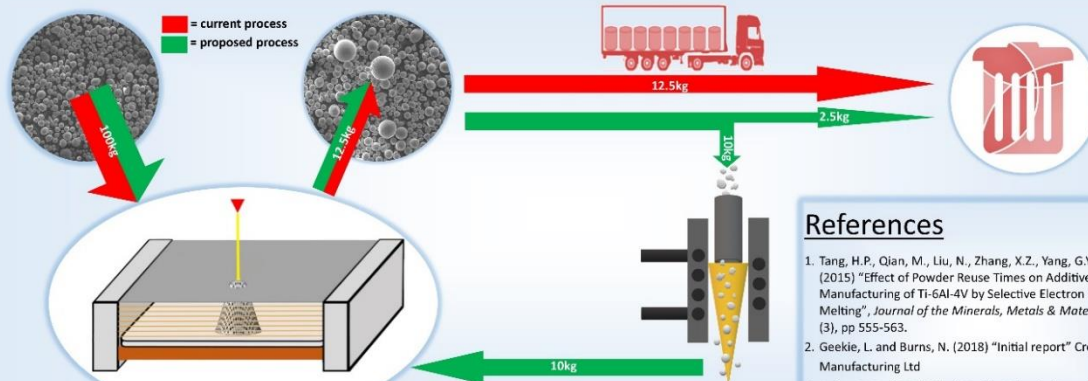
Powder that would have otherwise been sent to landfill can be used as feedstock in this process, producing powder of a similar quality to virgin powders used in additive manufacturing.



Type of powder	Oxygen content	Nitrogen content	Hydrogen content
Pre-spheroidised <sup>3</sup>	0.164%	0.047%	0.001%
Plasma spheroidised <sup>3</sup>	0.057%	0.009%	0.0007%

### Conclusions

Approximately 80% of waste powder is believed to be suitable for upcycling through plasma spheroidisation for reuse in additive manufacturing. This would result in a 10% reduction in the quantity of virgin powder needing to be produced each year, reducing both raw material usage and energy consumption.



### References

1. Tang, H.P., Qian, M., Liu, N., Zhang, X.Z., Yang, G.Y. and Wang, J. (2015) “Effect of Powder Reuse Times on Additive Manufacturing of Ti-6Al-4V by Selective Electron Beam Melting”, *Journal of the Minerals, Metals & Materials Society*, 67 (3), pp 555-563.
2. Geekie, L. and Burns, N. (2018) “Initial report” Croft Additive Manufacturing Ltd
3. Kelkar, R. M. (2018) “High Quality Spherical Powders for Additive Manufacturing Processes Along With Methods of Their Formation” US20190061005A1

## CENTRE FOR GLOBAL ECO-INNOVATION CO<sub>2</sub>e Calculator

<b>Name:</b> Daniel Powell			
<b>Project:</b> CGE 98 – Recycling and reuse of powders for various applications in additively manufactured products			
<b>Industry Partner:</b> Croft Additive Manufacturing Ltd			
<b>Academic Supervisors:</b> Dr Allan Rennie, Dr Vesna Najdanovic			
<b>Description of project:</b>			
<p>The layer-by-layer fabrication process employed by additive manufacturing has the potential to create very little waste; only the material that is required for the component and the support structures is used in the build process. This allows the surrounding metallic powder to be recycled and reused, but as the powder is continually reused its properties change, rendering it unsuitable for the manufacture of high value or safety critical components in some industrial sectors. This project will develop an alternative utilisation strategy to provide a more economical and environmentally friendly means of using the ‘waste’ powder at the end of its useful life, rather than simply disposing of it.</p>			
<b>Summary of GHG emission reduction:</b>			
<p>The majority of GHG emitted comes from electrical power consumed during the Selective Laser Melting (SLM) process. This remains unchanged. However, there is a reduction in the quantity of virgin powder that needs to be produced each year through atomisation, as plasma spheroidisation repurposes end of life powder instead. This process consumes less power than atomisation and prevents waste powder being sent to landfill, resulting in a reduction in GHG emissions.</p> <p>The given GHG emission reduction value is focused solely on Croft AM Ltd’s current powder usage. Croft represent a very small portion of the entire AM industry. If the practices highlighted were adopted by the wider AM industry and applied to other materials, the impact of this research could be greatly increased.</p>			
<b>GHG emissions before support</b>	<b>Current GHG emissions</b>	<b>Total GHG reduction</b>	<b>Percentage of reduction</b>
1.556 tCO <sub>2</sub> e	1.545 tCO <sub>2</sub> e	0.0115 tCO <sub>2</sub> e	0.71%

**Section one – Baseline of CO<sub>2</sub>e emissions relating to original process, service or product**

**Scope one – Direct emissions from company owned and controlled operations**

**Scope two – Indirect emissions purchased by company**

**CO<sub>2</sub>e from purchased energy for own use (electricity, steam, heating and cooling)**

*Energy required in the SLM process*

Can vary from build to build. An example of the SLM process using a machine similar to Croft AM Ltd's was carried out by Baumers *et al.* (2011), found to be 111.60 MJ/kg = 31.00 kWh

@ 0.28307 kgCO<sub>2</sub>e/kWh = 8.775 kgCO<sub>2</sub>e per kilogram of powder converted into product (UK Government, 2018).

140 kilograms of powder used each year, therefore **1228.52 kgCO<sub>2</sub>e produced each year.**

**Scope three – Other indirect emissions from the supply chain owned and/or purchased by suppliers and consumers**

**Upstream e.g. suppliers**

**CO<sub>2</sub>e embodied in fuel and energy related activities (extraction, production and transportation before consumption)**

*Energy required producing virgin SS316L Powder through atomisation*

Shown by Morrow *et al.* (2007) to be between 17.62-31.81 MJ/kg. Average is therefore 24.72 MJ/kg = 6.87 kWh

@ 0.28307 kgCO<sub>2</sub>e/kWh = 1.945 kgCO<sub>2</sub>e per kilogram of powder produced.

Need to supply 140 kilograms of powder each year, therefore **272.30 kgCO<sub>2</sub>e produced each year.**

### CO<sub>2</sub>e embodied in transportation and distribution

#### *Energy required for deliveries*

Use of a Class II Diesel Van for deliveries.

16.8 miles to Croft HQ from LPW for deliveries. Therefore 33.6 miles round trip.

@0.37773 kgCO<sub>2</sub>e per mile = 12.692 kgCO<sub>2</sub>e per delivery (UK Government, 2018).

Assume 50 kilograms purchased at a time (based on a confidential report from Croft AM Ltd).

Using 140 kilograms a year requires 2.8 deliveries, theoretically producing 35.54 kgCO<sub>2</sub>e each year.

However, this is, practically, the same as 3 deliveries each year, resulting in **38.08 kgCO<sub>2</sub>e produced each year.**

### CO<sub>2</sub>e embodied in waste generated in operations

#### *Energy wasted through atomisation*

12.5% of powder produced is "waste" (Croft AM Ltd, 2018). Therefore, through atomisation,  $0.125 \times 24.72 = 3.09$  MJ/kg = 0.858 kWh/kg is entirely wasted for every kg of powder produced.

@ 0.28307 kgCO<sub>2</sub>e/kWh = 0.243 kgCO<sub>2</sub>e per kilogram of powder produced.

Use 140 kilograms a year, therefore **34.02 kgCO<sub>2</sub>e TOTALLY WASTED each year** of the 272.3 kgCO<sub>2</sub> used to make virgin powder each year.

#### *Energy required sending powder to landfill*

@ 9 kgCO<sub>2</sub>e per tonne of metal to landfill = 0.009 kgCO<sub>2</sub>e per kg of powder disposed of (UK Government, 2018).

12.5% waste of 140 kilograms leads to 17.5 kilograms of waste sent to landfill each year, therefore **0.1575 kgCO<sub>2</sub>e produced each year.**

*Energy required scrapping support structures and heat sinks*

Remelting steel uses 6.25 MJ = 1.74 kWh (Morrow *et al.*, 2007).

@ 0.28307 kgCO<sub>2</sub>e/kWh = 0.493 kgCO<sub>2</sub>e per kilogram of scrap steel.

Support structures account for between 19-50% of the powder consumption. Assuming 25% of powder is used to create support structures (Piller *et al.*, 2018; Zelinski, 2015), 35 kilograms of support structures are made each year (0.25 \* 140 kg). Therefore, **17.26 kgCO<sub>2</sub>e produced each year** through scrapping.

**Downstream e.g. consumers (sold products)**

**Biogenic emissions – Other emissions related to flora, fauna, land and water**

**Total baseline emissions figure**

Assuming 140 kilograms of powder usage each year, based on Croft AM Ltd's current usage data:

Electrical energy consumption for SLM machine = **1228.52 kgCO<sub>2</sub>e**

Energy consumption for atomisation process = **272.30 kgCO<sub>2</sub>e** of which **34.02 kgCO<sub>2</sub>e** is entirely wasted, producing unusable powder

Emissions from delivery vehicle emissions = **38.08 kgCO<sub>2</sub>e**

Energy consumption from powder sent to landfill = **0.1575 kgCO<sub>2</sub>e**

Energy consumption from scrapping support structures and heat sinks = **17.26 kgCO<sub>2</sub>e**

**TOTAL BASELINE EMISSIONS:**

**1556.318 kgCO<sub>2</sub>e every year**

**= 1.556 tCO<sub>2</sub>e per annum**

**Section two – Reduction of CO<sub>2</sub>e emissions relating to new process, service or product**

**Scope one – Direct emissions from company owned and controlled operations**

**Scope two – Indirect emissions purchased by company**

CO<sub>2</sub>e from purchased energy for own use (electricity, steam, heating and cooling)

*Energy required in the SLM process – NO CHANGE*, the SLM process used by Croft AM Ltd will not be affected by this project.

**Scope three – Other indirect emissions from the supply chain owned and/or purchased by suppliers and consumers**

**Upstream e.g. suppliers**

CO<sub>2</sub>e embodied in fuel and energy related activities (extraction, production and transportation before consumption)

*Energy required producing virgin SS316L Powder through plasma spheroidisation*

Plasma spheroidisation through Tekna TekSphero-200 is expected to require 14.4MJ = 4kWh per kilogram of powder produced.

@0.28307 kgCO<sub>2</sub>e/kWh = 1.132 kgCO<sub>2</sub>e produced per kilogram of powder produced.

Assuming 80% of waste powder can be reclaimed (Powell, 2019; based on Sartin *et al.*, 2017), this is 10% of all produced powder (as 12.5% of produced powder is considered waste, therefore  $0.8 * 12.5\% = 10\%$ ). This corresponds to 14 kg of powder produced through spheroidisation ( $0.1 * 140$  kg). Therefore  $1.132 * 14 = 15.848$  kgCO<sub>2</sub>e produced each year through plasma spheroidisation.

HOWEVER, this reduces the need for 14 kilograms (i.e. 10% of all produced virgin powder) of replacement virgin powder to be produced through atomisation.

Therefore  $0.1 * 272.3 = 27.230$  kgCO<sub>2</sub>e reduced every year.

**Overall reduction of 27.230 – 15.848 = 11.382 kgCO<sub>2</sub>e every year from powder production.**

### CO<sub>2</sub>e embodied in transportation and distribution

#### *Energy required for deliveries*

16.8 miles to Croft HQ from LPW for deliveries. Therefore 33.6 miles round trip.

@0.37773 kgCO<sub>2</sub>e per mile = 12.692 kgCO<sub>2</sub>e per delivery.

Assume 50 kilograms purchased at a time.

Now only require 126 kilograms a year as can produce 14 kilograms themselves, requires 2.52 deliveries, theoretically producing 31.984 kgCO<sub>2</sub> produced each year.

This results in a theoretical reduction of 3.56 kgCO<sub>2</sub>e per year from less deliveries.

However, this is, practically, the same as 3 deliveries each year, resulting in 38.08 kgCO<sub>2</sub>e produced each year, and therefore **NO CHANGE**.

### CO<sub>2</sub>e embodied in waste generated in operations

#### *Energy wasted through atomisation*

Assume that 80% of the unused powder can be reclaimed from the 12.5% of waste powder, with the remainder (20%) being sieved out, stuck in filters or otherwise unrecoverable. Therefore, only 2.5% of powder produced is not used to make useful products, wasting only  $0.025 * 272.3 = 6.81$  kgCO<sub>2</sub>e each year when producing virgin powder instead of the previously calculated 34.02 kgCO<sub>2</sub>.

#### *Energy required sending powder to landfill*

Only 2.5% of powder is now sent to landfill, producing  $(0.025 * 140 * 0.009) = 0.0315$  kgCO<sub>2</sub>e per year.

**Overall reduction of 0.1260 kgCO<sub>2</sub>e per year** from less powder in landfill.

#### *Energy required scrapping support structures and heat sinks*

**NO CHANGE** in stainless steel, the procedure identified only saves energy if the scrapped material is reformed into powder, but this is not a reasonable assumption to make for all 35kg of support structure produced. The baseline calculation did not assume powder was going to be formed from the scrap support structures.

**Downstream e.g. consumers (sold products)**

**Biogenic emissions – Other emissions related to flora, fauna, land and water**

**Total reduction emissions figure (savings)**

Assuming 140 kilograms of powder usage each year, based on Croft AM Ltd's current usage data:

Electrical energy consumption for SLM machine = **NO CHANGE**

Energy consumption for atomisation process = **11.382 kgCO<sub>2</sub>e** with only **6.81 kgCO<sub>2</sub>e** being entirely wasted and producing unusable powder

Emissions from delivery vehicle emissions = **NO CHANGE**

Energy consumption from powder sent to landfill = **0.1260 kgCO<sub>2</sub>e**

Energy consumption from scrapping support structures and heat sinks = **NO CHANGE**

**TOTAL REDUCTION OF EMISSIONS:**

**11.50 kgCO<sub>2</sub>e every year**

**= 0.0115 tCO<sub>2</sub>e per annum**

## References

Baumers, M., Tuck, C., Wildman, R., Ashcroft, I. and Hague, R. (2011) "Energy inputs to additive manufacturing: does capacity utilization matter?" SFFS Symposium 2011, Texas

Croft AM Ltd (2018) "Croft Initial Report", unpublished document.

Morrow, W.R., Qi, H., Kim, I., Mazumder, J. and Skerlos, S.J. (2007) "Environmental aspects of laser-based and conventional tool and die manufacturing", *Journal of Cleaner Production*, 15 (10), pp. 932-943.

Piller, F.T., Poprawe, R., Schleifenbaum, H.J., Schuh, G., Barg, S., Dolle, C., Hinke, C., Jank, M. -H., Jiang, R., Meiners, W., Riesener, M., Schrage, J. and Ziegler, S. (2018) "Introducing a Holistic Profitability Model for Additive Manufacturing: An Analysis of Laser-powder Bed Fusion," *2018 IEEE International Conference on Industrial Engineering and Engineering Management (IEEM)*, pp.1730-1735. <https://doi.org/10.1109/IEEM.2018.8607729>

Powell, D. & Rennie, A. (2019) "Reducing waste in additive manufacturing: the powder problem" *Eco-Innovation Conference*, Lancaster, UK, 19<sup>th</sup>-20<sup>th</sup> September 2019.

Sartin, B., Pond, T., Griffith, B., Everhart, W., Elder, L., Wenski, E., Cook, C., Wieliczka, D., King, W., Rubenchik, A., Wu, S., Brown, B., Johnson, C. and Crow, J. (2017) "316l Powder Reuse For Metal Additive Manufacturing" *28th Annual International Solid Freeform Fabrication Symposium – An Additive Manufacturing Conference*, 7<sup>th</sup>-8<sup>th</sup> August, Austin, Texas

Tekna (n.d.) "TekSphero-200 – Plasma Powder Spherodization" [online] Available here: <http://www.tekna.com/landing-page/teksphero-200> (Accessed: 1st August 2019)

UK Government, 2018, 'Government emission conversion factors for greenhouse gas company reporting.' <https://www.gov.uk/government/collections/government-conversion-factors-for-company-reporting> [Accessed 21/10/2019].

Zelinski, P. (2015) "Additive's Idiosyncrasies", [blog] Additive Manufacturing, Available at: <https://www.additivemanufacturing.media/blog/post/additives-idiosyncrasies> [Accessed 30/01/2019]

## Appendix C – Programme of work for plasma spheroidisation

[External Sender] Royce Facilities PhD Access Scheme Enquiry - ref 19/0059



Luke A Benson Marshall

Tue 08/10/2019 16:12

To: Powell, Dan (Student)

Cc: Vahid Nekouie



Hi Dan, Vahid.

Thanks for the call, I think we are at a good point. In summary of the call;

Currently the virgin powder and in use powder are sized as follows and a target input for spheroidisation;

D10 D50 D90 (micron)

15 25 43 Virgin

14 24 50 Used

15 N/A 60 Target

The program of work will entail;

- 1) PSD of incoming powder
- 2) Sieving a sample of powder to determine how much powder actually needs sieving to have enough input material for spheroidisation.
- 3) PSD of sieved powder
- 4) Spheroidisation initial trial (100-150g)
- 5) PSD of product, used as a feedback loop to determine subsequent parameters x5
- 6) Spheroidisation trials (100-150g) x5
- 7) PSD of product x5
- 8) Return of spheroidised powder and input material (7 samples total) to D. Powell
- 9) Delivery of all PSD results and specifications of all equipment used and associated trial parameters

In addition to this Vahid is required to purchase sieve screens to avoid cross contamination.

The timeframe for the work is to perform steps 1)-5) before Nov 23rd and to complete 6)-9) in the subsequent 2 weeks, this is designed to provide Dan with the opportunity to attend and see the equipment if possible.

Finally, acknowledgements for the final Thesis will include Royce for this work (I will give more details on how we would like to be referenced closer to the time) and Vahid has offered publication support with a view to co-authorship, providing agreement between Vahid, Dan and Dan's academic supervisor can be reached and is appropriate.

Hopefully this covered everything we discussed.

[External Sender] Royce Fa...

(No subject)

